EGG-SAAM-6476
December 1983

RELAP5 THERMAL-HYDRAULIC ANALYSES OF PRESSURIZED THERMAL SHOCK SEQUENCES FOR THE H. B. ROBINSON UNIT 2 PRESSURIZED WATER REACTOR

C. D. Fletcher
M. A. Bolander
M. E. Waterman
J. D. Burtt
B. D. Stitt
C. M. Kullberg
C. B. Davis
D. M. Ogden

Idaho National Engineering Laborato
Operated by the U.S. Department of Energy

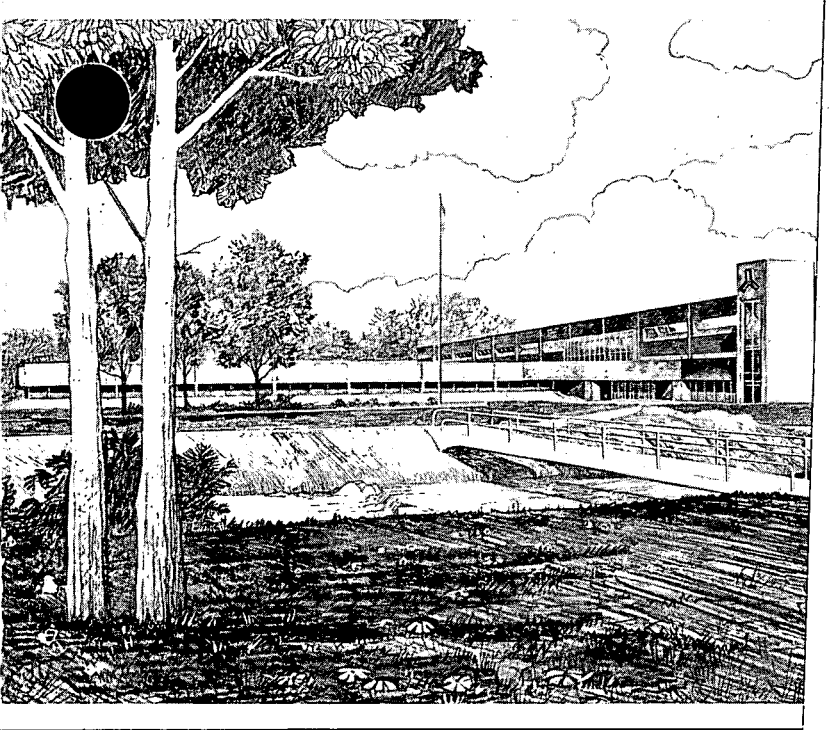

This is an informal report intended for use as a

Prepared for the
U.S. NUCLEAR REGULATORY COMMISSION
Under DOE Contract No. DE-AC07-76ID01570
FIN No. A6047

EG&G Idaho

EGG-SAAM-6476

RELAP5 THERMAL-HYDRAULIC ANALYSES OF PRESSURIZED THERMAL SHOCK SEQUENCES FOR THE H. B. ROBINSON UNIT 2 PRESSURIZED WATER REACTOR

C. D. Fletcher
M. A. Bolander
M. E. Waterman
J. D. Burtt
B. D. Stitt
C. M. Kullberg
C. B. Davis
D. M. Ogden

Published December 1983

EG&G Idaho, Inc.
Idaho Falls, Idaho 83415

Prepared for the
U.S. Nuclear Regulatory Commission
Washington, D.C. 20555
Under DOE Contract No. DE-AC07-76ID01570
FIN No. A6047

ABSTRACT

Thermal-hydraulic analyses of eleven hypothetical pressurized thermal shock (PTS) scenarios for the H. B. Robinson, Unit 2 pressurized water reactor were performed at the Idaho National Engineering Laboratory (INEL) using the RELAP5 computer code. The scenarios, which were developed at Oak Ridge National Laboratory (ORNL), contain significant conservatisms concerning equipment failures, operator actions, or both.

The results of the thermal-hydraulic analyses presented here, along with additional analyses of multidimensional and fracture mechanics effects will be utilized by ORNL, integrator of the PTS study, to assist the U. S. Nuclear Regulatory Commission in resolving the pressurized thermal shock unresolved safety issue.

FIN No. A6047--Code Assessment and Applications (Transient Analysis)

SUMMARY

Thermal-hydraulic analyses were performed at the Idaho National Engineering Laboratory (INEL) using the RELAP5 computer code to support the U. S. Regulatory Commission's investigation of the pressurized thermal shock (PTS) unresolved safety issue.

The plant analyzed was the H. B. Robinson, Unit 2 pressurized water reactor (PWR) which is of Westinghouse three-loop design with a rated thermal power of 2300 MW. An extensive computer model of the plant was developed specifically to perform the calculations needed for the analyses presented in this report. The model contains detailed thermal-hydraulic representations of pertinent PWR primary and secondary systems including the feedwater train and steam lines. Detailed models are also included for the steam dump, steam generator level, pressurizer level, and other plant control systems.

The model was quality-assured in four ways. First, the development of each model component was documented on worksheets which include references to the plant documents supporting the development. Second, the worksheets were independently reviewed by an analyst other than the one who developed them. Third, utility analysts, already familiar with design and modeling of the plant, reviewed the model at various stages of completion and the calculational results. Fourth, the simulation of a plant transient was performed with the completed model and results were compared with measured plant data. The comparison appears in this report.

Eleven scenarios of PTS interest are analyzed in this report. The scenarios were defined at Oak Ridge National Laboratory (ORNL), the integrator of the PTS study. Computer simulations of the scenario event sequences were performed using best estimate conditions and assumptions. However, the scenarios themselves contain significant conservative assumptions concerning equipment failures, operator actions or omissions, or combinations of these.

The scenarios analyzed were initiated by main steam line break, stuck open steam line valve, steam generator overfeed, small hot leg break, stuck open pressurizer valve, steam generator tube rupture, and loss of secondary heat sink events. Some scenarios start with the plant operating at full power while others start from hot standby conditions.

The results of the thermal-hydraulic analyses in this report represent part of the information required by ORNL for the assessment of the PTS issue. The results of this report are not to be used directly as an indication of pressurized thermal shock severity for the scenarios investigated. For this purpose, comprehensive results of the analyses (far beyond the results shown here) have been transmitted to ORNL. Following additional analyses of multi-dimensional and fracture mechanics effects, ORNL will integrate all results and publish a report that estimates the likelihood of reactor vessel failure and identifies important event sequences, operator and control actions, and uncertainties.

ACKNOWLEDGMENTS

The authors wish to acknowledge the timely efforts of text processors Joan Mosher and Louise Judy in the compilation of this document and of Operation Technicians Erma Jenkins and Nancy Thornley in the development of the graphics presented here.

The authors also wish to thank Rudy Oliver, Scott Lucas, Jerry Phillips and others of Carolina Power and Light Company and Dan Speyer (CP&L consultant) for their assistance in providing plant information and reviewing models and results. Their assistance proved invaluable and provided an extra degree of confidence in the analytical results.

CONTENTS

FIGURES

TABLES

1. INTRODUCTION

Rapid cooling of a reactor pressure vessel during a transient or accident accompanied by high coolant pressure is referred to as pressurized thermal shock (PTS). In late 1981 the U. S. Nuclear Regulatory Commission (NRC) designated PTS as an unresolved safety issue and developed a task action plan (TAP A-49) to resolve the issue.

The safety issue exists because rapid cooling at the reactor vessel wall inner surface produces thermal stresses within the wall. As long as the fracture toughness of the reactor vessel is high, overcooling transients will not cause vessel failure. However, NRC staff analyses (SECY-85-465) showed certain older plants with copper impurities in vessel weldments may become sensitive to PTS in a few years as the nil-ductility transition temperature of the weld material gradually increases. The purpose of the thermal-hydraulic analyses presented in this report is to better understand the behavior of a plant during various kinds of postulated severe overcooling transients with multiple failures of equipment and without operator corrective action. The understanding gained from these detailed calculations will be used to interpolate coolant temperature and pressure responses in the downcomer for other postulated transients using a simplified mass-and-energy balance approach. For each of these postulated transients, Oak Ridge National Laboratory (ORNL) will then calculate the reactor vessel temperature distribution and stresses during the transient and the conditional probability of vessel failure if the transient should occur. ORNL will publish a report that integrates these results to estimate the likelihood of PTS driving a crack through the reactor vessel wall and to identify important event sequences, operator and control actions, and uncertainties.

This series of analyses is intended to provide information to help the NRC staff confirm the bases for the screening criteria in the proposed PTS rule (proposed 10CFR 50.61) and determine the content required for licensees' plant-specific safety analysis reports and the acceptance criteria for corrective measures.

The computer simulations presented in this report were performed using "best estimate" modeling assumptions for plant conditions and responses to the events specified in the scenario descriptions. The reader is cautioned, however, that for bounding purposes the scenario descriptions were based on extremely conservative assumptions concerning equipment malfunctions, operator actions and omissions, or combinations of these. Thus while the computer simulations represent "best estimate" plant responses to the scenarios as defined, they do not represent the "most probable" plant responses to the scenario initiating events.

Analyses presented in this report were performed for the H. B. Robinson, Unit 2 pressurized water reactor operated at Hartsville, South Carolina by Carolina Power and Light Company. The reactor is of Westinghouse three-loop design and is currently being operated at a reduced power due in part to steam generator tube plugging. The simulation of the plant transient presented in Section 3, was performed at a thermal power of 2200 MW to agree with the operating power at the time of the transient. The simulation of Scenarios 1 through 11, presented in Sections 4 through 14 were performed assuming a full rated thermal power of 2300 MW. This is the power level at which the plant is expected to operate following an imminent replacement of steam generators. Other plant changes anticipated to be made at that time were also incorporated into the analyses of the scenarios.

Table 1-1 briefly identifies Scenarios 1 through 11 as defined at ORNL. Full scenario descriptions appear in Sections 4 through 14. Analyses were performed for a 2-hour period starting at the beginning of cooldown. For all except Scenario 11 the period started at the time of the initiating event. For Scenario 11 the period started at the time of steam generator dryout, approximately 1 hour after the initiating event.

This report is organized in the following format: a description of the computer model is given in Section 2, a comparison of computer simulated and measured data for a plant transient is presented in Section 3, analyses of PTS Scenarios 1 through 11 are presented in

TABLE 1-1. SUMMARY OF SCENARIOS ANALYZED

Scenario Number	Initial Plant Condition	Initiating Event	Analysis Section in This Report
1	Hot standby	1.0 ft^2 break in main steam line	4.0
2	Hot standby	Double-ended main steam line break	5.0
3	Hot standby	Stuck-open steam line PORV	6.0
4	Full power	Three steam dump valves fail open	7.0
5	Full power	Overfeed with auxiliary feedwater	8.0
6	Full power	Small hot leg break	9.0
7	Full power	Stuck open pressurizer PORV	10.0
8	Hot standby	Small hot leg break	11.0
9	Hot standby	Steam generator tube rupture	12.0
10	Full power	Steam generator tube rupture	13.0
11	Full power	Loss of heat sink with primary system feed-and-bleed recovery	14.0

Sections 4 through 14 followed by an overview and conclusions in Section 15. Appendix A presents a timing survey that discusses the computer run time required to perform the calculations.

2. MODEL DESCRIPTION

This section describes the RELAP5 H. B. Robinson PWR model used for three steady state initializations and subsequently for each of the PTS transient calculations and a simulation of a H. B. Robinson plant trip transient. Subsection 1 of this section describes the thermal-hydraulic components of the model, subsection 2 describes the control system model, subsection 3 presents the steady state conditions for each steady state initialization calculation, and subsection 4 describes the documentation control used for the models and code for these calculations.

The model was quality-assured in four ways. First, the development of each model component was documented on worksheets which include references to the plant documents supporting the development. Second, the worksheets were independently reviewed by an analyst other than the one who developed them. Third, utility analysts, already familiar with design and modeling of the plant, reviewed the model at various stages of completion and the calculational results. Fourth, the simulation of a plant transient was performed with the completed model and results were compared with measured plant data. The comparison appears in Section 3 of this report.

2.1 Thermal-Hydraulic Model

The RELAP5 model is a detailed representation of the H. B. Robinson PWR power plant describing all the major flow paths for both primary and secondary systems, including the main steam and feed systems. Also modeled are primary and secondary power operated relief valves (PORV), and safety valves. The emergency core cooling system (ECCS) was included in modeling the primary side and the auxiliary feedwater system was included in the secondary side modeling. The model contained 224 volumes, 242 junctions and 218 heat structures. A description of the primary and the secondary systems are presented in the following sections.

2.1.1 Primary System

The H. B. Robinson PWR plant has three primary coolant loops and each loop is represented in the RELAP5 model. The loops are designated as A, B, and C. Each modeled loop contained a hot leg, U-tube steam generator, pump suction leg, pump, and cold leg as shown in Figure 2-1. Attached to the C loop was the pressurizer, and the pressurizer spray lines were attached to the B and C loop cold legs as shown in Figure 2-1. Attached to each cold leg was a low pressure injection (LPI) port and an accumulator with its associated piping. Also attached to the cold leg was a high pressure injection (HPI) port. The LPI and HPI models were set up to inject one third of the total HPI and LPI flow into each loop. Attached also to the Loop B cold leg was the chemical and volume control system (CVCS). Makeup and letdown were modeled with a single junction. Heat structures were added to each volume in the primary loops to represent the metal mass of the piping and steam generator tubes. Heat structures were also used to represent the pressurizer proportional and back-up heaters.

Figure 2-2 shows the RELAP5 nodalization used to represent the H. B. Robinson vessel. Represented in the RELAP5 vessel model was the downcomer, downcomer bypass, lower plenum, core, upper plenum and upper head. The following leakage paths were represented in the vessel model; downcomer to upper plenum, downcomer to downcomer bypass, downcomer bypass to lower plenum, cold leg inlet annulus to upper plenum, and upper plenum to the upper head via the guide tube. Heat structures represented external and internal metal mass of the vessel as well as the core rods. Decay heat was assumed to be at the ANS standard rate.

There were 130 volumes associated with the primary loops and 33 volumes associated with the vessel.

2.1.2 Secondary System

The RELAP5 H. B. Robinson PWR secondary system model is shown in Figure 2-3 and 2-4. The steam generator secondary model, shown in Figure 2-3, represents the major flow paths in the secondary and includes

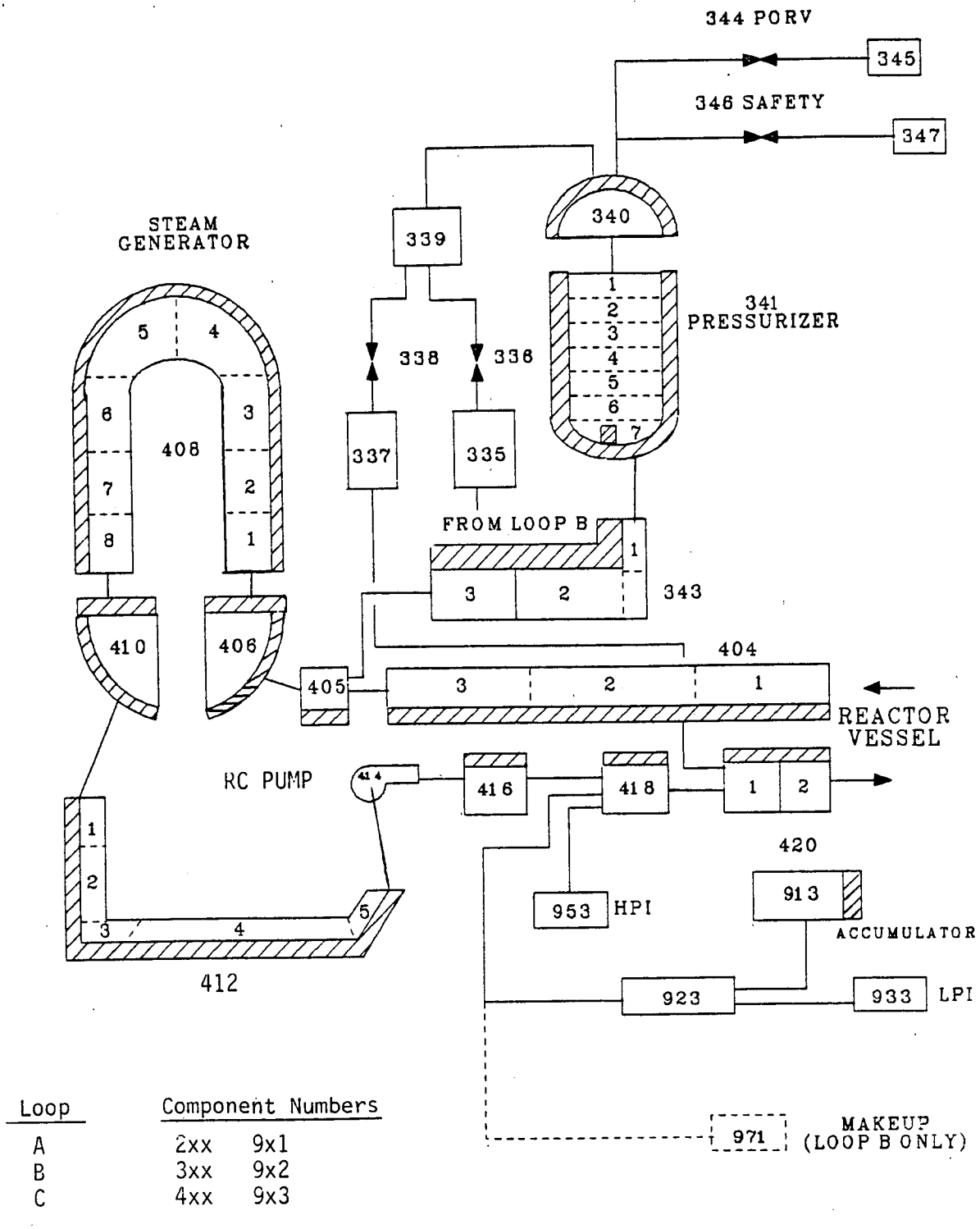

Loop	Component Numbers	
A	2xx	9x1
B	3xx	9x2
C	4xx	9x3

Figure 2-1. Nodalization of Primary Coolant Loops (loop C shown).

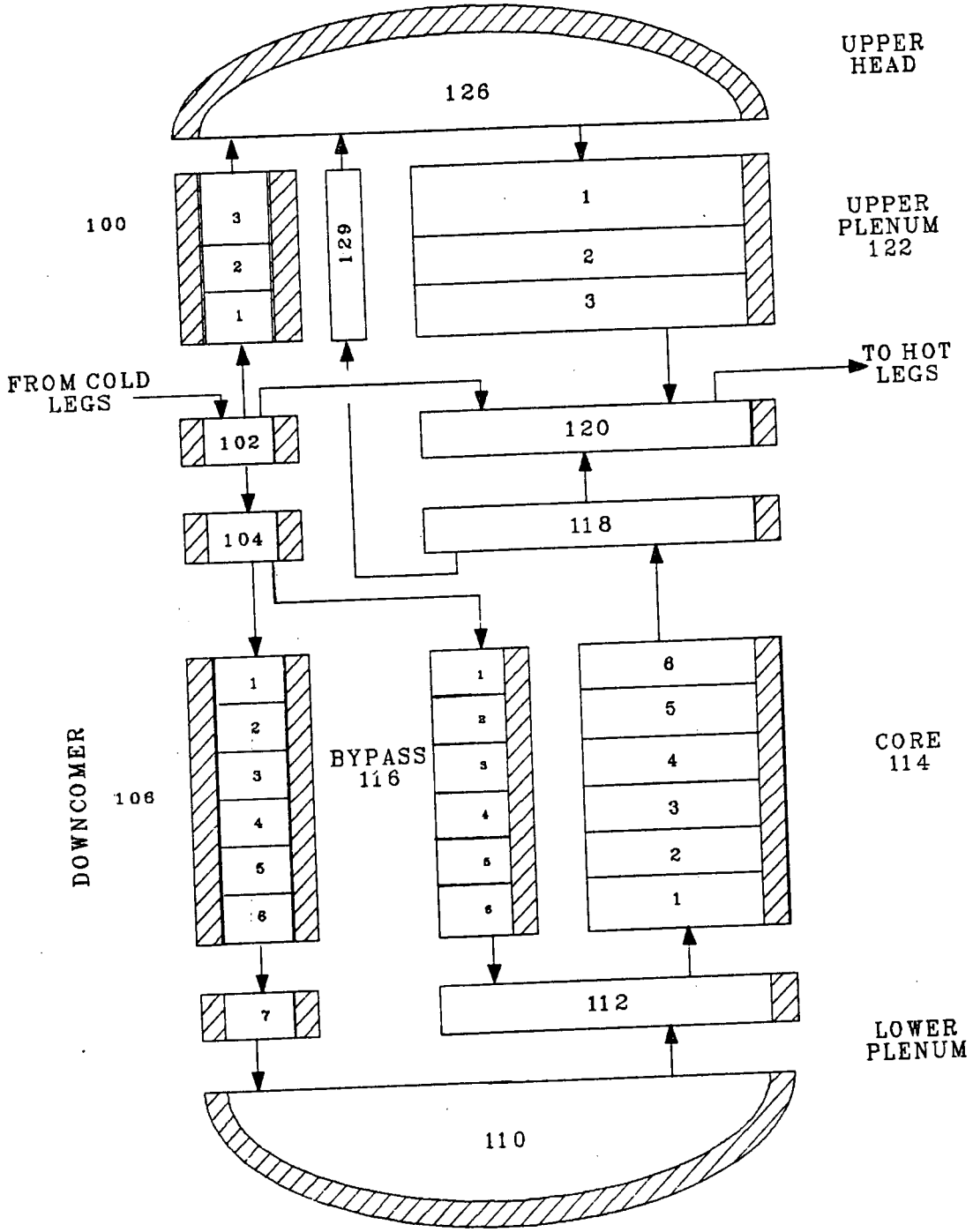

Figure 2-2. Nodalization of Reactor Vessel.

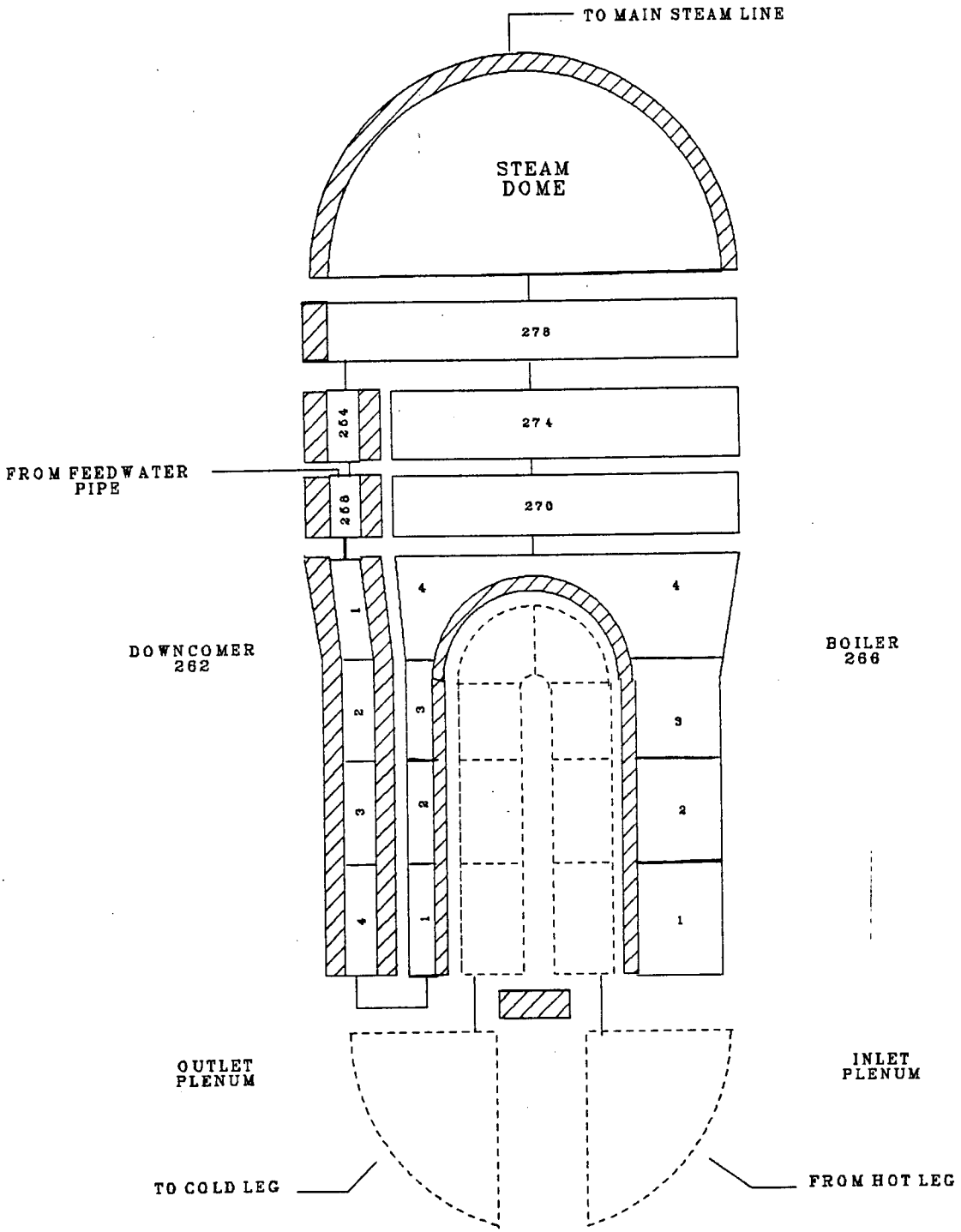

Loop	Component Numbers
A	2xx
B	3xx
C	4xx

Figure 2-3. Nodalization of Steam Generator (SGA shown).

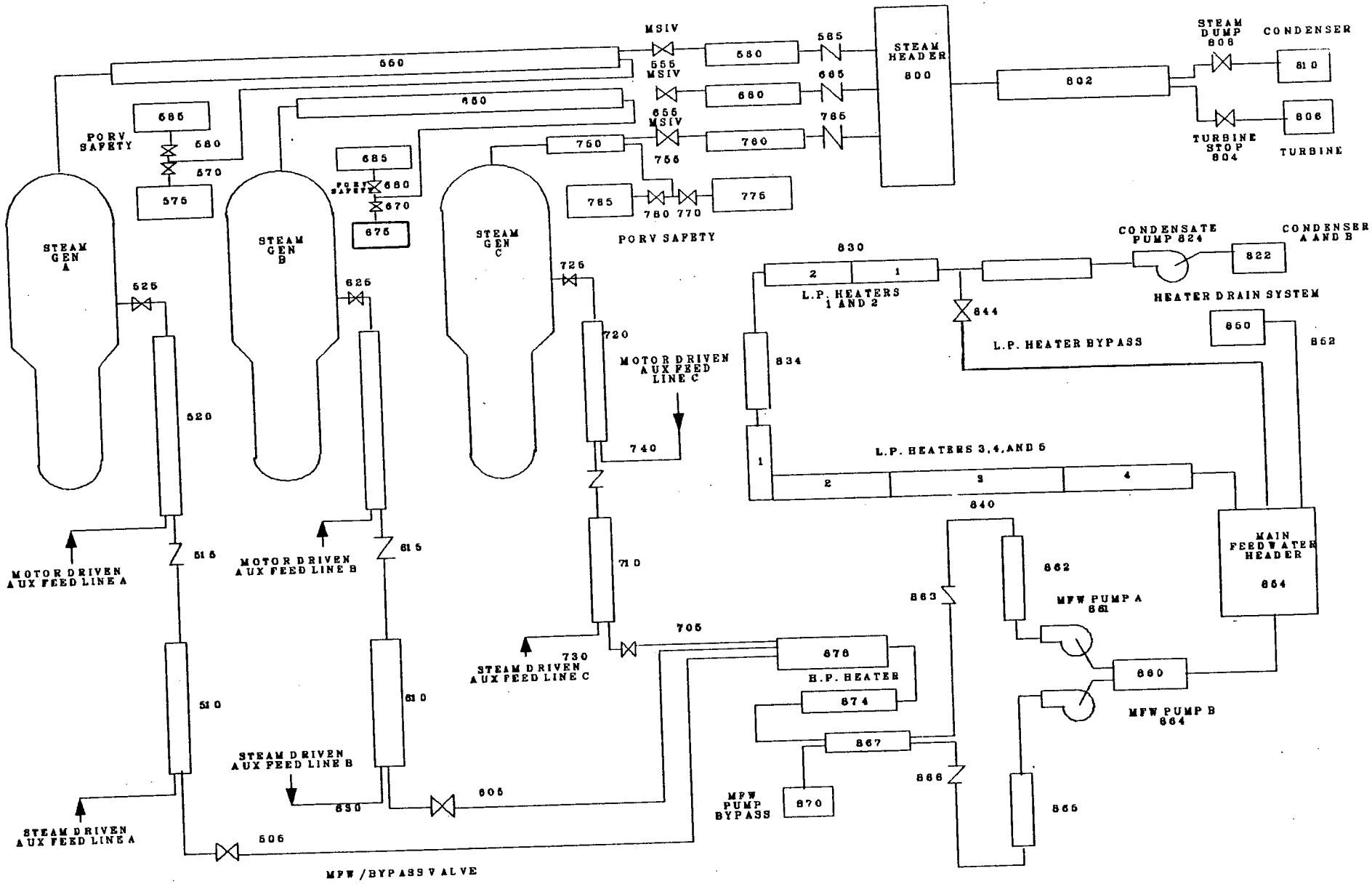

Figure 2-4. Nodalization of Feedwater and Steam Systems.

the downcomer, boiler region, separator and dryer region, and the steam dome. Due to modeling constraints, the steam generator secondary separators and dryers were modeled within a single calculational volume. Separation in the model thus takes place at a single elevation rather than at two discrete elevations as in the prototype steam generator. The effect of this difference is a perturbation of the flow field at the upper steam generator level tap which affects the indicated level in a minor way. A further discussion of this effect appears in Section 3.

The major flow paths of the steam line out to the turbine governor valves were modeled, and are shown in Figure 2-4. Each line from the steam generator secondary out to the common steam header was modeled individually and included a main steam isolation valve (MSIV), a check valve, safety and PORV valves. The flow restrictor was modeled in combination with the flow nozzle at the top of the steam dome. From the header to the turbine governor valves the north and south lines were modeled as one line. The steam dump valve banks were modeled as one valve with appropriate control logic to simulate the opening of each valve in the banks.

The major flow paths of the feedwater system were modeled and are shown in Figure 2-4. The feedwater system consisted of the condensate system, main feedwater system, and the auxiliary feedwater system. The components included in modeling the condensate system were the A and B condensate pumps, low pressure feedwater heaters, low pressure heater bypass, heater drain system, and the main feedwater pump suction header. The condensers were modeled using a constant temperature boundary condition. The components included in modeling the main feedwater system were both main feedwater pumps, main feedwater pump recirculation, high pressure feedwater heaters, main feedwater header tank, main feedwater/bypass valves, and piping to the steam generators including the feedwater header ring. The auxiliary feedwater system modeling included the motor driven and steam driven systems, with a common header for each system and valves from the header to each feed line.

Heat structures for the secondary system included the internal and external metal mass for each of the steam generator secondaries and the metal mass of the piping for both the steam line system and the feedwater system.

There were a total of 14 volumes representing the secondary for each steam generator. The steam line consisted of 16 volumes and the feedwater system contained 31 volumes.

2.2 Control System Model

The purpose of this section is to provide the reader with a general overview of the functions of the major control systems used in the 12 calculations to be described in subsequent sections. Detailed information regarding the setpoints of the Westinghouse control systems will not be provided due to the proprietary nature of the various control system specifications. In general, the control systems were modeled as closely as possible and are considered to be good representations of the actual systems.

The steam dump control system will be described in Section 2.2.1, followed by descriptions of the steam generator level control system in Section 2.2.2, the pressurizer pressure control system in Section 2.2.3, and pressurizer level control system in Section 2.2.4, and identification of additional systems in Section 2.2.5.

2.2.1 Steam Dump Control System

The purpose of the steam dump control system (SDCS) is to:

1. Permit the nuclear plant to accept sudden losses of load without tripping the reactor.

2. Remove stored energy and residual heat following a reactor trip and bring the plant to equilibrium no-load conditions without actuation of the steam generator safety valves.

3. Permit control of the steam generator pressure at no-load conditions and permit a manually controlled cooldown of the plant.

The above tasks are accomplished by three modes of steam dump control. Requirements 1 and 2 are met by control of the primary system average fluid temperature, Tave, whereas requirement 3 is met by controlling the secondary system steam pressure. The SDCS is divided into three separate systems, which are described in the following subsections.

2.2.1.1 Load Rejections Controller

The load rejections controller (LRC) is designed to control the primary system average temperature during periods of load rejection. Control of the primary system average temperature is performed by modulating the steam dump valves and, if the load rejection is greater than 70%, the steam line power-operated relief valves (PORVs). The turbine impulse stage pressure signal is linearly converted into the primary system average temperature setpoint; and, the filtered derivative of the turbine impulse stage pressure signal is used to determine whether or not a load rejection has occurred, and the size of the rejection when one does occur.

Modulation of the steam dump valves is blocked if the condenser does not have sufficient vacuum, or if the primary system average temperature decreases below the minimum temperature setpoint. Other bistables exist in the real plant but were not modeled because they would not have been used in the various calculations presented here.

2.2.1.2 Plant Trip Steam Dump Control

The function of the plant trip controller (PTC) is to bring the primary system average temperature down to the equilibrium no-load setpoint, 559 K (547°F) for the 2300 MW full power case, after the turbine

has been tripped. The PTC performs this function by modulating the steam dump valves. Unlike the LRC, the PTC does not have any control over the steam line relief valves.

Modulation of the steam dump valves is blocked if the condenser does not have sufficient vacuum, or if the primary system average temperature decreases below the minimum temperature setpoint. Steam dump control system operation using the PTC is replaced with the steam pressure controller when the primary system average temperature is decreased to the no-load setpoint, with the additional constraint that 60 s must have expired since the plant was tripped. The 60 s delay is used to simulate the reactor operator response time.

2.2.1.3 Steam Pressure Control

The steam pressure controller (SPC) is used to regulate the secondary system steam header pressure. This system is used when the plant is at no-load conditions, or to replace the PTC. The steam header pressure is controlled by modeling the steam dump valves. The setpoint pressure is 7.03 MPa (1020 psia). No modulation of the steam line PORVs is performed by this system.

Modulation of the steam dump valves is blocked if the condenser does not have sufficient vacuum, or if the primary system average temperature decreases below the minimum temperature setpoint; however, unlike the LRC and PTC systems, the minimum temperature condition may be overridden by the plant operator to enable plant cooldown to cold shutdown conditions.

2.2.2 Steam Generator Level Control System

The steam generator level control system (SGLCS) is designed to regulate the liquid level in the steam generator (SG) downcomer. This control system uses three input signals to regulate the feedwater flow rate into each of the three steam generators. These three signals are 1) the steam generator liquid level, 2) the steam flow rate measured in the steam

line at the SG outlet, and 3) the feedwater flow rate measured downstream of the feedwater regulating valve. The SGLCS is only used when the plant load is above 15%.

The steam generator liquid level is determined by measuring the differential pressure between pressure taps in the SG downcomer. The liquid level is inferred from this differential pressure, and can be perturbed by events that influence these two taps in a nonsynchronous manner; for example, a main steam line break or turbine stop valve closure. The steam generator liquid level signal is compared to the setpoint level, which is a function of the turbine impulse stage pressure, and the resulting error is then used as an input signal to a proportional-integral (P-I) controller.

The feedwater and steam flow rate signals are compared to determine the feed-steam mismatch signal. This signal is added to the level error signal and the result is used as the input signal for another P-I controller. The output of this P-I controller is used to modulate the appropriate feedwater valve.

The SGLCS is not used when the plant load is less than 15%. Instead, the main feedwater valves are closed and feedwater control is performed manually using the feedwater bypass valves to maintain the desired steam generator level. Additionally, one main feedwater pump and one condensate pump are used, instead of two of each as in the full power case.

The conditions that can result in main feedwater isolation in the plant have been incorporated into the SGLCS model. These conditions include plant trip, main feedwater pump trip, and initiation of the engineered safety features actuation signal (ESFAS).

2.2.3 Pressurizer Pressure Control System

The purpose of the pressurizer pressure control system (PPCS) is to maintain the desired primary system pressure. This function is performed using spray valves, relief valves, proportional heaters, and back-up heaters.

The pressurizer pressure is compared to the setpoint pressure to determine the pressurizer pressure error. This error signal is used as the input signal to a P-I controller. The output of the P-I signal is used to control the function of both spray valves, the proportional and back-up heater source demands, and the valve area of one of the two pressurizer PORVs. The other PORV area is a function of the uncompensated pressurizer pressure signal.

The PPCS is modeled as accurately as possible and includes all the trips and setpoints in the actual plant with two exceptions. First, the spray valves do not maintain a minimum flow as in the plant because of difficulties incurred due to thermal-hydraulic considerations. The minimum flow requirement is imposed in the plant to maintain the spray line temperature at the temperature of the primary system cold legs. This is required to avoid the possibility of thermally stressing the spray lines when pressurizer spray is demanded. To compensate, the model spray lines were initialized at cold leg temperatures and no heat losses from the lines to containment were considered. The other modeling exception is in the amount of power supplied to the proportional heaters during steady state operation. The heaters normally operate at 2000 kW to make up for plant heat losses and pressure decay due to the minimum continuous spray operation. Since the pressurizer tank walls were modeled as perfectly insulated heat structures, and the spray valves were completely isolated during the steady state initialization phase, this 2000 kW heater source was subtracted from the total possible proportional heater source of 4000 kW.

2.2.4 Pressurizer Level Control System

The purpose of the pressurizer level control system (PLCS) is to maintain the desired amount of liquid inventory in the primary coolant system. The amount of water inventory in the primary coolant system may be inferred from the liquid level in the pressurizer, which varies as a function of the primary system average coolant temperature.

The pressurizer setpoint level is specified as a function of the primary system average coolant temperature. The setpoint level is

subtracted from the actual level determined from a set of differential pressure taps located in the pressurizer. The pressurizer level error signal is used as the input signal in a P-I controller. The output of the P-I controller specifies the amount of change in the charging pump speed to effect the desired change in the primary system coolant inventory.

The level error signal is also used to actuate the back-up heaters when the pressurizer level error exceeds the setpoint level by 5%. Pressurizer heater demand is blocked when the pressurizer level becomes less than the low-level limit of 14%.

The PLCS is modeled to include the reactor coolant pump seal injection contribution in addition to the charging flow demanded by the compensated pressurizer level error signal. All the pump seal injection flow is added to only one loop, but is quantitatively correct.

2.2.5 Additional Control Systems

Included in the control system package are miscellaneous controllers and trips that are modeled to represent various system functions that cannot be classified in any of the aforementioned systems. These controllers perform functions such as 1) feedwater recirculation to the condenser during periods of low feedwater demand, 2) low pressure feedwater heater bypass due to low main feedwater pump suction pressure, 3) specification of turbine impulse stage pressure as a function of steam flow rate and turbine governor valve area, and 4) control of the auxiliary feedwater systems.

2.3 Steady State Conditions

Three steady state initialization calculations were performed with the RELAP5 H. B. Robinson model. The calculations were performed with the core power at 2300 MW, 2200 MW, and 8.29 MW (hot standby). Each of the subsequent transient calculations used either the 2300 MW power steady state or the hot standby steady state. The 2200 MW power steady state was

used for a plant trip transient performed for model check out purposes. The following subsections present the steady state conditions for each of the three power levels.

2.3.1 2300 MW Steady State

The initial conditions for the 2300 MW steady state were representative of H. B. Robinson operating conditions at the proposed 100% rated core power. Table 2-1 compares initial values of the selected parameters from the RELAP5 model with desired initial conditions which were obtained from a revised precautions, limitations and setpoints document and other documents describing the initial conditions for the proposed 2300 MW power for H. B. Robinson. The RELAP5 initial conditions were obtained from a steady-state run that used control systems to represent the behavior of the primary pressure control and loop flow, the chemical and volume control system, the secondary liquid level, and main feedwater and steam control valves. The table shows that the actual initial conditions were generally in excellent agreement with the desired initial conditions.

2.3.2 2200 MW Steady State

The initial conditions for the 2200 MW steady state were representative of H. B. Robinson operating conditions at the time of the plant trip transient. Table 2-2 compares initial values of selected parameters from the RELAP5 model with desired initial conditions which were obtained from start-up data and other documents describing the operating conditions of the H. B. Robinson Plant at 2200 MW core power. The RELAP5 initial conditions were obtained from a steady state run that used control systems to represent the behavior of the primary pressure control and loop flow, the chemical and volume control system. RELAP5 secondary initial conditions were obtained from the use of control systems that represented manual control of the feedwater bypass valve to maintain level in the generators and action of the steam dump valves in plant trip control mode. The table shows that the actual initial conditions were generally in excellent agreement with the desired initial conditions.

TABLE 2-1. 2300 MW INITIAL CONDITIONS

Parameter	RELAP5	Desired
Core power, MW	2300	2300
Pressurizer pressure, MPa (psia)	15.5 (2250)	15.5 (2250)
Hot leg temperature, K (°F)	591.4 (604.8)	591.4 (604.5)
Cold leg temperature, K (°F)	558.9 (546.3)	558.9 (546.3)
Pressurizer level, %	54.5	53.3
Reactor coolant flow, Kg/s (lbm/s)	12726 (28055.5)	12726 (28056)
Reactor coolant pump speed, RPM	1247.1	1190
Net makeup flow, gpm	0.001	0
Steam pressure, MPa (psia)	5.5 (804)	5.7 (828)
Steam generator level, %	53.7	52
Steam flow (each), Kg/s (lbm/s)	425 (937)	424.2 (935.2)
Steam generator mass (each), Kg (lbm)	44253 (97560)	42302 (93260)
Condenser temperature, K (°F)	312 (102)	312 (102)
Feedwater temperature, K (°F)	500.4 (441)	500.6 (441.5)
Heater drain flow, Kg/s (lbm/s)	335.3 (783.2)	--[a]
Feedwater recirculation, gpm	0.0	--

a. No data available.

TABLE 2-2. 2200 MW INITIAL CONDITIONS

Parameter	RELAP5	Desired
Core power, MW	2192	2192
Pressurizer pressure, MPa (psia)	15.5 (2250)	15.62 (2265)
Hot leg temperature, K (°F)	585.6 (594.4)	583.2 (590)
Cold leg temperature, K (°F)	555.9 (541.0)	552.6 (535.0)
Pressurizer level, %	43	40
Reactor coolant flow, Kg/s (lbm/s)	13275.3 (29267)	12458.3 (27466)
Reactor coolant pump speed, RPM	1244	1190
Net makeup flow, gpm	34.8	--[a]
Steam pressure, MPa (psia)	5.16 (748)	5.20 (754.7)
Steam generator level, %	~52	~52
Steam flow (each), Kg/s (lbm/s)	401.7 (885.7)	426.3 (939.8)
Steam generator mass (each), Kg (lbm)	43650 (96232)	42302 (93260)
Condenser temperature, K (°F)	312 (102)	312 (102)
Feedwater temperature, K (°F)	498 (437)	498 (437)
Heater drain flow, Kg/s (lbm/s)	353 (783)	--
Feedwater recirculation, gpm	0.0	--

a. No data available.

2.3.3 Hot Standby Steady State

The initial conditions for the hot standby steady state were representative of H. B. Robinson operating conditions at hot standby. Table 2-3 compares initial values of selected parameters from the RELAP5 model with desired initial conditions obtained from documents describing hot standby conditions for the H. B. Robinson plant. The RELAP5 initial conditions were obtained from a steady state run that used control systems to represent the behavior of the primary pressure control and loop flow, and the chemical and volume control system. RELAP5 secondary initial conditions were obtained from the use of control systems that represented manual control of the feedwater bypass valve to maintain level in the generators and action of the steam dump valves in steam pressure control mode. The table shows that the actual initial conditions were generally in excellent agreement with the desired initial conditions.

2.4 Documentation Control of Codes and Models

The computer code used to perform the calculations presented in this report was an updated version of RELAP5/MOD1.6 cycle 16. A compiled version of this code and the updates which modified cycle 16 are stored at INEL under configuration control number FO1419.

Input decks used to perform the steady-state and transient calculations are stored at INEL under configuration control number FO1418. Table 2-4 shows the order in which the input decks have been assembled on the configuration control tape. The H. B. Robinson plant transient calculation was initiated from the 800 s point of the 2200 MW steady state calculation. Calculations of Scenarios 4, 5, 6, 7, 10, and 11 were initiated from the 800 s point of the 2300 MW steady state calculation. Calculations of Scenarios 1, 2, 3, 8, and 9 were initiated from the 600 s point of the hot standby steady state calculation.

TABLE 2-3. HOT STANDBY INITIAL CONDITIONS

Parameter	RELAP5	Desired
Core power, MW	8.29	8.29
Pressurizer pressure, MPa (psia)	15.5 (2250)	15.5 (2250)
Hot leg temperature, K (°F)	560.3 (548.9)	559 (547)
Cold leg temperature, K (°F)	560.04 (548.4)	559 (547)
Pressurizer level, %	23.6	24.4
Reactor coolant flow, Kg/s (lbm/s)	12629 (27841.9)	12626.8 (27837)
Reactor coolant pump speed, RPM	1226	1190
Net makeup flow, gpm	0	0
Steam pressure, MPa (psia)	7.03 (1020)	7.03 (1020)
Steam generator level, %	38.4	39
Steam flow (each), Kg/s (lbm/s)	2.27 (5.0)	--[a]
Steam generator mass (each), Kg (lbm)	57788 (127400)	54432-61689 (120000-136000)
Condenser temperature, K (°F)	299.8 (80)	--
Feedwater temperature, K (°F)	299.8 (80)	--
Heater drain flow, Kg/s (lbm/s)	0.0	--
Feedwater recirculation, gpm	1500	--

a. No data available.

TABLE 2-4. CONFIGURATION CONTROL OF INPUT DECKS

Purpose	Number of Decks on This File	File Number on Configuration Control Tape
2200 MW full power steady state	6	1
2300 MW full power steady state	1	2
Hot standby steady state	1	3
HBR plant trip	1	4
Scenario 1	2	5
Scenario 2	4	6
Scenario 3	4	7
Scenario 4	6	8
Scenario 5	3	9
Scenario 6	5	10
Scenario 7	2	11
Scenario 8	1	12
Scenario 9	5	13
Scenario 10	5	14
Scenario 11	8	15

3. SIMULATION OF HBR PLANT TRIP FROM 2200 MW

The results of the plant trip calculation are presented in this section. This calculation was performed to assess the ability of the model to simulate the responses of the corresponding plant thermal-hydraulic and control systems to a trip from the full power state. Although the plant trip simulation did not exercise the thermal-hydraulic models as fully as did the PTS sequences, the control system models were exercised fully.

A description of the plant trip test that was simulated by this calculation is presented in Section 3.1. The results of the calculation are compared to the plant data in Section 3.2. Conclusions regarding the performance of the control system models is discussed in Section 3.3.

3.1. Description of Plant Trip Test

A description of the plant trip calculation is presented in this section. Information concerning the plant trip test sequence of events was obtained from the H. B. Robinson plant startup data. Additional details may be obtained from Section 43 of the Plant Startup Test Report (WCAP-7844).

The plant trip test was initiated from the 2200 MW full power steady state. 2300 MW is the proposed 100% power level that will be used after the plant is upgraded with new steam generators, however 2200 MW was the power level at which the plant was operating at the time of the test. Approximately one hour of plant data was reported in the startup test report. The first 900 s of this data was considered the most significant since this was the period when the various control systems were required to operate in a transient recovery mode.

The plant trip test was performed to demonstrate the ability of the plant control systems to bring the plant to equilibrium no-load conditions following a plant trip from full power.

The test was initiated by tripping the turbine. All control systems operated as designed, with the partial exception of the main feedwater control valves, which failed to immediately close when the turbine was tripped. The main feedwater system was isolated 50 s after the start of the test.

3.2 Comparison of Results

The results of the plant trip calculation are presented in this section. Similarities and discrepancies between the calculated results and the measured plant data are addressed for each of the major plant control systems described in Section 2.2.

In comparing measured plant with code-calculated data, the reader should be aware that the former is generally not in a form that allows for easy comparison. Data was taken from strip charts that covered a 2-hour period during the test. As such, the width of the lines representing the measured data were approximately 60 s. Therefore the occurrences of events in time were subject to some interpretation.

3.2.1 Steam Dump Control System Response

The functioning of the SDCS may be inferred from the response of the primary system auctioneered high average temperature, T-ave. The calculated and measured responses of this parameter are shown in Figure 3-1. The difference in steady state initial temperatures is only 2.5 K (4.5°F) which is insignificant due to the nature of the temperature response during the test.

The response of the calculated T-ave is in close agreement with the measured T-ave through the initial period of temperature decrease following the plant trip. The rate of increase of the calculated temperature was somewhat faster than the measured increase. This discrepancy in primary system heatup rates is due to the difference in the total feedwater flow rates.

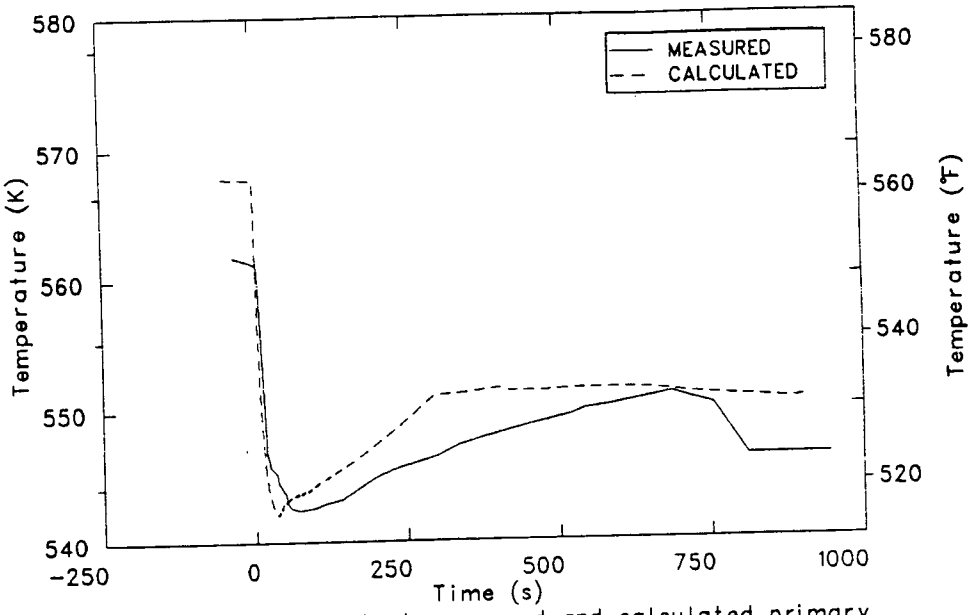

Figure 3-1. Plant trip test measured and calculated primary system highest average temperature responses.

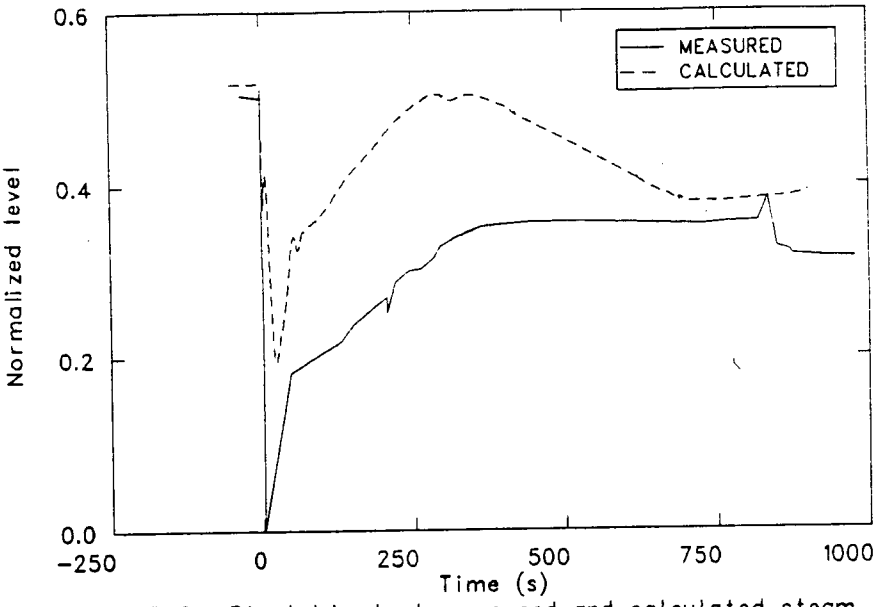

Figure 3-2. Plant trip test measured and calculated steam generator level responses.

Steam generator levels are compared in Figure 3-2. The measured steam generator levels decreased to 0% at the start of the test, while the calculated levels decreased to 20%. Consequently, steam-driven auxiliary feedwater was initiated in the test but not in the calculation (a requirement for initializing steam-driven auxiliary feedwater is 2/3 steam generators with 15% NR level). The additional feedwater in the test resulted in higher primary to secondary heat transfer rates than those calculated. These higher rates resulted in the slower primary system temperature responses indicated by the data.

The discrepancy between the measured and calculated steam generator NR levels will be addressed in the discussion of the steam generator level control system (SGLCS).

It is important to note that while the differences in primary system temperature responses between measured data and calculated results appear to be significant, the maximum difference was only 2.6 K (4.7°F), which is probably within the plant's temperature measurement uncertainty. The general trend of the calculated response is the same as the measured response which indicates that the SDCS model adequately simulated the response of the actual system.

3.2.2 Steam Generator Level Control System Response

The functioning of the SGLCS may be determined using the response of the steam generator narrow range (NR) levels, and the feedwater and steam flow rates. The three steam generator calculated responses were essentially identical; therefore, the discussion of SGLCS response will be centered on the responses of Steam Generator B (SGB). The measured and calculated SGB NR level responses are shown in Figure 3-2. The trends were qualitatively the same with two important exceptions.

The first discrepancy between the calculated and measured level responses was in the size of the downward spike at the start of the test. The measured data indicated that the NR level temporarily decreased to 0% before recovering; whereas, the calculated level only decreased to 20%.

This discrepancy is significant because the SG NR level determines the demand from the auxiliary feedwater systems (and the main feedwater as well). These differences appear to be associated with the uncertainty in behavior of the feedwater control valve. Sensitivity calculations indicate that modulation of the valves will reproduce the response seen in the plant data.

The second discrepancy was in the response of the level taps after the feedwater to the steam generators had been terminated in the calculation, which happened when the NR level reached 39%. The measured data indicated that once the level reached 39% no further increase in level occurred; whereas, the calculated level continued to increase for an additional 200 s.

A complete explanation for these two discrepancies has not been determined. Important factors are uncertainties in the plant data relative to the modulation of the main feedwater and steam dump valves. The effect of modeling the separators and dryers at a single elevation (see Section 2.1.2) was found to be only a minor perturbation in indicated level due to flow effects at the upper reference pressure tap. The continued increase in calculated level following termination of AFW was found to be caused by a redistribution of liquid from the boiler region to the downcomer. Further investigations are being conducted to understand these discrepancies.

The steam generator total feedwater flow rate response is shown in Figure 3-3. The main feedwater control valves were reported to have not closed during the first 50 s of the test due to a delay in the feedwater controller response. No other information was available regarding the actual response; therefore, the modeled valve areas were held constant for the first 50 s. After the first 50 s the calculated and measured feedwater flow rate responses were approximately the same, except for the period from 140 s to 660 s. During this period the modeled auxiliary feedwater system ceased flow due to the calculated recovery of steam generator level (the model regulated steam generator levels between 39% and 41%). Feedwater flow was resumed at 660 s when the NR level decreased below 39%. The

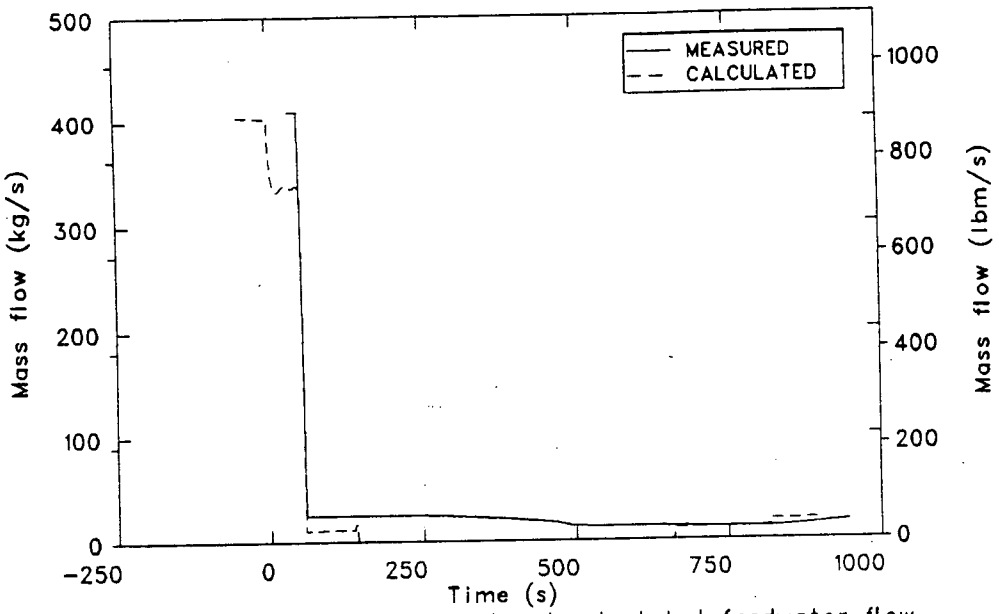

Figure 3-3. Plant trip measured and calculated feedwater flow rate responses.

measured feedwater flow rate did not decrease to zero because some feedwater was required to maintain SG level at the setpoint. This feedwater demand was required due to continuous steam flow out of the SG during this period.

The measured and calculated steam flow rate responses are shown in Figure 3-4. The calculated steam flow rate was less than the measured flow rate throughout the calculation. The higher measured flow rate was due to steam-driven auxiliary feedwater operating in the test but not in the calculation. The extra feedwater caused higher primary to secondary heat transfer, which in turn resulted in greater steam generation.

Overall, the largest discrepancy in SGLCS response was in the calculation of the NR levels. This discrepancy can be important when the steam-driven auxiliary feedwater system is required in addition to the motor-driven system due to low SG NR level. With the exception of the auxiliary feedwater discrepancy, the calculated feedwater and steam flow rate responses are in reasonable agreement with the measured plant data. Since these three parameters (NR level, feedwater and steam mass flow rates) are the input signals for the SGLCS it is concluded that the SGLCS is adequately modeled with the exception of the minor discrepancies in upper reference tap transient response characteristics. The reference tap problem is only important in those situations similar to the plant trip test. In situations where the NR level decreases below 15% for a prolonged period of time the modeled level tap response behaves in the desired manner; hence, there are few cases where the modeled SGLCS would not respond like the actual system. This response was evaluated for each of the 11 PTS calculations presented in this report and, in the few instances where a significant effect was noticed, discussed in the appropriate analysis section.

3.2.3 Pressurizer Pressure Control System Response

The PPCS measured and calculated responses may be inferred from the information presented in Figure 3-5, which illustrates the calculated and measured pressurizer pressure responses.

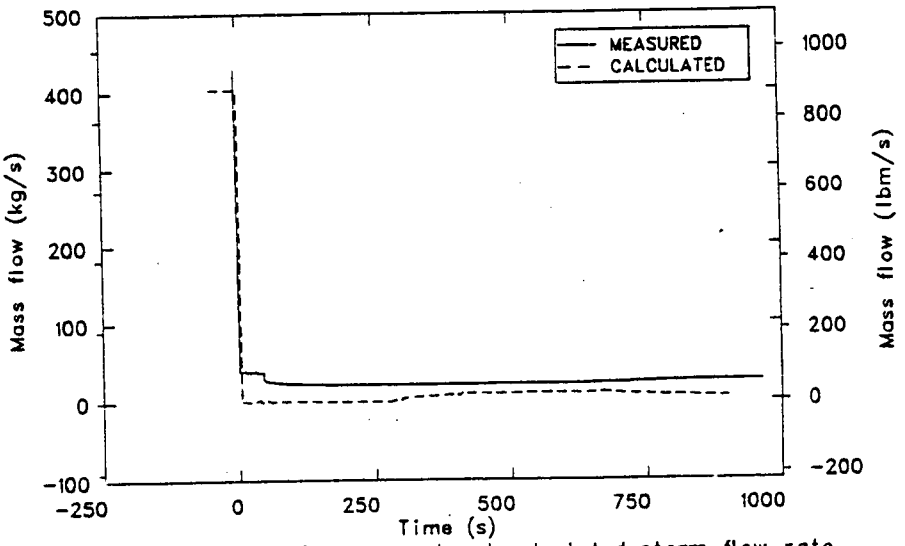

Figure 3-4. Plant trip measured and calculated steam flow rate responses.

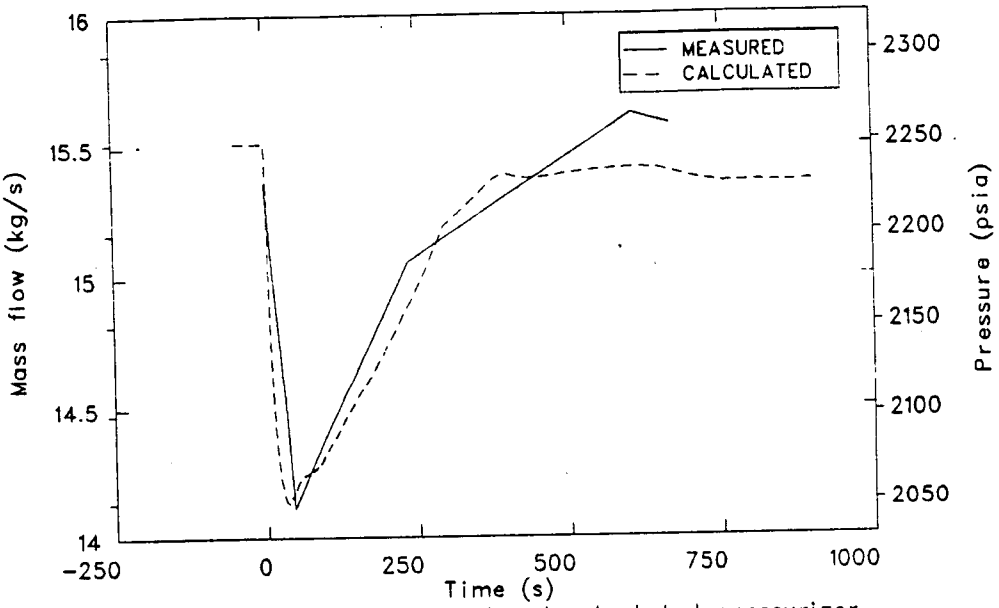

Figure 3-5. Plant trip measured and calculated pressurizer pressure responses.

The agreement between the measured and calculated data is very good through the first 400 s. The measured data indicate the pressure increased to approximately 15.65 MPa (2270 psia), whereas the calculated pressure did not increase beyond 15.41 MPa (2235 psia). This discrepancy was due to unresolved anomalies in the actual plant response (the setpoint pressure was 15.51 MPa, 2250 psia) and the apparent inability of the model to maintain the setpoint pressure at the lower pressurizer setpoint level.

Overall, the PPCS model performed adequately relative to the actual plant system.

3.2.4 Pressurizer Level Control System Response

The measured and calculated responses of the PLCS are inferred from the pressurizer level responses shown in Figure 3-6. The measured pressurizer setpoint level is also included to provide a characterization of the desired response.

The measured and calculated level responses were nearly identical with the exception of the minimum level achieved at approximately 100 s. This discrepancy was due to a lag element included in the level tap model to simulate instrument response time. The overall response of the calculated data indicates that the PPCS is adequately modeled.

3.3 Conclusions

A comparison of the calculated and measured data indicated generally good agreement, thus providing a limited, but useful, qualification of the plant model beyond the detailed quality assurance measures described in Section 2.

The modeled control systems appear to be sufficiently capable of simulating the plant control system responses that were expected to occur in the various PTS transients. The modeled thermal-hydraulic systems adequately simulated the plant trip test however the PTS transient responses were generally of larger magnitude than the plant trip test.

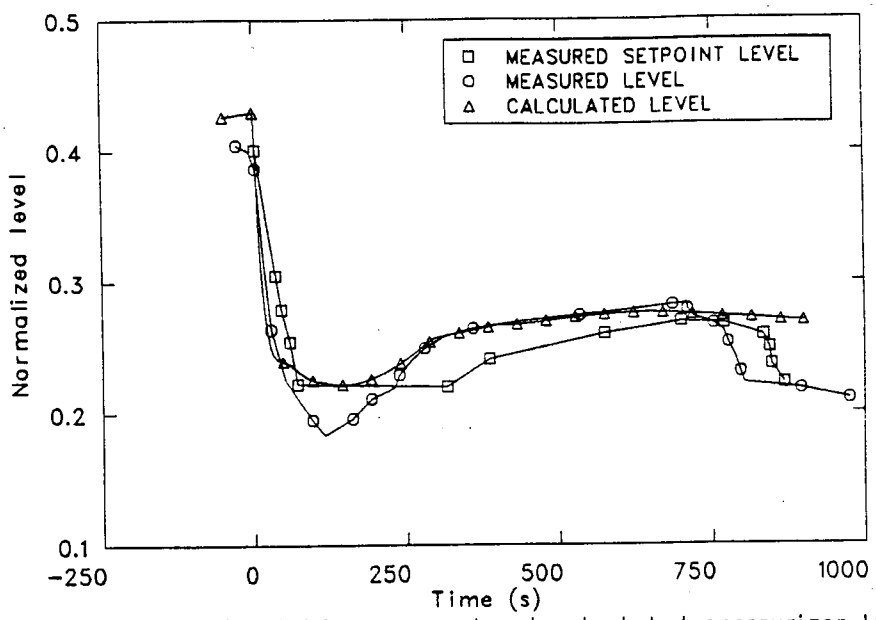

Figure 3–6. Plant trip measured and calculated pressurizer level responses.

Additional analysis is being performed relative to the SG NR level responses during periods of rapidly changing secondary system conditions. However, most of the PTS transients resulted in permanent changes of steam generator secondary conditions, which were adequately represented by the existing level tap model.

4. SCENARIO 1, 1.0 ft^2 STEAM LINE BREAK AT HOT STANDBY

The following section details the analysis of Scenario 1, a 0.093 m^2 (1.0 ft^2) break in Steam Line A, downstream of the flow restrictor and upstream of the main steam isolation valve (MSIV). The subsections contain a description of the scenario in Section 4.1, model changes effected to perform the calculation in Section 4.2, analysis of the results in Section 4.3, extrapolation of the key PTS parameters, and the conclusions drawn in Section 4.4.

Scenarios investigated in this report generally include conservative assumptions concerning equipment failures, operator actions, or combinations of these. Conclusions relative to pressurized thermal shock severity are not to be drawn directly from the results presented in this report (see Section 15).

4.1 Scenario Description

The description of Scenario 1, as provided by Oak Ridge National Laboratory, is shown in Table 4-1.

The transient was initiated by the occurrence of a 0.093 m^2 (1.0 ft^2) break in Steam Line A. All automatic plant functions were assumed to respond normally. Two operators actions were assumed as well. The first was to trip the reactor coolant pumps (RCPs) if the primary system pressure fell below 9.07 MPa (1315 psia), provided a SIAS signal had been generated. The second operator action was to stop auxiliary feedwater flow to the affected steam generator (ASG) 600 s after the transient initiation.

4.2 Model Changes

The basic RELAP5 model used to perform Scenario 1 is described in Section 2.

TABLE 4-1. SCENARIO DESCRIPTION NO. 1

Plant Initial State - Just prior to transient initiator

General Description: Hot 0% Power, 0% Power after 100 hrs of shutdown
System Status
Turbine: Not latched, TSVs closed
Secondary PORV: Automatic control
Steam Dump Valves: Automatic control
Charging System: Automatic control
Pressurizer: Automatic control
Engineering Safety Features: Automatic control
Power Operated Relief Valves (PORVs): Automatic control
Reactor Control: Manual
Main Feedwater: In bypass mode, manual control to provide 39% level in S/G's; 1 condensate pump, 1 MFWP operating.
Aux Feedwater: Automatic control
Main Steam Isolation Valves (MSIVs): Open, Automatic control
Main Feedwater Isolation Valves (MFIVs): Closed, Automatic control

Transient Initiator - A 1.0-ft^2 hole appears in steam line A outside containment upstream of the MSIV and downstream of the flow restrictor

Equipment Failures which occur during the transient if the equipment is demanded.

None

Operator Reactions to Reported Information

1. If Safety Injection Actuation Signal (SIAS) is generated, the operator will trip the reactor coolant pumps when RCS pressure reaches 1300 psig.

2. Stop AFW flow to the unaffected S/G when liquid carryover is observed in the main steamline.

3. Stop AFW flow to the affected S/G at 10 min or when carryover occurs.

The break in Steam Line A was simulated by the insertion of a break flow path at the downstream end of component 550. After 600 s of the transient calculation, all components upstream of the steam generators, including auxiliary feedwater headers and valves, and the main feedwater train, were deleted. These deletions were performed after the simulated isolation of the auxiliary feedwater flow to the ASG to decrease the computer memory requirements for the problem and thereby decrease run time. Deletion of the feed train was justified by the fact that it was completely isolated from the steam generators after the SIAS was generated.

4.3 Results

The following section contains the results of the Scenario 1 calculation. The first subsection discusses the results of the calculation. The second subsection discusses the extrapolation to 7200 s of the key PTS parameters and the uncertainties involved in the calculation.

4.3.1 Calculation Results

The sequence of events that occurred during the Scenario 1 calculation is shown in Table 4-2. The transient was initiated by the insertion of a 0.093 m^2 (1.0 ft^2) break junction to atmosphere in Steam Line A (component 550). Approximately 100 ms after break initiation a SIAS signal was generated by a high ΔP between the system header and Steam Line A. The SIAS signal shut down the operating main feedwater pump and activated motor driven auxiliary feedwater (AFW). Turbine driven AFW initiation required two-out-of-three low steam generator level indications and thus was not initiated. High Pressure Injection (HPI) flow was initiated at 68.5 s when the primary system pressure dropped below the pump's shutoff head of 10.13 MPa (1470 psia). HPI flow continued until 1214 s when the primary pressure rose above the shutoff head. At 72.2 s, when the pressure dropped below 9.07 MPa (1315 psia), the RCPs were tripped. At 600 s auxiliary feedwater flow was terminated as prescribed in the scenario description. By 1026 s heat transfer to the ASG had degraded to the point where core decay power exceeded the ASG's heat removal capability and the

TABLE 4-2. SCENARIO 1 SEQUENCE OF EVENTS

Time (s)	Event
0	Steam line ruptures
0.1	High steam line A ΔP SIAS signal Main feedwater pump tripped off Motor auxiliary feedwater tripped on
20.3	Pressurizer low level alarm
43	Pressurizer indicated empty
68.5	High pressure injection (HPI) initiated
72.2	Reactor coolant pumps tripped
400	Pressurizer level indication returned
600	Auxiliary feedwater tripped off
908	Pressurizer indicated full
1026	Downcomer temperature started to increase
1200	Pressurizer went water solid
1214	HPI shut off
1467	Power operated relief valves began cycling
1800	Transient terminated

primary coolant temperatures started to increase. At 1467 s, primary pressure had increased to the power operated relief valve (PORV) setpoint and the valve began cycling.

Figure 4-1 presents the primary and secondary pressure responses to the transient. Pressure in the ASG decreased continuously reaching near atmospheric conditions (0.14 MPa, 20 psia) by 900 s. Both unaffected steam generators (USGs) experienced a slight decrease in pressure early in the transient when the primary cooldown caused them to become primary system heat sources. Once the RCPs were tripped, the USGs were effectively isolated due to primary loop stagnation and their pressures stabilized.

In the primary system, the pressure decreased as the break induced heat transfer to the ASG peaked. As the ASG emptied and the tubes became surrounded by high quality fluid, heat transfer to the ASG degraded and, with the RCPs tripped, primary pressure stabilized around 6.55 MPa (950 psia). At 400 s the pressurizer began refilling, as shown in Figure 4-2, and experienced an extreme condensation spike that appeared to nearly fill the pressurizer. This condensation spike pulled the liquid out of the upper head toward the pressurizer in a manometer effect. It also caused a decrease in primary system pressure, between 410 s and 670 s (Figure 4-1). The magnitudes of the pressurizer insurge, and resultant depressurization, are unrealistic.

This pressurizer condensation phenomena was observed in several of the scenarios presented in this report, although it manifested itself most severely in Scenario 1. During pressurizer refill, as each pressurizer cell started to fill, there was an increase in the condensation rate in that cell. This increase caused primary system pressure to decrease, and the magnitude of the decrease was dependent upon the magnitude of the condensation. It is believed the the observed decreases in pressure were overstated by the condensation effect.

Actual condensation occurs at the interface between steam and liquid. When the subcooled primary coolant first enters the superheated steam environment of an empty pressurizer, high condensation rates can be

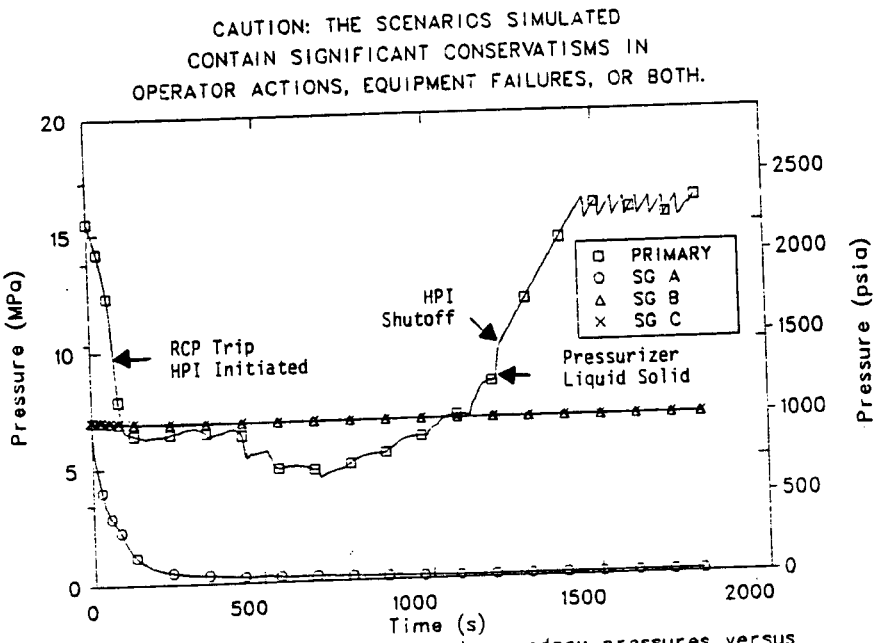

Figure 4–1. Scenario 1 primary and secondary pressures versus time.

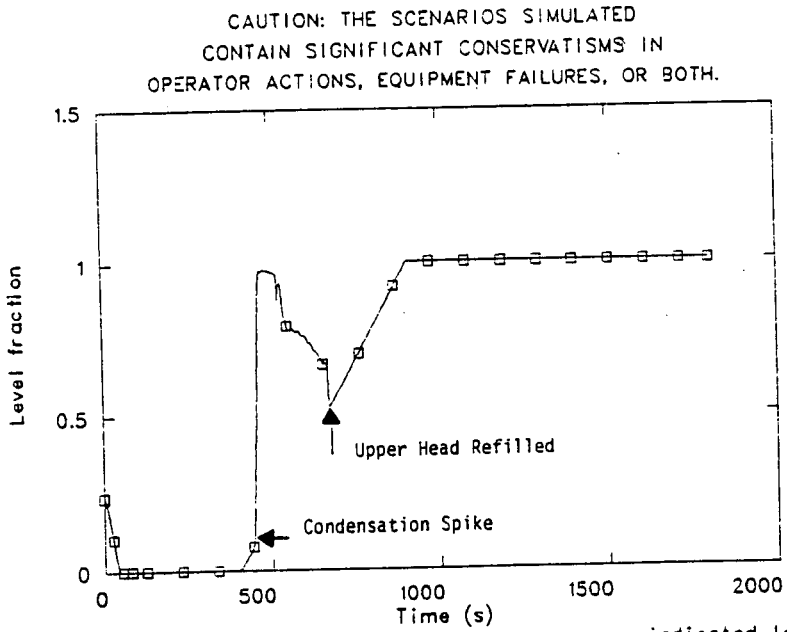

Figure 4–2. Scenario 1 pressurizer narrow range indicated level versus time.

expected, so the initial dips in pressure seen in Figure 4-1 are probably realistic. However, once a level has been established within the pressurizer, a layer of saturated liquid is believed to form at the liquid-steam interface decreasing the condensation rate significantly. This condensation would not be sufficient to dominate the pressure response of the pressurizer during refill. In RELAP5, however, it is the volume averaged subcooled liquid, not the saturated liquid boundary, that is used to calculate a condensation rate in each cell as it starts to fill. Thus, for each cell, after the lower pressurizer region is filled, the calculated condensation rate is likely too high, causing an unrealistic decline in pressure.

At 670 s, the reactor vessel upper head refilled due to continued HPI and charging flow. Once the upper head was filled, the pressurizer began to fill again and primary system pressure began to increase, accompanied, as mentioned, with periodic decrease as each successive pressurizer cell filled. At 1200 s, the pressurizer went liquid solid, increasing the repressurization rate. HPI shutdown lowered this rate slightly at 1214 s, but the nominal charging flow of 0.95 l/s (15 gpm) and the primary swell due to the energy imbalance between decay power and heat removal, continued the repressurization until, at 1467 s, the power operated relief valve (PORV) setpoint of 16.2 MPa (2350 psia) was reached. Primary system pressure continued to oscillate around the setpoint for the remainder of the transient calculation.

Figure 4-3a shows break flow over the first 60 s of the transient. Break flow, choked at the break junction, initially spiked, then fell as the ASG depressurized. At 1.5 s, the ASG's separators had filled due to the upsurge of moisture caused by the break. With the separator liquid full, moisture was passed through to the break junction, which caused lower quality fluid to be released and, thus, the mass flow rate to increase. This increase continued until the separators mixture level fell enough to allow the component to function and increase the break junction quality. From that point (6 s) break flow fell with ASG pressure. Figure 4-3b compares break flow with auxiliary feedwater flow. Motor driven auxiliary feedwater (AFW) flow was initiated with the SIAS signal at 0.15 s and

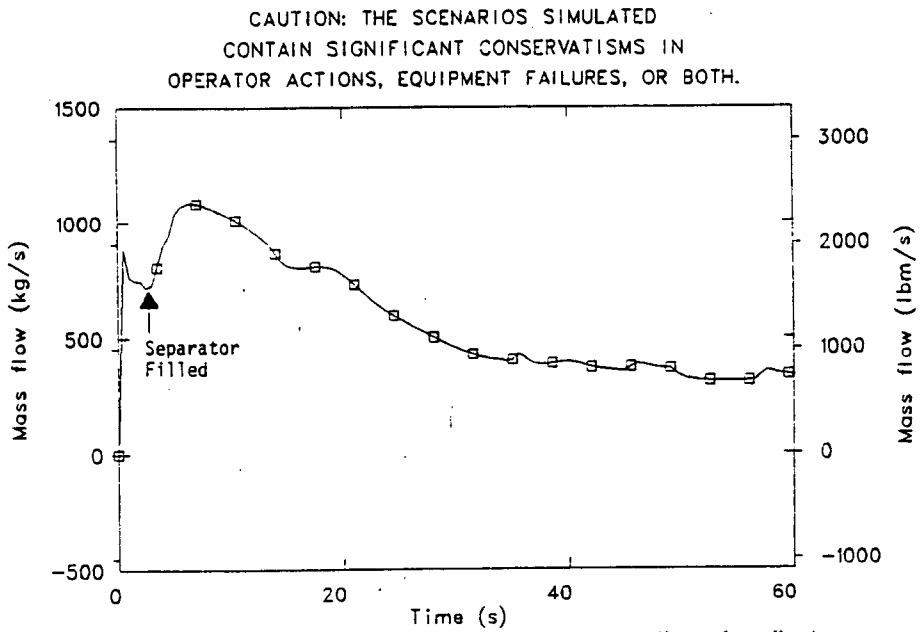

Figure 4-3a. Scenario 1 break mass flow versus time for first 60 s of transient.

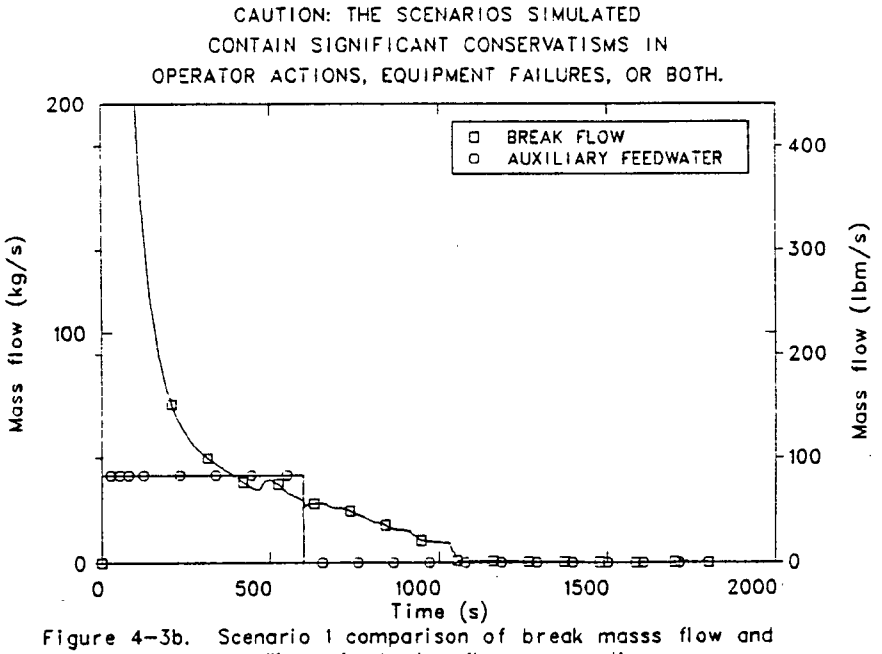

Figure 4-3b. Scenario 1 comparison of break masss flow and auxiliary feedwater flow versus time.

directed by the header to the ASG. Since the pressures of the ASG and AFW header were significantly lower than those of the USG, all AFW flow was delivered to the ASG. By 390 s auxiliary feedflow exceeded break flow and the ASG began to refill, as shown in Figure 4-4. This refill terminated at 600 s when auxiliary feedwater ceased as defined in the scenario description.

Figure 4-5a presents the mass flow rates in the cold legs of all three primary loops. Prior to the RCP trip, the mass flow in all loops increased due to the increased coolant density as the fluid cooled. Flow in Loop A was higher than in the two USG loops because the heat transfer into the ASG caused the Loop A fluid to be cooler and, thus, more dense. At 72.2 s the primary system pressure dropped to 9.07 MPa (1315 psia) and the RCPs were tripped. Flow in all three loops coasted down and established an asymmetric natural circulation condition. Figure 4-5b shows this flow condition in more detail. Loop A established a substantial flow, driven by the continued heat transfer to the ASG. This flow decreased as the heat transfer to the emptying ASG degraded. Loops B and C essentially stagnated, although both experienced flow reversals and perturbations during the pressurizer condensation spike and subsequent upper head void and fill process. The effective stagnation of the two USG loops allowed the ASG loop to dominate the thermal response of the transient.

Figures 4-6 and 4-7 show the temperature response in the hot leg, steam generator inlet, steam generator outlet, and cold leg in Loop B and Loop C, respectively. Both figures show similar responses. There is an initial decrease in all temperatures in response to the cooldown of Loop A. The steam generator outlet temperature became higher than the inlet temperature, signalling that the USGs were supplying heat to the primary. The stagnation in loop flow was reflected in the divergence between steam generator outlet and cold leg temperatures. The cold leg temperatures reflected the insurge of cold HPI fluid into the stagnant cold leg piping. Loop B cold leg temperatures, which reached a minimum value of 102.5°F, were colder than Loop C's cold leg temperatures primarily due to the absence of major flow perturbations caused by pressurizer behavior and because all makeup flow is injected into Loop B. Pressurizer behavior also

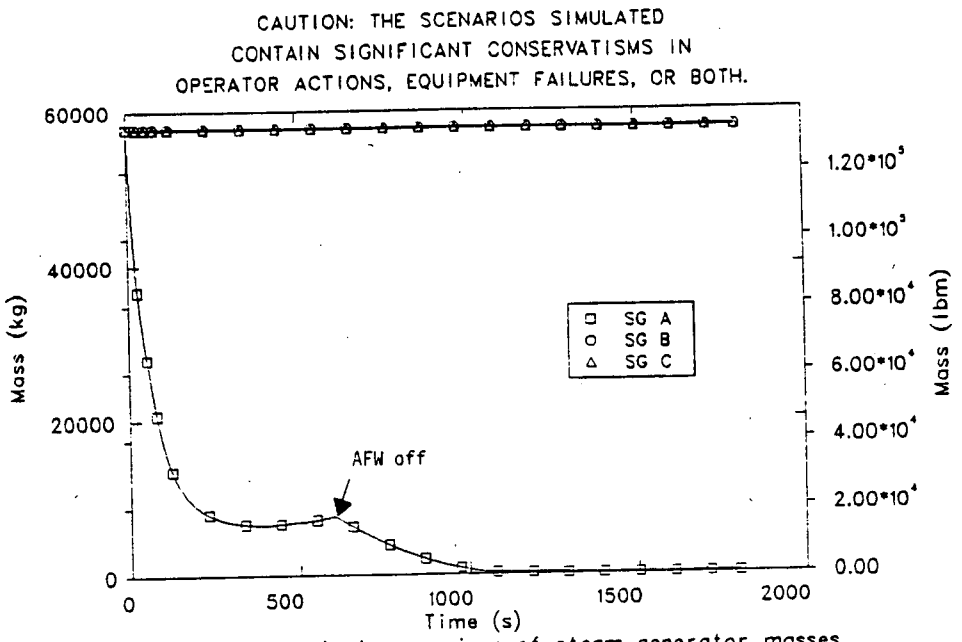

Figure 4-4. Sccenario 1 comparison of steam generator masses versus time.

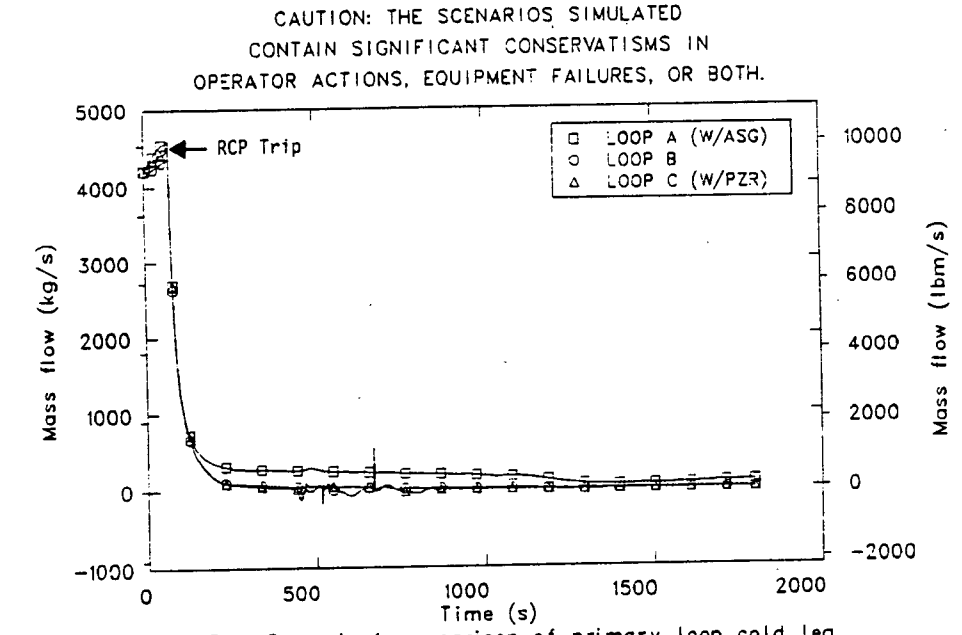

Figure 4-5a. Scenario 1 comparison of primary loop cold leg mass flows versus time.

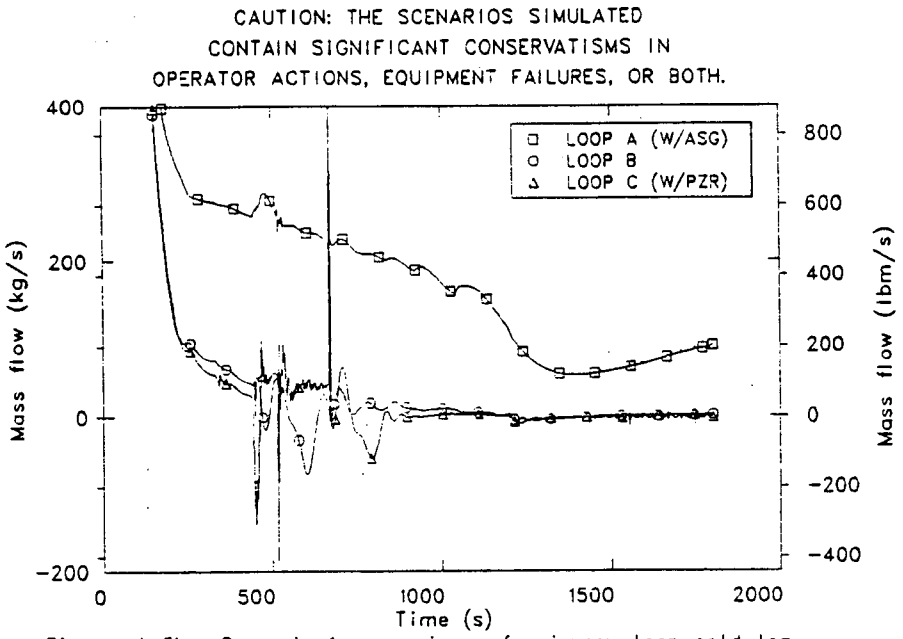

Figure 4-5b. Scenario 1 comparison of primary loop cold leg mass flows versus time (reduced scale).

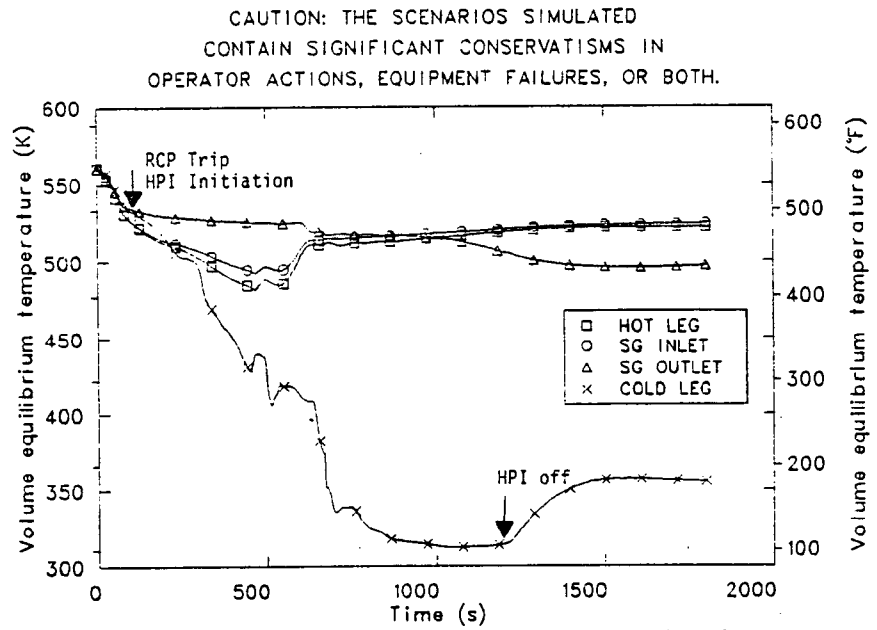

Figure 4-6. Scenario 1 fluid temperatures versus time in primary loop B.

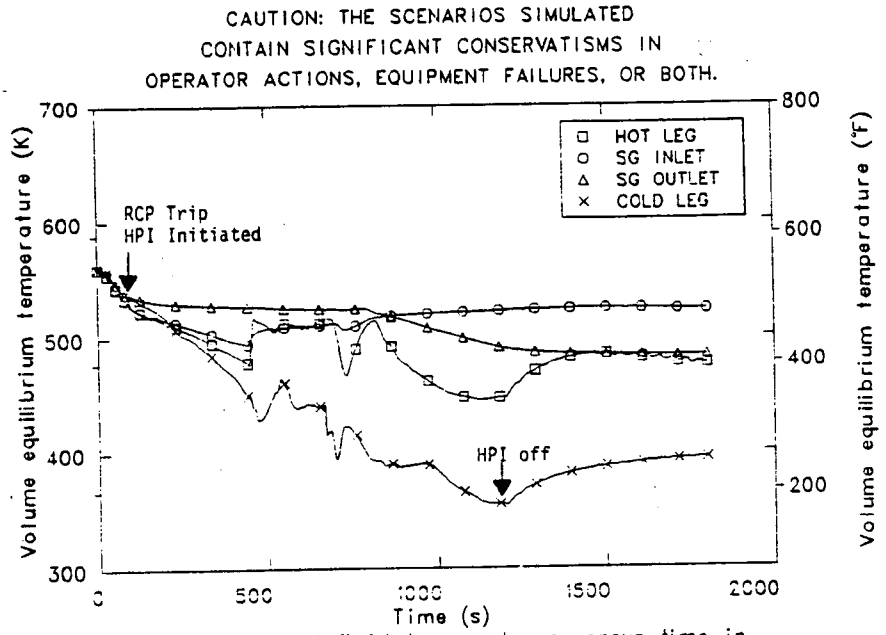

Figure 4-7. Scenario 1 fluid temperatures versus time in primary loop C (W/PZR).

accounted for the divergence between Loop C's hot leg temperature and its steam generator inlet temperature. The inlet was essentially stagnated and at thermal equilibrium with the steam generator, while the hot leg experienced flow out of the cooler reactor vessel.

Figure 4-8 shows the hot leg, steam generator inlet, steam generator outlet, and cold leg temperatures in Loop A. Both the cold leg and the steam generator outlet temperatures were always lower than the hot leg/steam generator inlet temperatures, reflecting the fact that the ASG acted as a heat sink throughout the transient. The close coupling of the temperature pairs was an indication of the natural circulation flow through the loop. After 1000 s, with the ASG empty, the effects of the heat transfer degradation caused hot and cold leg temperatures to converge. Termination of HPI flow caused the cold leg and steam generator outlet temperatures to converge after 1214 s.

Figure 4-9 presents a comparison between all three cold leg temperatures and the downcomer temperature. The downcomer temperature fell between the USG loop temperatures and the ASG loop temperature during the time the RCPs were operational and coasting down. Once the USG loops stagnated, the downcomer temperature converged on Loop A's cold leg temperature and they remained closely coupled throughout the transient.

The transient calculation was terminated at 1800 s. At this time, the ASG was completely empty, the primary system pressure was cycling around the PORV setpoint of 16.2 MPa (2350 psia) and the reactor vessel downcomer temperature was rising, having reached a minimum of 386.2 K (235.5°F) at 1026 s.

4.3.2 Extrapolations and Uncertainties

The following section presents and discusses the extrapolation of key PTS parameters out to 7200 s and the uncertainties involved with these parameters. The parameters discussed are downcomer pressure and fluid temperature, downcomer inner wall surface heat transfer coefficient, primary cold leg mass flows and fluid temperatures.

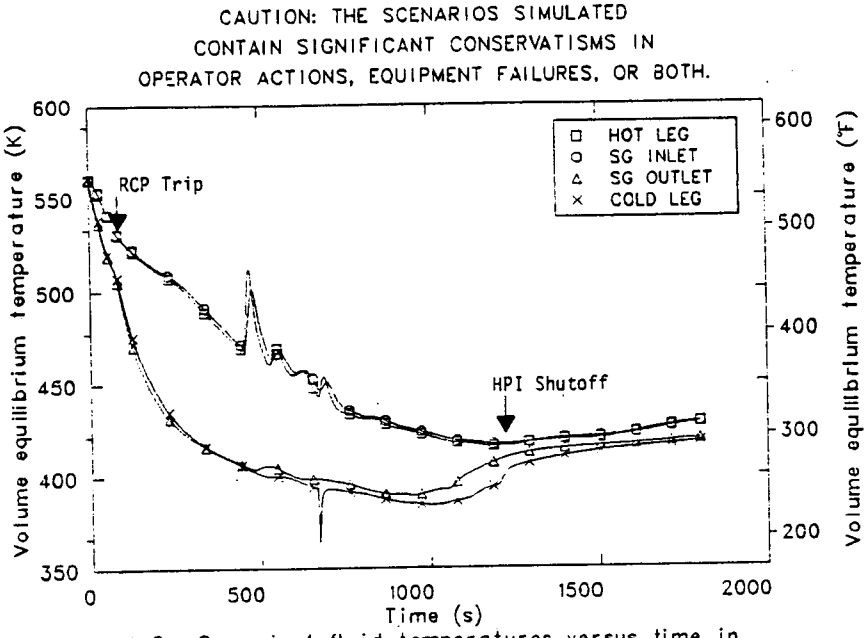

Figure 4-8. Scenario 1 fluid temperatures versus time in primary loop A (W/ASG).

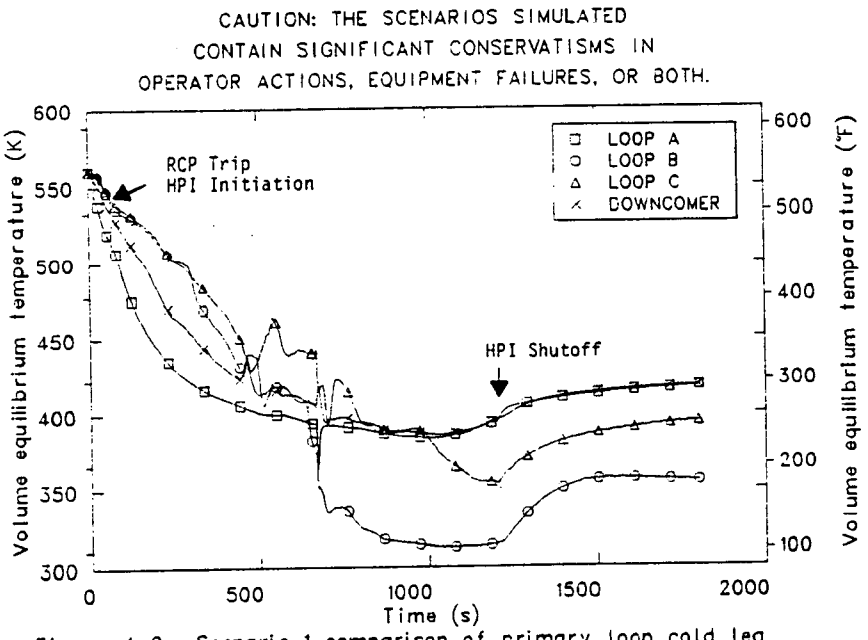

Figure 4-9. Scenario 1 comparison of primary loop cold leg temperatures and downcomer temperature versus time.

Figure 4-10 presents the extrapolation of reactor vessel downcomer pressure to 7200 s. At the time the transient was terminated, the heat removal from the primary was less than the heat supplied by the core's decay power. The primary system heatup will continue until the system reaches saturation. The pressure will remain at the PORV setpoint throughout the 2 hour period. The uncertainties in the pressure calculation involved the pressurizer condensation problem discussed in Section 4.3.1. If an adiabatic pressurization is assumed after the two lower volumes of the pressurizer filled, the pressure would rise to the PORV setpoint by 829 s, approximately 600 s earlier than calculated. This approximation is conservative. The actual PORV opening time is expected to fall between these two times.

Figure 4-11 shows the extrapolated downcomer temperature curve. The temperature was rising at a constant rate at the end of the calculation. Extrapolating the temperature rise using this rate resulted in an extrapolated downcomer temperature of 484.62 K (412°F). There was little uncertainty in this calculation. The downcomer temperature was a direct result of the affected loop flow and the heat removal (or lack of) to the ASG. An early HPI cutoff, due to the uncertainty in primary system pressure would not have significantly affected the downcomer temperature.

Figure 4-12 presents the extrapolated heat transfer coefficient for the inner wall surface of the reactor vessel downcomer. The correlation used for the subcooled single phase heat transfer occurring on the wall surface is the Dittus-Boelter correlation, which is dependent on flow and fluid conditions. In the Scenario 1 case flow is slightly decreasing during a fluid heat up. Ratioing key fluid parameters (Cp, μ, K, Pr, Re), an extrapolated heat transfer coefficient was calculated. There was more dependance on fluid properties than flow and the uncertainties were minimal in this extrapolation.

Figure 4-13 displays the extrapolated primary loop cold leg flows. The primary heat up establishes a very small positive flow (1 Kg/s, 2.2 lbm/s) in Loops B and C. Flow continued in Loop A. The rise observed at the end of the calculation was due to an increasing ΔT across the core and a further calculation was performed to determine if the flow

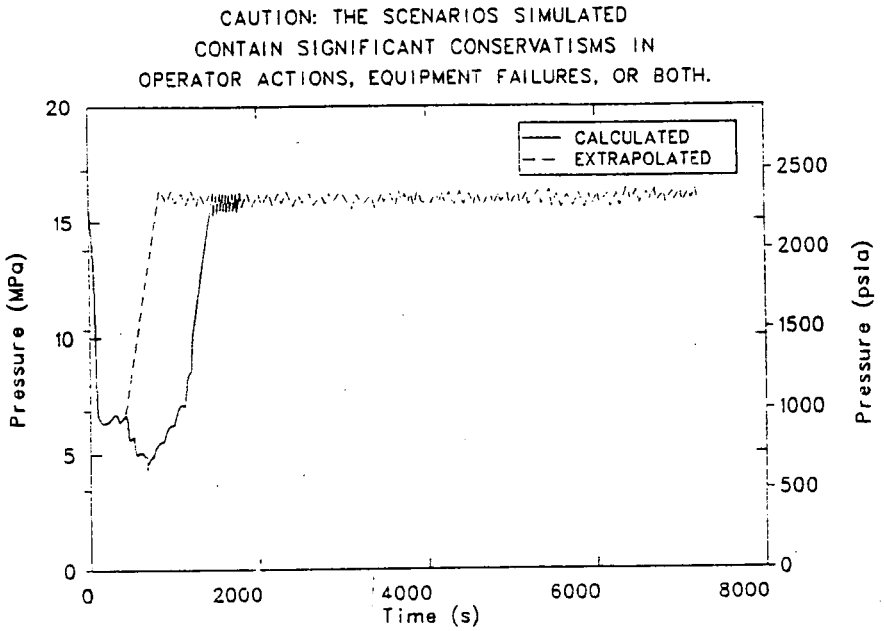

Figure 4-10. Scenario 1 extrapolated downcomer pressure versus time

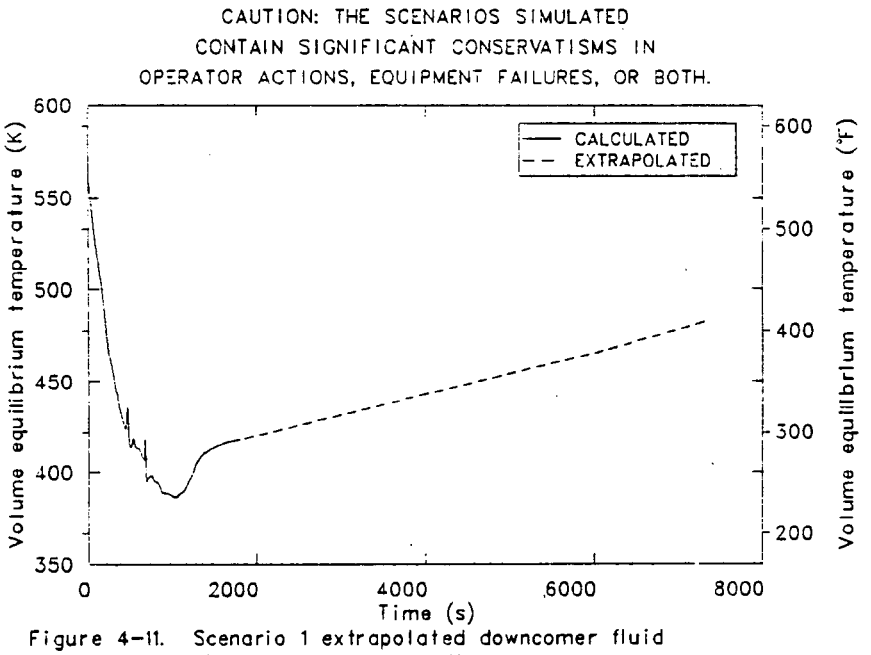

Figure 4-11. Scenario 1 extrapolated downcomer fluid temperature versus time.

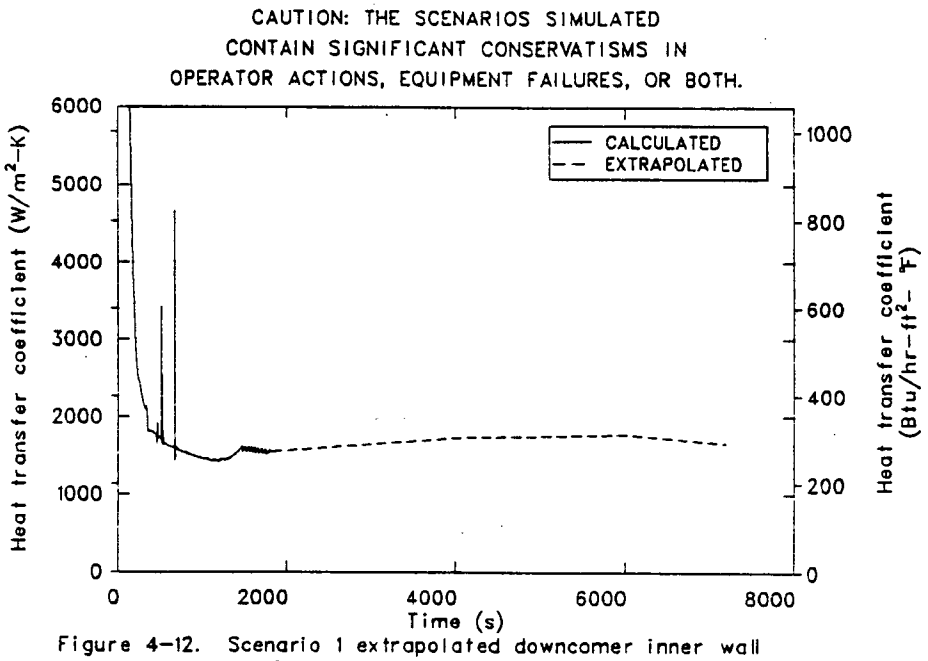

Figure 4-12. Scenario 1 extrapolated downcomer inner wall surface heat transfer coefficient versus time.

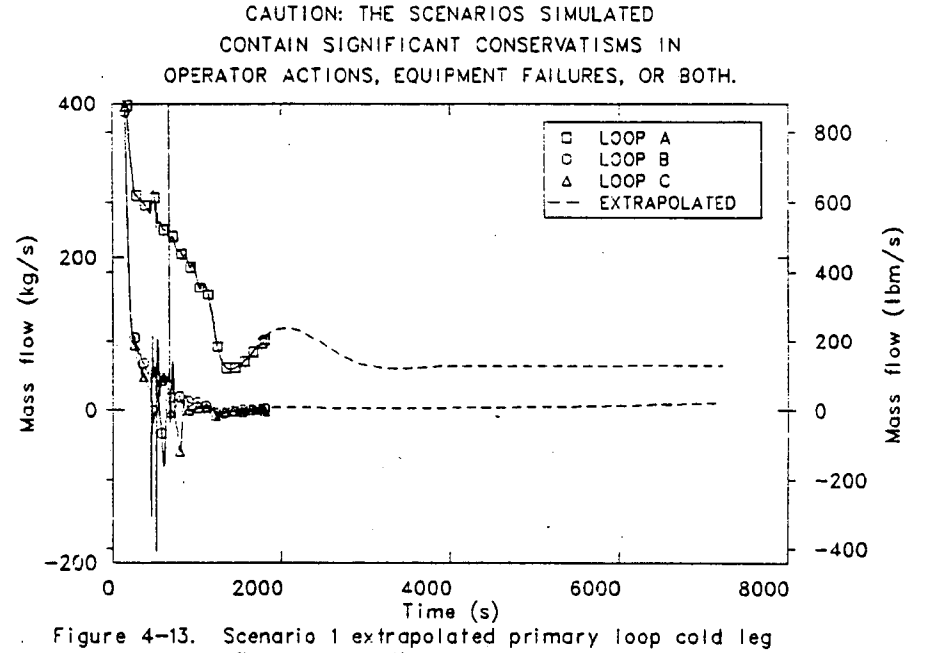

Figure 4-13. Scenario 1 extrapolated primary loop cold leg flows versus time.

again reversed and stabilized, which it did. Ratioing water properties in a single phase natural circulation correlation indicated that the flow would decrease slightly over the next 5400 s. Early in the transient both B and C loops experienced substantial oscillations in flow that were direct results of the pressurizer condensation problem, discussed in Section 4.3.1. The stagnant condition of these loops was very sensitive to flow changes in the loop. These flow spikes may or may not be real, however, the flow stabilized at the end of the transient and the effect of the uncertainties is minimal.

Figure 4-14 extrapolates the three primary loop cold leg temperatures to 7200 s. There is considerable divergence between the loops. Loop A had a relatively high flow and its temperature was extrapolated to rise the same amount as that of the downcomer temperature. Both Loop A's cold leg and the downcomer are tightly coupled by the flow. Loop C developed a very low positive flow and its temperature rise was expected to approach the Loop A cold leg temperature asymptotically. There is considerable uncertainty in this, however due to the temperature rise experienced during the period of pressurizer condensation between 400 and 700 s. If the condensation spike had not occurred, loop C's cold leg would have dropped to the same temperature Loop B did (312.3 K, 102.5°F). Loop B's cold leg temperature increased after HPI cutoff, then began to decrease due to continued stagnation and charging fluid injection. It's minimum temperature, however, occurred at 1050 s. The major uncertainty in the Loop B cold leg temperature was a function of the model used in the analysis. The model assumed that all pump seal injection makeup flow (0.32 l/s/pump, 5 gpm/pump) in the plant was injected into Loop B. This additional cold fluid depressed the temperature after the time of HPI cut off more than if the pump seal injection flow had been split among all three loops. If the flow had been split, the temperature profile in Loop B after HPI cut off would change but there would be no effect on the minimum temperature in the loop.

The pressurizer condensation problem would have some effect upon the temperature profiles just discussed. If the adiabatic compression calculation were correct HPI would have shut off at 568 s, causing both

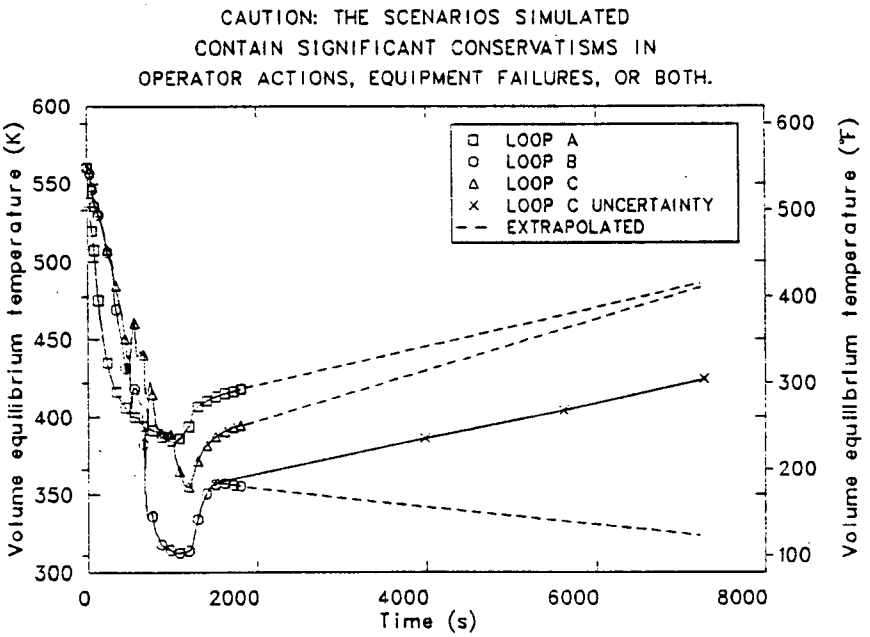

Figure 4-14. Scenario 1 extrapolated primary loop cold leg temperatures versus time.

C and B loop cold leg temperatures to turn around earlier than calculated. This early turnaround would have kept both B and C loop minimum temperature to near 400 K (260°F). Loop A's temperature would have been minimally impacted due to the flow that mixed the incoming HPI fluid with the fluid exiting the steam generator. And, as the downcomer temperature reflected close coupling with Loop A, this key PTS parameter would have been altered insignificantly

The next uncertainty is concerned with the representation of the reactor vessel with a one-dimensional computer model and the effect on hot leg fluid temperatures. The model by definition passes equal temperature fluids to the hot legs. This is a limitation where significant loop asymmetric behavior is to be expected and where sufficient fluid mixing does not occur within the reactor vessel. For the sequence being investigated here there is significant asymmetry between affected Loop A and unaffected Loops B and C. It is not known, however, to what extent the cold leg fluids are mixed as they pass through the reactor vessel. Therefore it is not possible to quantify the effect of this uncertainty on the parameters of interest. Qualitatively, little effect on primary system pressure is expected. The unaffected hot legs would likely be warmer and the affected hot leg cooler than calculated. As a result the unaffected loops would flow somewhat faster and the affected loop slower than calculated.

4.4 Conclusions

The calculation and extrapolation of Scenario 1 led to the following conclusions:

The peak primary pressure was calculated to be the PORV setpoint 16.2 MPa (2350 psia), which occurred between 829-1467 s and continued to the end of the 2 hour transient

The minimum downcomer temperature reached was 386.2 K (235°F) at 1026 s into the transient

The minimum cold leg temperatures reached were

Loop A	386.2 K (235°F) at 1026 s
Loop B	312.3 K (102.5°F) at 1050 s
Loop C	312.3 K (102.5°F) at 1050 s

The scenario developed into a continuing primary system cooldown until the ASG was emptied; then the decay heat source in the core overwhelmed the heat removal capacity of the system, which had developed an asymmetric natural circulation flow condition. This heat imbalance turned the temperatures around and a primary system heatup commenced.

5. SCENARIO 2, DOUBLE ENDED STEAM LINE BREAK AT HOT STANDBY

The following section details the analysis of Scenario 2, a double ended guillotine break in Steam Line A, downstream of the flow restrictor and upstream of the main steam isolation valve (MSIV). The subsections contain a description of the scenario, model changes effected to perform the calculation, analysis of the results, extrapolation of the key PTS parameters, and the conclusions drawn.

Scenarios investigated in this report generally include conservative assumptions concerning equipment failures. operator actions, or combinations of these. Conclusions relative to pressurized thermal shock severity are not to be drawn directly from the results presented in this report (see Section 15).

5.1 Scenario Description

The description of Scenario 2, as provided by Oak Ridge National Laboratory, is shown in Table 5-1.

The transient was initiated by the occurrence of a full double ended break in Steam Line A with the reactor at hot standby conditions. All automatic plant functions are assumed to respond normally. Operators were assumed to trip the RCPs when the primary pressure fell below 9.07 MPa (1315 psia), provided a SIAS signal had been generated previously. In addition, operators were assumed to fail to isolate auxiliary feedwater to the affected steam generator (ASG).

5.2 Model Changes

The basic RELAP5 model used to perform the Scenario 2 calculation is described in Section 2. The transient was initiated from the hot standby steady state presented in Section 2.3.3.

TABLE 5-1. SCENARIO DESCRIPTION NO. 2

Plant Initial State - Just prior to transient initiator

General Description: Hot 0% Power, 0% Power after 100 hrs of shutdown
System Status
- Turbine: Not latched, TSVs closed
- Secondary PORV: Automatic control
- Steam Dump Valves: Automatic control
- Charging System: Automatic control
- Pressurizer: Automatic control
- Engineering Safety Features: Automatic control
- PORVs: Automatic control
- Reactor Control: Manual
- Main Feedwater: In bypass mode, manual control to provide 39% level in S/G's; 1 condensate pump, 1 MFWP operating.
- Aux Feedwater: Automatic control
- MSIVs: Open, Automatic control
- MFIVs: Closed, Automatic control

Transient Initiator - Full double-ended guillotine pipe break in line A upstream of the MSIV and downstream of the flow restrictor.

Equipment Failures which occur during the transient if the equipment is demanded.

The operator fails to isolate AFW to the affected S/G.

Operator Reactions to Reported Information

1. If SIAS signal is generated, the operator will trip the reactor coolant pumps when RCS pressure reaches 1300 psig.

2. Stop AFW flow to the unaffected S/G when liquid carryover is observed in the main steamline.

The break in Steam Line A was simulated by the insertion of a break flow path in the downstream end of component 550, and the deletion of steam line components 555, 560, and 565. Trips were altered to insure continuous auxiliary feedwater to Steam Generator A throughout the transient after the time it is automatically tripped on.

After 100 s of the transient calculation, the feedtrain components upstream of and including the feedwater regulating valves (components 505, 605, 705) were deleted from the deck. The deletions were performed to lower computer memory requirements for the problem. The feedtrain after this time in the transient was completely isolated from the remainder of the model due to the closed main feedwater valves.

After 1250 s of the transient calculation, the calculation began experiencing water packing failures in the ASG downcomer and boiler. To get around this problem, a modeling change was used. This change reduced the number of volumes in the ASG downcomer (component 262) and ASG boiler (component 266) from four to two volumes each. This change allowed the calculation to continue an additional 330 s. Close examination of the results during this period revealed no adverse effects caused by the modeling change.

5.3 Results

The following section details the results of the Scenario 2 calculation. The first subsection discusses the results of the calculation. The second subsection discusses the extrapolation to 7200 s of the key PTS parameters and the uncertainties involved in the calculation.

5.3.1. Calculation Results

The sequence of events that occurred during Scenario 2 is shown in Table 5-2. The transient was initiated by the insertion of a 0.287 m^2 (3.094 ft^2) junction to atmosphere in Steam Line A (component 550). Approximately 50 ms after break initiation, an SIAS signal was generated by high ΔP in Steam Line A. The SIAS signal shut down the one operating

TABLE 5-2. SCENARIO 2 SEQUENCE OF EVENTS

Time (s)	Event
0	Steam line ruptures
0.05	High steam line ΔP SIAS signal Main feedwater pump tripped Motor auxiliary feedwater initiated
17	Pressurizer low level alarm
35	Pressurizer indicated empty
50.5	HPI initiated
53.05	Reactor coolant pumps tripped
310	Pressurizer level returned
1154	Pressurizer indicated full
1464	HPI turned off
1586	Calculation terminated

main feedwater pump and activated the motor driven auxiliary feedwater system. High pressure injection (HPI) flow into all 3 loops began at 50.5 s when primary pressure dropped below 10.13 MPa (1470 psia). HPI flow continued until 1464 s when the primary system had repressurized above the pump's shutoff head. Reactor coolant pumps (RCPs) were tripped at 53 s when the primary system pressure dropped below 9.07 MPa (1315 psia).

Figure 5-1 presents the primary and secondary system pressure responses during the transient. Pressure in the ASG fell in response to the break to near atmospheric pressure (0.14 MPa, 20 psia) by 140 s. The two unaffected steam generators (USGs) began to act as heat sources initially as the primary system cooled down and the secondary pressures dropped. Once the RCPs tripped at 53 s pressure in the USGs stabilized at 6.89 MPa (1000 psia) as the USGs were effectively isolated from the primary system by stagnant primary loop flows.

In the primary system, pressure decreased initially as the heat transfer to the ASG decreased average primary system temperature. The depressurization lasted until the ASG had emptied sufficiently to degrade its heat transfer and the RCPs had been tripped. Primary system pressure then began to increase as HPI flow refilled the primary system. The erratic nature of the repressurization was a result of the condensation effects in the pressurizer as discussed in Section 4.3.1.

Figure 5-2a shows break flow for the first 30 s of the transient. Initially the break flow peaked at a value of 2300 kg/s (5070.6 lbm/s) then became choked downstream of the break at the 0.13 m^2 (1.4 ft^2) flow restrictor in the steam generator outlet nozzle. The flow rate fell until 1.5 s when the separator in the ASG filled with liquid and moisture began being carried over to the break, thus decreasing the void fraction of the exit fluid. This decreased void fraction increased the mass lost and break mass flow increased until 4.5 s, when the separators again became effective, cutting off the liquid flow to the break. Once the break quality began to increase, break flow became a function only of pressure, increasing or decreasing as the ASG pressure responded to the transient. Figure 5-2b shows a comparison of break flow and auxiliary feedwater flow

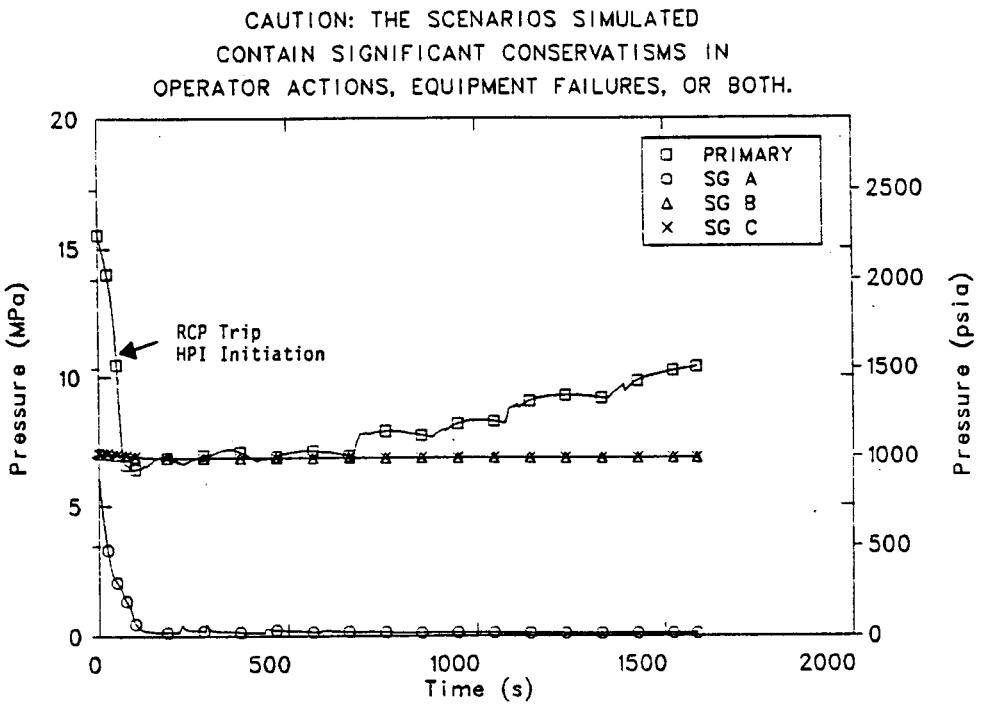

Figure 5-1. Scenario 2 primary and secondary pressures versus time.

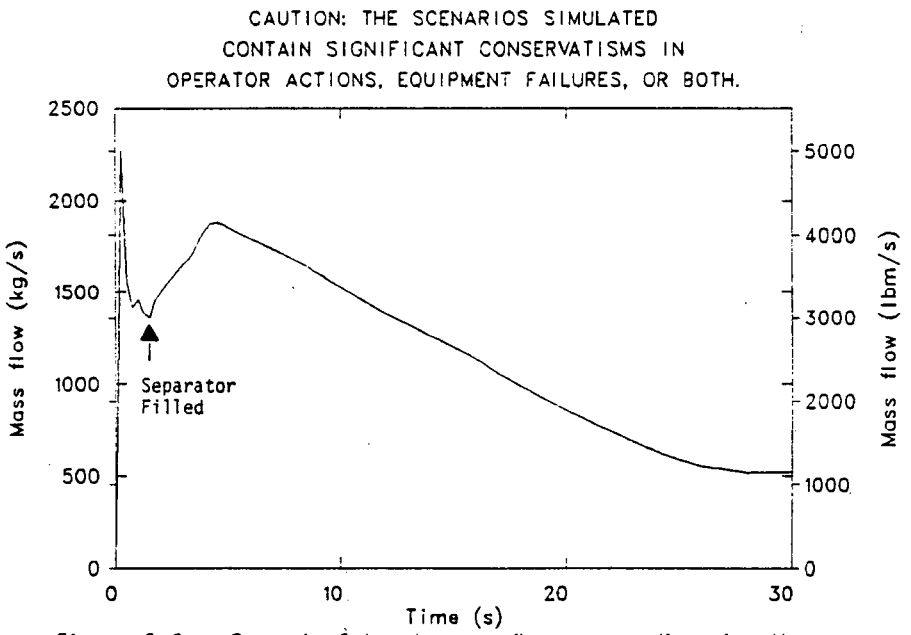

Figure 5-2a. Scenario 2 break mass flow versus time for the first 30 s of transient.

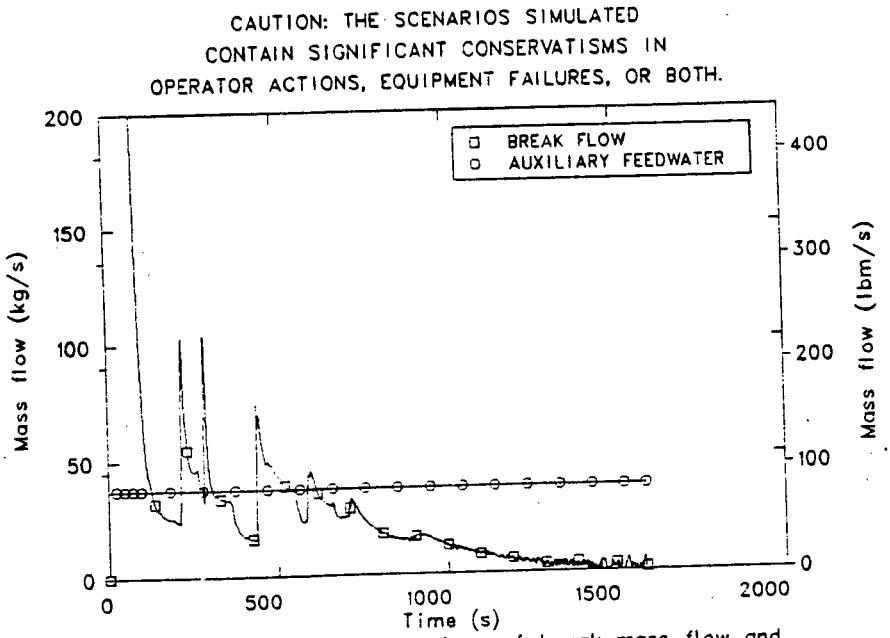

Figure 5-2b. Scenario 2 comparison of break mass flow and auxiliary feedwater flow versus time.

during the transient. From 120 s, except for four spikes caused by momentary pressure surges, auxiliary feedwater flow exceeded break flow and began refilling the ASG. This steam generator refill is shown graphically in Figure 5-3.

Figure 5-4a presents the mass flow rate in the three primary loop cold legs. All three loops experienced an increase in mass flow prior to the RCP trip due to the cooldown of the primary system which increased the density of the reactor coolant. After the pumps were tripped at 53 s, an asymmetric natural circulation condition was established, with flow in Loop A much higher than either of the other loops. This higher flow was due to the greater density head in the loop caused by the continued heat removal through the ASG. Figure 5-4b shows this asymmetric flow in more detail. As shown, flow in Loops B and C essentially stagnated and occasionally reversed. The unaffected loop flows were nearly two orders of magnitude less than the circulation in Loop A. This stagnant condition isolated the USGs from the primary system and allowed Loop A to dominate the downcomer thermal response during the transient.

Figures 5-5 and 5-6 present the temperatures in the hot leg, steam generator inlet and outlet, and cold leg in Loops B and C, respectively. In the initial part of transient, prior to the RCP trip, the cooldown of the primary caused the unaffected steam generators to become heat sources. This is reflected in the figures by the steam generator outlet temperatures being greater than the steam generator inlet temperatures. Once the RCPs had been tripped, the cold leg temperature diverged from that in the steam generator outlet as a result of the flow stagnation discussed previously and the injection of cold HPI liquid into the cold legs. Once the HPI flow terminated at 1464 s, both cold leg temperatures began to rise.

Figure 5-7 presents the fluid temperatures in the hot leg, steam generator inlet and outlets, and cold leg of Loop A, the affected loop. Over the entire transient, the steam generator outlet temperature was lower than the inlet temperature, reflecting the continued heat removal through the ASG. The close coupling of the steam generator outlet and cold leg temperatures, as well as the hot leg and steam generator inlet

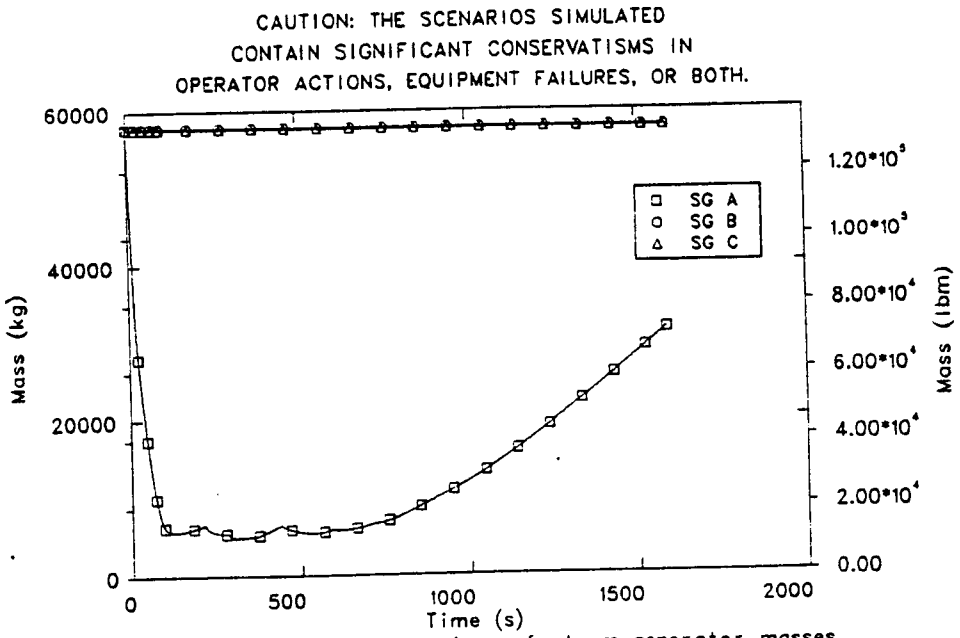

Figure 5-3. Scenario 2 comparison of steam generator masses versus time.

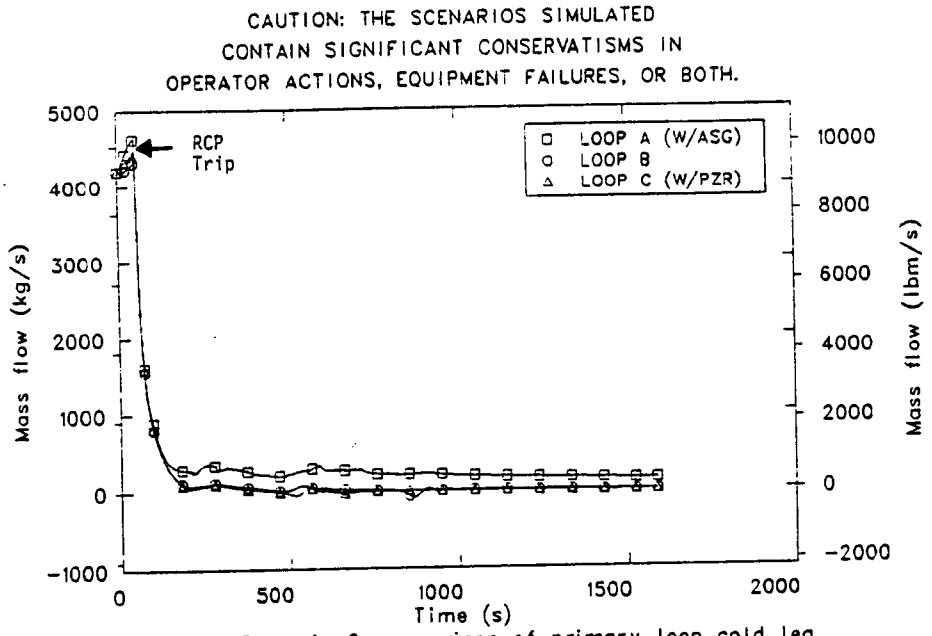

Figure 5-4a. Scenario 2 comparison of primary loop cold leg flows versus time.

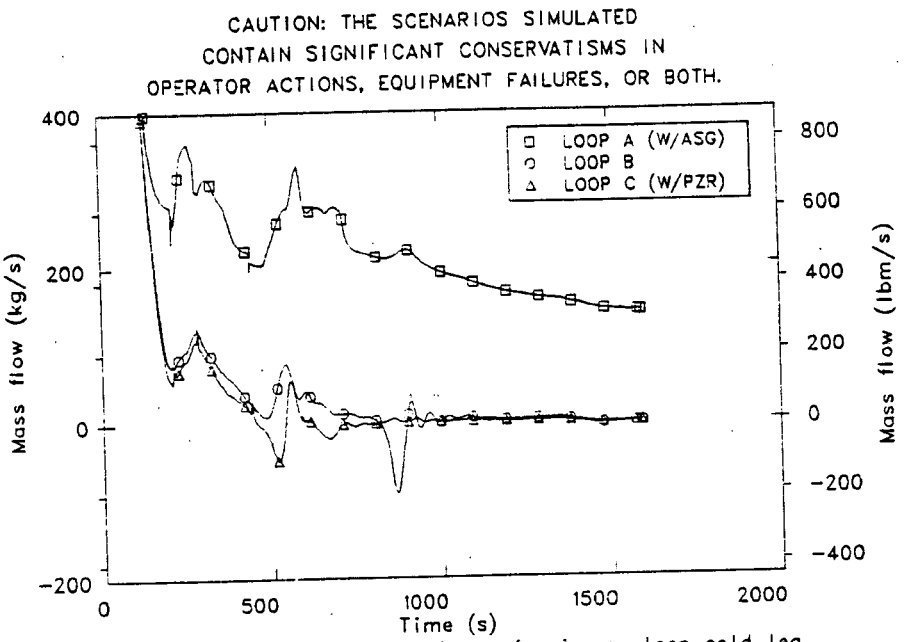

Figure 5-4b. Scenario 2 comparison of primary loop cold leg flows versus time (reduced scale).

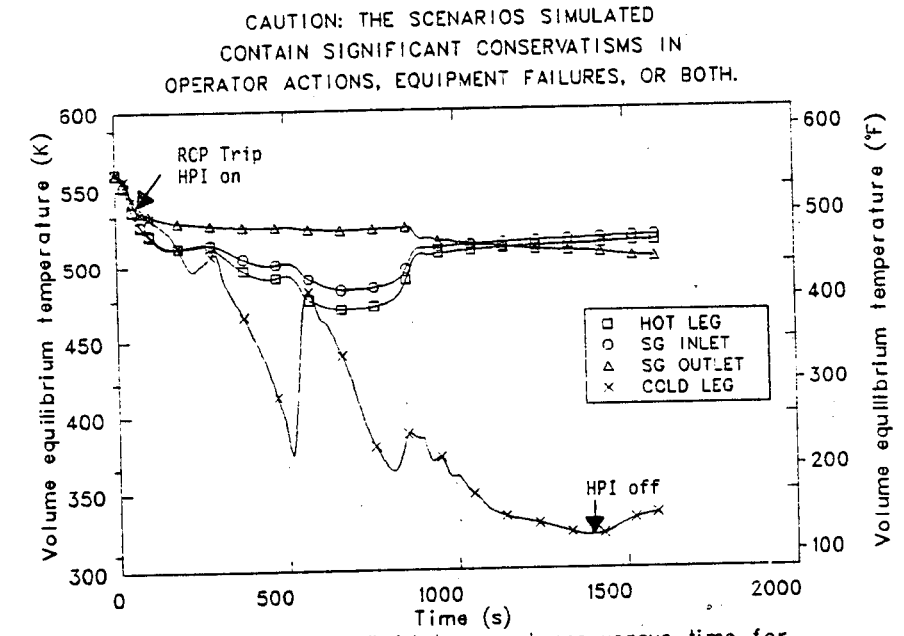

Figure 5-5. Scenario 2 fluid temperatures versus time for primary loop B.

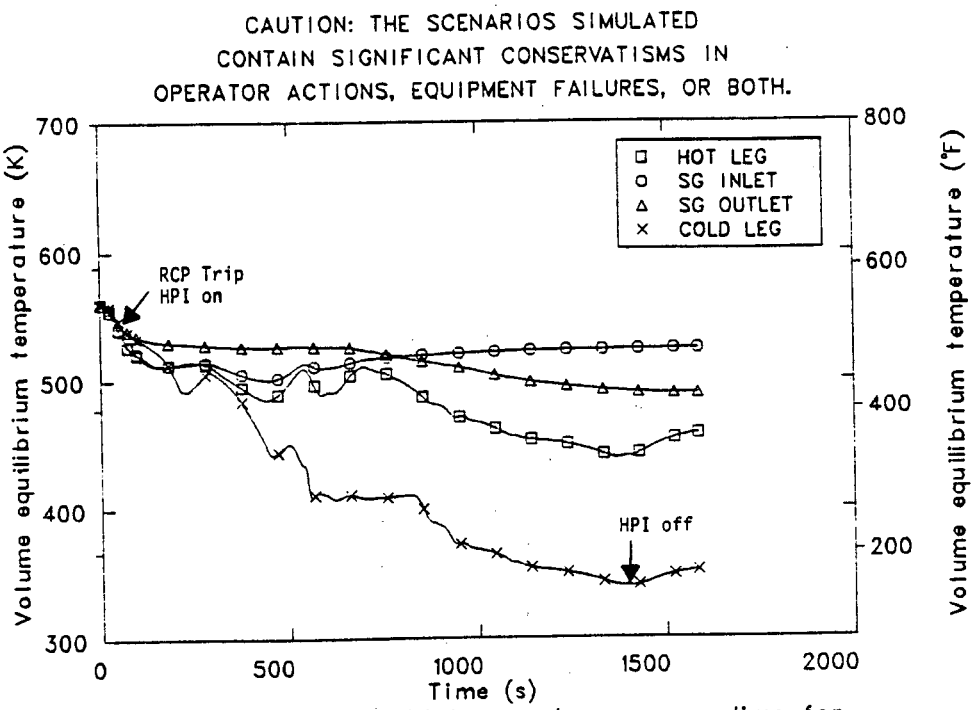

Figure 5-6. Scenario 2 fluid temperatures versus time for primary loop C (W/PZR).

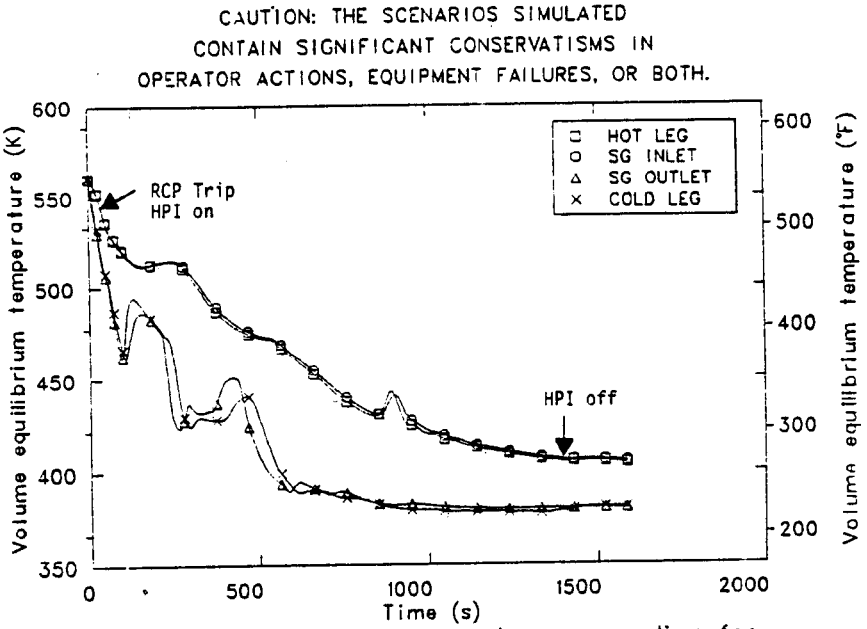

Figure 5-7. Scenario 2 fluid temperatures versus time for primary loop A (W/ASG).

temperatures, resulted from the high mass flow in the loop during forced convection and natural circulation. The HPI shutoff was reflected by a rise in cold leg temperatures to coincide completely with temperature in the steam generator outlet.

Figure 5-8 shows a comparison of the three loop cold leg temperatures with the downcomer fluid temperature. Once the RCPs were tripped, the dominate loop in the system was Loop A, as seen by the close coupling of the affected loop's cold leg and the downcomer temperature. Both unaffected loops have lower cold leg temperatures due to stagnant condition of the loop, and continued HPI flow.

The calculation was terminated at 1586 s when trends suitable for extrapolation had been established. At the time of termination the primary pressure was steadily increasing, the downcomer temperature was decreasing and the ASG was still filling.

5.3.2 Extrapolations and Uncertainties

The following section presents and discusses the extrapolation of key PTS parameters out to 7200 s and the uncertainties involved in these parameters. The parameters discussed are downcomer pressure and fluid temperature, downcomer wall inner surface heat transfer coefficient, primary loop cold leg mass flows and fluid temperatures.

Figure 5-9 presents the extrapolation of downcomer pressure. At the time the transient was terminated, pressure was still rising due to the continued influx of makeup flow. It was extrapolated that this rise would continue until the PORV setpoint of 16.2 MPa (2350 psia) was reached. From the stable repressurization rate achieved at the transient termination, the setpoint would be reached at approximately 3854 s. The final repressurization rate was used as there is no mechanism to increase or decrease the pressurization rate.

The main uncertainty involved in the pressure calculation was the pressurizer behavior. Using an adiabatic calculation, it was estimated

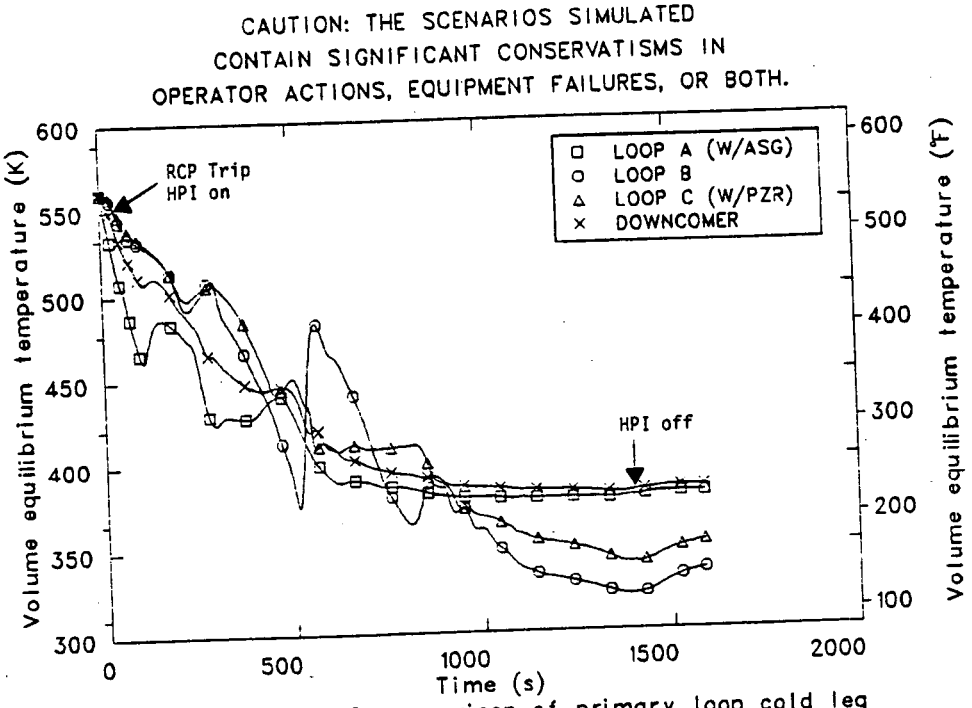

Figure 5-8. Scenario 2 comparison of primary loop cold leg temperatures and downcomer temperature versus time.

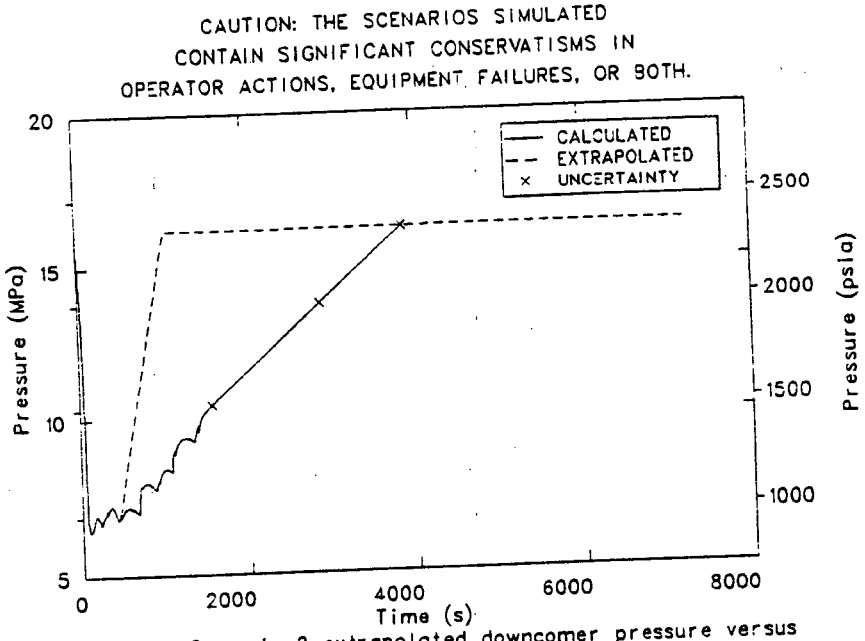

Figure 5-9. Scenario 2 extrapolated downcomer pressure versus time.

that the pressure would have reached the PORV setpoint much earlier, at 1018 s. This calculation used the following assumptions:

(1) it was assumed that the RELAP5 condensation effects, discussed in Section 4.3.1 were correct for refill of the lower two pressurizer volumes.

(2) after the lower two volumes were filled, no condensation was assumed from any source. The existing steam bubble was simply compressed.

This adiabatic calculation is conservative. The actual time to the PORV opening would likely fall somewhere between the code calculated and adiabatic times.

Figure 5-10 shows the extrapolated downcomer temperature. The key to extrapolating this parameter was its close coupling to the affected loop's cold leg temperature. Once the HPI flow stops, the Loop A cold leg temperature rises to the ASG outlet temperature. With auxiliary feedwater continuing to fill the ASG with cold water, the ASG will become subcooled and continue to bring down the primary temperatures. This conclusion was based on the results of Scenario 3 (Section 6.3.1). Using the downcomer temperature at the end of the calculation, coupled with the rate of temperature decrease in the ASG outlet temperature, the extrapolated temperature at 7200 s is 369.8 K (206.1°F).

The uncertainty in this downcomer temperature is the Pressure/HPI response. If the pressure rises as shown in the uncertainty curve of Figure 5-9, HPI would cut off at 631 s. The effect of an early HPI cutoff would be to cause an early jump in downcomer temperature due to the rise in cold leg temperatures. However, the affected steam generator outlet temperature will not change and the downcomer temperature will rise insignificantly. Therefore, assuming a mixed downcomer temperature based on relative flow rates in each loop, there are no major uncertainties in the downcomer temperature.

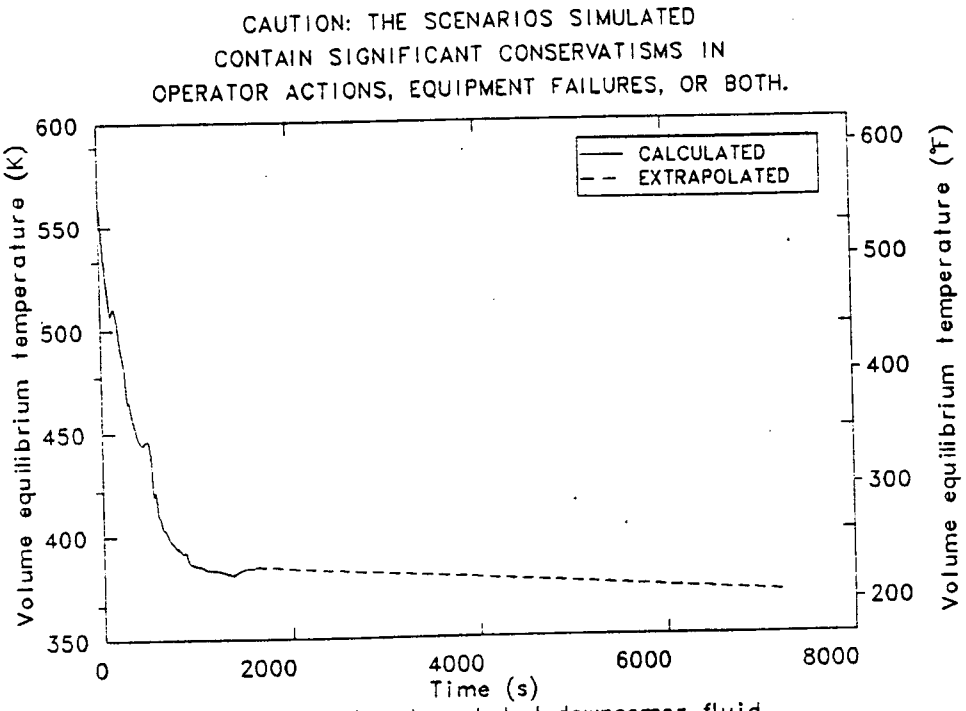

Figure 5–10. Scenario 2 extrapolated downcomer fluid temperature versus time.

Figure 5-11 presents the extrapolated heat transfer coefficient at the downcomer wall inner surface. The heat transfer coefficient in the low flow, subcooled regime in the downcomer is found using the Dittus-Boelter correlation, which decreases as flow decreases. Using extrapolated water properties and the flow extrapolation shown in Figure 5-12, the heat transfer coefficient was calculated at 7200 s. There are no important uncertainties in this extrapolation.

Figure 5-12 shows the three cold leg flows extrapolated to 7200 s. Both Loop B and Loop C will remain stagnant, given the assumption of no operator action on the USG secondary side. Cold leg flow in the affected loop is very sporadic but generally drifting down as the cold leg temperature drifts down. Using the slope of the curve at the end of the transient, the flow was extrapolated to 7200 s. In a natural circulation environment, temperature gradients and density heads affect flows considerably, and thus uncertainties in temperatures are mirrored in flow uncertainties. For example, early cutoff of HPI would decrease the density driving head in Loop A and drop the flow immediately. However the end points would remain close to the same.

Figure 5-13 extrapolates the three cold leg temperatures to 7200 s. For Loop A, the ΔT calculated between the end of the calculation and 7200 s was identical to the ΔT used to extrapolate the downcomer temperature in Figure 5-10. Cold leg temperatures in the stagnant loops rose as a very small reverse flow was present. This drew warmer fluid out of the inlet annulus and into the cold legs. Projecting this flow to continue, cold leg temperatures in Loops B and C would rise asymptotically to the downcomer temperature. Temperature uncertainties in the affected loop were minimal due to the constant flow through the loop. In the unaffected loops, flow behavior posed a substantial uncertainty. For example, Loop B experienced a flow reversal around 600 s which caused its cold leg temperature to rise 110 K (198°F). If that flow reversal had not occurred the Loop B cold leg temperature could have gone down to very near the HPI injection temperature, 305 K (90°F).

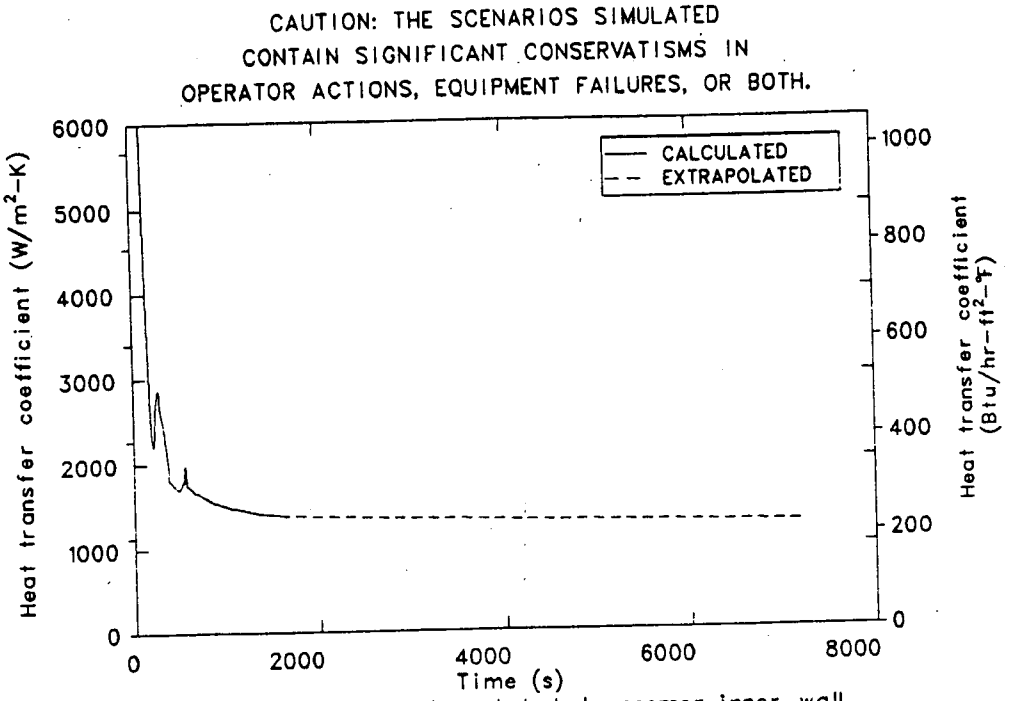

Figure 5-11. Scenario 2 extrapolated downcomer inner wall surface heat transfer coefficient versus time.

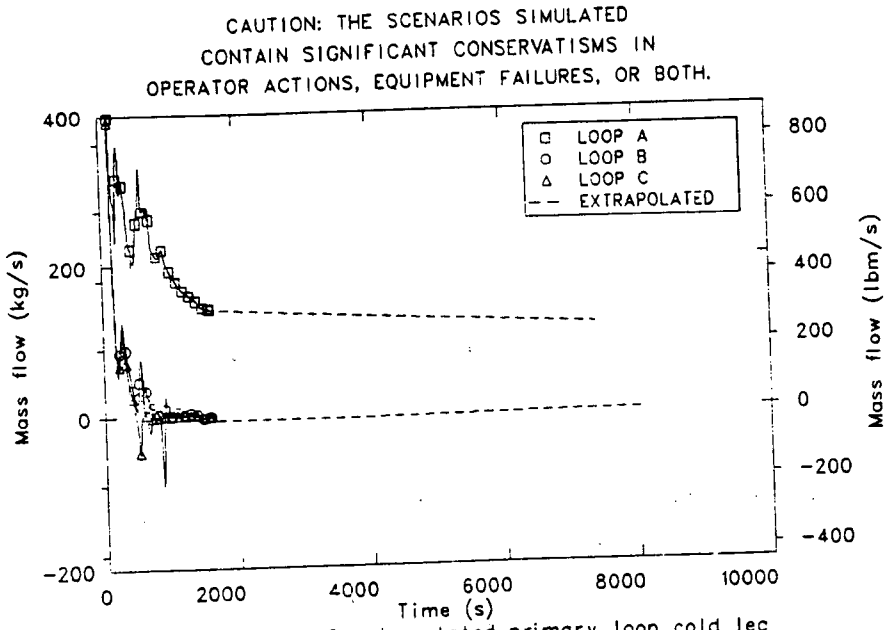

Figure 5-12. Scenario 2 extrapolated primary loop cold leg flows versus time.

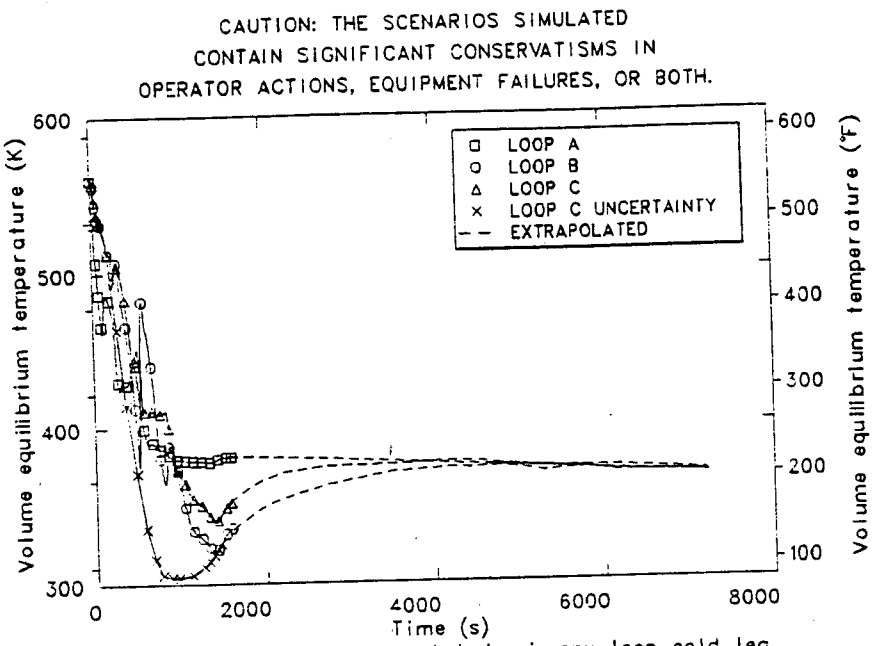

Figure 5-13. Scenario 2 extrapolated primary loop cold leg temperatures versus time.

An additional source of uncertainty concerning Scenario 2 is discussed in Section 4.3.2, the possible asymmetric flow and temperature behavior in the vessel.

5.4 Conclusions

The Scenario 2 calculation and extrapolation led to the following conclusions:

Peak pressure was extrapolated to be 16.2 MPa (2350 psia), the PORV setpoint.

Minimum downcomer fluid temperature was extrapolated to be 369.8 K (206°F).

Minimum cold leg temperatures were

A loop	366.8 K (200.6°F)
B loop	320.6 K (117.4°F)
C loop	339.3 K (151.1°F)

The Scenario 2 calculation resulted in a continuous cooldown of the primary system due to the continued flow of auxiliary feedwater into the ASG. The primary system developed an asymmetric natural circulation condition with flow in the affected loop and stagnation in the remaining two loops.

6. SCENARIO 3, STUCK OPEN STEAM LINE PORV AT HOT STANDBY

The following section describes the investigation of Scenario 3. This calculation was performed to evaluate the consequences of a postulated transient initiated by the failure-open of a single steam line power operated relief valve (PORV) with the reactor at hot standby conditions.

A description of the scenario is provided in Section 6.1, followed by a discussion of the model changes required to perform the calculation in Section 6.2. The results of the calculation, the extrapolated results, and the uncertainties associated with the calculation are described in Section 6.3. The conclusions regarding the calculation are presented in Section 6.4.

Scenarios investigated in this report generally include conservative assumptions concerning equipment failures, operator actions, or combinations of these. Conclusions relative to pressurized thermal shock severity are not to be drawn directly from the results presented in this report (see Section 15).

6.1 Scenario Description

A description of the scenario as developed at Oak Ridge National Laboratory appears in Table 6-1.

The scenario is initiated with the failing open of the PORV on Steam Line A with the reactor at hot standby conditions. Operator action is assumed to trip off reactor coolant pump (RCP) power when primary system pressure falls below 9.07 MPa (1315 psia). It is assumed the operator fails to isolate auxiliary feedwater (AFW) to the affected steam generator.

TABLE 6-1. SCENARIO DESCRIPTION NO. 3

Plant Initial State - Just prior to transient initiator

General Description: Hot 0% Power, 0% Power after 100 hrs of shutdown
System Status
Turbine: Not latched
Secondary PORV: Automatic control
Steam Dump Valves: Automatic control
Charging System: Automatic control
Pressurizer: Automatic control
Engineering Safety Features: Automatic control
PORVs: Automatic control
Reactor Control: Manual
Main Feedwater: In bypass mode, manual control to provide 39% level in S/G's; 1 condensate pump, 1 MFWP operating.
Aux Feedwater: Automatic control
MSIVs: Open, Automatic control
MFIVs: Open, Automatic control

Transient Initiator - A hole appears in steam line A outside containment upstream of the MSIV and downstream of the flow restrictor. The hole size corresponds to that of the steam line PORV.

Equipment Failures which occur during the transient if the equipment is demanded.

The operator fails to isolate AFW to S/G "A".

Operator Reactions to Reported Information

If SIAS signal has been generated the operator will trip the reactor coolant pumps when RCS pressure reaches 1300 psig.

6.2 Model Changes

With the exception of trip changes necessary to simulate the stuck open valve, the model used to perform this calculation is described in Sections 2.1 and 2.2. The transient was initiated from the hot standby conditions presented in Section 2.3.3.

6.3 Results

The following sections describe the analysis results for a calculation of Scenario 3 and extrapolation and uncertainty of those results.

6.3.1 Calculation Results

A sequence of events for the calculation appears in Table 6-2.

This sequence assumes the PORV in Steam Line A fails open at time zero and the operator fails to isolate auxiliary feedwater (AFW) to the affected steam generator. The break size used was 0.009035 m^2 (0.0978952 ft^2). This was the size of the PORV required for the RELAP5 model to pass 73.08 kg/s (161 lbm/s) of saturated steam to atmosphere at a pressure of 5.45 MPa (790 psia). At the time of sequence initiation the reactor was at hot standby conditions. Initial reactor power was 8.29 Mw representing decay heat at 100 hr after reactor shutdown.

Upon opening the break, the Steam Generator A (SGA) secondary pressure fell rapidly as shown in Figure 6-1. Steam Generators B and C (SGB and SGC) were isolated from the effects of the break because of the steam line check valves in each steam line upstream of the common steam line header. As a result SGB and SGC secondary pressures remained elevated except for the minor downward drift associated with the changing heat balance among the steam generators shown in Figure 6-2. Following the break the SGA heat removal rate increased dramatically while SGB and SGC became heat sources to the primary coolant system. The peak in the SGA heat removal rate corresponds to the time at which the SGA downcomer fluid flashed and removed the subcooling effect on the outside of steam generator

TABLE 6-2. SCENARIO 3 SEQUENCE OF EVENTS

Time (s)	Event
0	Break opens, stuck open PORV in steam line A, reactor at hot standby
2	Pressurizer proportional heaters powered
13	Pressurizer backup heaters powered
27	Safety injection actuation signal (SIAS) on high steam line differential pressure
	Immediate actions caused by SIAS: FW bypass valves closed, main FW pump tripped, MFW pump recirculation flow terminated, motor-driven AFW initiated, HPI and LPI pumps started (shutoff heads HPI: 1470 psia, LPI: 145 psia), letdown isolated
30	Steam generator B becomes primary system heat source
33	Steam generator C becomes primary system heat source
81	Low pressurizer level indication, pressurizer heaters tripped off and makeup rate increased
205	Pressurizer level indication zero (less than 1%)
441	HPI flow starts (1470 psia primary system pressure
999	RC pump trip (1315 psia primary system pressure)
1161	RC pump rotors stopped
1204	Makeup reduced to 15 gpm RC pump seal injection only, pressurizer level > level setpoint
2532	Affected SG narrow range level indication reaches 100%
2916	Affected SG separator water filled, liquid carryover to break begins
3288	Primary pressure recovers to HPI shutoff head
3787	End of RELAP5 calculation

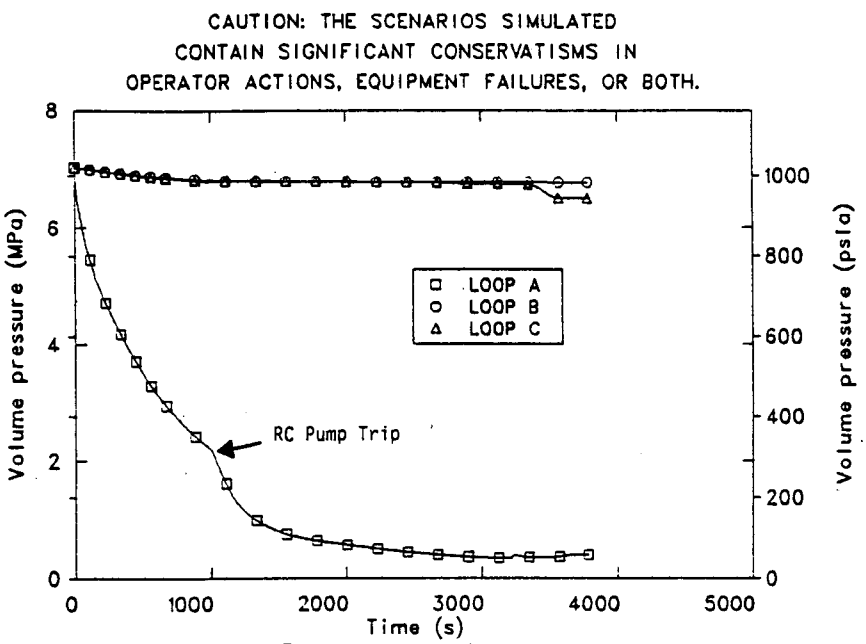

Figure 6-1. Scenario 3 secondary system pressures.

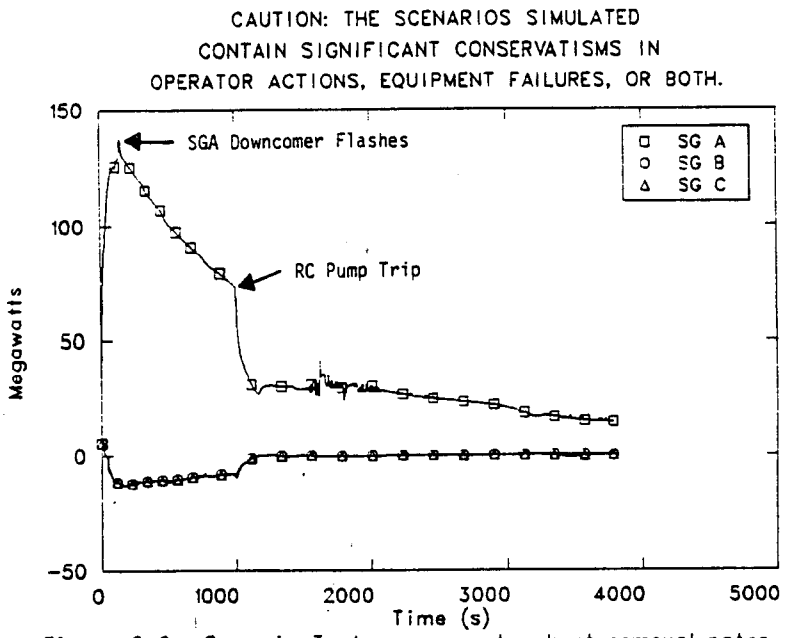

Figure 6-2. Scenario 3 steam generator heat removal rates.

tubes in the lower boiler section. The effect of losing rapid forced circulation heat transfer, due to RCP trip, on the inside of SGA tubes is also evident in Figure 6-2.

The primary system pressure response is shown in Figure 6-3. The pressure initially fell as primary liquid volume shrank due to the high SGA heat removal rate. The falling pressure caused the pressurizer heaters to be fully powered at 13 s. As shown on Figure 6-3, when the pressurizer emptied the depressurization rate increased.

At 27 s a safety injection activation signal (SIAS) was generated due to high differential pressure between the common steam line header and Steam Line A. Immediate actions caused by the generation of the SIAS were: closure of the feedwater (FW) bypass valves, tripping of power to the operating main feedwater (MFW) pump, termination of MFW pump recirculation flow, initiation of motor-driven auxiliary feedwater (AFW) and isolation of letdown flow. The SIAS also caused the high pressure injection (HPI) and low pressure injection (LPI) pumps to be started. However no flow could be delivered from these pumps unless primary system pressure fell below their respective shutoff heads. Turbine-driven AFW flow was not initiated during this sequence because 2-of-3 steam generators are required to have low level indications and this condition was met only in SGA.

Figure 6-4 presents a comparison of break and auxiliary feedwater mass flow rates for SGA. The break flow initially peaked, then declined along with the SGA secondary pressure shown in Figure 6-1. The AFW flow was essentially constant after AFW initiation at 27 s at a rate which represented total motor-driven AFW capacity. All AFW was directed to SGA because in the H. B. Robinson Unit 2 Plant a common AFW header is used to feed all steam generators. Due to the break in the SGA secondary system and the previously mentioned effective isolation of SGB and SGC, the pressure in the AFW header was below that of SGB and SGC. As a result all AFW flow was directed to SGA.

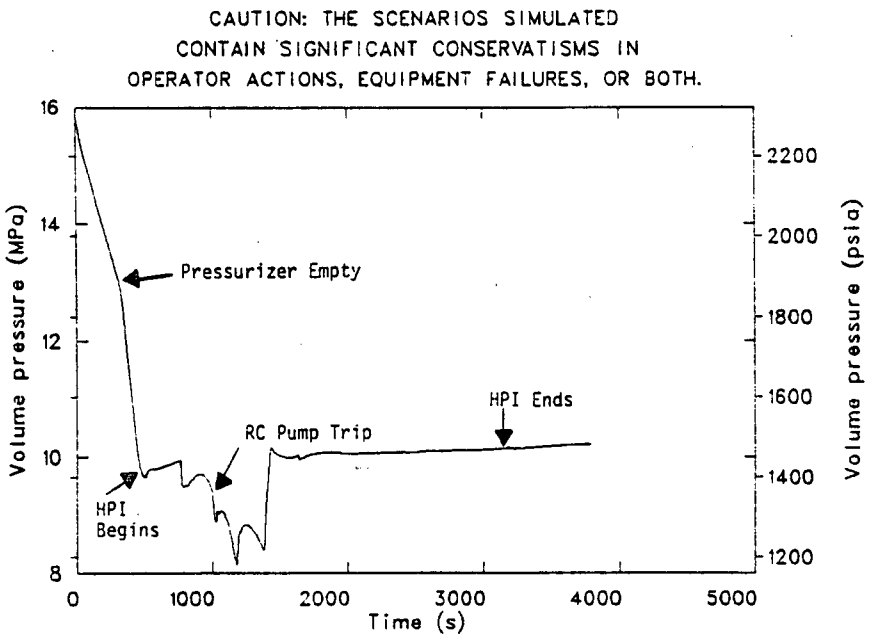

Figure 6-3. Scenario 3 reactor vessel downcomer pressure.

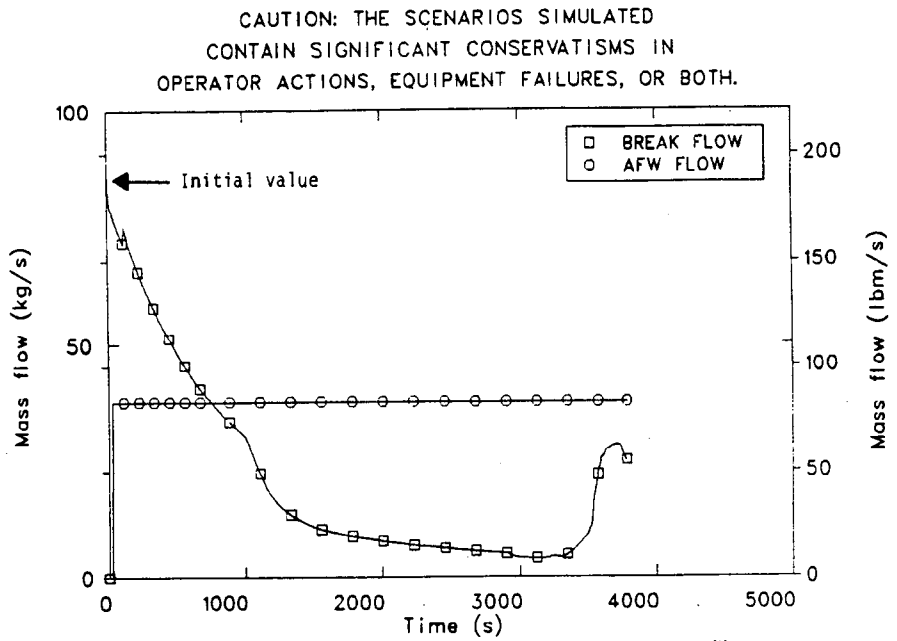

Figure 6-4. Scenario 3 affected steam generator auxiliary feedwater and break mass flowrates.

Figure 6-5 presents the pressurizer level indicated response. At 81 s the low level indication caused the termination of pressurizer heater power and an increase in the makeup rate to full makeup capacity. The level indication was essentially zero at 205 s.

The primary system pressure continued to fall as shown in Figure 6-3 and, at 441 s, the pressure fell below the HPI pump shutoff head. The HPI mass flow rate response, per loop, is shown in Figure 6-6. HPI flow is inversely proportional to the primary system pressure. The volume addition rate to the primary system due to HPI flow more than offset the continuing shrinkage rate due to cooling and the primary system depressurization was reversed shortly after initiation of HPI. As HPI injection continued, however the pressurizer began to refill with liquid which was highly subcooled. The interaction in the surge line and pressurizer between the subcooled liquid and superheated steam resulted in rapid condensation of the steam. This condensation process removed vapor volume from the pressurizer which continued the decrease in primary system pressure. At 999 s the reactor coolant pumps were tripped when the pressure fell to 9.07 MPa (1315 psia). As was discussed in Section 4.3.1, pressurizer condensation effects may be overstated by RELAP5 during the later stages of the pressurizer insurge. This is because vertical thermal stratification within the liquid phase inside the pressurizer may limit the physical condensation potential and this stratification is not well calculated by the model. During the early portion of the insurge discussed here, however, the pressurizer is essentially voided such that direct mixing of cold liquid and hot steam is promoted. Thus the calculated condensation effects during the initial portion of the insurge are likely physical.

Following the trip of the reactor coolant pump power at 999 s, the pumps coasted down with the rotors stopping at 1161 s. Figure 6-7 shows that, following coastdown, Loop A natural circulation continued while Loop B and C flows approached stagnation. This difference was caused by the different steam generator heat removal rate characteristics shown in Figure 6-2. By about 2400 s flow rates in both Loops B and C were virtually zero. Stagnation of Loops B and C occurred because SGB and SGC were heat sources to the primary system and the heat added caused a

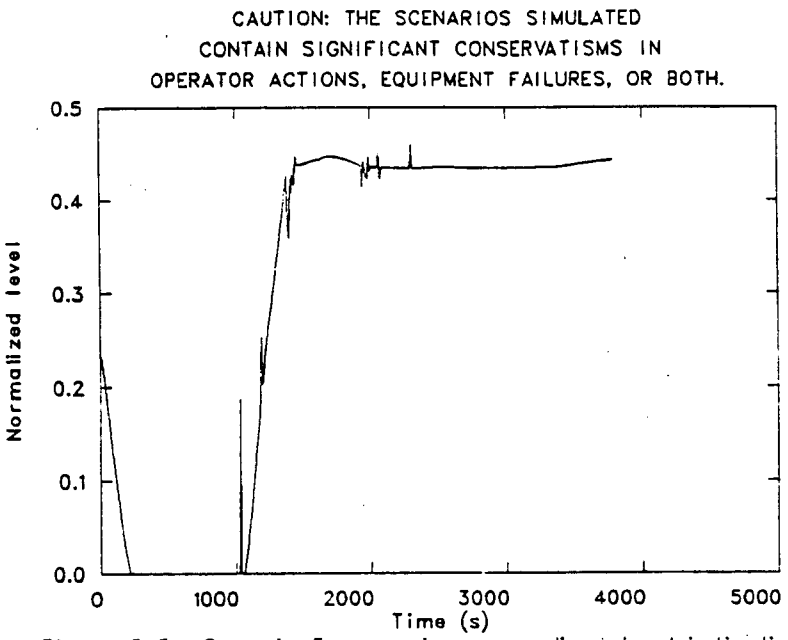

Figure 6–5. Scenario 3 pressurizer normalized level indication.

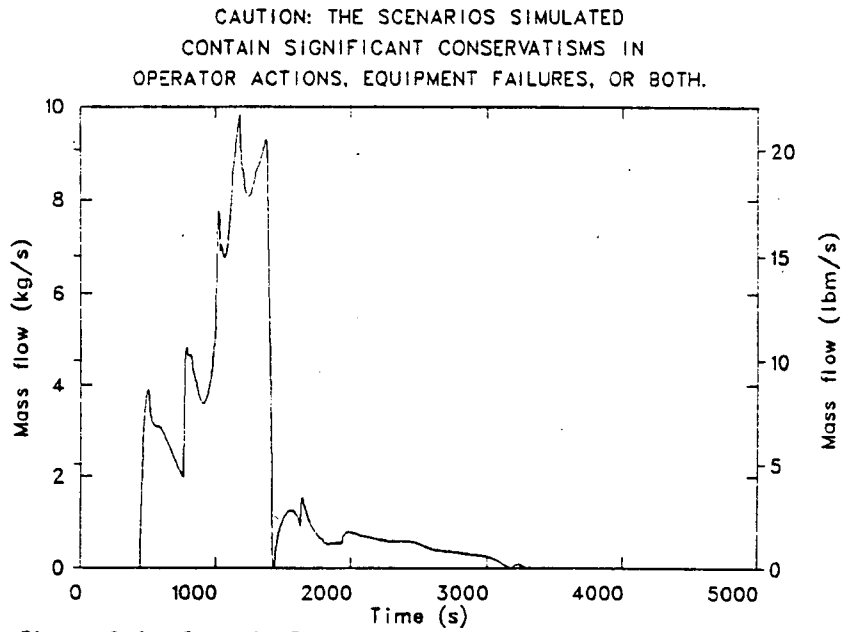

Figure 6–6. Scenario 3 high pressure injection mass flow rate (per loop)

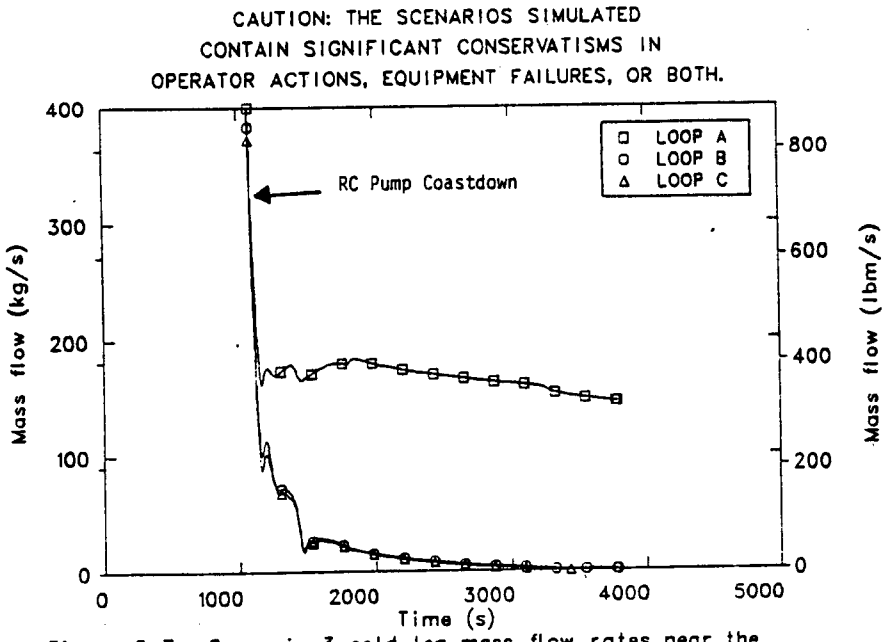

Figure 6-7. Scenraio 3 cold leg mass flow rates near the reactor vessel.

sufficient density head difference to balance the pressure head which was driving fluid through Loop A. Stagnation was not a result of voiding within the SGB and SGC tubes.

At 1204 s the pressurizer level indication had advanced to the setpoint level and makeup flow was reduced to a constant 0.95 liters/s (15 gpm) for the remainder of the sequence. This rate represents the net reactor coolant pump seal injection rate expected during this period. Due to model restrictions the makeup flow was injected only into the Loop B cold leg. This difference had no major effect on the results except for the Loop B and C cold leg temperatures which will be discussed in Section 6.3.2.

Continued HPI flow caused the pressurizer to continue filling and the primary system pressure stabilized at about 1400 s just below the HPI shutoff pressure. At this time there was a near balance between primary system volume addition from the HPI and makeup flows and volume shrinkage due to contraction of the cooling primary fluid. The pressurizer level and pressure continued to slowly increase, however until 3288 s when the HPI shutoff pressure was exceeded. After this time primary system pressure was very slowly increasing due to the action of the small makeup flow alone.

The affected steam generator initially lost mass due to the effect of the break. However after about 800 s the AFW flow to SGA exceeded the break flow as shown in Figure 6-4 and the secondary began to refill. Figure 6-8 shows the steam generator secondary masses and Figure 6-9 shows the corresponding narrow-range level indications. The dip and recovery in the SGA level at about 120 s was caused by flashing of the SGA downcomer fluid during the blowdown. At 2532 s the SGA narrow-range level indication reached 100%. At 2916 s the affected steam generator separator became water-filled and liquid carryover to Steam Line A commenced.

Figure 6-10 shows the fluid temperature responses in each of the cold legs near the reactor vessel and in the reactor vessel downcomer at the elevation corresponding to the top of the core. The Loop A cold leg was generally the coldest as a result of the continued SGA heat removal as indicated in Figure 2. Following RC pump trip the Loop B and C cold legs

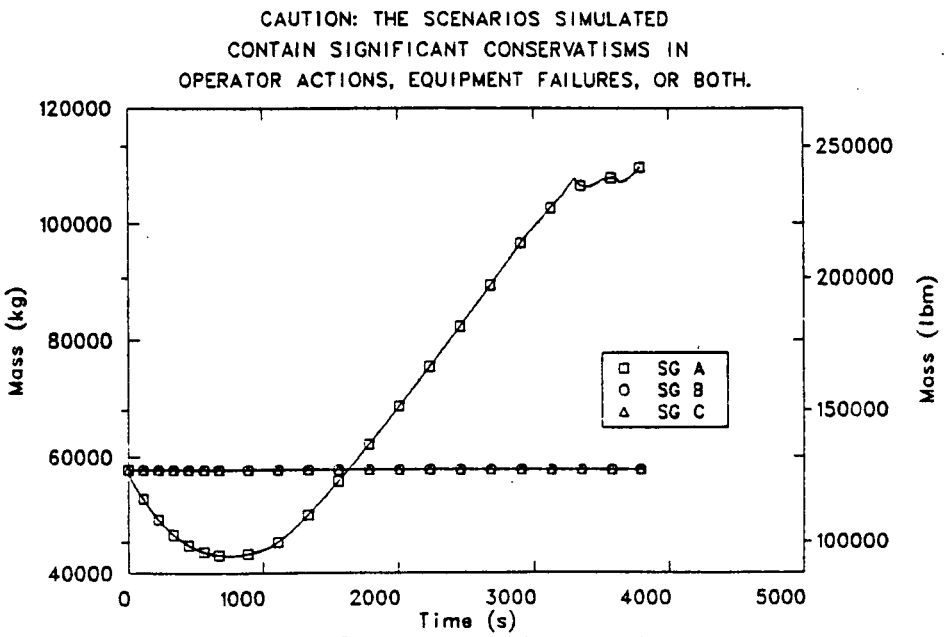

Figure 6-8. Scenario 3 steam generator secondary masses.

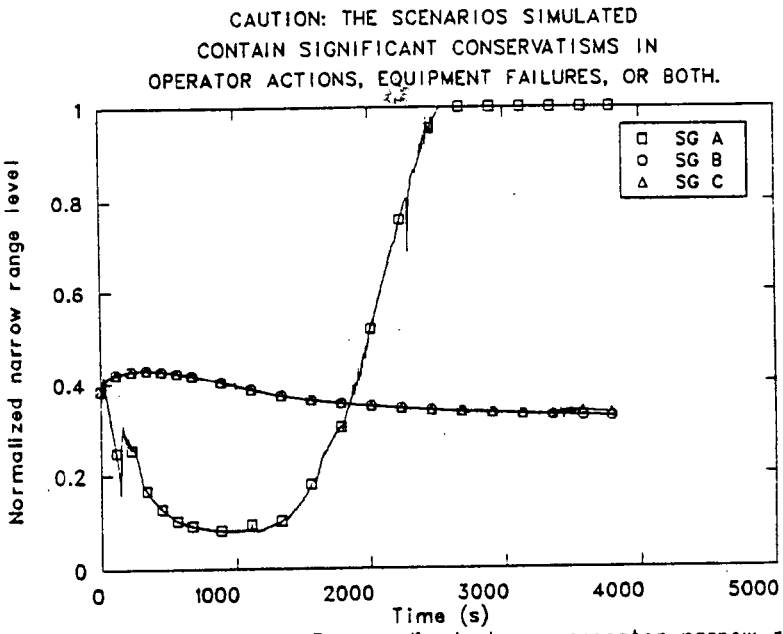

Figure 6-9. Scenario 3 normalized steam generator narrow range indicated levels.

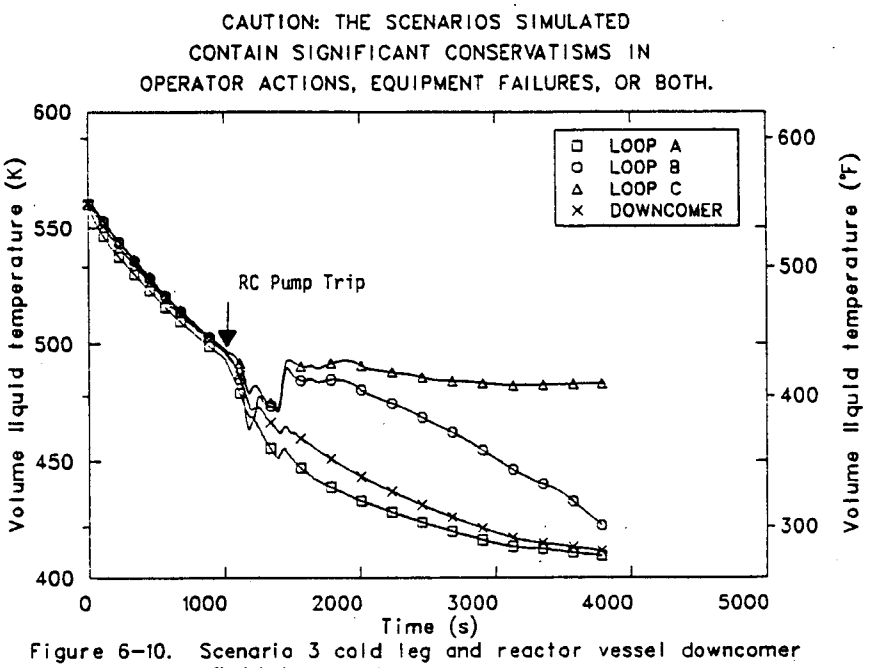

Figure 6–10. Scenario 3 cold leg and reactor vessel downcomer fluid temperatures.

were essentially stagnant, however, the minor Loop B and C flows shown in Figure 6-7 were sufficient to prevent the Loop B and C cold leg temperatures from plunging. In general the Loop B cold leg fluid temperature is below that of Loop C because, in the model, makeup is injected only into Loop B.

The calculation was terminated at 3787 s because a suitable indication of trends existed to allow an extrapolation of results to 7200 s. At the end of the calculation the primary system pressure was 10.14 MPa (1471 psia) and rising slowly and the reactor vessel downcomer fluid temperature was 411 K (281°F) and falling slowly. The affected steam generator separator was flooded and 30% of its steam dome was also flooded. Loop A continued to circulate.

6.3.2 Extrapolations and Uncertainties

The calculation was terminated at 3787 s. This section describes the extrapolation of results to 7200 s and adjustment of results to account for uncertainties in the computer calculation.

Three uncertainties in the calculation will be addressed: pressurizer effects, asymmetric hot leg temperatures, and makeup effects.

As discussed in Sections 4.3.1 and 6.3.1, it is suspected that calculated condensation rates are overstated during the later stages of the pressurizer refill process. As a result, the primary system pressure is depressed artificially during this portion of the transient. Adjustments have been made on the figures shown in this section to account for this effect. The adjustments were accomplished by assuming that during refill of the lower two cells of the pressurizer (23% of its height) the code calculated results were correct. For the remainder of the refill, however, the parameters were adjusted based on an adiabatic compression of the vapor in the pressurizer. The reactor coolant pump (RCP) trip due to low primary system pressure occurred when the bottom pressurizer cell was filling. As stated above, the calculated effects during this period appear physical, therefore the occurrence of the RCP trip is physical as well.

Next is the uncertainty due to asymmetric loop behavior discussed in Section 4.3.2. For the sequence being investigated here there is significant asymmetry between affected Loop A and unaffected Loops B and C. It is not known, however, to what extent the cold leg fluids are mixed as they pass through the reactor vessel. Therefore it is not possible to quantify the effect of this uncertainty on the parameters of interest. Qualitatively, little effect on primary system pressure is expected. The unaffected hot legs would likely be warmer and the affected hot leg cooler than calculated. As a result the unaffected loops would flow somewhat faster and the affected loop slower than calculated.

As discussed in Section 6.3.1, the makeup injection was modeled into the Loop B cold leg. After 1204 s the makeup flow was reduced to a constant 0.95 ℓ/s (15 gpm) representing the net seal injection flow to all three reactor coolant pumps. To be properly modeled this injection rate should have been split into thirds and each portion injected at the reactor coolant pumps. This difference has a minor effect on the parameters of interest except the cold leg temperatures in the unaffected loops during low flow conditions. As calculated, the Loop B cold leg is too cool and Loop C cold leg is too warm. This effect has been quantified as shown on the adjusted results in this section.

Extrapolations to 7200 s, and adjustments based on the above effects, are shown on Figures 6-11 through 6-15 as dashed lines. These dashed lines represent the best estimate responses for this scenario.

Figure 6-11 shows the extrapolated and adjusted primary system pressure. The dashed line was drawn by assuming an adiabatic compression of the pressurizer vapor space after the time the bottom two cells of the pressurizer had filled with liquid. The extrapolated pressure at 7200 s is 11.12 MPa (1632 psia).

Figure 6-12 shows the extrapolated and adjusted reactor vessel downcomer fluid temperature at an elevation equivalent to the top of the core. The effect on temperature of the different HPI rate due to the pressure differences discussed in the previous paragraph is minor. This is

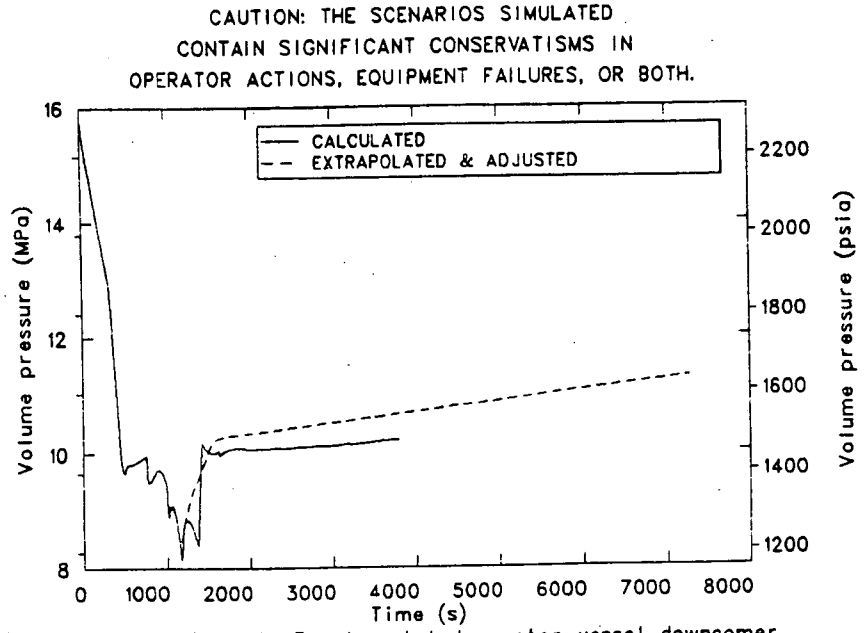

Figure 6–11. Scenario 3 extrapolated reactor vessel downcomer fluid pressure.

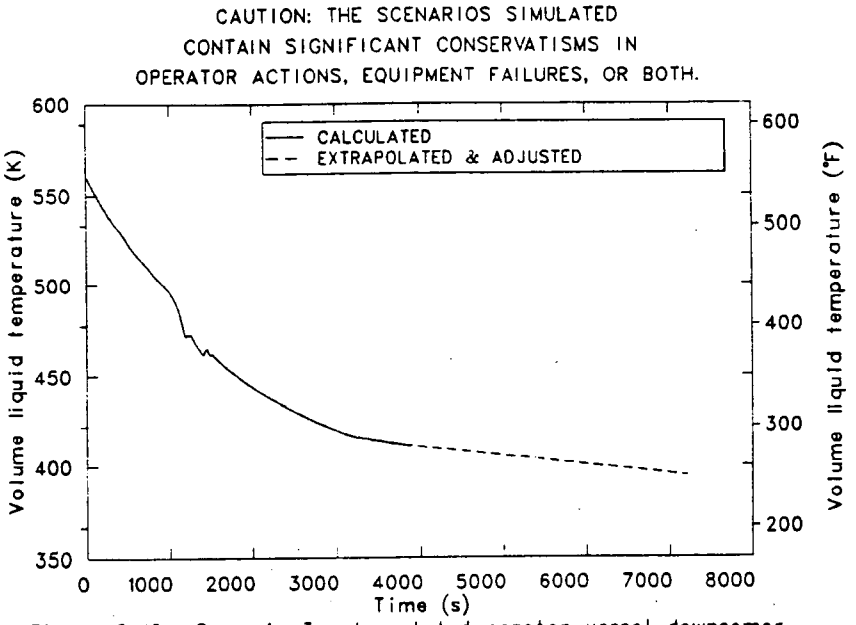

Figure 6–12. Scenario 3 extrapolated reactor vessel downcomer fluid temperature.

so because the temperature response is dominated by the affected steam generator heat removal rate and not by different subcooling effects of HPI due to the minor differences in primary pressure response indicated in Figure 6-11. The extrapolation from the end of the calculation to 7200 s assumes that the existing cooldown continues. This is based on an affected steam generator heat removal rate of 14.4 MW and a core decay heat of 8.2 MW. The temperature extrapolated at 7200 s is 397 K (256°F).

Figure 6-13 shows the extrapolation of the heat transfer coefficient on the inside surface of the reactor vessel downcomer wall. The extrapolation was performed simply by extending the trend present at the end of the calculation. This is justified because trends in flow conditions and temperatures are well established at the end of the calculation.

Figure 6-14 shows the extrapolated cold leg mass flow rates between the HPI sites and reactor vessel. Conditions present at the end of the calculation are expected to continue through 7200 s. Loop A is expected to continue in natural circulation while Loops B and C remain virtually stagnant.

Figure 6-15 shows the cold leg fluid temperatures between the HPI sites and the reactor vessel. The Loop A extrapolation used the results of the downcomer temperature extrapolation from Figure 6-12 and the relationship between the downcomer and Loop A cold leg temperature indicated in Figure 6-10. The minimum extrapolated Loop A cold leg temperature is 395 K (252°F). The calculated results for Loop B and C temperatures exhibit the effects of the aforementioned improper split in makeup flow. After 1204 s the reactor coolant pump seal makeup should have been injected equally into all three loops. In the calculation it was all injected into Loop B, hence the decreasing Loop B cold leg temperature during the latter part of the calculation. The adjusted and extrapolated Loop B and C temperatures shown are identical and are based on constant 0.32 liters/sec (5 gpm) pump seal injection into each of the three cold legs. Note that, because Loop A natural circulation flow continued, no adjustment of Loop A temperature was made for this effect.

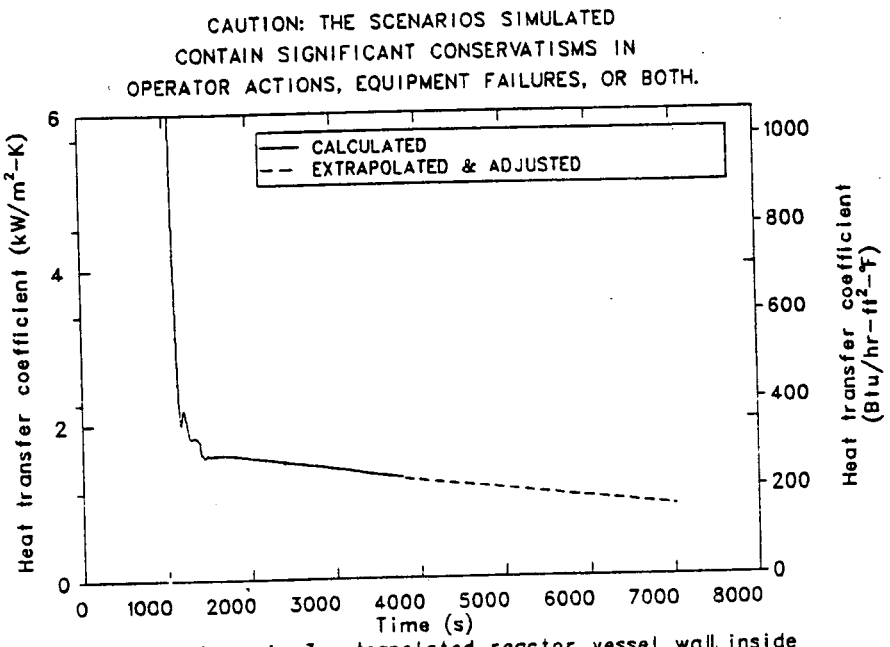

Figure 6-13. Scenario 3 extrapolated reactor vessel wall inside surface heat transfer coefficient.

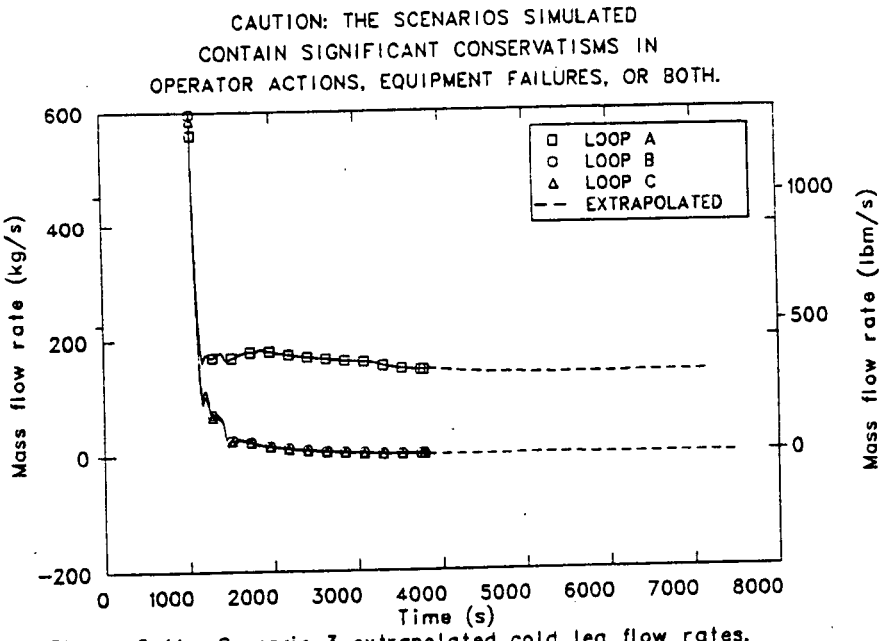

Figure 6-14. Scenario 3 extrapolated cold leg flow rates.

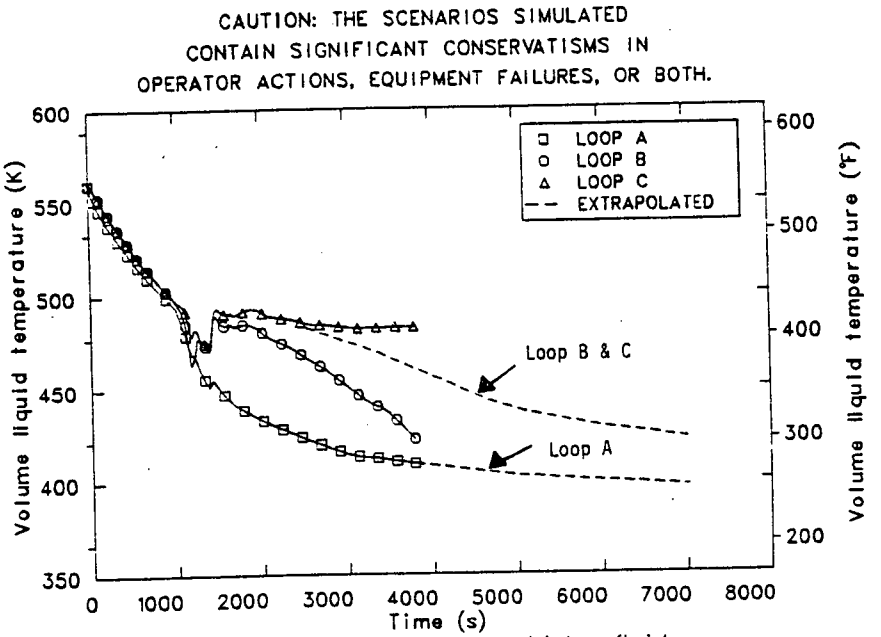

Figure 6-15. Scenario 3 extrapolated cold leg fluid temperatures.

6.4 Conclusions

The minimum reactor vessel downcomer fluid temperature occurred at the end of the two-hour period. The extrapolated minimum temperature is 397 K (256°F). The extrapolated primary system pressure at that time is 11.12 MPa (1632 psia).

7. SCENARIO 4, THREE STEAM DUMP VALVES FAIL OPEN AT FULL POWER

The following section describes the investigation of Scenario 4. The simulation was performed to evaluate the consequences of three steam dump valves failing open with the reactor at full power. Section 7.1 contains the scenario description, Section 7.2 modeling changes effected to perform the transient calculation, Section 7.3.1 analysis of the transient results, Section 7.3.2 extrapolation of the results and Section 7.4 conclusions drawn from the analysis.

Scenarios investigated in this report generally include conservative assumptions concerning equipment failures, operator actions, or combinations of these. Conclusions relative to pressurized thermal shock severity are not to be drawn directly from the results presented in this report (see Section 15).

7.1 Transient Scenario Description

A description of Scenario 4 appears in Table 7-1. This sequence definition was developed at Oak Ridge National Laboratory (ORNL).

The transient was initiated from full power steady state conditions by locking open 3 out of 5 main steam line dump valves. All automatic plant functions with the exception of the main steam isolation valve (MSIV) for Loop A are assumed to be operative. It was assumed that the Loop A MSIV fails to close if a MSIV trip signal is generated, however this condition was not reached during the transient. The reactor is tripped at 41.1 s into the transient and operator actions are assumed to trip the reactor coolant pumps on a low pressurizer pressure signal.

7.2 Model Changes

The basic RELAP5 model used to perform the three dump steam valves failure open transient calculation is described in Section 2. The

TABLE 7-1. SCENARIO DESCRIPTION NO. 4

Plant Initial State - Just prior to transient initiator

General Description: 100% Power steady state
System Status
- Turbine: Automatic control
- Secondary PORV: Automatic control
- Steam Dump Valves: Automatic control
- Charging System: Automatic control
- Pressurizer: Automatic control
- Engineering Safety Features: Automatic control
- PORVs: Automatic control
- Reactor Control: Automatic
- Main Feedwater: Automatic control
- Aux Feedwater: Automatic control
- MSIVs: Open, Automatic control
- MFIVs: Open, Automatic control

Transient Initiator - Three (3) steam dump valves fail open.

Equipment Failures which occur during the transient if the equipment is demanded.

1. The affected steam dump valves will not close.
2. MSIV "A" fails to close.

Operator Reactions to Reported Information

1. If SIAS signal is generated, the operator will trip the reactor coolant pumps when RCS pressure reaches 1300 psig.

2. Stop AFW flow to the unaffected S/G when liquid carryover is observed in the main steamline.

3. Stop AFW flow to S/G "A" 10 min after attempted MSIV closure or when carryover occurs.

following changes were made to the control system model to simulate the transient. The reactor was manually tripped at 41.1 s to simulate an overpower trip caused by moderator cooldown effects. The steam dump control system was modified such that at the beginning of the transient the total steam dump valve area was set at a constant value representing the 3 stuck open dump valve condition.

For this transient both the motor and steam-driven auxiliary feedwater systems are activated. The motor-driven auxiliary system was left on once activated. The steam-driven feedwater auxiliary was assumed to degrade to zero flow after the steam generator steam dome pressures reached 0.69 MPa (100 psia).

The transient calculation was initiated from the full power steady state described in Section 2.3.1.

7.3 Results

The following section details the results of the Scenario 4 calculation. The first subsection discusses the results of the calculation. The second subsection discusses extrapolation of results to 7200 s and uncertainties involved in the calculation.

7.3.1 Calculation Results

The following section describes the investigation of Scenario 4. The calculation was performed to evaluate the consequence of three steam dump valves failing open with the reactor at full power. A sequence of events for this simulation is summarized in Table 7-2.

At zero time 3 out of 5 steam dump valves failed open in the steam line. This hypothetical equipment malfunction is equivalent to a 0.043 m^2 (0.465 ft^2) steam line break that affects all three steam generators. After the break was initiated the secondary pressure began to drop which resulted in a subsequent primary system cooldown. The reactor was tripped at 41.1 s after transient initiation. This trip was imposed to

TABLE 7-2. SCENARIO 4 SEQUENCE OF EVENTS

Time (sec)	Event
0.0	Three steam dump valves fail open
1.0	Proportional heaters on
5.0	Proportional heaters reach maximum power
17.35	Backup heaters on
41.10	Trip reactor
41.10	Trip turbine
42.0	Turbine stop valve closed
49.85	Main feedwater valves start to close
52.9	Trip feedwater pumps
52.9	Main feedwater valves closed
52.9	Motor-driven auxiliary feed on
89.30	Backup and proportional heaters latched off
98.95	Steam-driven auxiliary feed on
132.30	SI signal on low pressurizer pressure (1730 psia)
132.30	CVCS flow reaches maximum due to letdown isolation
132.30	HPI pumps activated
175.0	HPI shutoff head overcome
180.0	Pressurizer emptied
181.0	RCP pumps tripped
300.0	Transition to natural circulation loop flow--HPI reaches maximum flow

TABLE 7-2. (continued)

827.7	CVCS drops to minimum (after letdown isolation) flow rate of 15 gpm
850.0	Steam driven auxiliary feed off
1250.0	Primary side pressure stabilizes at 10 MPa (1450 psia)
2500.0	End of calculation

account for reactor overpower conditions caused by moderator cooldown effects. The reactor trip is based on a separate effects calculation used to estimate the reduced average moderator temperature needed to induce overpower conditions. The results of this separate effects calculation were consistent with the time frame given by ORNL for the plant trip to occur.

The primary and secondary system pressure responses are shown in Figure 7-1. After reactor trip the primary depressurization rate increased significantly. The increased depressurization rate was a consequence of enhanced primary system cooldown caused by a large mismatch between the core decay power and the much larger total power removal through the steam generators (Figure 7-2). The primary pressure reached a minimum of 6.9 MPa (1000 psia) at 300 s. Although the primary cooldown continued after 300 s, repressurization was induced by liquid volumetric addition from both the HPI and CVCS injection. Although the secondary system pressure initially dropped, a substantial pressure increase occurred after the steam turbine valves shut [peak value of 6.1 MPa (885.0 psia) at 50 s]. This phenomena was caused when the secondary steam production rate temporarily exceeded the steam mass flow rate out the stuck open dump valves. As the reactor power dropped however, the total secondary side steam generation rate decreased below the mass flow rate out the dump valves and the secondary sides began to depressurize again.

Throughout the simulation, the auxiliary feedwater played a key role in maintaining enough steam generator mass inventory to sustain primary side cooldown. After the main feedwater train was isolated at 52.9 s the motor and then steam-driven auxiliary feedwater systems where activated at 52.9 s and 98.2 s respectively (Figures 7-3 and 7-4). The trip signal that caused the feedwater valves to close was triggered by a low primary average temperature [less than 563 K (554°F)]. Final feedwater valve closure occurred over a 4.0 s period. For each loop partial feedwater valve closure had occurred prior to the reactor trip. This was a consequence of the feedwater control system responding to conditions induced by the stuck open dump valves. The reduced feedwater flow induced a trip signal to both feedwater pumps which in turn activated the motor-driven auxiliary

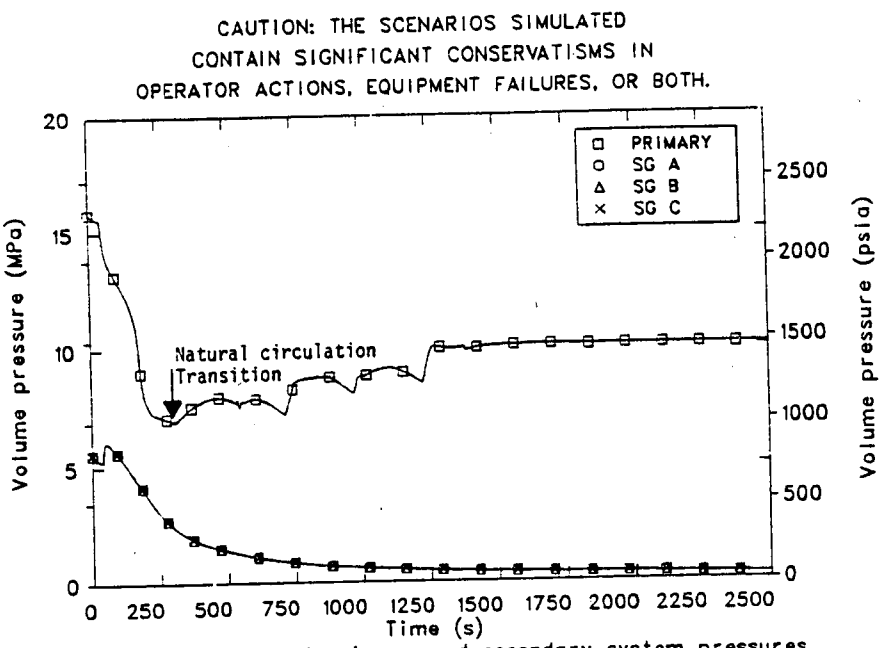

Figure 7-1. Scenario 4 primary and secondary system pressures.

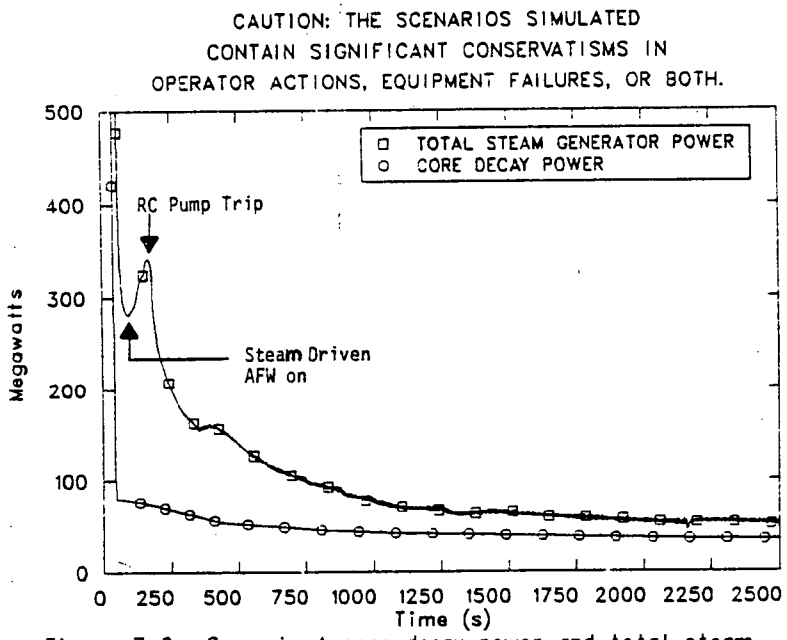

Figure 7-2. Scenario 4 core decay power and total steam generator power.

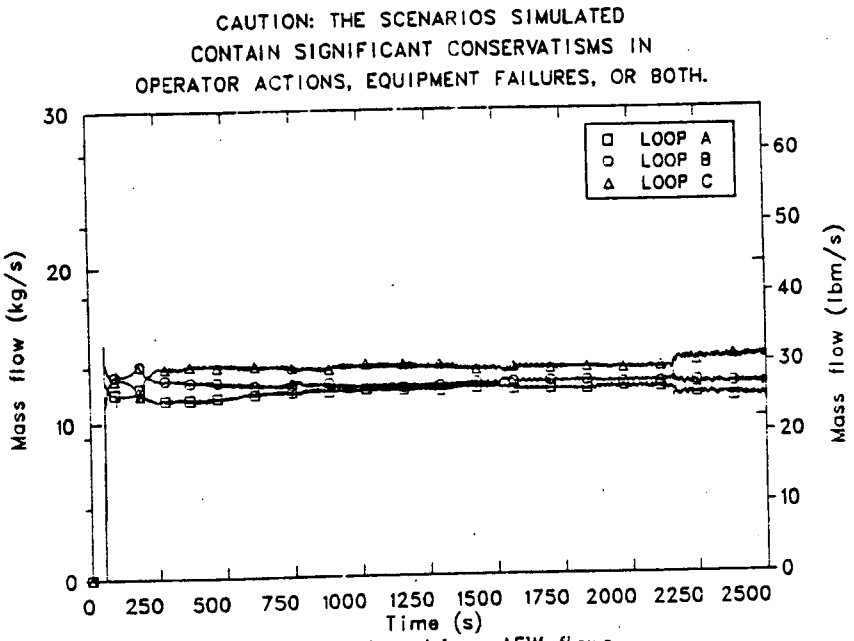

Figure 7-3. Scenario 4 motor driven AFW flows.

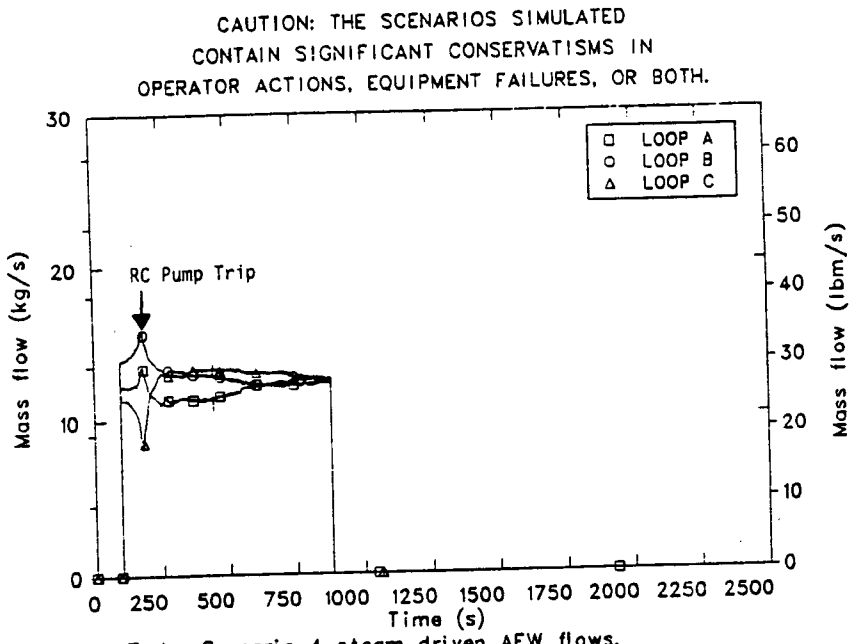

Figure 7-4. Scenario 4 steam driven AFW flows.

feedwater pumps. As each steam generator continued to lose mass inventory, a 2-out-of-3 narrow range low level signal (narrow range less than 15% of full span) activated the steam-driven auxiliary feedwater system.

Presented in Figure 7-5 are the steam generator mass inventories for the three loops. Each steam generator is characterized by approximately the same response with the mass inventories being somewhat larger in Steam Generators B and C since the feedwater lines to these two steam generators are shorter than that connected to Steam Generator A. Thus Steam Generators B and C received more auxiliary feedwater. During the initial 600 s of the transient each steam generator lost approximately 40% of its total mass inventory.

After approximately 600 s the steam generator pressures were reduced to 1.03 MPa (150 psia) such that the total auxiliary feedwater mass flow rate exceeded the mass flow rate through the steam dump valves. Thus, each steam generator began to refill. At 850 s the steam-driven auxiliary steam feedwater system was no longer available due to insufficient steam generator pressure needed to drive this system (Figure 7-4). Thereafter, each steam generator continued to refill as a consequence of the motor-driven feedwater system. At 2157 s the steam generator mass inventories exhibited slightly discontinuous behavior. This behavior was the result of renodalization of the steam generator boilers when the simulation was restarted at 2157 s. It was judged that this discontinuous behavior was not significant in affecting the overall system response. At the end of the simulation each steam generator was at saturation conditions at a pressure of 0.26 MPa (38 psia).

For a brief period of time the auxiliary feedwater flow contributed to increasing the energy removal between the primary and secondary sides. This enhanced removal rate occurred at approximately the time the steam-driven auxiliary feedwater system was activated (Figure 7-2). This additional flow approximately doubled the amount of liquid going to each steam generator. However, this enhanced cooldown continued only until the primary reactor coolant pumps were tripped at the pressurizer pressure

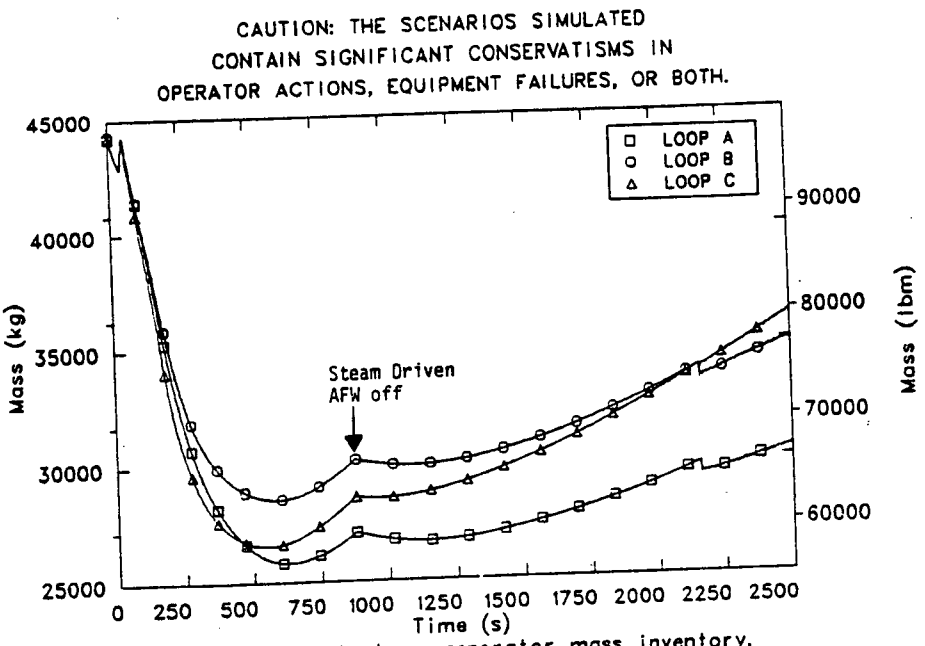

Figure 7-5. Scenario 4 steam generator mass inventory.

setpoint of 9.07 MPa (1315 psia). The subsequent primary coolant flow reduction resulted in an immediate reduction in primary to secondary heat transfer.

By 300 s the primary reactor coolant flow in all three loops had transitioned to natural circulation (Figure 7-6). During the remainder of the simulation the loop flows remained relatively stable at approximately 150 kg/s (330 lbs/sec). Generally, the natural circulation loop mass flowrates were at least an order of magnitude larger than either the HPI or CVCS flows (Figures 7-7 and 7-8). The mixing effects due to HPI were apparent from Figure 7-9, which presents the downcomer coolant temperature. At 1250 s there was a significant reduction in HPI flow, that induced approximately a 3.3 K (6.0°F) increase in the downcomer fluid temperature. Although, HPI contributed to cooling the primary fluid after 300 s, heat removal to the steam generators was the dominant mechanism by which the primary coolant temperature was reduced. Variations in CVCS injection did not significantly perturb the downcomer temperatures or produce significant temperature differences in the cold legs (only Loop B had CVCS injection).

Both the HPI and CVCS systems were responsible for the repressurization of the primary coolant system. Initially, the HPI was significantly larger than the CVCS mass flow rate. Prior to 1250 s the HPI flow was the principal cause for repressurization of the primary coolant. This condition changed around 1250 s when the primary pressure approached the HPI shutoff head (Figure 7-7). The increased primary system mass inventory eventually caused a repressurization of the primary system along with a refilling of the pressurizer (Figure 7-10). The refilling of the pressurizer led to anomalous behavior in both the primary pressure response and HPI injection mass flow rates. It was determined that this behavior was similar to the problems related to the simulation in Section 4.3.1. Uncertainties related to this problem are discussed in Section 7.3.2.

At 1250 s the pressurizer pressure reached a plateau of approximately 10 MPa (1450 psia). At this time the primary coolant shrinkage rate due to cooldown effects was balanced by approximately the same amount of liquid

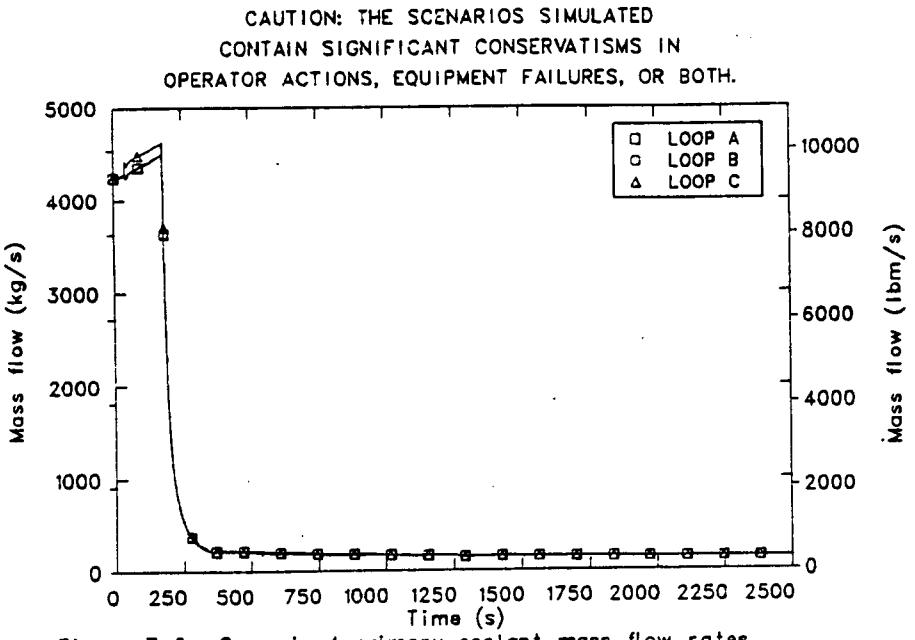

Figure 7-6. Scenario 4 primary coolant mass flow rates.

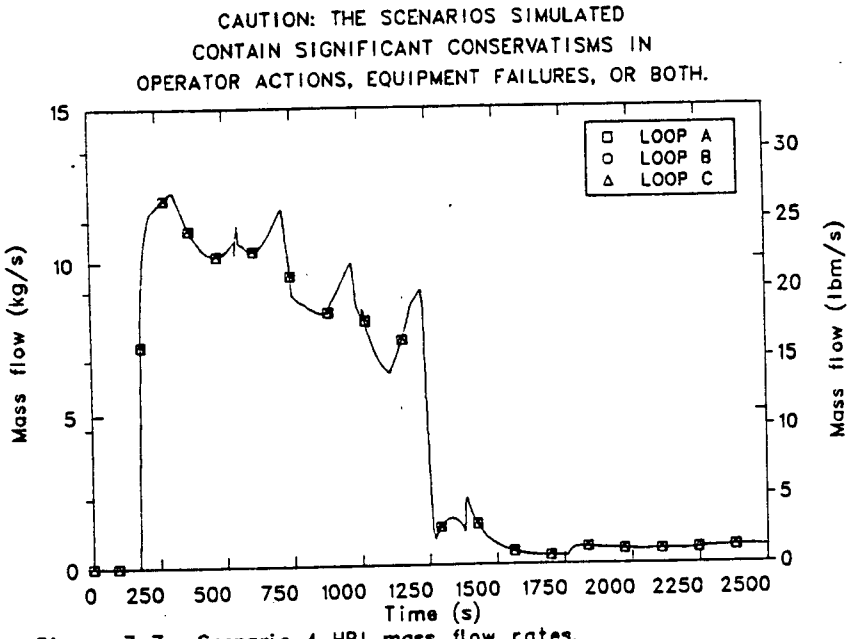

Figure 7-7. Scenario 4 HPI mass flow rates.

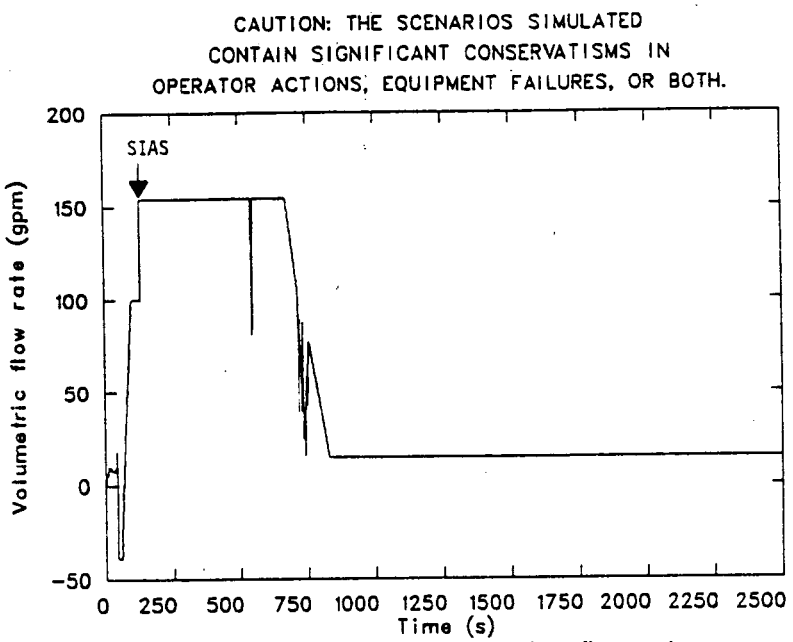

Figure 7-8. Scenario 4 CVCS net injection flow rate.

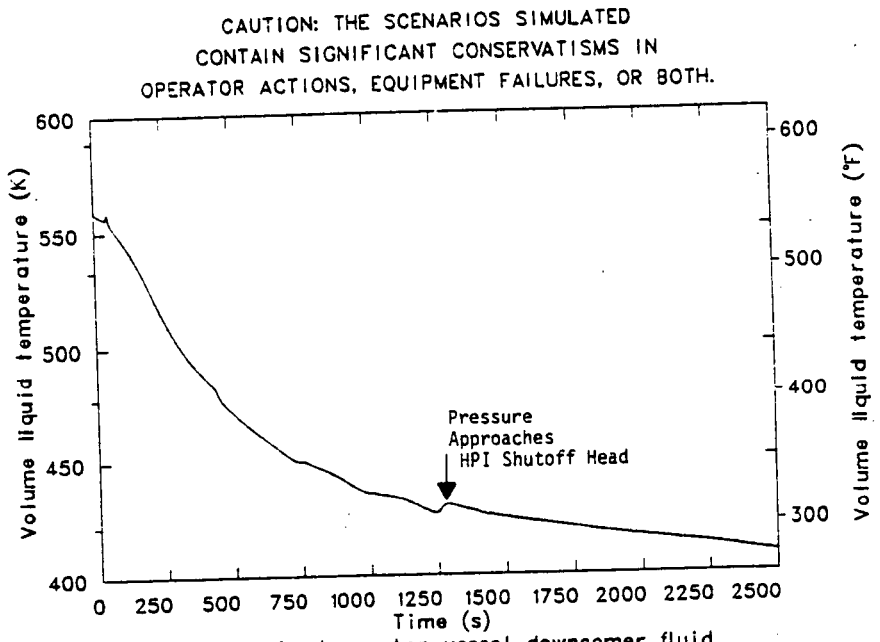

Figure 7-9. Scenario 4 reactor vessel downcomer fluid temperature.

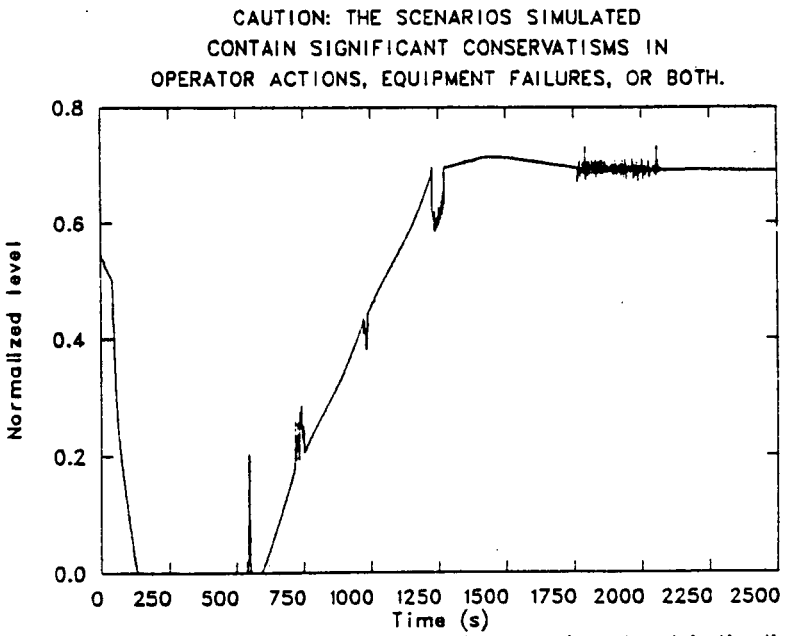

Figure 7-10. Scenario 4 normalized pressurizer level indication.

volume injected from the HPI and CVCS systems. During the remainder of the simulation the primary system pressure was maintained at approximately 10 MPa (1450 psia) as the primary system cooldown continued.

7.3.2 Extrapolations and Uncertainties

Figure 7-11 presents the extrapolated pressure response in the reactor vessel downcomer at an elevation adjacent to the top of the core. Part of the extrapolation includes the period from 750 to 1250 s when anomalous pressurizer pressure behavior occurred. Using the same methods employed in Section 4.3.1 the pressure response was recalculated out to the time which the pressurizer pressure reached a plateau.

At 4830 s primary side repressurization was predicted to occur at the time the steam generator secondary sides reached atmospheric pressure conditions and the secondary depressurization stopped. It was concluded that the core decay power matched the total steam generator heat removal rate. As a consequence, when the secondary depressurization and cooldown stopped, shrinkage of the primary coolant ceased. Continued CVCS injection then caused a gradual primary side repressurization. By 7200 s the system pressurized to 11.8 MPa (1711 psia) with an estimated uncertainty of 1.4 MPa (203 psia). The principal source of uncertainty in the final primary pressure was the estimated time at which the steam generators would blow down to atmospheric conditions.

Coincident with the stabilization of the secondary side conditions was a stabilization of the primary side downcomer and cold leg temperatures (Figures 7-12 and 7-13). After natural calculation had been established in the primary coolant loops the temperatures of the fluid exiting the primary side steam generator outlets were approximately equal to the secondary side steam generator boiler saturation temperatures. It was concluded this trend would persist out to 7200 s. This is because of relatively low primary loop mass flows and because the core decay power out to 7200 s is adequate to maintain the liquid in the steam generator boiler sections at saturation conditions. At 4830 s when the steam generators reached atmospheric conditions both the downcomer and cold leg temperatures were

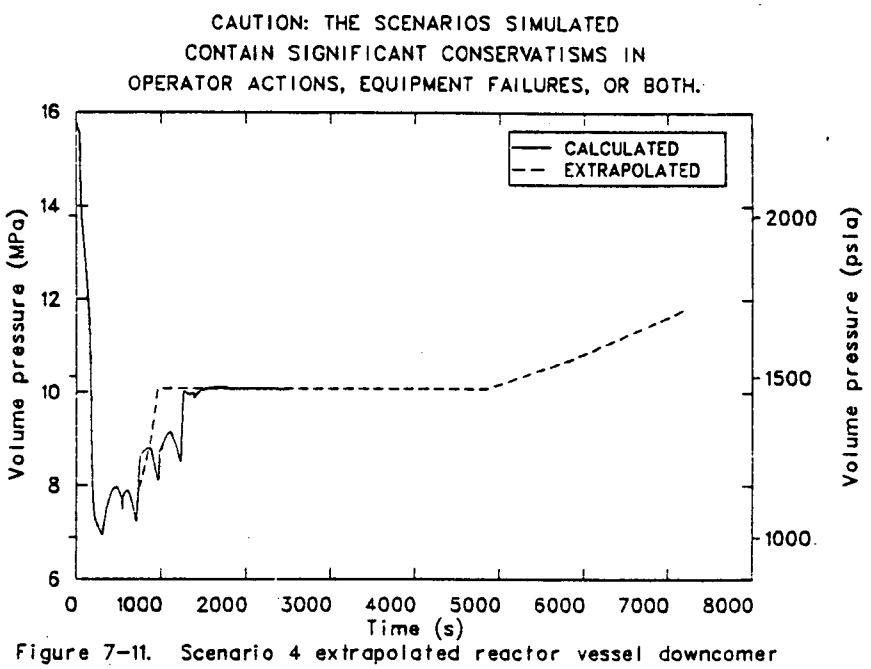

Figure 7-11. Scenario 4 extrapolated reactor vessel downcomer pressure.

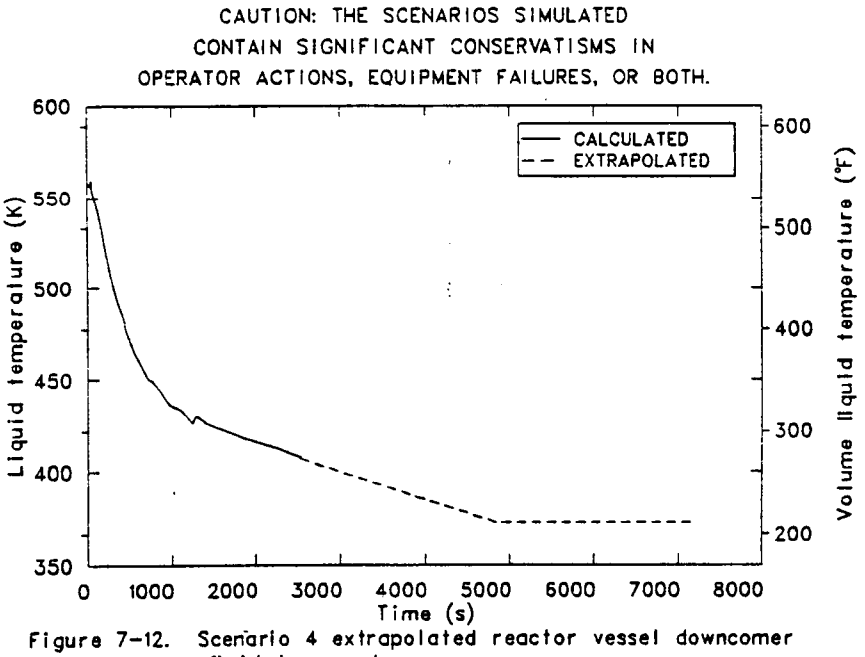

Figure 7-12. Scenario 4 extrapolated reactor vessel downcomer fluid temperature.

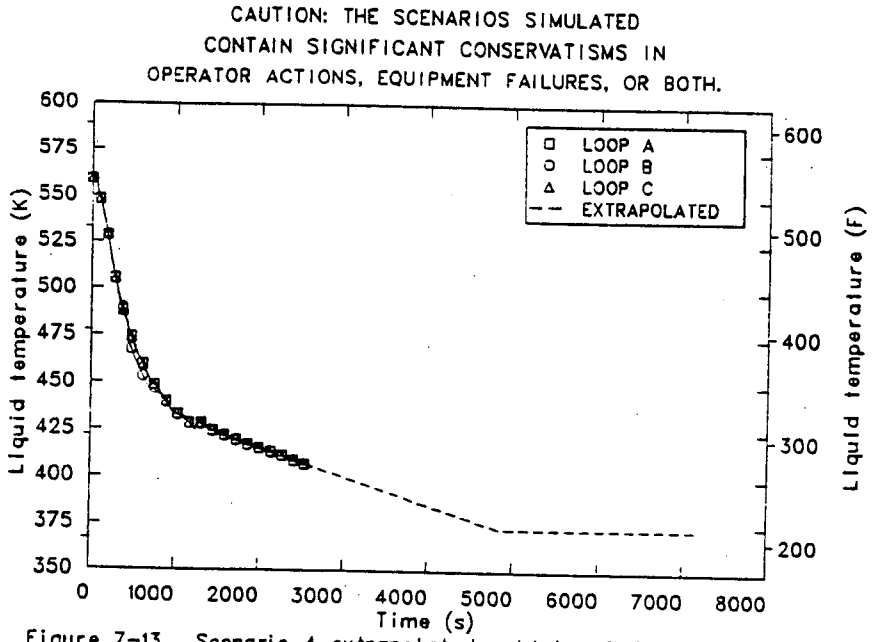

Figure 7-13. Scenario 4 extrapolated cold leg fluid temperatures.

estimated to stabilize at 373 K (212°F). This temperature corresponds to atmospheric saturation conditions without accounting for the steam generator boiler hydrostatic head effects which would slightly increase the boiler saturation temperature.

The extrapolated primary cold leg temperatures were symmetric as a consequence of nearly symmetric secondary side conditions. The temperature mixing effects caused by CVCS injection into Loop B were not significant. This is because the loop natural circulation mass flow rate is much greater than the CVCS mass flow rate. The minimum downcomer/cold leg temperatures were extrapolated to 373 K (212°F) with an estimated uncertainty of +5 K (9.8°F). The principal uncertainty in estimating the extrapolated downcomer and cold leg temperatures responses was a function of when the steam generator secondaries reach atmospheric conditions.

The extrapolated values for the cold leg loop flows and downcomer heat transfer coefficient were maintained at the values calculated at 2500 s (Figures 7-14 and 7-15). These estimates were made using the assumption that the primary system density gradients that drive the natural circulation loop flows would not significantly change in the 2500 to 7200 s period. The extrapolated cold leg mass flow rates and downcomer heat transfer coefficient had uncertainties as a consequence of the assumption that the primary system density gradients did not significantly change from 2500 to 7200 s. These extrapolations are biased on the high side since both the loop flows and downcomer heat transfer coefficients decrease as a consequence of core power decay and secondary side stabilization.

7.4 Conclusions

The simulation of Scenario 4 indicated that the primary coolant system initially experienced a rapid cooldown and depressurization until about 300 s, followed by a gradual cooldown as natural circulation continued and heat was transferred to the steam generators. As a consequence of CVCS and HPI operation, partial recovery of the primary system pressure occurred. The minimum downcomer fluid temperature and subsequent maximum pressure were extrapolated to 373 K (212°F) and 11.8 MPa (1711 psia) at 7200 s respectively.

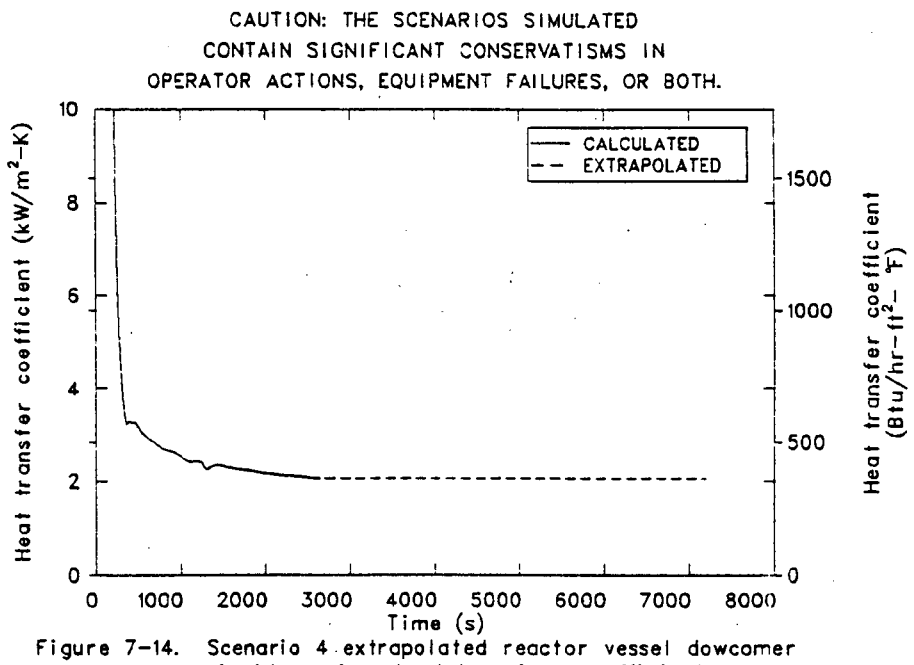

Figure 7-14. Scenario 4 extrapolated reactor vessel dowcomer inside surface heat transfer coefficient.

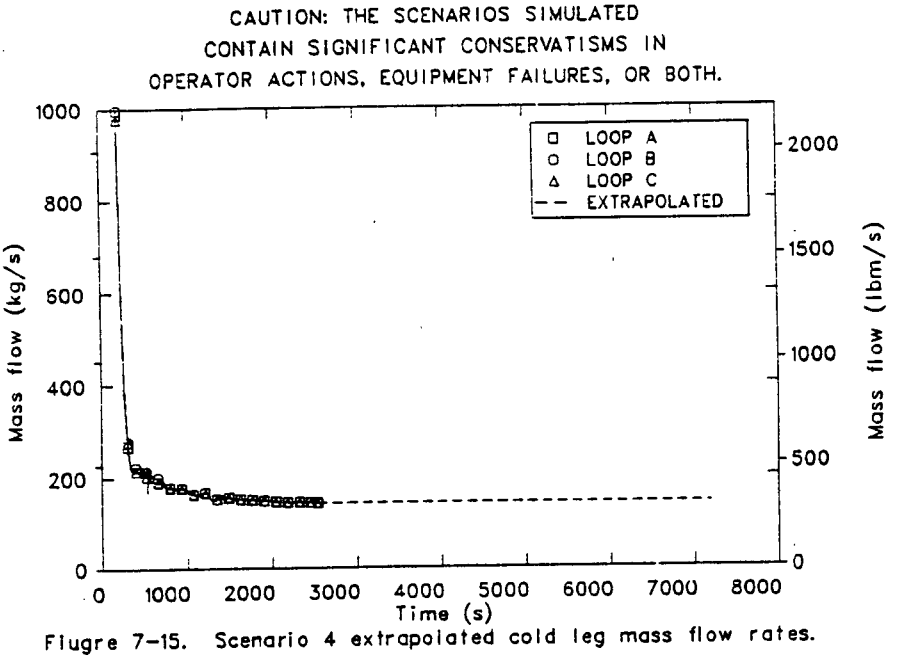

Flugre 7-15. Scenario 4 extrapolated cold leg mass flow rates.

The temperature responses in all three loops were characterized as being relatively symmetric throughout the simulation. The principal mechanism for the cooldown of the primary coolant was natural circulation.

By extrapolating the simulation results to 7200 s it was found that the primary system was maintained in a natural circulation cooldown mode with the downcomer and cold leg fluid temperatures stabilizing at approximately 4830 s.

8. SCENARIO 5, OVERFEED WITH AUXILIARY FEEDWATER AT FULL POWER

The following section describes the investigation of Scenario 5. This calculation was performed to evaluate the consequences of a postulated steam generator overfeed with auxiliary feedwater with the reactor at full power conditions.

A description of the scenario is provided in Section 8.1, followed by a discussion of the model changes required to perform the calculation in Section 8.2. The results of the calculation, the extrapolated results, and the uncertainties with the calculation are described in Section 8.3. The conclusions regarding the calculation are presented in Section 8.4.

Scenarios investigated in this report generally include conservative assumptions concerning equipment failures, operator actions, or combinations of these. Conclusions relative to pressurized thermal shock severity are not to be drawn directly from the results presented in this report (see Section 15).

8.1 Scenario Description

Table 8-1 gives the description of the desired scenario as supplied by ORNL. The transient was initiated from full power steady state conditions by tripping both main feedwater (MFW) pumps. The auxiliary feedwater (AFW) pumps failed to start when first demanded but, at 8 minutes into the transient, both motor and turbine driven auxiliary feedwater pumps were manually started and set to provide maximum flow. The auxiliary feedwater was terminated when the void fractions in the volumes representing the steam domes of all the steam generators dropped below 50%. This cutoff point simulated the time when liquid carryover would be observed in the steam line.

All other control systems operated in their automatic modes.

TABLE 8-1. SCENARIO DESCRIPTION NO. 5

Plant Initial State - Just prior to transient initiator

General Description: 100% Power steady state

System Status

Turbine: Automatic control
Secondary PORV: Automatic control
Steam Dump Valves: Automatic control
Charging System: Automatic control
Pressurizer: Automatic control
Engineering Safety Features: Automatic control
PORVs: Automatic control
Reactor Control: Automatic
Main Feedwater: Automatic control
Aux Feedwater: Automatic control
MSIVs: Open, Automatic control
MFIVs: Open, Automatic control

Transient Initiator - Both Main Feedwater pumps trip simultaneously.

Equipment Failures which occur during the transient if the equipment is demanded.

Aux feedwater pumps fail to start.

Operator Reactions to Reported Information

1. Operator initiates actions to correct Aux flow problem and restarts all AFW pumps to provide max flow at 8 minutes. Aux feedwater flow at maximum to all 3 steam generators, and all AFW pumps started (Feedwater source: Condensate tank)).

2. Stop all AFW flow when liquid carryover is observed in the main steamlines.

8.2 Model Changes

No changes in the hydrodynamic model were necessary. The only changes in the model were the trips which controlled the main feedwater pumps, turbine trip, and the auxiliary feedwater system. The changes to the main feedwater pump and the auxiliary feedwater control systems implement the scenario described above.

8.3 Results

This section is divided into two subsections. The first presents the calculated results, and the second extrapolates the calculated results to two hours, and discusses uncertainties associated with the calculation and extrapolation.

8.3.1 Calculation Results

The sequence of events for this transient is presented in Table 8-2. The transient was initiated by tripping both MFW pumps. This trip caused an immediate turbine trip which then tripped reactor power. The steam control valve closed by 1 s, simulating the closure of the turbine isolation valve. Also at 1 s, the steam dump valves opened on a load rejection signal. Hot leg temperatures dropped immediately as core power dropped. This cooldown shrank the primary system fluid volume and caused an outsurge from the pressurizer, which in turn caused primary system pressure to fall, as shown in Figure 8-1. At 3 s, the pressurizer heaters came on as a result of the drop in pressure.

At 4 s, the steam dump valves were closed as shown in Figure 8-2 and at 29 s were modulated open to control the primary system average temperature to 559 K (547°F). The primary pressure continued to fall until approximately 90 s, at which time the pressurizer heaters overcame the effect of the cooldown, and primary system pressure began to rise. It rose steadily until it reached the heater control point of 15.6 MPa (2270 psia) at 674 s. The pressurizer heaters then cycled on and off to hold the pressure at that point. The primary system pressure never dropped low

TABLE 8-2. SCENARIO 5 SEQUENCE OF EVENTS

Time (s)	Event
0	Tripped MFW pumps; turbine tripped; reactor tripped
1	Turbine isolation valve closed; steam dump valves opened on load rejection; proportional pressurizer heaters turned on
3	Backup pressurizer heaters turned on
4	Steam dump valves closed
5	Main feedwater valves closed
29	Steam dump valves opened
480	AFW, motor and turbine, turned on manually
674	Backup pressurizer heaters turned off (cycle on and off until approximately 950 s)
784	AFW shifted to SGC
854	Steam dump valves closed
880	High Tave dropped below 547°F, steam dump control shifted from plant trip control (PTC) to steam pressure control (SPC)
970	AFW flow shifted to SGB; pressurizer proportional heaters turned off
991	Pressurizer sprays turned on (cycle on and off until approximately 1100 s)
1540	AFW flow splits between all 3 SGs
1924	AFW flow shifts to SGA
1976	Pressurizer heaters turned off on low pressurizer level
2015	SIAS signal on high differential pressure between Steam Line A and header; letdown flow isolated

TABLE 8-2. (continued)

Time (s)	Event
2352	SGA filled and isolated; AFW flow shifted to SGB
2693	SGB filled and isolated; AFW flow shifted to SGC
3027	SGC filled and isolated; AFW flow turned off
3131	Pressurizer spray turned on
3201	Makeup flow at minimum value
3600	End of calculation

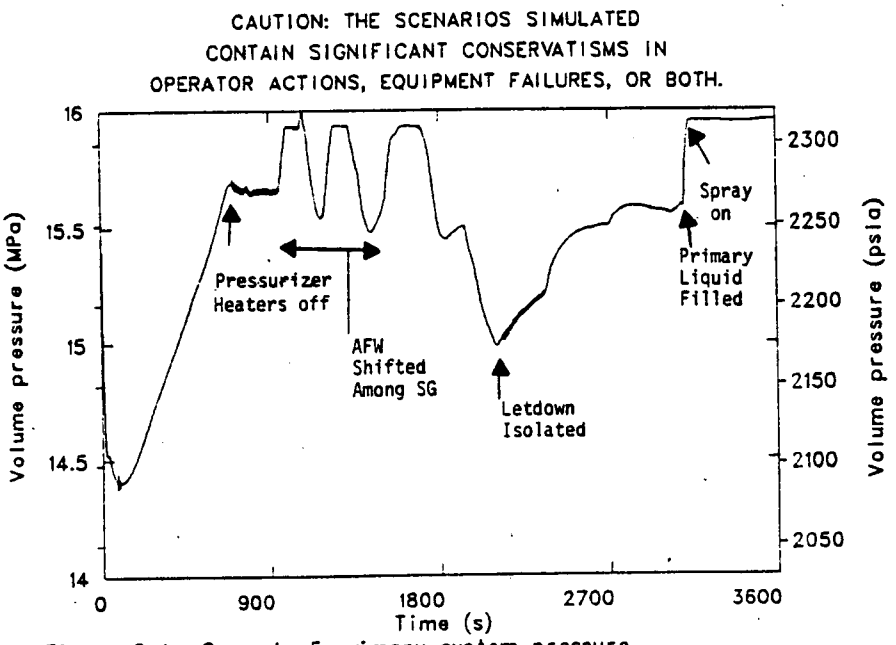

Figure 8-1. Scenario 5 primary system pressure.

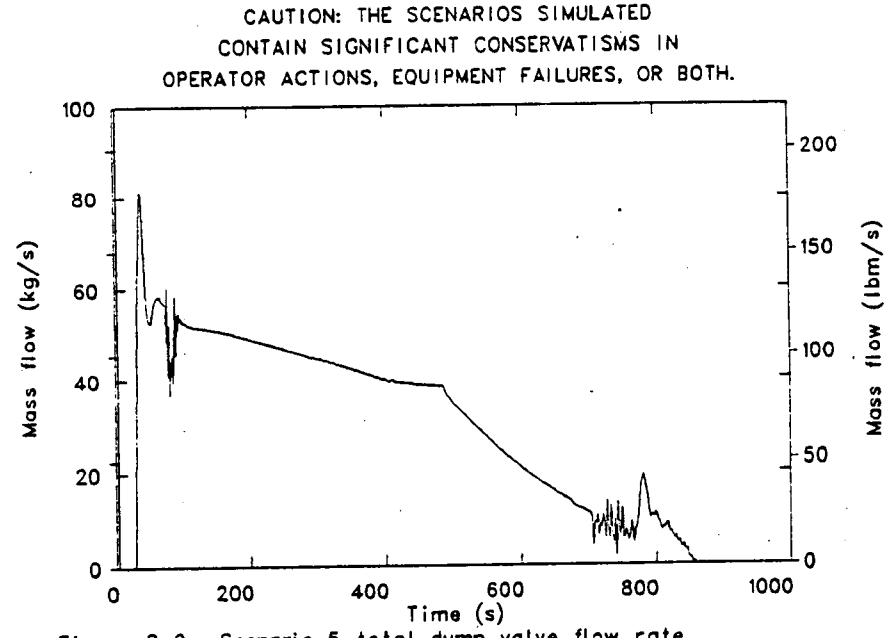

Figure 8-2. Scenario 5 total dump valve flow rate.

enough to turn on the HPI, or trip off the reactor coolant pumps. Figure 8-3 presents the three cold leg flow rates.

Energy removal out the steam dump valves kept the primary system temperatures near 560°F (548°F) from 29 to 480 s. At 480 s, AFW flow was initiated (see Figure 8-4). The initial AFW fluid did not cause a significant cooldown in the primary system. This was because the fluid initially injected to the steam generators was the relatively warm fluid which had stagnated in the feedwater lines. Figure 8-5 shows the feedwater temperatures for each of the steam generators. As more cold AFW fluid was injected into the feedwater lines, the temperatures in the lines dropped, and colder water was injected into the steam generators.

During this stage of the transient, the liquid levels in the steam generators were below the elevation of the feedwater ring. As a result, the feedwater was injected into steam filled volumes. At 784 s, the temperature of the feedwater entering Steam Generator C had dropped to the point where it induced an increase in condensation in that generator, and dropped the pressure slightly. This drop in pressure diverted all the AFW flow from the two other steam generators and delivered it all to Steam Generator C. This extra flow dropped the feedwater temperature even further, and kept the generator pressure depressed. At 970 s, the volume which received the feedwater flow in Steam Generator C filled with liquid, and the condensation induced depressurization ended. The AFW flow then diverted to Steam Generator B. At 1300 s the feedwater injection volume filled in Steam Generator B and the AFW flow shifted to Steam Generator A. At 1540 s the same volume filled in Steam Generator A and the AFW flow split between the three steam generators.

Figure 8-5 shows the total energy transferred from the primary system to all three steam generators. As the flow shifted between generators, different temperature water was delivered to one of the generators, therefore total heat transfer changed. Also, there was a time lag between when cold feedwater was injected into the top of the steam generator downcomer, and when it arrived at the tube bundle. The result of these

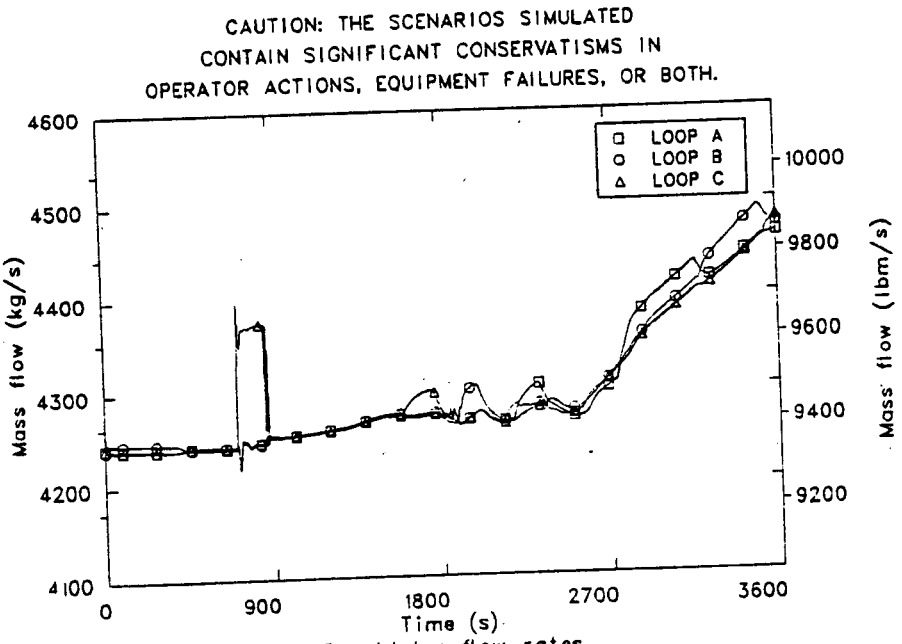

Figure 8-3. Scenario 5 cold leg flow rates.

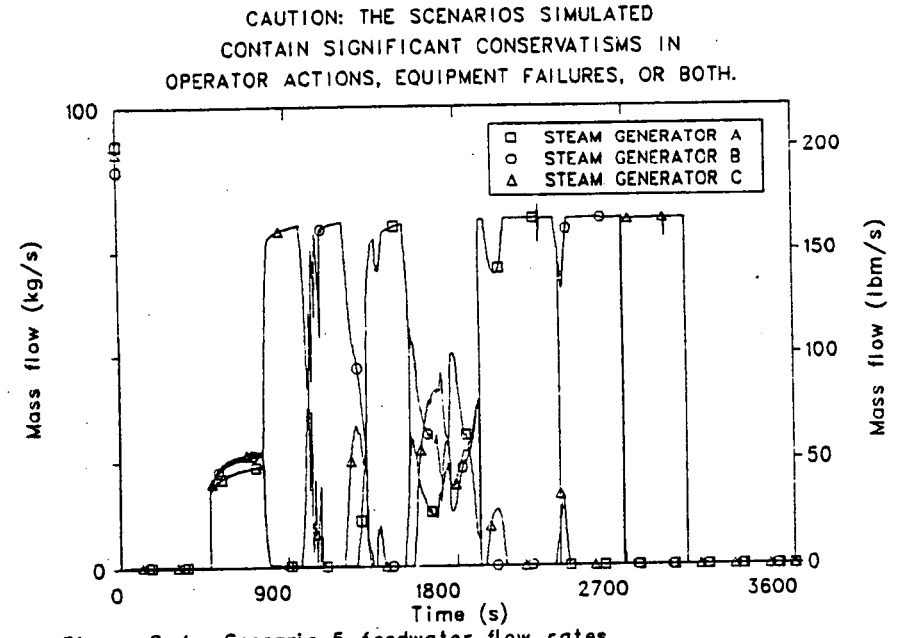

Figure 8-4. Scenario 5 feedwater flow rates.

CAUTION: THE SCENARIOS SIMULATED
CONTAIN SIGNIFICANT CONSERVATISMS IN
OPERATOR ACTIONS, EQUIPMENT FAILURES, OR BOTH.

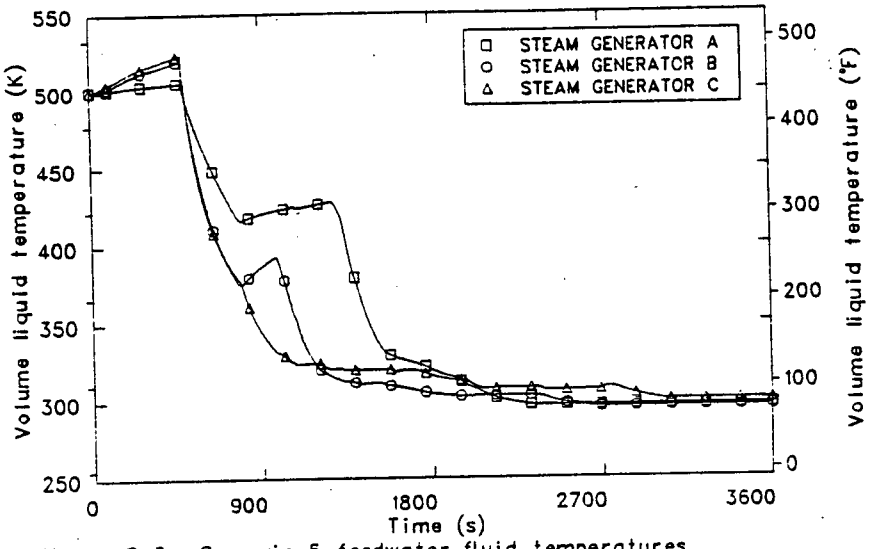

Figure 8-5. Scenario 5 feedwater fluid temperatures.

shifts in feedwater flow and temperatures were the oscillations seen in Figure 8-6. These oscillations in energy removal rate caused the oscillations seen in the downcomer and cold leg temperatures between 900 and 1800 s, as shown in Figures 8-7 and 8-8. The oscillations in primary system temperature caused the oscillations in primary pressure over the same time interval by alternating swelling and shrinking the primary fluid. The oscillations are also seen in the pressurizer liquid level, shown in Figure 8-9. The changes in primary system pressure were limited by the pressurizer heaters and sprays, which turned on and off throughout this period as determined by their respective controllers.

By 1800 s, the effects of the shifting AFW flows damped out as all the warm water in the feedwater lines was flushed out. The AFW flows shifted around again between 1924 and 3027 s due to condensation induced pressure drops, but since the feedwater temperatures to all the steam generators were the same, it made no difference which generator received the feed flow. Between 1800 and 3027 s, the primary system experienced a gradual cooldown as energy was removed from the primary system by the cold AFW flow. The pressurizer heaters attempted to recover the drop in primary system pressure associated with this cooldown until 1976 s, when the heaters were shut off on low pressurizer level.

At 2015 s, the A steam generator was receiving all the AFW flow, and that flow caused a sufficient depressurization in the A steam line to cause an SIAS signal on high ΔP between the A steam line and the steam header. The only significant result of the SIAS signal was that the letdown flow was isolated. This resulted in a net increase of 3.3×10^{-3} m^3/s (54 gpm) in the makeup flow. This increase in flow was sufficient to overcome the volumetric shrink as the primary system cooled, and therefore, pressurizer level began to increase and primary system pressure began to rise.

Figure 8-10 shows the narrow range liquid levels of the three steam generators. At 2352 s Steam Generator A filled with water, and feedwater to that generator was isolated. Steam Generator B filled and isolated at 2693 s, and Steam Generator C filled and isolated at 3027 s. After Steam

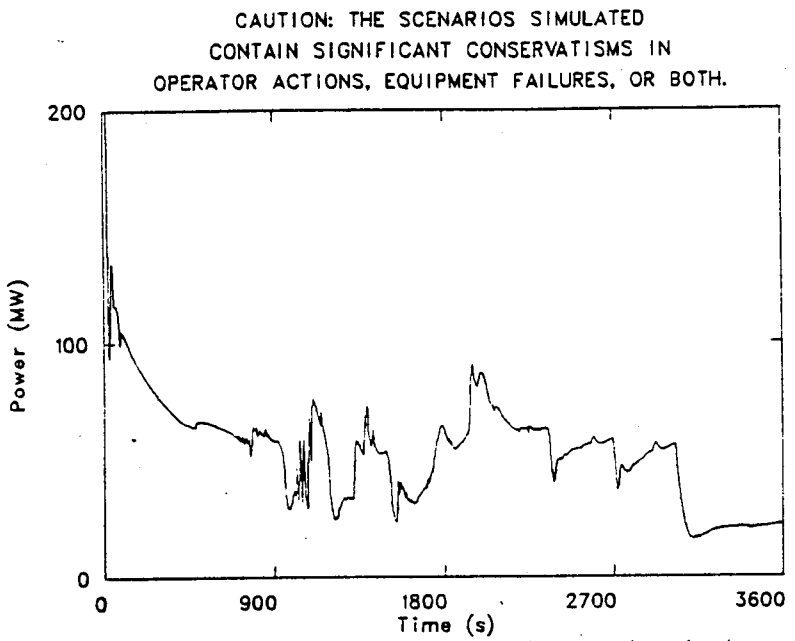

Figure 8-6. Scenario 5 total primary to secondary heat transfer.

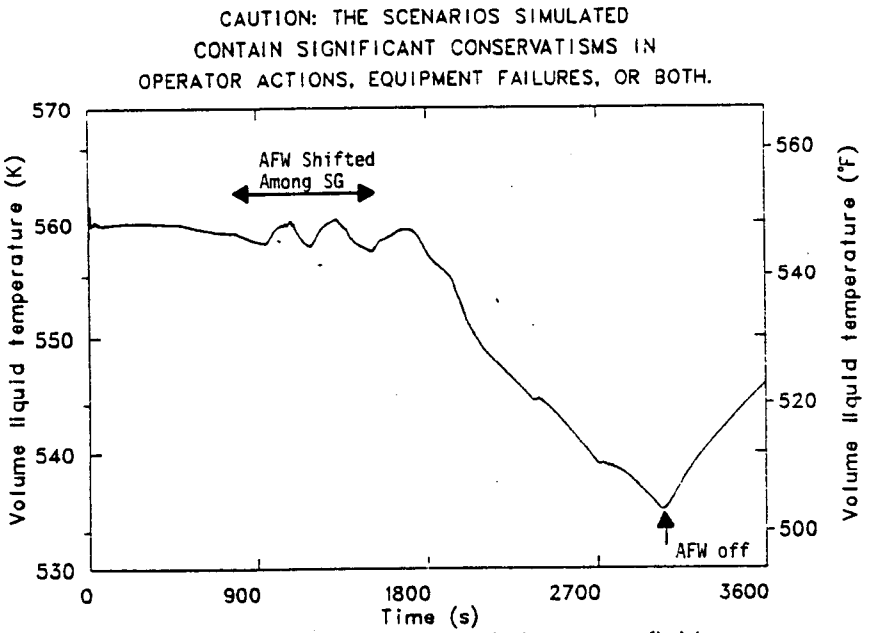

Figure 8-7. Scenario 5 reactor vessel downcomer fluid temperature.

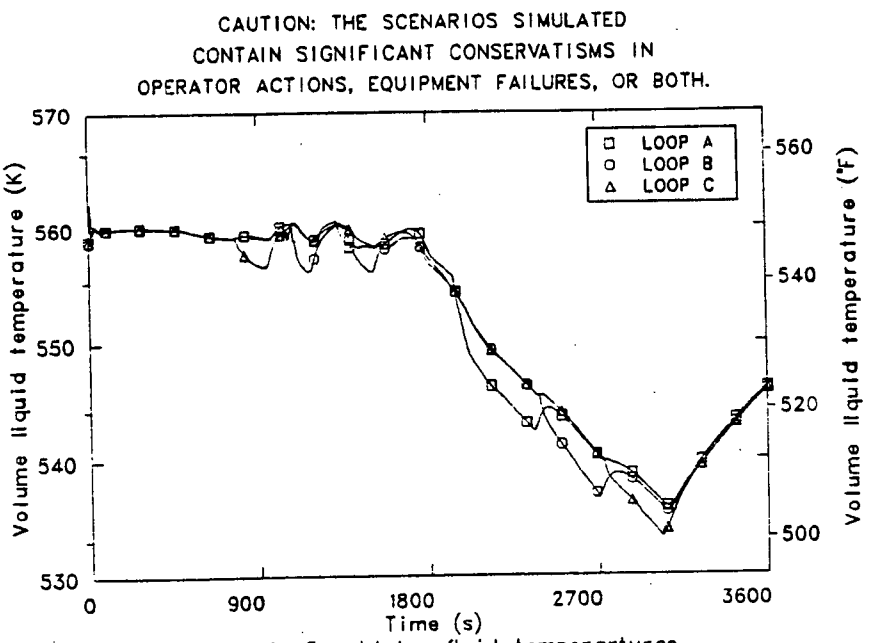

Figure 8-8. Scenario 5 cold leg fluid temperartures.

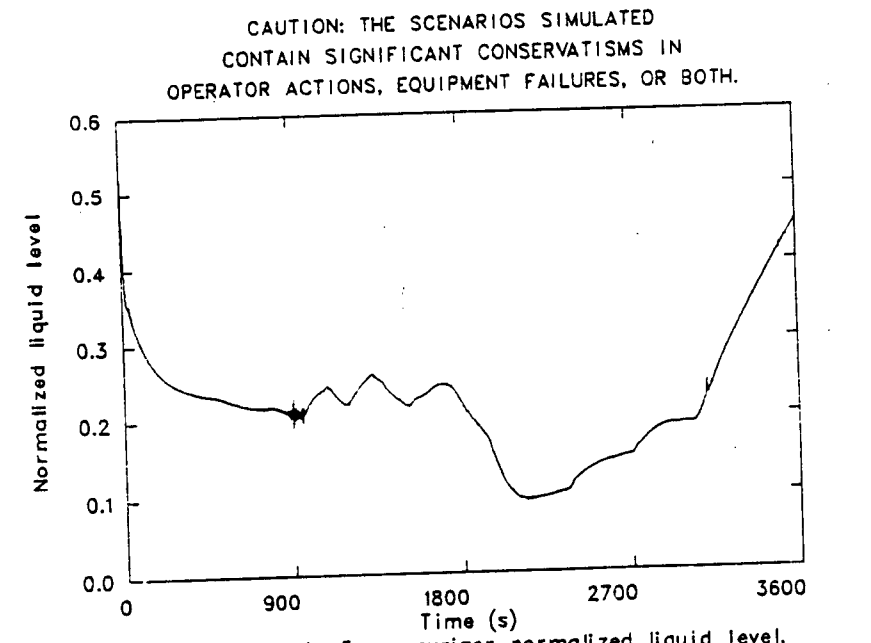

Figure 8-9. Scenario 5 pressurizer normalized liquid level.

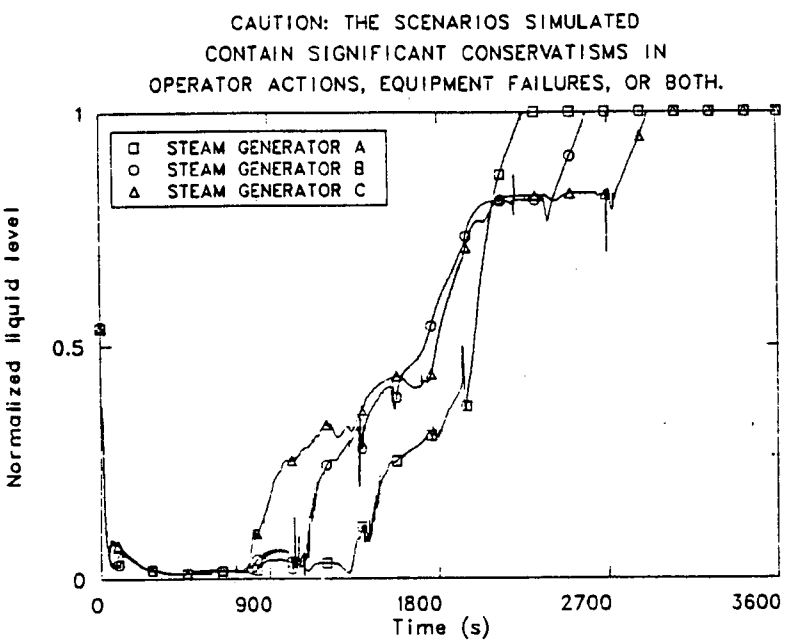

Figure 8-10. Scenario 5 steam generator narrow range normalized liquid levels.

Generator C isolated, all AFW flow was stopped, and the energy transferred out of the primary system dropped immediately. As a result, primary system temperatures started to rise. Primary system pressure also started to rise more rapidly as the heatup caused an insurge into the pressurizer. At 3131 s, pressurizer sprays came on and held the primary system pressure at approximately 16.0 MPa (2320 psia). At the end of the calculation, 3600 s, primary system pressure was stable at 16.0 MPa (2320 psia) and the reactor vessel downcomer fluid temperature was at 546 K (523°F) and rising steadily.

8.3.2 Extrapolations and Uncertainties

Figures 8-11 and 8-12 show the downcomer pressure and temperature extrapolated to 7200 s. Pressurizer sprayer capacity is sufficient to control primary system pressure during the heatup experienced at the end of this transient. Therefore, the primary system pressure would stay at approximately 16.0 MPa (2320 psia) through 7200 s. Primary and secondary system temperatures would stay closely coupled and would rise until the secondary pressure reached 7.03 MPa (1020 psia) at about 4600 s, at which time the steam dump valves would open to hold steam generator pressure at that point. This pressure corresponds to a saturation temperature of 559 K (547°F). The primary temperature would therefore rise until it reached 559 K (547°F) and then stay there through 7200 s. The cold leg temperatures would be essentially the same as the downcomer temperature through 7200 s because the primary coolant pumps would stay on. Cold leg flow rates would also stay nearly constant through 7200 s because of primary coolant pump operation. Figure 8-13 shows the heat transfer coefficient at the outer wall of the downcomer, extrapolated to 7200 s.

There were no major uncertainties associated with the calculation.

8.4 Conclusions

This transient was mild primarily for two reasons. The primary system never depressurized enough to initiate HPI or to trip the RCPs. Because no HPI was injected the primary system did not cool as quickly, and more importantly, because the RCPs did not trip, the primary fluid was kept well

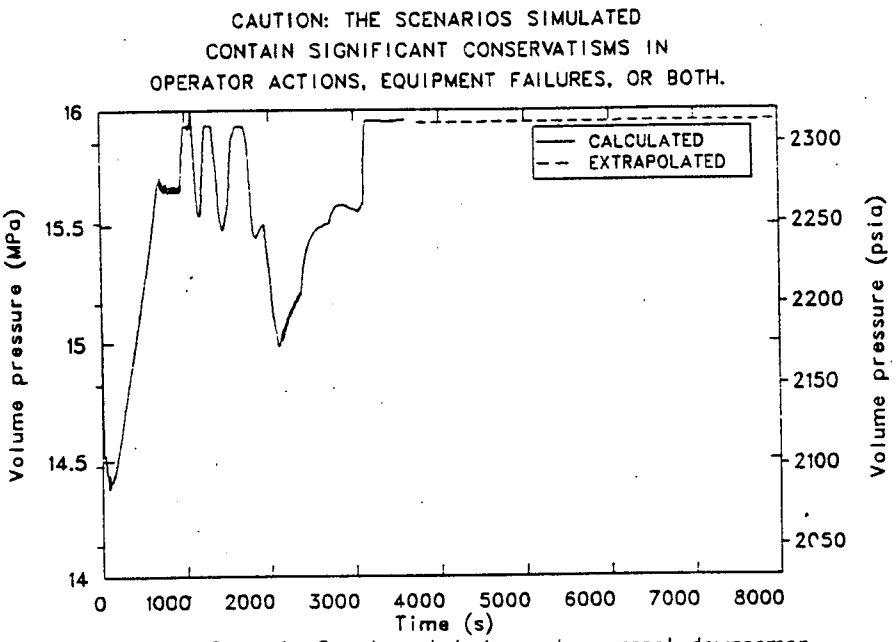

Figure 8–11. Scenario 5 extrapolated reactor vessel downcomer pressure.

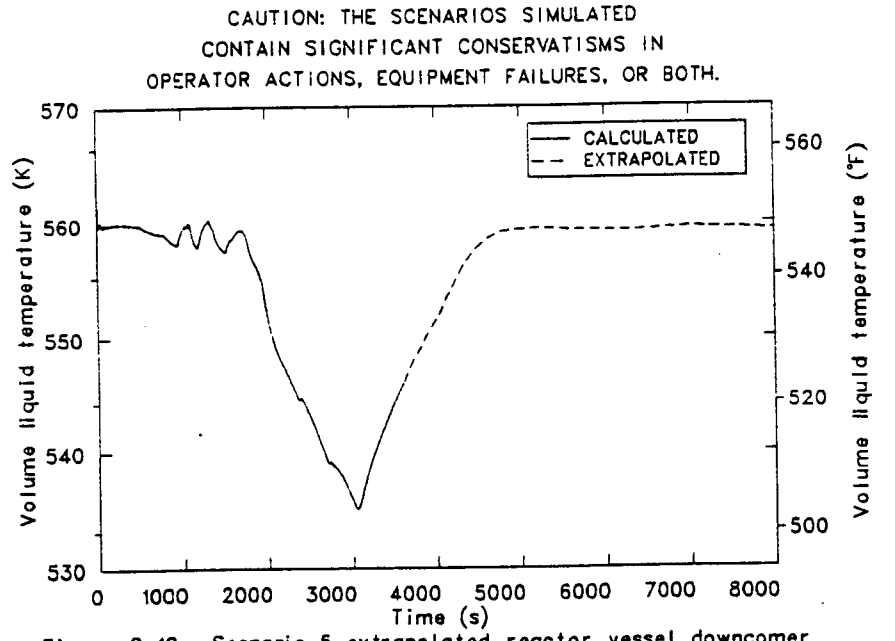

Figure 8–12. Scenario 5 extrapolated reactor vessel downcomer fluid temperature.

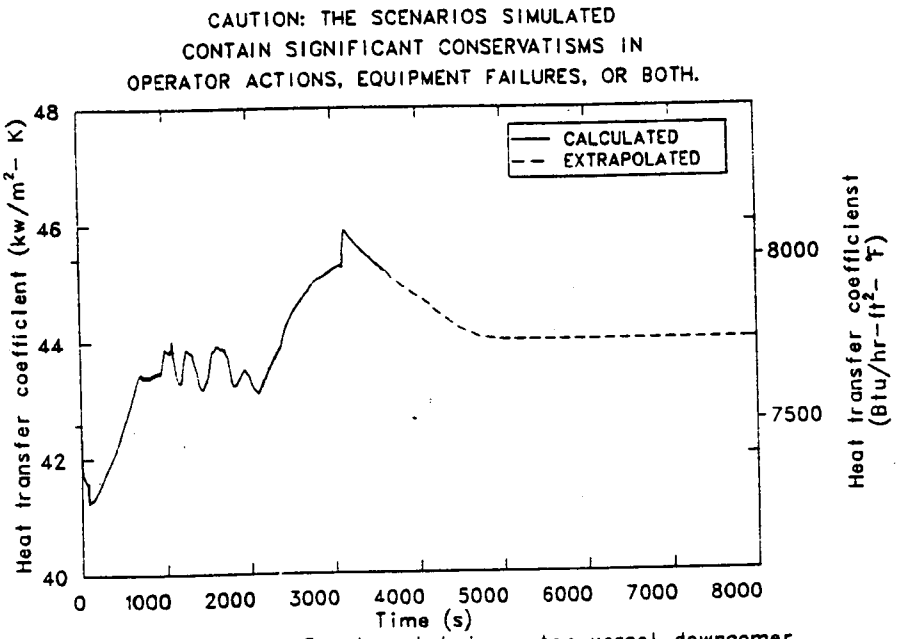

Figure 8-13. Scenario 5 extrapolated reactor vessel downcomer heat transfer coefficient.

mixed throughout the transient. Secondly, the AFW flow rates were not sufficiently large to cause a serious cooldown. The minimum reactor vessel downcomer temperature reached was 535 K (503°F), and occurred at 3027 s. The maximum reactor vessel downcomer pressure after this time was 16.0 MPa (2320 psia). After extrapolating the results out to 7200 s, the downcomer pressure and temperature would be 16.0 MPa (2320 psia) and 559 K (547°F) respectively.

9. SCENARIO 6, SMALL HOT LEG BREAK AT FULL POWER

The following section presents the transient scenario description, modeling changes effected to perform this calculation, detailed analysis of the transient results, extrapolations and uncertainty analyses, and conclusions drawn from the analysis for Scenario 6; a small hot leg break at full power.

Scenarios investigated in this report generally include conservative assumptions concerning equipment failures, operator actions, or combinations of these. Conclusions relative to pressurized thermal shock severity are not to be drawn directly from the results presented in this report (see Section 15).

9.1 Scenario Description

The transient is initiated from full power steady state (nominal temperature and pressure), and all control systems are in automatic control. The transient is initiated by a 0.0635 m (2.5 in.) diameter hole appearing in the bottom of the horizontal section of the C loop hot leg, just upstream of the pressurizer surge line connection. It is assumed that all systems operate automatically as designed. The only operator actions assumed to take place are: (1) trip the reactor coolant pumps when the primary pressure reaches 9.1 MPa (1315 psia) if a SIAS signal has been generated, (2) throttle auxiliary feedwater flow to maintain a 40% narrow range level in each of the steam generators. A transient scenario is provided in Table 9-1.

9.2 Model Changes

Changes made to the steady state model to initiate the small hot leg break included the addition of a break valve in the C loop hot leg connected to a time dependant volume set at atmospheric conditions. The break components were set to represent a break at the bottom of the hot leg pipe. The valve was set to open at the initiation of the transient.

TABLE 9-1. SCENARIO DESCRIPTION NO. 6

Plant Initial State - Just prior to transient initiator

General Description: 100% Power steady state
System Status
- Turbine: Automatic control
- Secondary PORV: Automatic control
- Steam Dump Valves: Operative/Automatic control
- Charging System: Automatic control
- Pressurizer: Automatic control
- Engineering Safety Features: Automatic control
- PORVs: Automatic control
- Reactor Control: Automatic
- Main Feedwater: Automatic control
- Aux Feedwater: Automatic control
- MSIVs: Open, Automatic control
- MFIVs: Open, Automatic control

Transient Initiator - A 2.5-in. hole appears in the hot leg.

Equipment Failures which occur during the transient if the equipment is demanded.

None

Operator Reactions to Reported Information

1. If SIAS signal is generated, the operator will trip the reactor coolant pumps when RCS pressure reaches 1300 psig.

2. The operator will throttle AFW flow to maintain 40% S/G level.

9.3 Results

This section presents the results, and extrapolations and uncertainties of the small hot leg break transient at full power.

9.3.1 Calculation Results

A sequence of events of the transient is provided in Table 9-2.

The small break was assumed to occur at time zero in the bottom of the Loop C hot leg. The primary system rapidly depressurized as shown in Figure 9-1. Both the proportional and backup heaters were turned on to recover the pressure. Also, as a result of the break, the pressurizer level rapidly decreased, as shown in Figure 9-2, and the makeup flow increased to compensate for the lost liquid inventory.

At approximately 16 s, the reactor tripped on a 2/3 reactor over-temperature delta T signal. The turbine stop valves closed and secondary pressures began to increase as shown in Figure 9-3. The primary depressurization rate increased due to the rapid reduction in core power and a lag in the response of the primary to secondary heat removal rate as shown in Figure 9-4. The steam dump control system changed from load rejection mode to plant trip control mode at the time of reactor trip to bring the plant average temperature down to 559 K (547°F). The steam dump valves opened and closed as shown in Figure 9-5, due to a large mismatch between the plant average temperature and the temperature setpoint in the plant trip control mode, and an undershoot of a lead-lag controller in the plant trip control system logic.

Also as a result of reactor trip, the break mass flow rate increased as shown in Figure 9-6. This increase was due primarily to an increase in the pressurizer surge line outflow rate. At the time of reactor trip the primary system depressurized, however, the pressurizer did not depressurize as fast due to the energized pressurizer heaters trying to maintain 15.5 MPa (2250 psia). This increased the driving potential of the fluid in

TABLE 9-2. SCENARIO 6 SEQUENCE OF EVENTS

Time (s)	Event
0.0	0.0635 m. (.2083 ft) diameter break appeared in bottom of C loop hot leg. Primary system depressurizes and pressurizer heaters energized.
16	Reactor tripped on 2/3 reactor over-temperature ΔT signal. Turbine stop valves close. Steam dump system switches to plant trip control mode.
25	Pressurizer heaters are deenergized due to pressurizer level dropping below 14.4% of measured level.
27	SI signal received on low pressurizer pressure, main feedwater pumps trip, main feed valves close, motor-driven auxiliary feedwater initiated.
40	HPI flow initiated, steam-driven auxiliary feedwater initiated.
50	Pressurizer empty, steam dump valves open.
55	Reactor coolant pumps trip, vessel upper head begins to void.
295	Tave dropped below 559 K (547°F), steam dump system switched to steam pressure control mode, steam dump valves close.
400	Hot legs and steam generator tubes void, natural circulation to Loops A and B stopped.
607	Auxiliary feedflow to Steam Generator C stopped due to 40% narrow range level criteria.
849	Auxiliary feedflow to Steam Generator B stopped due to 40% narrow range level criteria.

TABLE 9-2. (continued)

Time (s)	Event
989	Auxiliary feedflow to Steam Generator A stopped due to 40% narrow range level criteria.
1000	Natural circulation to Loop C stopped.
2440	Accumulator flow initiated.
2800	Transient terminated. Reactor vessel downcomer pressure and temperature are 3.6 MPa (522 psia), 362 K (193°F) respectively.

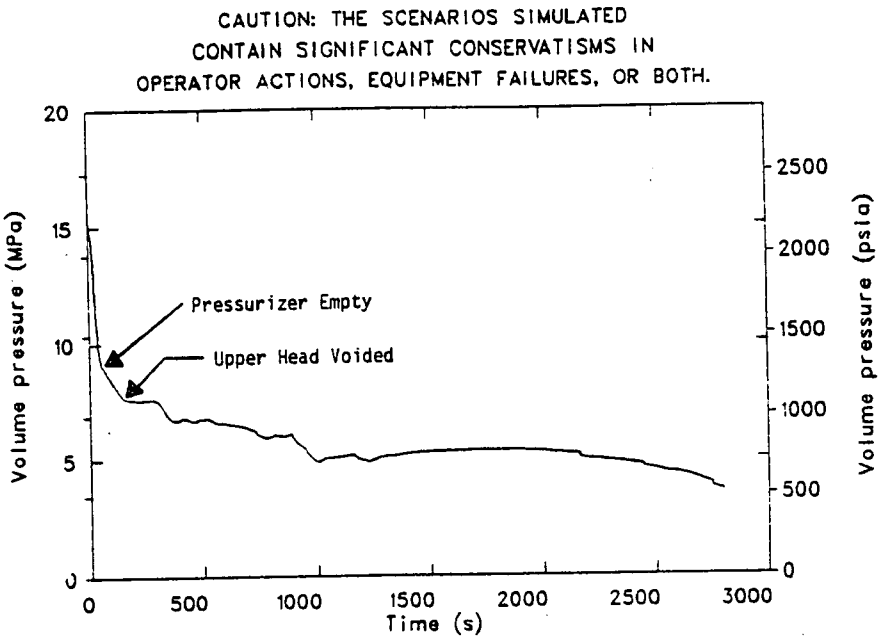

Figure 9–1. Scenario 6 primary system pressure.

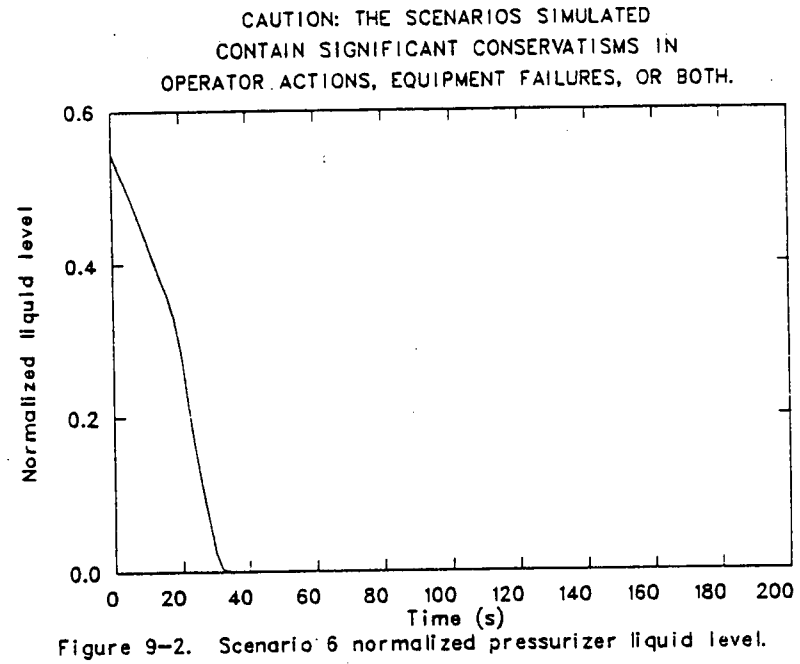

Figure 9–2. Scenario 6 normalized pressurizer liquid level.

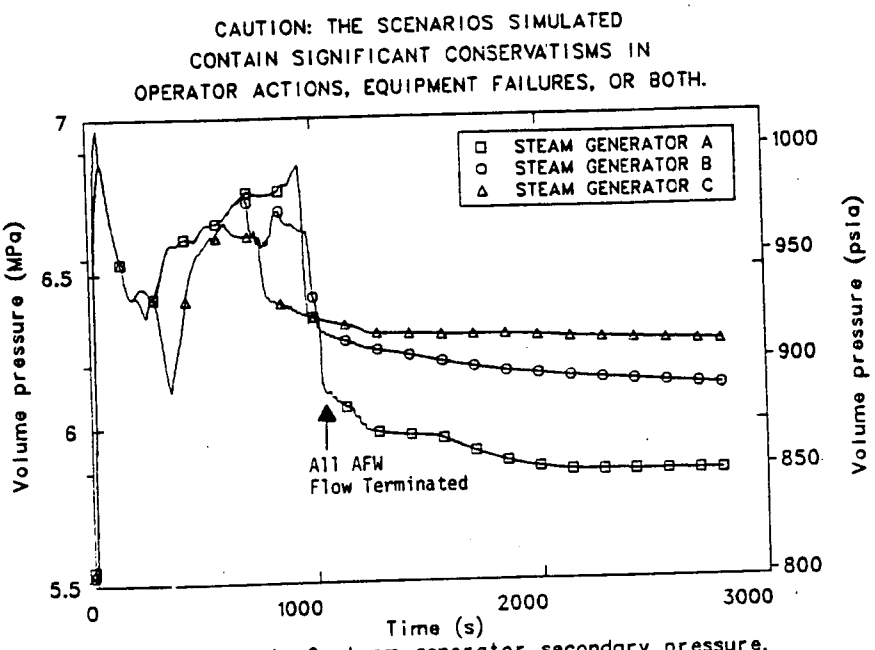

Figure 9–3. Scenario 6 steam generator secondary pressure.

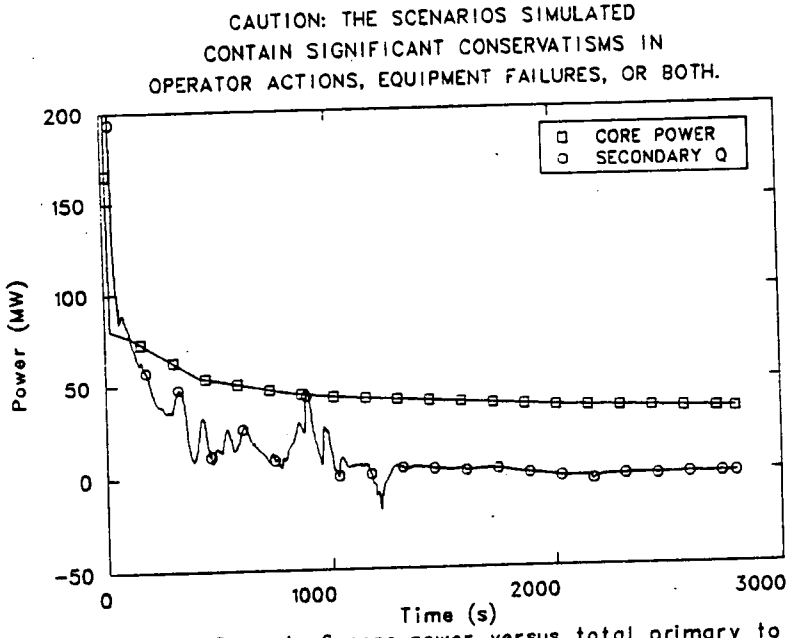

Figure 9–4. Scenario 6 core power versus total primary to secondary heat transfer rate.

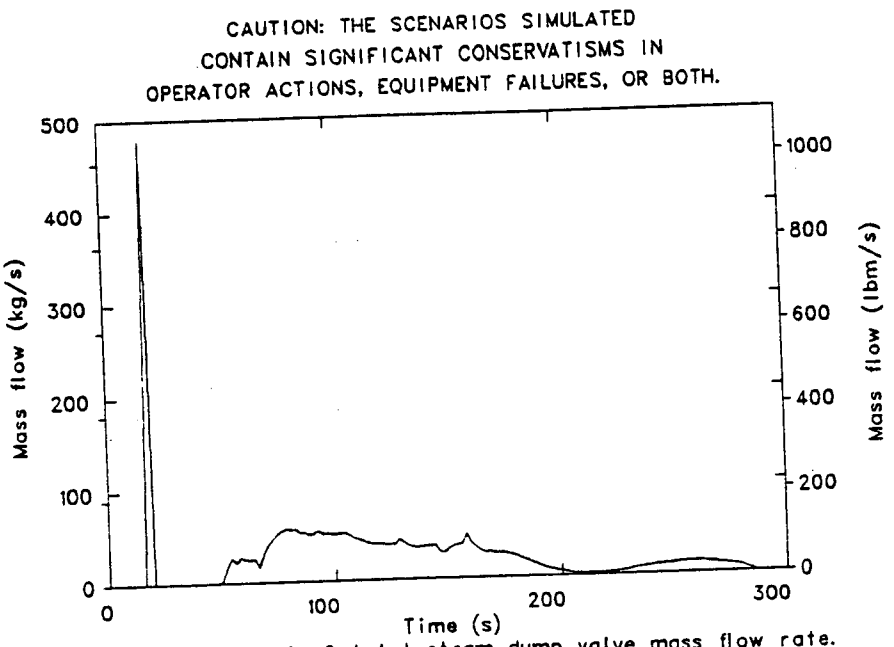

Figure 9-5. Scenario 6 total steam dump valve mass flow rate.

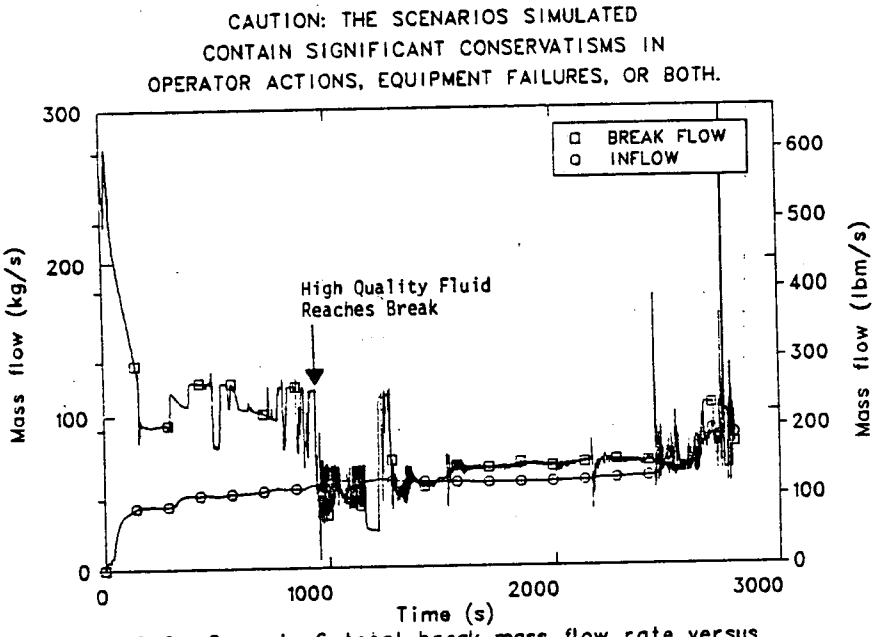

Figure 9-6. Scenario 6 total break mass flow rate versus total ECC/CVCS mass flow rate.

the pressurizer surge line resulting in the increased mass flow. At approximately 24 s the pressurizer level dropped below 14.4%, the heaters were turned off, the driving potential decreased, and the break mass flow rate decreased.

At approximately 27 s the primary system pressure had dropped to 11.9 MPa (1730 psia) actuating the SIAS signal. As a consequence the main feedwater valves closed, isolating main feedwater from the steam generator secondaries. The main feedwater pumps tripped on low flow and the heater drain flow was terminated. At the termination of the main feedwater pump power the motor-driven auxiliary feedwater system was activated and auxiliary feedwater began flowing into the A and B steam generators as shown in Figure 9-7. Due to the use of a common header for both the motor and steam-driven auxiliary feedwater systems, the differential pressures between the header and the steam generators determined which steam generators received the flow. At the initiation of the motor-driven auxiliary feedwater flow the C steam generator pressure was slightly higher than the other two, therefore, only the A and B steam generators received auxiliary feedflow.

Primary system pressure had dropped below the HPI shutoff head by approximately 40 s and flow from this system was established to each cold leg. Also at this time, two out of three steam generators had reached the low-low level signal setpoint and the steam-driven auxiliary feedwater flow was initiated to the generators. Only the A and B steam generators received the steam-driven auxiliary feedflow at this time as shown in Figure 9-8. No auxiliary feedflow was delivered to Steam Generator C because of its slightly higher pressure. With both the motor and steam-driven auxiliary feedwater systems operating, the level in Steam Generators A and B began to increase as shown in Figure 9-9.

Between 50 and 55 s several events occurred. At approximately 50 s the undershoot of the lead-lag controller in the plant trip control system had corrected itself and the steam dump valves opened as shown in Figure 9-5. Also by this time, the pressurizer was completely empty. At approximately 55 s the primary system pressure had dropped below 9.1 MPa

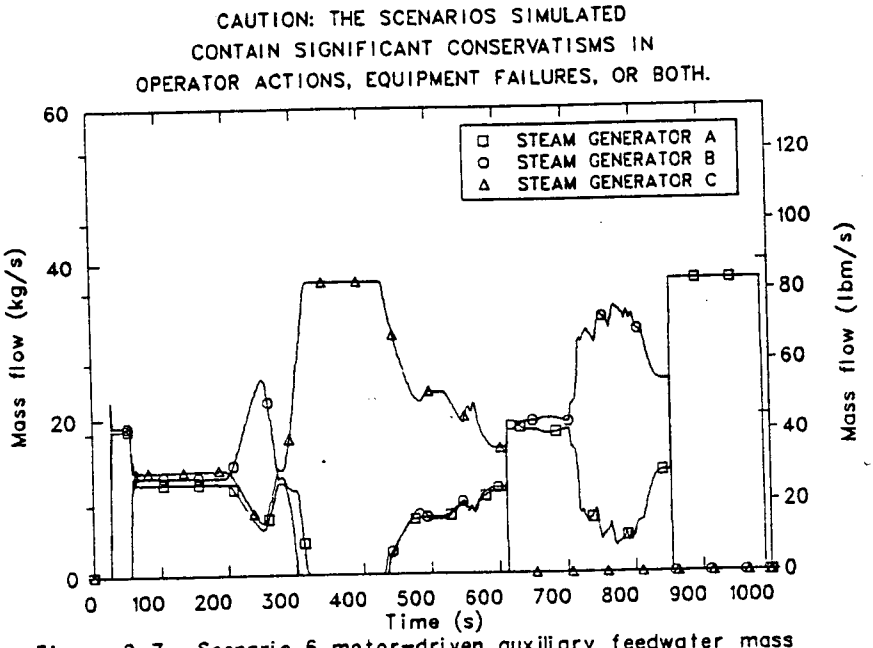

Figure 9-7. Scenario 6 motor-driven auxiliary feedwater mass flow rate.

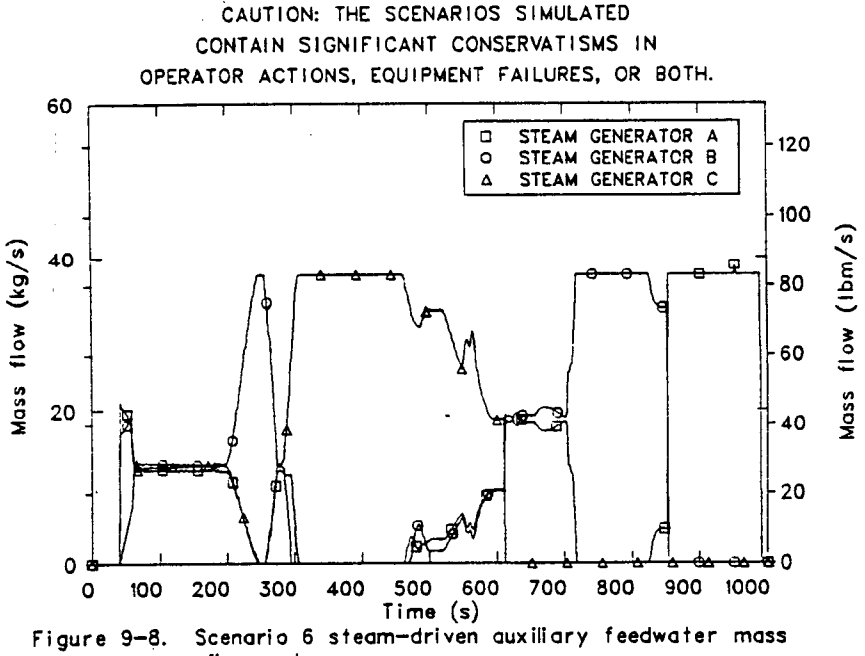

Figure 9-8. Scenario 6 steam-driven auxiliary feedwater mass flow rate.

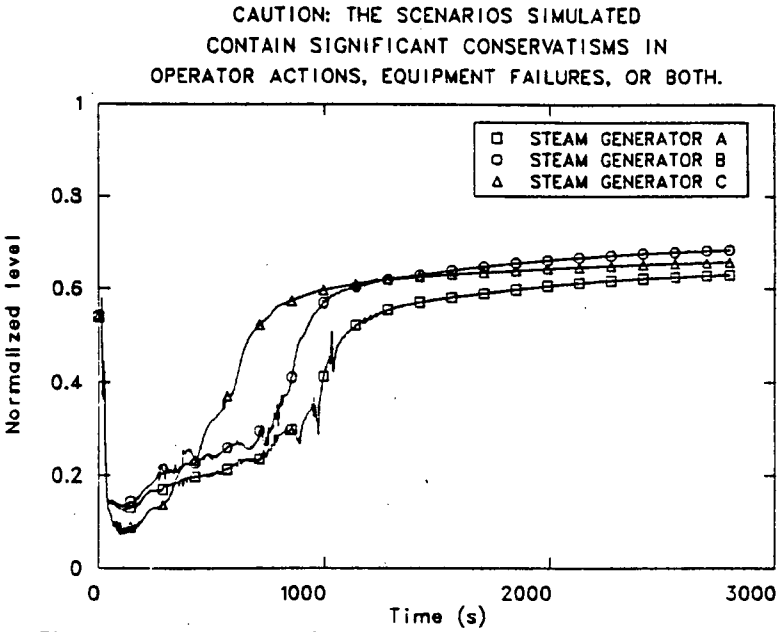

Figure 9–9. Scenario 6 normalized steam generator narrow range liquid level.

(1315 psia) and the reactor coolant pumps were tripped. As the pumps coasted down, the loop flow transitioned from full flow to natural circulation as shown in Figure 9-10. Primary system heat removal was nearly equal to decay power (see Figure 9-4) and the secondary pressures began to decrease due to the influence of the cold auxiliary feedwater and heat removal through the steam dump valves. Auxiliary feedflow to the C steam generator was established at this time. Primary system depressurization was slowed as a result of the equalization between decay heat generation and removal, and vapor generation in the reactor vessel upper head as a result of the pressure there reaching the saturation temperature of the fluid.

At approximately 150 s the reactor vessel upper head had completely voided and voiding in the upper plenum, downcomer above the inlet annulus, and hot legs commenced. Two phase fluid reached the break and the break mass flow drastically dropped as shown in Figure 9-6. Vapor generation in the vessel upper plenum and the reduction in the break flow rate resulted in a stabilization of the primary system pressure for approximately 150 s as shown in Figure 9-1.

At approximately 300 s, the auctioneered high average temperature dropped below 559 K (547°F) and the steam dump system control changed from plant trip control mode to steam pressure control mode. The steam dump valves closed, and secondary system depressurization was continued solely due to cooldown effects from the addition of cold auxiliary feedflow. Between 300 and 1000 s vapor generation and condensation effects resulted in perturbations in the primary system pressure response, shown in Figure 9-1, as the loops and upper plenum drained. Two phase flow periodically reaching the break also contributed to the pressure oscillations. Also contributing to the primary system pressure response during this time, was the primary-to-secondary heat removal rate shown in Figure 9-4. The heat removal rate was affected by the amount of auxiliary feedwater which the steam generators were receiving. The common header for each auxiliary feedwater system (steam and motor-driven) was modeled and the flow to each generator was determined by the differential pressure between the header and the generator. At times one generator received all

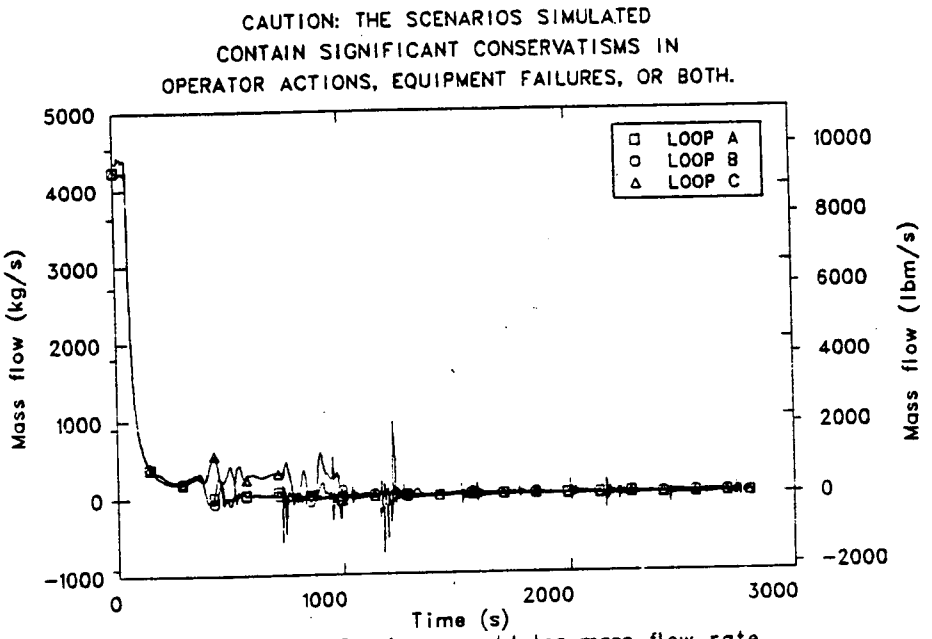

Figure 9–10. Scenario 6 primary cold leg mass flow rate.

of the flow as shown in Figures 9-7 and 9-8. As specified in the scenario, the operator controlled the secondary level around the 40% narrow range level. At approximately 600 s the level in the C steam generator reached the 40% level and auxiliary feedflow to that generator was terminated. At approximately 849 and 989 s respectively, auxiliary feedflow to the A and B steam generators was terminated. The termination of auxiliary feedwater to each steam generator stopped the cooldown and depressurization of that secondary as shown in Figure 9-3.

By approximately 400 s enough voiding in the A and B loops had occurred that natural circulation had stopped and these loops were very nearly stagnant throughout the remainder of the calculation as shown in Figure 9-10. The C loop, however continued to circulate due to the effects of the break, until approximately 1000 s. At this time the liquid in the loop C steam generator tubes and hot leg had drained and natural circulation was lost.

The cold leg and reactor vessel downcomer fluid temperature responses are shown in Figure 9-11. Between 400 and 1500 s the liquid temperature decreased at a faster rate in the A and B loops than in the C loop because those loops has stagnated and mixing of the warmer loop flow with the incoming cold HPI liquid was minimized. When the C loop stagnated at approximately 1000 s, the cold leg temperature in that loop decreased at a rate similar to the other loops. The oscillations in the fluid temperature during this period were due to oscillations in the loop flow shown in Figure 9-10. The reactor vessel downcomer fluid temperature was higher than in the cold legs due to heat addition to the cold leg fluid as it entered the steam filled environment in the downcomer, downcomer wall heat transfer, and warm fluid entering the downcomer through the vessel internal leakage paths.

When the C loop hot leg had drained at 1000 s high quality fluid was at the break, resulting in the sharp decrease in the break mass flow observed in Figure 9-6. The total primary inflow from the HPI and makeup after this time equaled or exceeded the break mass flow as shown in Figure 9-6. The primary system depressurization was stopped and a slow

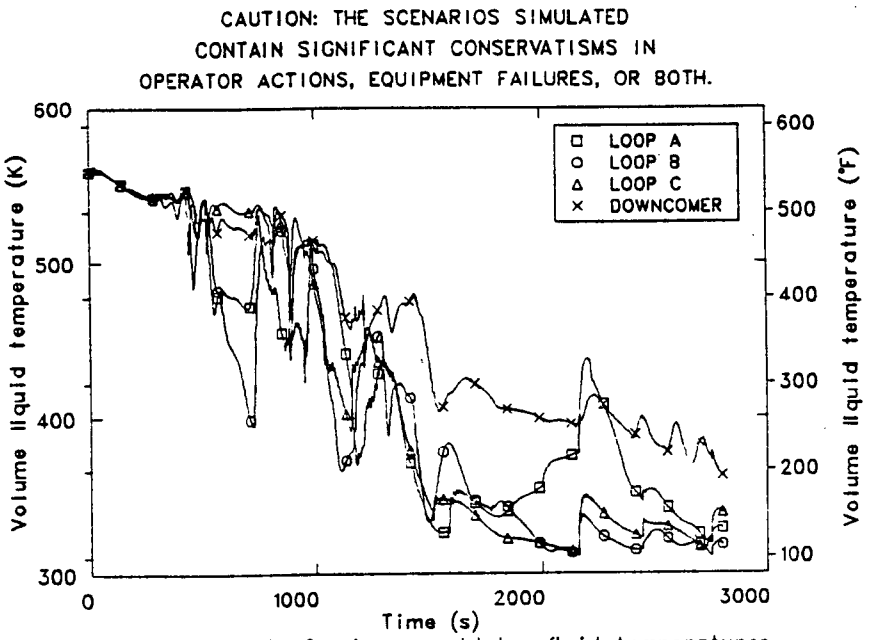

Figure 9–11. Scenario 6 primary cold leg fluid temperatures and vessel downcomer fluid temperatures.

repressurization began due mainly to volume expansion from vapor generation in the primary loops and vessel, and wall heat transfer to the fluid. The repressurization continued until approximately 1800 s when the energy removal at the break exceeded core power and energy addition from primary metal mass (heat removal through the steam generators was negligible at this time). From 1800 s to the termination of the calculation, primary system pressure decreased as shown in Figure 9-1 due mainly to energy removal at the break.

Between 1800 and 2200 s flow oscillations in the A loop allowed more mixing of the warm loop fluid and the cold ECC fluid, resulting in an increase in the cold leg fluid temperature as shown in Figure 9-11. At approximately 2160 s a flow reversal in all three loops occurred and the temperature in all three cold legs increased due to warmer liquid from the downcomer entering the cold legs. After 2200 s the oscillations in the A loop subsided somewhat and the temperature in that loop decreased.

At approximately 2440 s the primary system pressure dropped below 4.6 MPa (673 psia) and accumulator injection began. With accumulator flow, the total mass inflow to the primary system and the break mass flow were nearly equal as shown in Figure 9-6. The calculation was terminated at 2800 s and the primary system was slowly refilling. The primary system pressure at the termination of the calculation was 3.6 MPa (522 psia) and decreasing, and the reactor vessel downcomer fluid temperature was 363 K (193°F) and decreasing.

9.3.2 Extrapolations and Uncertainties

This section presents the extrapolations of the vessel downcomer pressure, fluid temperature and wall inside surface heat transfer coefficient. Also, extrapolations of the cold leg flow rates and fluid temperatures are shown. Any known uncertainties in the calculation are also addressed.

An extrapolation to two hours of the pressure, temperature and heat transfer coefficient curves in the reactor vessel downcomer and the mass flow rate and temperature curves in the cold legs are shown in Figures 9-12

through 9-16. Parameters in the downcomer are shown for the elevation adjacent to the top of the core. At the termination of the transient, heat removal from the primary to the secondary was nearly zero and the primary system was gaining very little mass due to the total ECC mass inflow (including accumulator flow) equaling the break mass flow rate. It is estimated the primary system would continue to depressurize as shown in Figure 9-12, until the break flow and total ECC inflow was balanced and energy removal through the break or steam generators was balanced with the core decay power. It was estimated this steady state would occur around a pressure of .9 MPa (142 psia), which is just below the LPI shutoff head, and would occur at approximately 3200 s. The addition of LPI fluid appeared to be sufficient to hold the pressure at .9 MPa (142 psia) through the two hour period of PTS concern.

Figure 9-13 shows the extrapolation of the reactor vessel downcomer temperature. Loop mass flows at the end of the calculation were nearly equal to the ECC flow rate (essentially stagnant), and the downcomer temperature was approaching the temperature of the ECC fluid temperature of 305 K (90°F). It is estimated the reactor vessel downcomer temperature will be dominated by the ECC fluid temperature because of loop flow stagnation, and will decrease until it approaches the temperature of the ECC fluid. Mixing of the cold leg fluid coming from the upper head and plenum leakage paths will keep the reactor vessel downcomer temperature slightly above the cold leg temperature. The estimated reactor vessel downcomer temperature at two hours is 310 K (100°F).

Figure 9-14 shows the extrapolation of the reactor vessel downcomer inner surface wall heat transfer coefficient. After reactor vessel coolant pump trip occurred, the wall to fluid heat transfer regime changed to a natural circulation/pool boiling mode as the loop flow transitioned from forced flow, to natural circulation, to stagnation. After 2800 s it is estimated the wall heat transfer coefficient will not change significantly.

Figures 9-15 and 9-16 show the mass flow rate and fluid temperature extrapolations for each of the three cold legs. At the termination of the calculation (2800 s), loop flow was stagnant because the steam generator

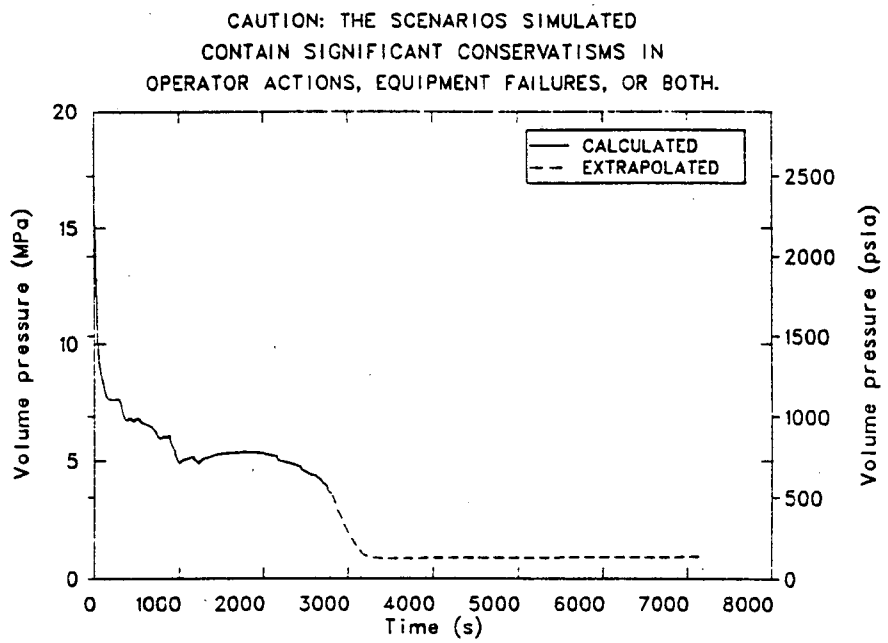

Figure 9–12. Scenario 6 extrapolated reactor vessel downcomer fluid pressure elevation equal to the top of the core.

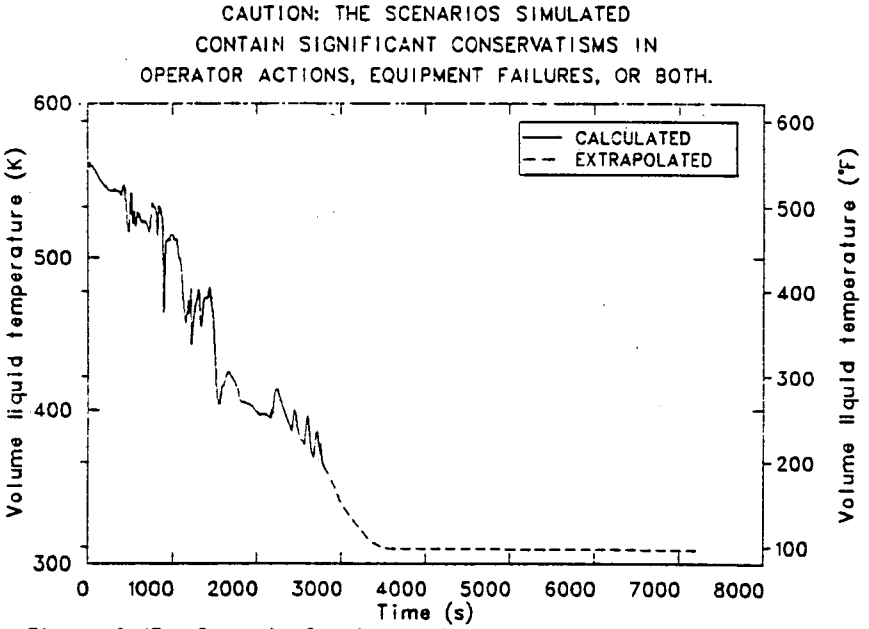

Figure 9–13. Scenario 6 extrapolated reactor vessel downcomer fluid temperature at elevation equal to the top of the core.

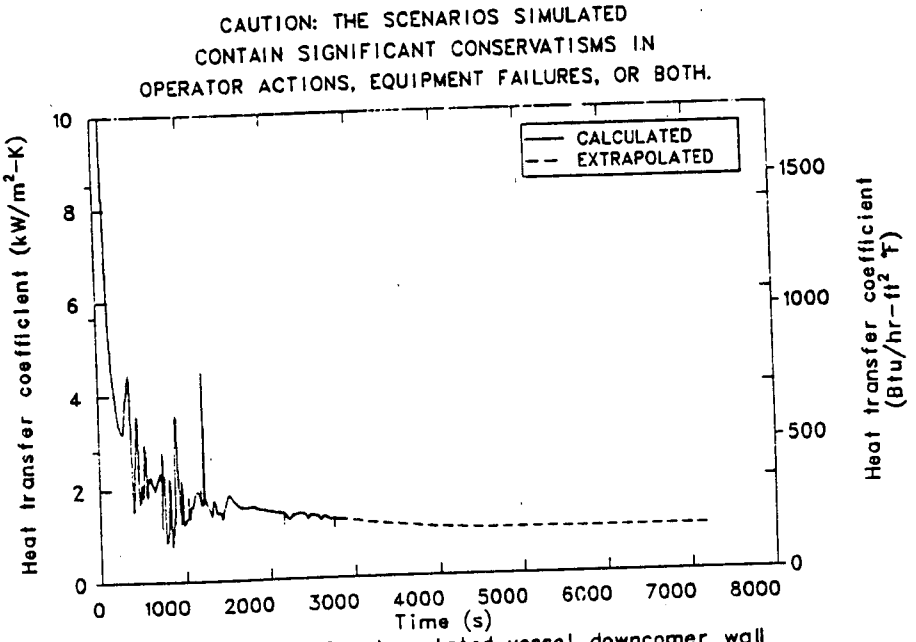

Figure 9–14. Scenario 6 extrapolated vessel downcomer wall inside surface heat transfer coefficient at elevation equal to the top of the core.

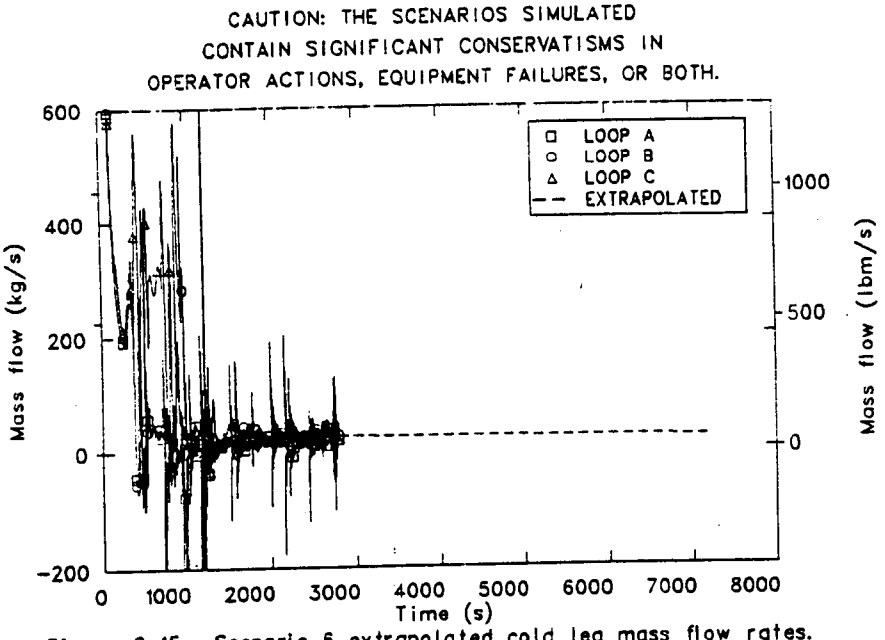

Figure 9–15. Scenario 6 extrapolated cold leg mass flow rates.

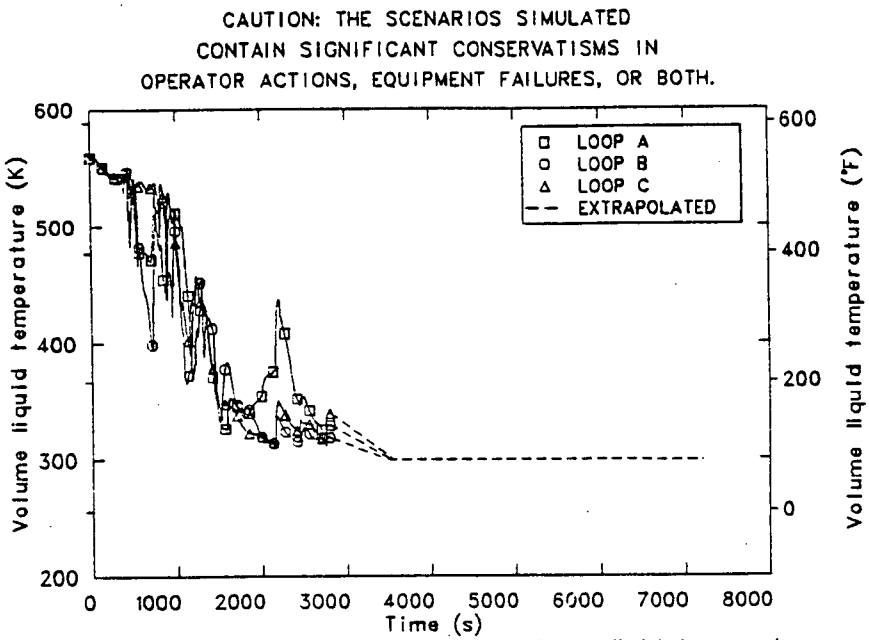

Figure 9–16. Scenario 6 extrapolated cold leg fluid temperature.

tubes and hot legs were voided. To reestablish loop flow (natural circulation), enough fluid volume in the primary system to essentially fill the hot legs and steam generator tubes, and the establishment of primary heat removal through the steam generators would be required. At 2800 s the steam generators were heat sources because the fluid temperatures were slightly higher than the primary, and the break flow essentially equaled the total ECC inflow, thus no primary side fluid volume gain. It is estimated these conditions will exist throughout the two hour period, therefore, loop flow will remain stagnant. The cold leg temperatures will decrease and approach the ECC fluid temperature of 305 K (90°F).

There were no significant uncertainties that affected the overall results of the calculation.

9.4 Conclusions

As a consequence of the size of the hot leg break it was shown that the break was capable of removing core decay power. Therefore there was no mechanism which would allow the primary system to repressurize. It was estimated that primary system pressure would stabilize at approximately .9 MPa (142 psia). Also, because of primary mass inventory loss, natural circulation was lost and the minimum reactor vessel downcomer temperature was estimated to be 310 K (100°F), slightly above the ECC fluid temperature.

10. SCENARIO 7, STUCK OPEN PRESSURIZER PORV AT FULL POWER

The following section describes the investigation of Scenario 7. This calculation was performed to evaluate the consequences of a stuck open primary PORV with the reactor at full power conditions.

A description of the scenario is provided in Section 10.2. The results of the calculation, the extrapolated results, and the uncertainties associated with the calculation are described in Section 10.3. The conclusions regarding the calculation are presented in Section 10.4.

Scenarios investigated in this report generally include conservative assumptions concerning equipment failures, operator actions, or combinations of these. Conclusions relative to pressurized thermal shock severity are not to be drawn directly from the results presented in this report (see Section 15).

10.1 Scenario Description

Table 10-1 gives the description of the desired scenario as supplied by ORNL. The transient was initiated from full power steady state conditions by opening one primary power operated relief valve (PORV). The PORV was closed 10 minutes into the transient to simulate an operator closing a block valve. It was assumed this block valve would prevent any further flow through either PORV.

All other control systems operated in their automatic modes.

10.2 Model Changes

No changes in the thermal-hydraulic model were necessary. The only change in the control system model was in the trips which controlled the primary PORVs. The transient was initiated from the full-power steady state conditions presented in Section 2.3.1.

TABLE 10-1. SCENARIO DESCRIPTION NO. 7

Plant Initial State - Just prior to transient initiator

General Description: 100% Power steady state
System Status
- Turbine: Automatic control
- Secondary PORV: Automatic control
- Steam Dump Valves: Operating/automatic control
- Charging System: Automatic control
- Pressurizer: Automatic control
- Engineering Safety Features: Automatic control
- PORVs: Automatic control
- Reactor Control: Automatic
- Main Feedwater: Automatic control
- Aux Feedwater: Automatic control
- MSIVs: Open, Automatic control
- MFIVs: Opening, Automatic control

Transient Initiator - Pressurizer PORV transfers full open.

Equipment Failures which occur during the transient if the equipment is demanded.

PORV blocking valve will not close until 10 minutes into transient.

Operator Reactions to Reported Information

1. The operator shuts PORV blocking valve at 10 minutes into transient.

2. If SIAS signal is generated, the operator will trip the reactor coolant pumps when RCS pressure reaches 1300 psig.

10.3 Results

This section is divided into two subsections. The first presents the calculated results, and the second extrapolates the calculated results to two hours, and discusses uncertainties associated with the calculation and extrapolation.

10.3.1 Calculation Results

The sequence of events for this transient is presented in Table 10-2. The transient was initiated by opening one primary PORV. Primary system pressure, as shown in Figure 10-1, began to fall as mass was lost out of the PORV. However, almost all other parameters in the plant remained essentially unchanged until 33.4 s, at which time the reactor was tripped. The reactor tripped on a 2-out-of-3 loop high reactor delta temperature. The reference delta temperature used to determine the overtemperature is based on the primary system pressure, so as the primary system pressure dropped, the reference delta temperature dropped. Therefore, the over delta temperature was reached without the primary system temperatures changing appreciably.

Following reactor trip, the primary system pressure dropped more rapidly as the primary system cooled. Hot and cold leg fluid temperatures are shown in Figure 10-2. By 45 s, the turbine isolation valve closed, and the steam dump valves opened on a load rejection signal, and stayed open for 3 s. The feedwater valves also began to close following reactor trip and by 52 s were completely closed. The main feedwater pumps tripped off and both motor and turbine-driven auxiliary feedwater pumps began delivering feedwater at 53 s. At 72 s the steam dump valves modulated open and brought the primary system average temperature down to 560 K (547°F).

At 113 s, primary system pressure dropped below 10.1 MPa (1470 psia), and HPI flow was initiated.

TABLE 10-2. SCENARIO 7 SEQUENCE OF EVENTS

Time (sec)	Event
0.0	PORV opened
33.4	Reactor tripped on 2/3 reactor over delta temperature; turbine stop valve closed; feedwater valves began to close.
34	Steam dump valve opened
37	Steam dump valve closed
52	Feedwater valves closed
54	MFW pumps tripped
72	Steam dump valve opened
113	HPI flow initiated on low primary system pressure
139	Reactor coolant pumps tripped on low primary system pressure
180	Reactor vessel upper head fluid saturated and began to flash
272	Steam dump valve control shifted to steam pressure control (SPC) mode, dump valve closed
278	Normalized pressurizer level went off scale high
600	PORV block valve closed
620	AFW flow shifted SGC
674	AFW flow isolated from SGC, diverted to SGB
706	AFW flow isolated from SGB, diverted to SGA
848	AFW flow isolated from SGA, all AFW flow stopped
947	Minimum reactor vessel downcomer temperature, 538 K (509°F), reached

TABLE 10-2. (continued)

Time (sec)	Event
1490	Reactor vessel upper head refilled with liquid
1506	Primary system pressure rose above HPI shutoff head, HPI flow stopped
1840	Steam dump valves opened
2088	Pressurizer safety relief valve opened, then immediately closed
2200	End of calculation

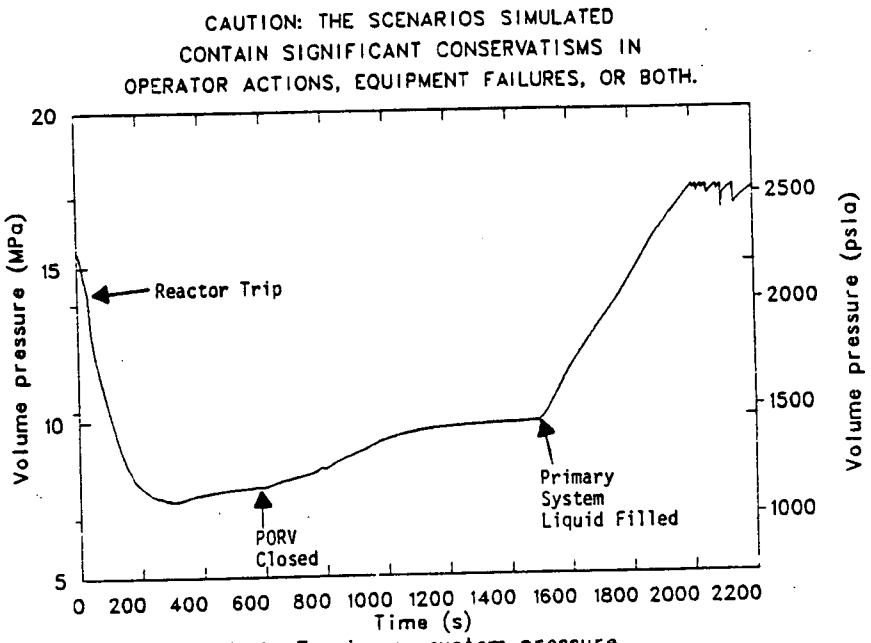

Figure 10-1. Scenario 7 primary system pressure.

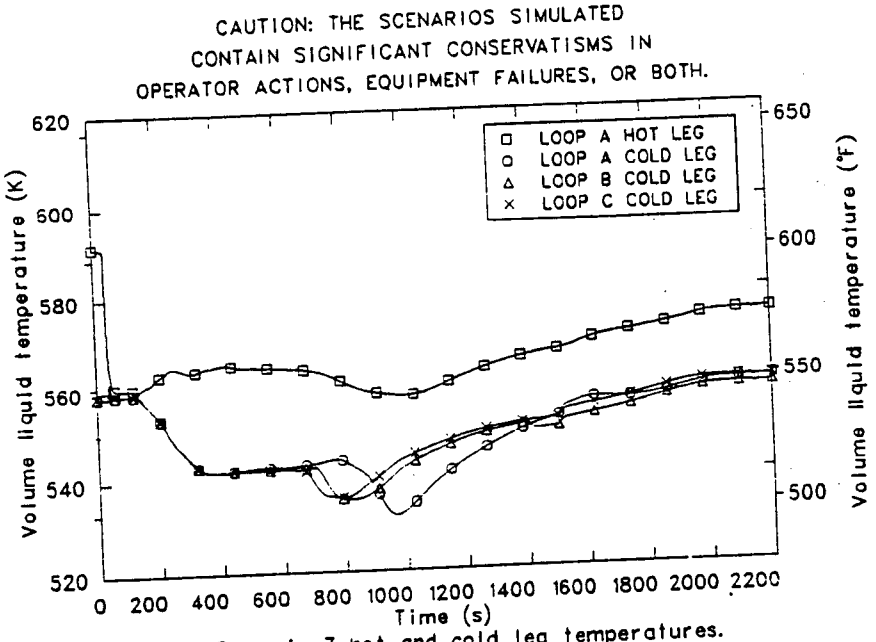

Figure 10-2. Scenario 7 hot and cold leg temperatures.

At 139 s, primary system pressure dropped below 9.07 MPa (1315 psia), and the primary coolant pumps were tripped. Hot leg temperatures then increased and cold leg temperatures decreased as the loop flow rate dropped. By approximately 300 s, a stable natural circulation flow was established in all three loops as energy was added to the primary fluid from decay heat, and removed through the steam generators. The cold leg flow rates for the three loops are shown in Figure 10-3. By 180 s, the primary system pressure had dropped to the saturation pressure of the fluid in the reactor vessel upper head, and the fluid there began to flash. The void fraction within the reactor vessel upper head and in the volume at the top of the reactor vessel downcomer are shown in Figure 10-4. As liquid was forced out of the upper head when the bubble there grew, liquid surged into the pressurizer, rapidly increasing the pressurizer level, shown in Figure 10-5. The pressurizer level exceeded its indicated range at 278 s, although the pressurizer was not completely full. Some voids also formed in the volume at the top of the reactor vessel downcomer, as seen in Figure 10-4.

At 272 s, the steam dump valve control shifted to the steam pressure control (SPC) mode, and the dump valves closed. Secondary pressures, shown in Figure 10-6, began to rise but there was no significant effect on primary conditions because the cold auxiliary feedwater removed sufficient energy from the primary fluid without having to draw steam off the steam generators.

The total HPI flow rates, and the flow rate out the PORV are shown in Figure 10-7. The total HPI flowrate rate exceeded the flow out the PORV very soon after HPI initiation. At approximately 300 s, the volumetric injection of the HPI system exceeded the volume lost out the PORV, and the primary system began to repressurize. Repressurization was very slow at first. At 600 s, the PORV was closed simulating the closure of a block valve by an operator. The rate of repressurization increased at that time, but was still fairly slow as the voids in the reactor vessel upper head and downcomer collapsed.

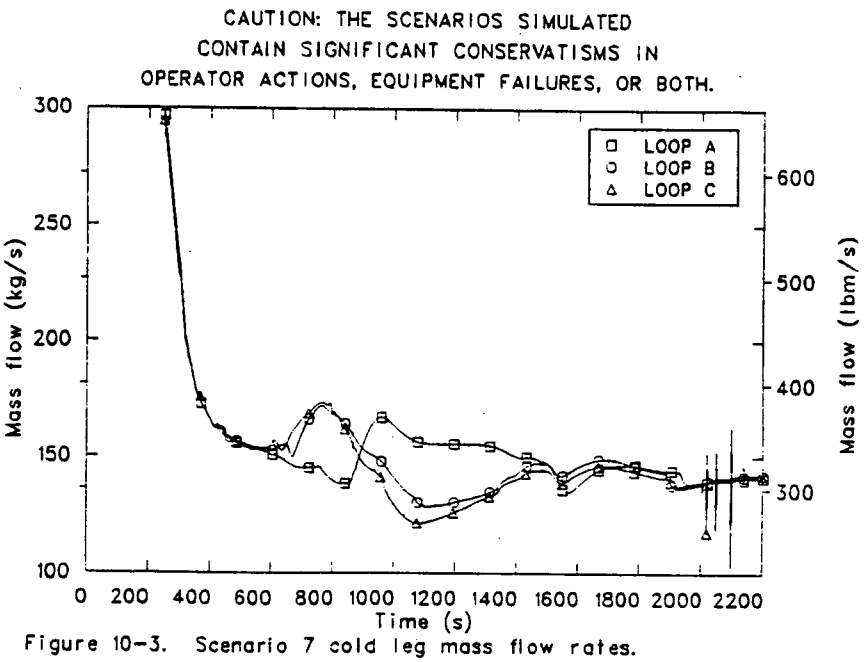

Figure 10-3. Scenario 7 cold leg mass flow rates.

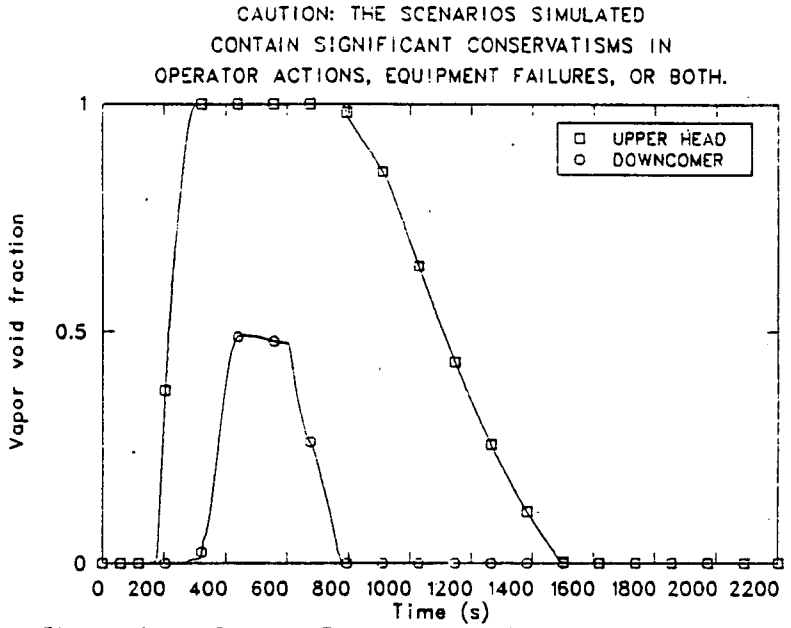

Figure 10-4. Scenario 7 reactor vessel upper head and top of downcomer void fractions.

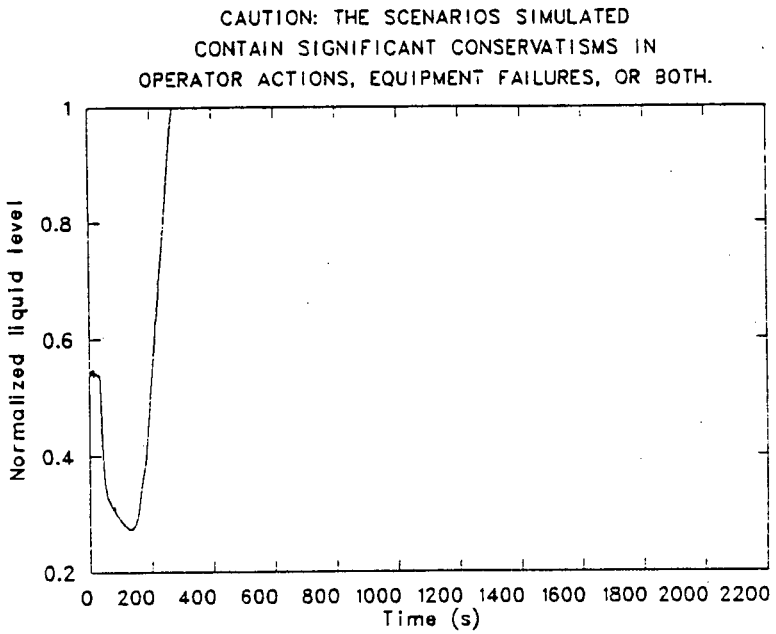

Figure 10-5. Scenario 7 normalized pressurizer level.

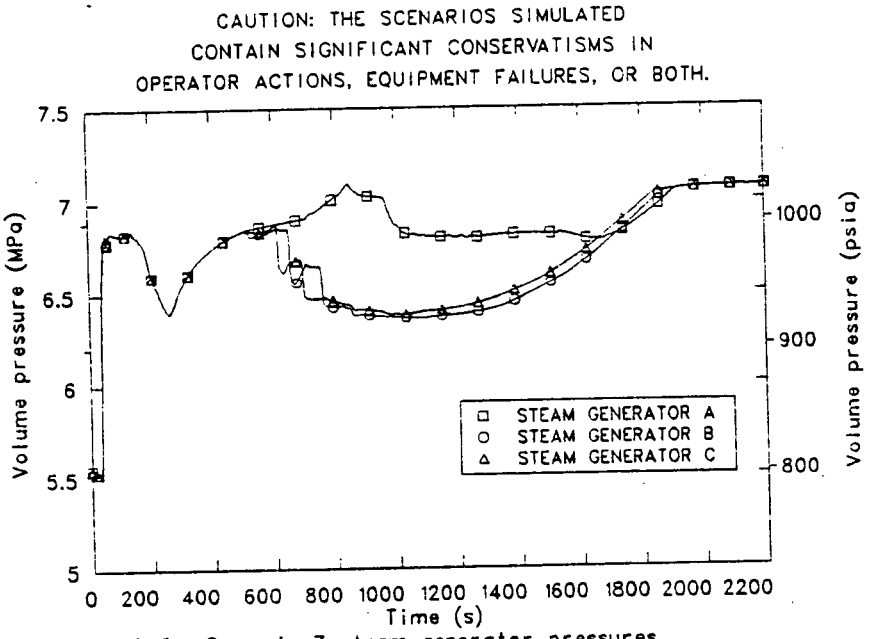

Figure 10-6. Scenario 7 steam generator pressures.

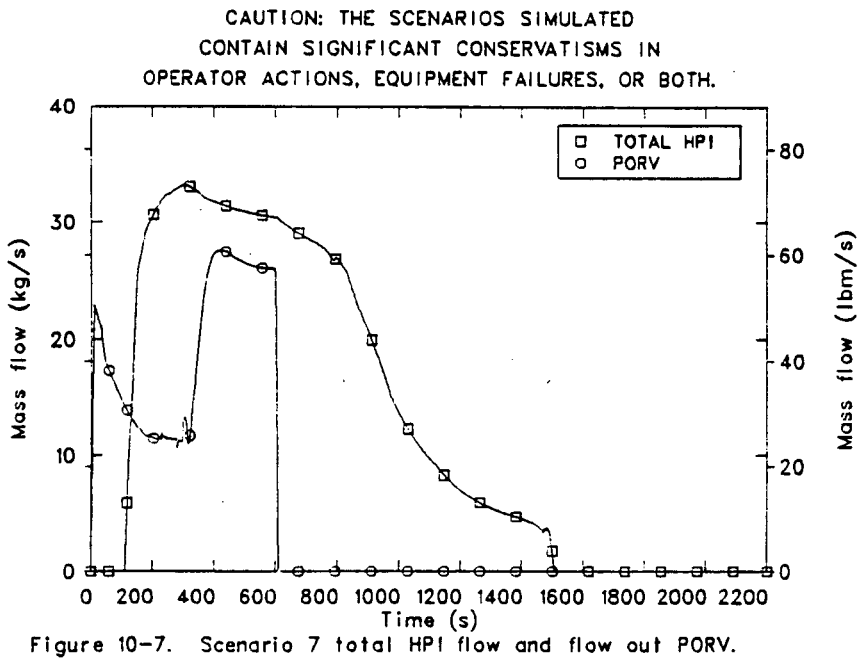

Figure 10-7. Scenario 7 total HPI flow and flow out PORV.

During the early stages of this transient, the liquid levels in the steam generators were below the elevations of the feedwater rings. As a result, the feedwater was injected into steam filled volumes. At 620 s, the temperature of the feedwater entering Steam Generator C had decreased to the point where it induced an increase in the condensation in that generator, and dropped the pressure slightly. This drop in pressure diverted all the AFW flow from the other two steam generators and delivered it all to Steam Generator C, as shown in Figure 10-8. The steam generator narrow range levels are presented in Figure 10-9. At 674 s, the liquid level in Steam Generator C reached the 40% control point, and feedflow to that generator was isolated. The AFW then diverted entirely to Steam Generator B. The feedflow to that generator was isolated at 706 s as the liquid level exceeded 40%. Steam Generator A then received all the feedwater until 848 s when its liquid level rose to 40% and all AFW flow was isolated.

The effect of these shifts in AFW flow are the temporary drops in the cold leg temperatures between 600 and 1200 s, as seen in Figure 10-2. As the AFW flow shifted to a specific steam generator, the energy removed by that generator increased, while the energy removed by the other two generators decreased. As a result, the cold leg temperature in the loop receiving all the feedwater dropped below the temperature in the other two loops. After the AFW was isolated to a given steam generator, the cold leg temperature in that loop began to rise. After all AFW flow was isolated, all three cold legs temperatures converged. The shifts in AFW flow did not significantly affect the primary system pressure.

After the isolation of the AFW system, the heat sink for the primary system was lost, and the primary system began heating up. The primary system was also being filled by the HPI flow. At 934 s, the pressurizer went liquid full, and at 1490 s, the upper head of the reactor vessel completely filled with liquid. Primary system pressure rose rapidly after this time. Primary system pressure rose above the HPI shutoff head of 10.1 MPa (1470 psia) at 1506 s, and HPI flow stopped. The pressure continued to increase because the primary fluid was swelling as it heated up, and because the CVCS was still injecting water at its minimum rate, $9.2 \times 10^{-4} m^3/s$ (15 gpm).

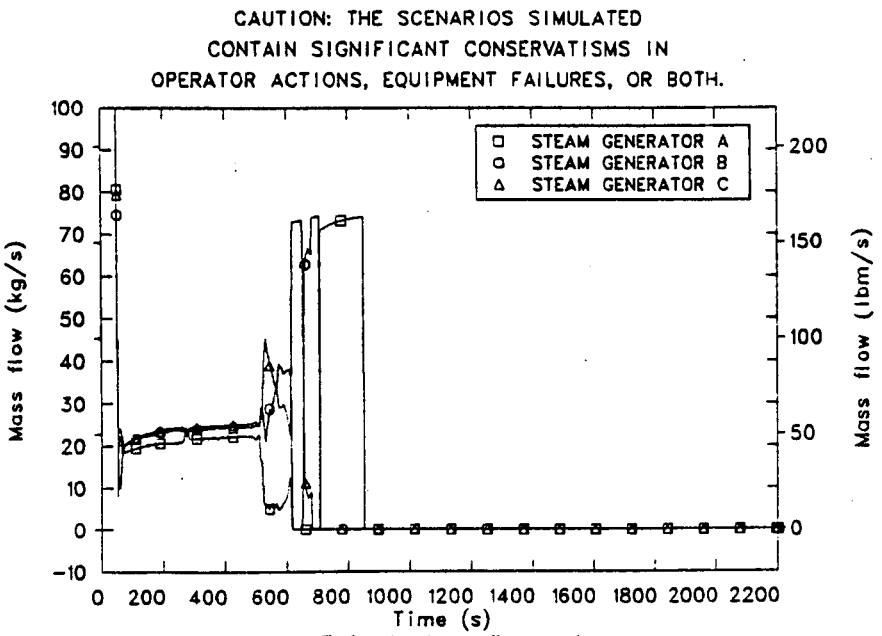

Figure 10-8. Scenario 7 feedwater flow rates.

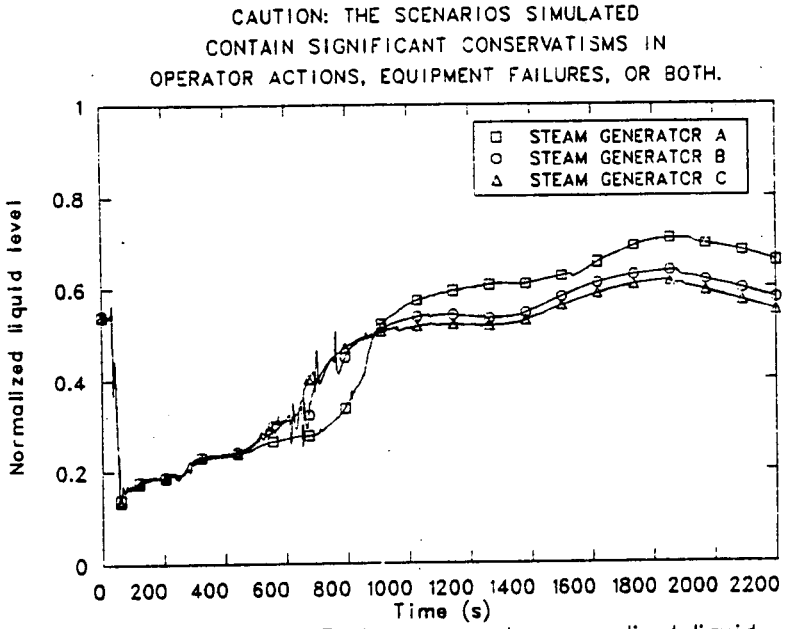

Figure 10-9. Scenario 7 steam generator normalized liquid levels.

The primary and secondary systems were closely coupled throughout this transient. At 1840 s, secondary pressures had risen to 7.03 MPa (1020 psia), and the steam dump valves opened to hold the pressure at that point. This pressure corresponds to a saturation temperature of 559 K (547°F). Therefore, the steam dumps modulated to control the primary and secondary fluid temperatures close to 559 K (547°F) through the end of the calculation. Primary system pressure rose high enough to open the primary safety relief valve once, very briefly, at 2088 s. The primary system pressure then stayed stable at just under the safety relief valve setpoint, 17.5 MPa (2535 psia), through the end of the calculation. At the end of the calculation, 2200 s, both downcomer pressure and temperature were stable at 17.5 MPa (2535 psia), and 560 K (548°F), respectively.

10.3.2 Extrapolations and Uncertainties

Figures 10-10 and 10-11 show the downcomer pressure and temperature extrapolated to 7200 s. Steam dump valve capacity was more than sufficient to remove decay heat, so the primary system temperatures would stay very close to 560 K (548°F) out through 7200 s. Because mass is still being added to the primary system by the CVCS, the safety relief valve would occasionally open to relieve pressure, and the primary system would remain at the safety relief valve setpoint, 17.5 MPa (2535 psia) out through 7200 s. Figure 10-12 presents the cold leg mass flow rate extrapolated to 7200 s. All three loops would act symetrically, and since a stable natural circulation flow had been established, the flow rates would stay essentially constant from the end of the calculation out through 7200 s. The heat transfer coefficient in the downcomer, Figure 10-13, is a strong function of the mass flow rate, and would also remain essentially constant through 7200 s.

There were no major uncertainties associated with this calculation.

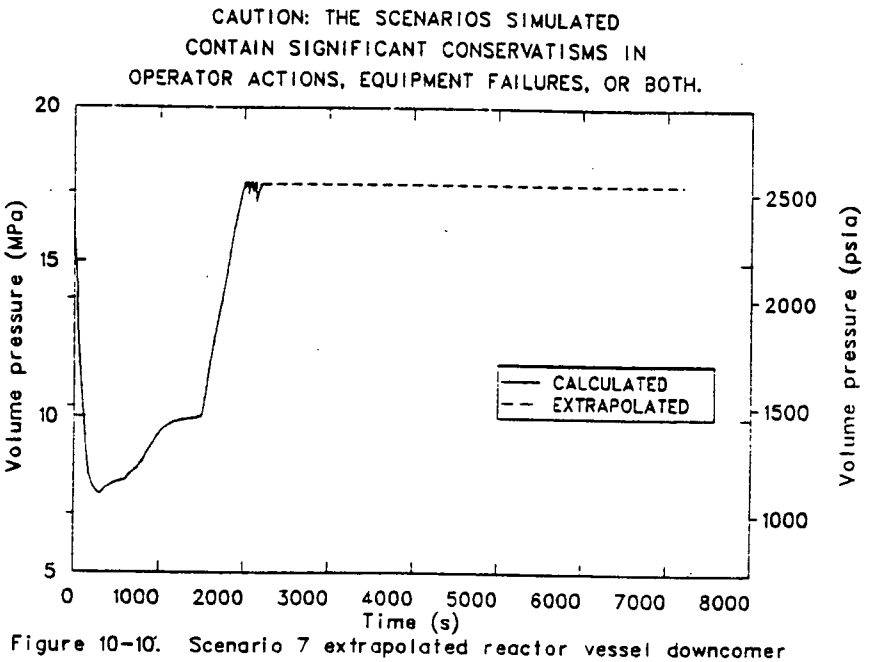

Figure 10-10. Scenario 7 extrapolated reactor vessel downcomer pressure.

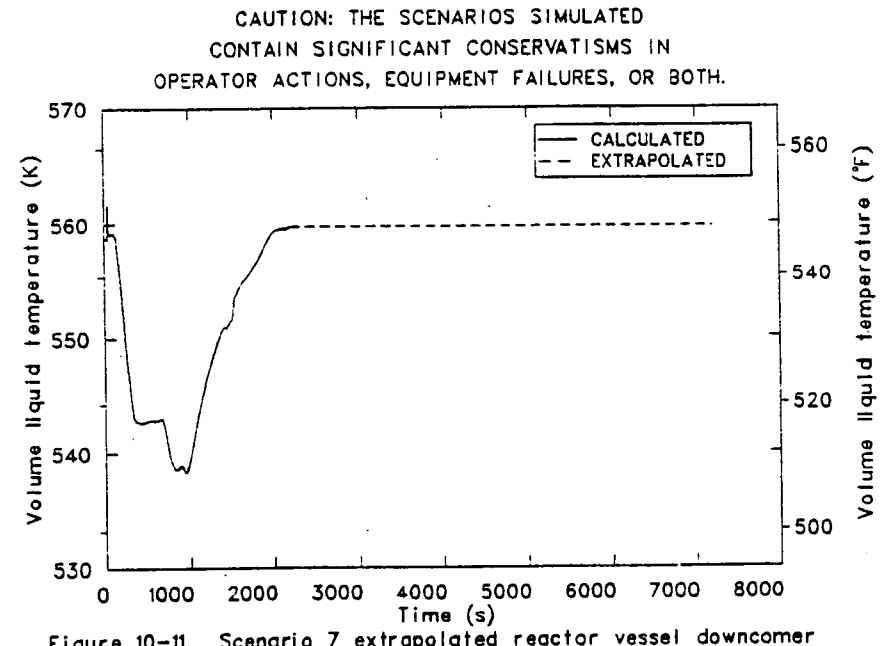

Figure 10-11. Scenario 7 extrapolated reactor vessel downcomer temperature.

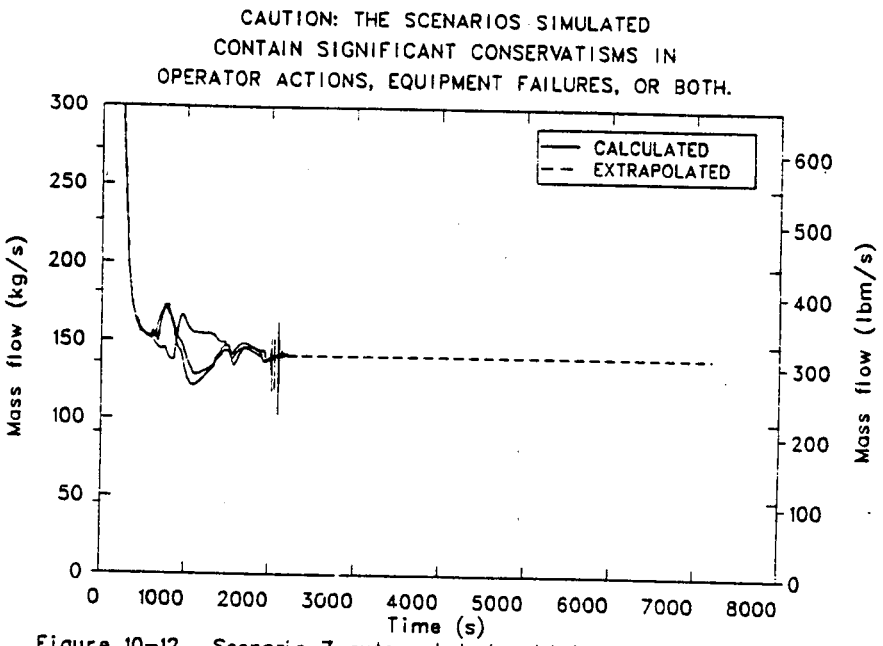

Figure 10-12. Scenario 7 extrapolated cold leg mass flow rates.

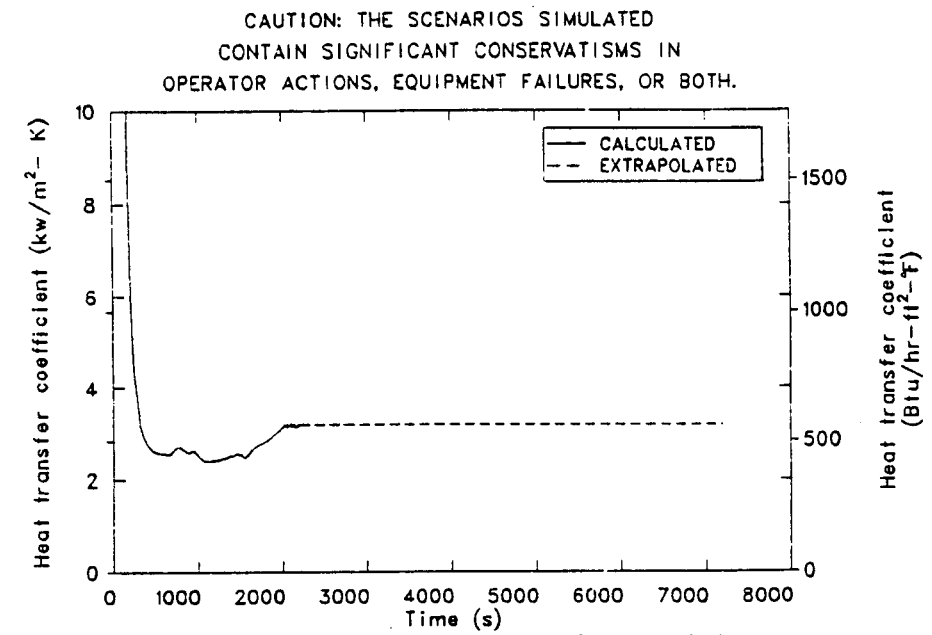

Figure 10-13. Scenario 7 extrapolated reactor vessel downcomer heat transfer coefficient.

10.4 Conclusions

This transient was mild primarily for two reasons. First, the open PORV was not large enough to void the primary system and stagnate the loop flows. Secondly, the energy removed by the PORV and AFW flow was not sufficient to cause a serious cooldown. The minimum reactor vessel downcomer temperature reached was 538 K (509°F), and occurred at 947 s. The maximum primary system pressure after this time was 17.5 MPa (2535 psia). After extrapolating the results out to 7200 s, the reactor vessel downcomer pressure and temperature would be 17.5 MPa (2538 psia), and 560 K (548°F), respectively.

11. SCENARIO 8, SMALL HOT LEG BREAK AT HOT STANDBY

The following section describes the investigation of Scenario 8. This calculation was performed to evaluate the consequences of a postulated small hot leg break with the reactor at hot standby conditions.

A description of the scenario is provided in Section 11.1, followed by a discussion of the model changes required to perform the calculation in Section 11.2. The results of the calculation, the extrapolated results, and the uncertainties with the calculation are described in Section 11.3. The conclusions regarding the calculation are presented in Section 11.4.

Scenarios investigated in this report generally include conservative assumptions concerning equipment failures, operator actions, or combinations of these. Conclusions relative to pressurized thermal shock severity are not to be drawn directly from the results presented in this report (see Section 15).

11.1 Scenario Description

The description for this scenario, as defined by ORNL, appears in Table 11-1. The transient was assumed to be initiated by a small hot leg break while the reactor was at hot standby. The break was located at the bottom of the C hot leg, near the connection to the pressurizer surge line, and had a diameter of 0.0635 m (2.5 in.). The operators were assumed to trip the reactor coolant pumps when the primary coolant pressure dropped below 9.07 MPa (1315 psia). The operators were also assumed to throttle auxiliary feedwater (AFW) flow to maintain steam generator narrow range levels at 40%.

11.2 Model Changes

The model used to perform this calculation was essentially the same as that described in Sections 2.1, 2.2, and 2.3.3 except for nodalization changes required to represent a small hot leg break. A junction (597) and

TABLE 11-1. SCENARIO DESCRIPTION NO.8

Plant Initial State - Just prior to transient initiator

General Description: Hot 0% Power, 0% Power after 100 hrs of shutdown
System Status
- Turbine: Not latched, TSVs closed
- Secondary PORV: Automatic control
- Steam Dump Valves: Automatic control
- Charging System: Automatic control
- Pressurizer: Automatic control
- Engineering Safety Features: Automatic control
- PORVs: Automatic control
- Reactor Control: Manual
- Main Feedwater: In bypass mode, manual control to provide zero power level in S/G's; 1 condensate pump, 1 MFWP operating
- Aux Feedwater: Automatic control
- MSIVs: Open, Automatic control
- MFIVs: Closed, Automatic control

Transient Initiator - A 2.5 in. hole appears in the hot leg.

Equipment Failures which occur during the transient if the equipment is demanded.

None

Operator Reactions to Reported Information

1. If SIAS signal is generated, the operator will trip the reactor coolant pumps when RCS pressure reaches 1300 psig.

2. The operator will throttle AFW flow to maintain 40% S/G level.

time-dependent volume (599) were added to the model to simulate the break and containment, respectively. The break was attached to the bottom of volume 40403 (refer to Figure 2-1)

11.3 Results

This section is divided into two subsections. The first presents the calculated results, and the second extrapolates the calculated results to two hours, and discusses uncertainties associated with the calculation and extrapolation.

11.3.1 Calculation Results

The calculated sequence of events for this scenario is presented in Table 11-2. The transient started when the break opened at 0.0 s. The backup and proportional heaters were energized within 1 s and were tripped at 6 s because of low pressurizer level. The makeup pumps delivered maximum flow after 7 s. A safety injection actuation signal (SIAS) was generated at 21 s when the pressurizer pressure dropped to 11.93 MPa (1730 psia). The SIAS caused the following actions: the HPI pumps started, the operating main feedwater pump tripped, the main feedwater bypass valves closed, motor-driven AFW flow started, and the letdown isolation valve closed. The reactor coolant pumps were tripped at 32 s to simulate an operator action taken when pressurizer pressure dropped to 9.07 MPa (1315 psia).

Calculated pressurizer pressure is shown in Figure 11-1. Flow out the break caused the pressure to decrease rapidly. HPI was delivered to the cold legs after 29 s, when the pressure dropped below 10.1 MPa (1470 psia), the shutoff head of the HPI pumps. The depressurization rate slowed at 53 s when flashing began in the steam generator U-tubes. The steam generator secondaries began acting as heat sources at 57 s. The pressure remained nearly constant between 57 s and 370 s because of heat transfer, first from the steam generators and then later from the core. The heat transfer produced enough steam to compensate for the volumetric flow out the break. The steam production in the core dropped near 370 s because of an increase in flow into the reactor vessel that caused the core to subcool. Without the steam production in the core to maintain the pressure, the break was able to depressurize the reactor coolant system.

TABLE 11-2. SCENARIO 8 SEQUENCE OF EVENTS

Time (s)	Event
0.0	Break opened
1	Heaters on
6	Heaters off
7	Maximum makeup flow
17	Pressurizer emptied
21	SIAS; MFW pump tripped; bypass valves closed; AFW initiated, letdown isolated; HPI pumps started
29	HPI initiated
32	RCPs tripped
53	Flashing in U-tubes
57	Steam generator secondaries acting as heat source
100	Voiding begins in upper head
125	Voiding begins in core
300	Upper head completely voided
400	Core subcooled
470	AFW off
800	U-tubes voided
1040	Accumulator flow initiated
1300	Break recovered
1650	Vessel refilled; U-tubes refilling
1740	Calculation terminated

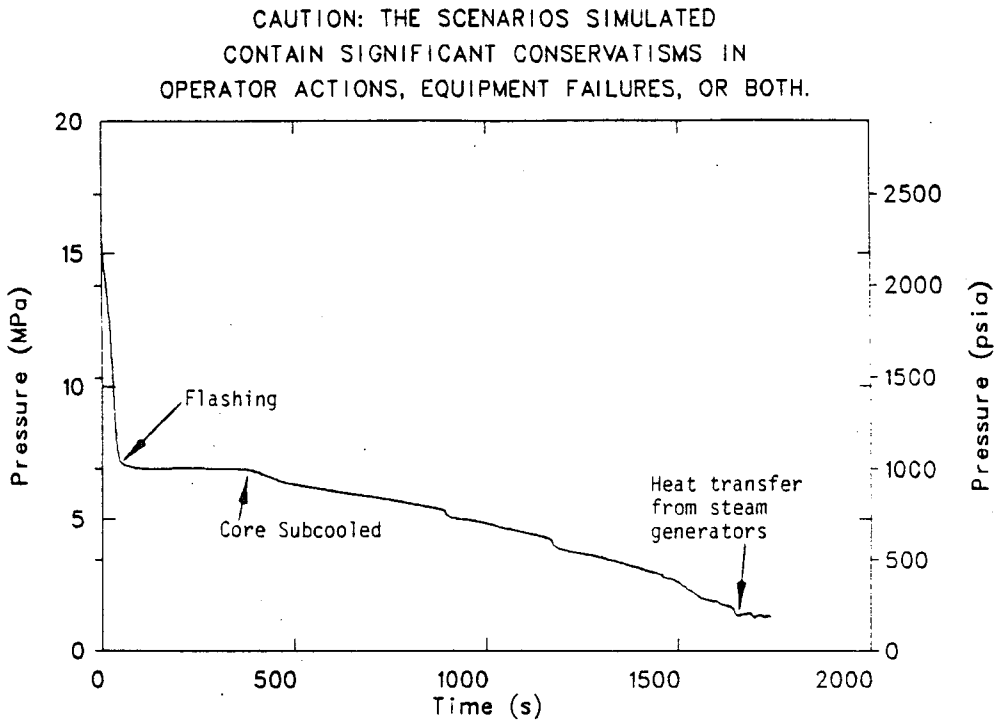

Figure 11-1. Scenario 8 pressurizer pressure.

The reactor coolant pressure dropped to the accumulator pressure of 4.65 MPa (675 psia) at 1040 s, initiating accumulator flow. The pressure remained nearly constant after 1650 s when the reactor coolant system was refilled to the point where liquid droplets entered the U-tubes. The subsequent heat transfer from the hot steam generator secondaries stopped the depressurization of the reactor coolant system.

Figure 11-2 shows the break mass flow rate and the sum of the HPI and makeup flow rates. The break flow rate decreased during the first 53 s of the transient and then reached a plateau, similar to the reactor coolant pressure curve that was described previously. The break flow then remained relatively constant until 900 s when the break partially uncovered. The break was generally covered with liquid before 900 s, as illustrated by Figure 11-3 which shows the void fraction of the fluid exiting the break. A two-phase mixture flowed through the break between 900 s and 1300 s. The break was usually covered with liquid again after 1300 s. The partial uncovering of the break at 900 s caused a sharp reduction in break mass flow rate. The mass flow rate tended to increase after 1300 s when the break recovered. Although the calculated flow rate and void fraction at the break were relatively noisy after 900 s, the trends were reasonable. HPI flow was initiated at 29 s and increased during the transient as the reactor coolant pressure decreased. By the end of the calculation, the sum of the HPI and makeup flows approximately equaled the break flow.

Calculated accumulator liquid volumes are shown in Figure 11-4. Flow from the accumulators began at 1040 s when the reactor coolant pressure dropped below the accumulator pressure of 4.65 MPa (675 psia). The accumulators retained about 20% of their initial liquid volume at the end of the calculation. The average accumulator flow after 1040 s slightly exceeded the sum of the HPI and makeup flows. Before accumulator injection began, the break flow generally exceeded the sum of the HPI and makeup flows, causing the void in the reactor coolant system to increase. After accumulator injection began, the total injection flow generally exceeded the break flow, refilling the reactor coolant system.

The voiding and refilling of the reactor coolant system are illustrated by Figure 11-5, which shows void fraction in the upper head and

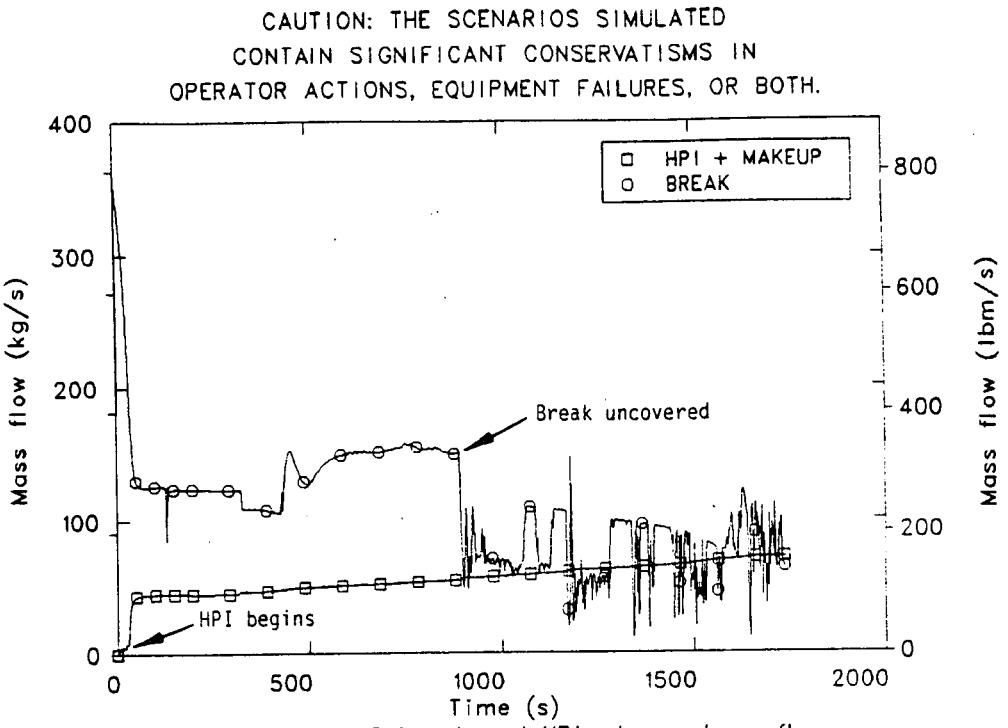

Figure 11-2. Scenario 8 break and HPI plus makeup flows.

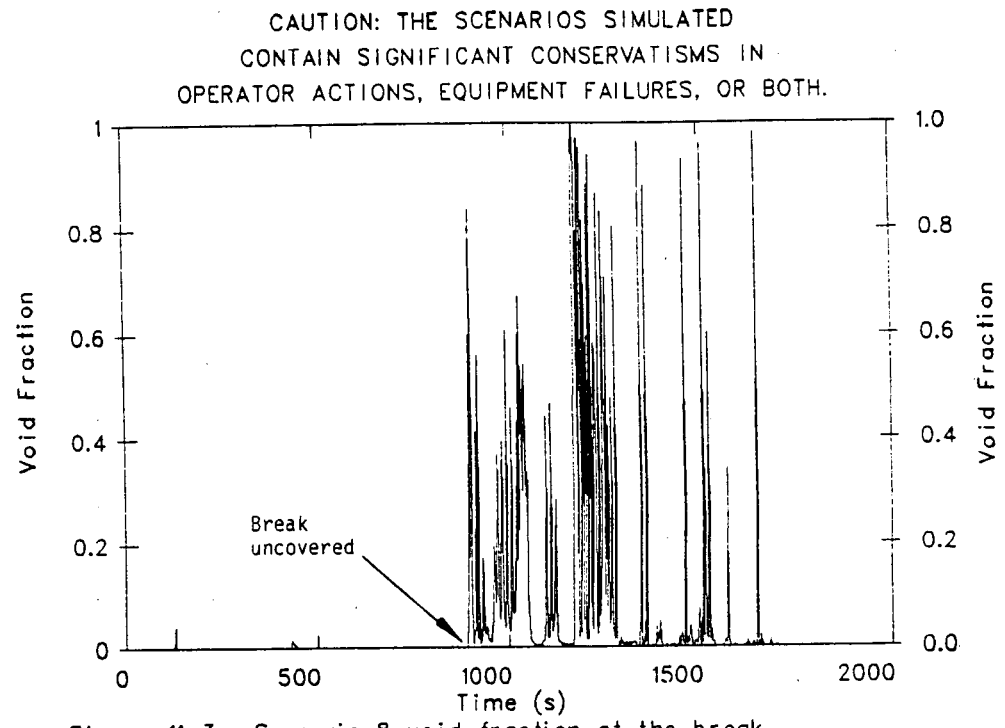

Figure 11-3. Scenario 8 void fraction at the break.

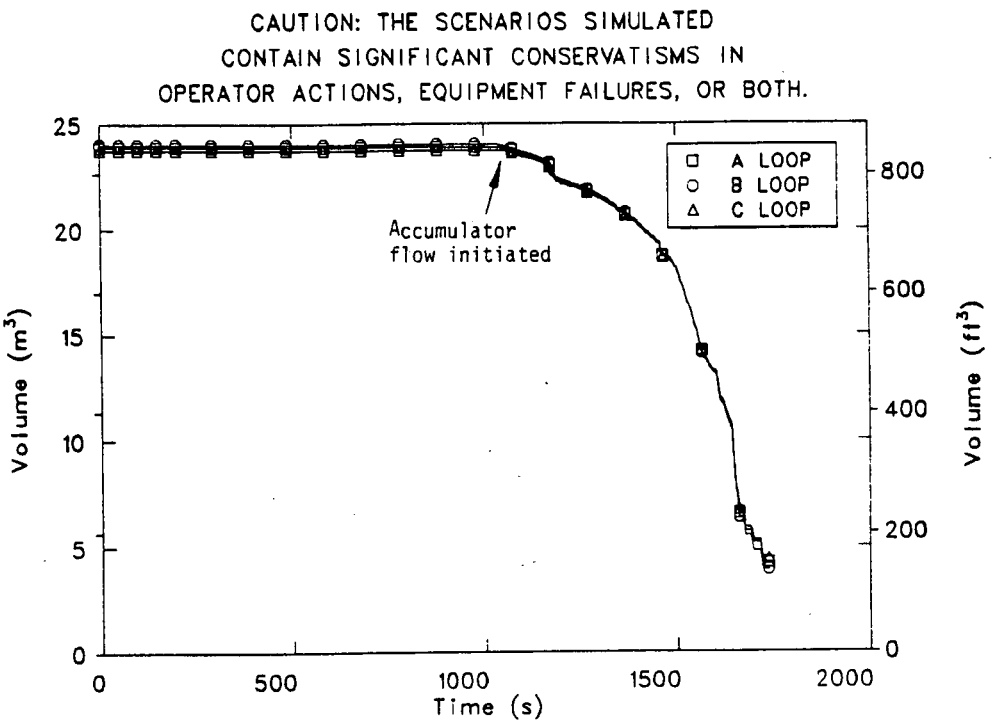

Figure 11-4. Scenario 8 accumulator liquid volumes.

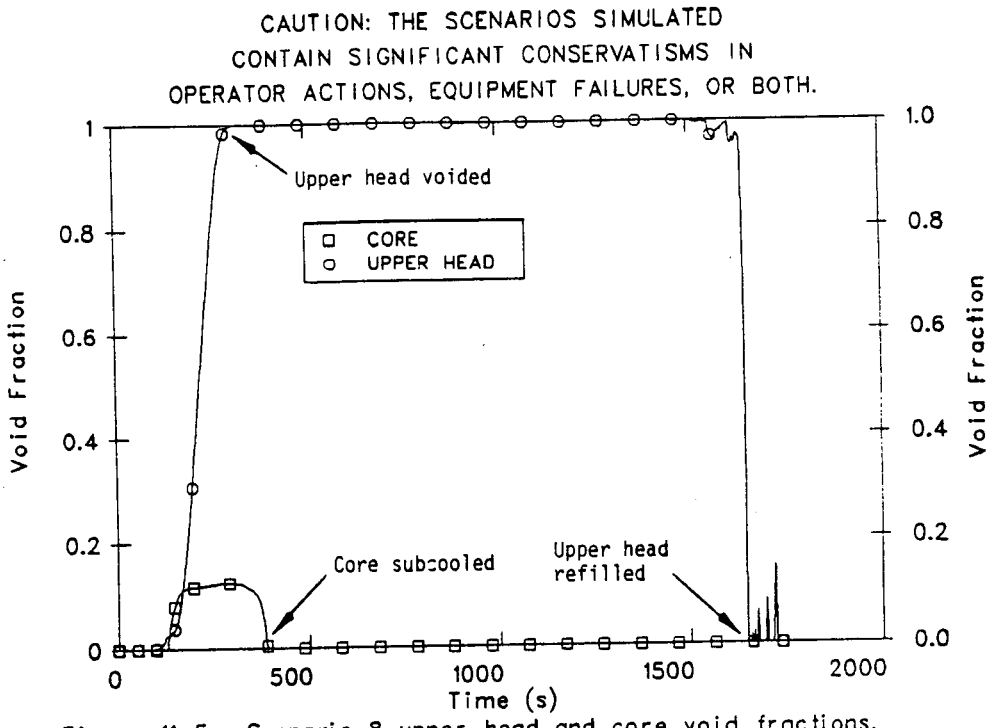

Figure 11-5. Scenario 8 upper head and core void fractions.

near the center of the core. Voids first appeared in the reactor coolant system in the steam generator U-tubes at 53 s. The upper head began draining at 100 s and was completely voided by 300 s. Voids formed in the core at 125 s due to a reduction in flow following the reactor coolant pump trip at 32 s. An increase in core inlet flow at 370 s brought subcooled liquid into the core, causing the voids in the core to disappear by 400 s. The core was subcooled for the remainder of the calculation. The steam generator U-tubes were voided completely by 800 s, and by 900 s the loops had drained down to the elevation of the hot leg nozzles. Accumulator injection began at 1040 s, starting the refill of the reactor coolant system. The reactor vessel had completely refilled at 1650 s as evidenced by the void fraction in the upper head going to zero. By 1650 s, the hot legs had nearly refilled and liquid drops were entering the U-tubes.

The rate of heat transfer to each steam generator secondary is shown in Figure 11-6. The heat transfer into the C steam generator increased at the start of the transient because of an increase in the C hot leg fluid temperature that was caused by an outsurge of flow from the pressurizer. The heat transfer into the C steam generator decreased shortly after the pressurizer emptied at 17 s. The steam generator secondaries began acting as a heat source at 57 s. The steam generators were generally heat sources for the remainder of the calculation, although they were heat sinks between 370 s and 480 s because of cooling effects related to AFW. The steam generators were nearly thermally isolated after the U-tubes voided at 800 s. Consequently, the steam generators remained hot even though the primary coolant system was cooling. Liquid droplets began entering the U-tubes at 1650 s, resulting in a large heat transfer rate from the hot steam generators to the reactor coolant.

Calculated cold leg mass flow rates are shown in Figure 11-7. The vertical scale has been limited to present an expanded view of the flow rates after completion of pump coastdown. The mass flow rates decreased rapidly following the trip of the reactor coolant pumps at 32 s. The loop flows nearly stagnated at 125 s when the volume expansion due to vapor production in the core approximately balanced the volumetric flow out the break. In fact, between 125 s and 330 s the flow in the A and B loops was from the vessel backwards through the pump towards the steam generator.

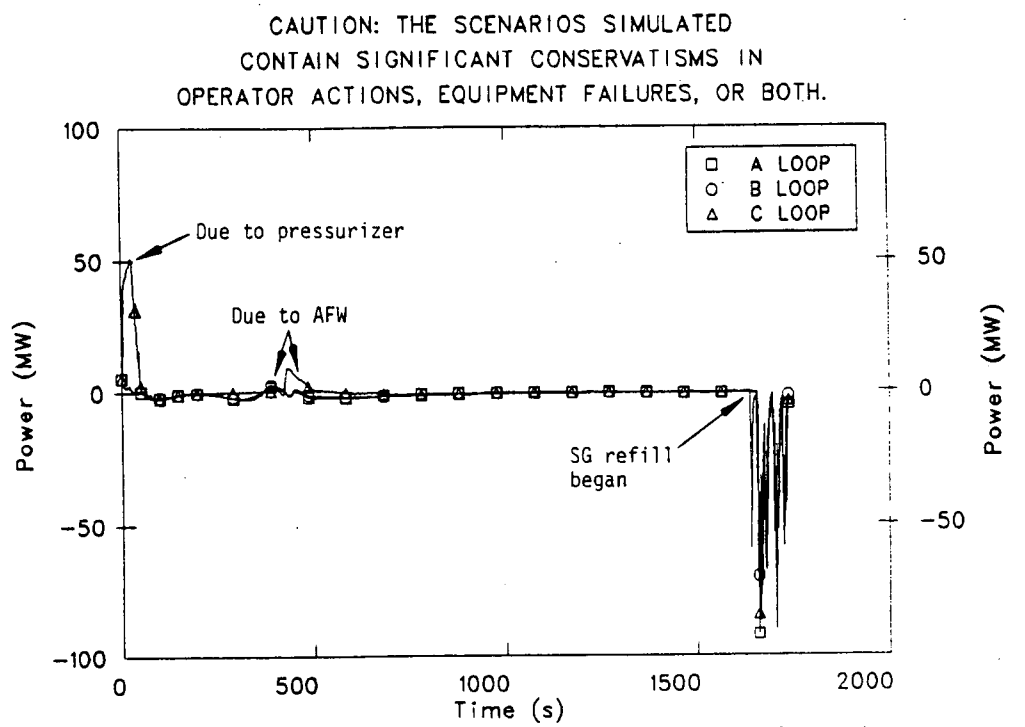

Figure 11-6. Scenario 8 steam generator heat transfer rates.

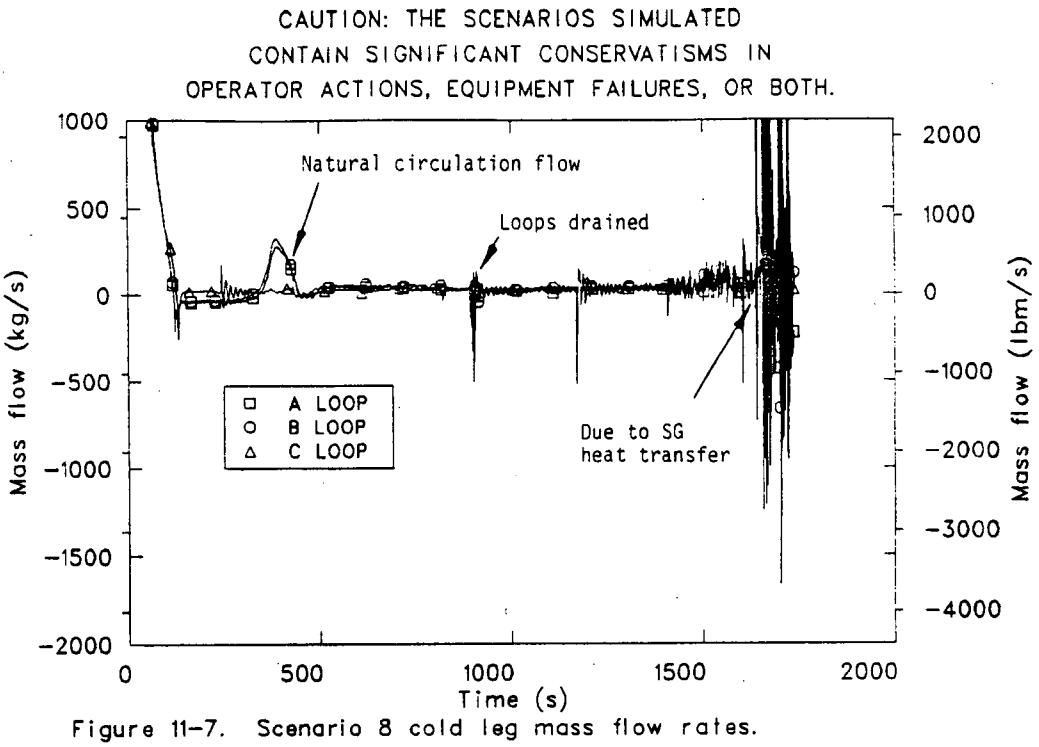

Figure 11-7. Scenario 8 cold leg mass flow rates.

Between 125 and 300 s, the density difference between the core and downcomer was balanced by a difference in liquid level in the uphill and downhill sides of the steam generator U-tubes. Because of the reverse flow in the A and B cold legs, the HPI refilled the U-tubes at 350 s and the density difference between core and downcomer could no longer be balanced within the steam generator, resulting in a positive natural circulation flow in the A and B loops. The increase in flow caused the voids in the core to disappear as the core subcooled at 400 s. The driving potential for natural circulation decreased as the voids in the core disappeared, and the loop mass flow rates nearly stagnated again. The low mass flow rates in the cold leg between 450 and 900 s were primarily due to draining of the downhill side of the U-tubes and loop seal piping down to the elevation of the hot leg nozzle. After the loops stopped draining at 900 s, the mass flow in the cold leg was mostly due to HPI and accumulators. The calculated mass flow rates became very noisy after 1650 s when the reactor coolant system refilled sufficiently for water droplets to reach the U-tubes. A simultaneous reflooding of three hot steam generators would probably be an oscillatory process, but the magnitudes of the calculated flow oscillations are probably too large.

Calculated cold leg and downcomer fluid temperatures are shown in Figure 11-8. Significant differences between cold leg temperatures were calculated between 125 and 900 s. After the loop mass flow stagnated at 125 s, slight differences in the direction and magnitude of cold leg flows caused relatively large differences between the cold leg temperatures in different loops. The cold leg temperatures decreased rapidly at 900 s when the loops drained down to the elevation of the hot leg nozzles. After the loops finished draining, the cold leg flows were due primarily to the ECC flows, and consequently the cold leg temperatures decreased nearly to the ECC temperature. The minimum cold leg temperature was about 310 K (100°F), just 5.6 K (10°F) above the HPI temperature. The downcomer temperature, although generally higher than the cold leg temperatures, also decreased after 900 s. The downcomer was warmer than the cold legs primarily because of leakage of warmer fluid from the upper plenum, upper head, and downcomer bypass regions into the downcomer. The cold leg and downcomer temperatures increased after 1650 s due to mixing caused by the flow oscillations that accompanied the refill of the steam generator U-tubes.

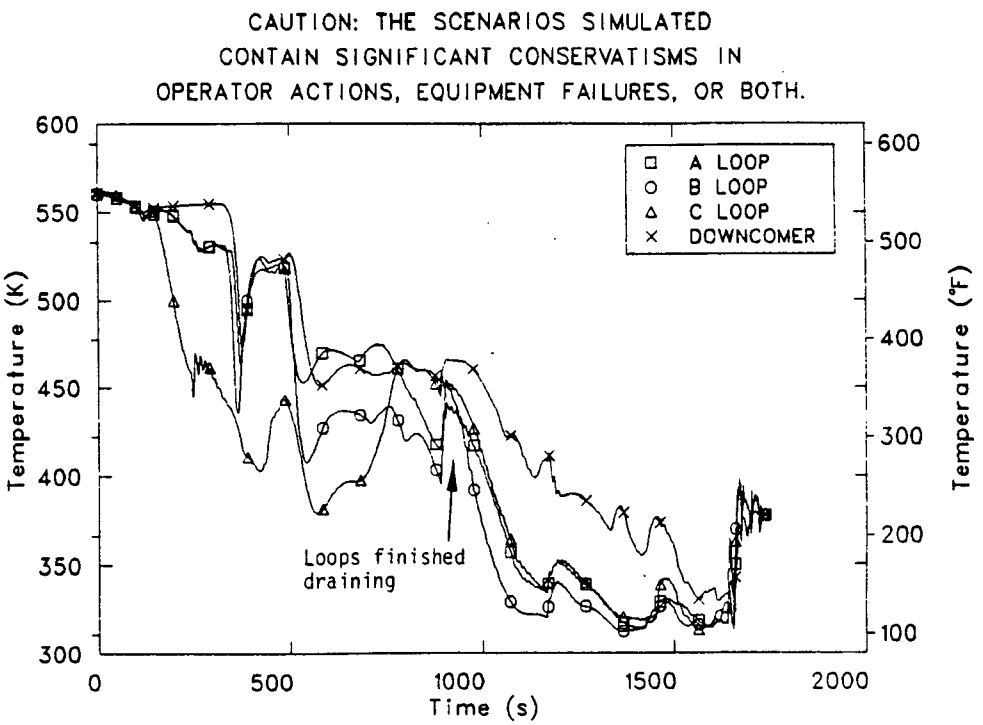

Figure 11-8. Scenario 8 cold leg and downcomer fluid temperatures.

11.3.2 Extrapolations and Uncertainties

No significant offsets or biases due to uncertainties were apparent in the calculation.

Downcomer fluid pressure is shown in Figure 11-9. The pressure was calculated by the code prior to 1740 s and extrapolated by hand after 1740 s. The extrapolated pressure was constant at 1.3 MPa (190 psia) until 2700 s when the steam generator secondaries would have cooled to the primary saturation temperature, based on the calculated heat transfer rate at 1740 s. The pressure then decreased to below the shutoff head of the LPI pumps and remained constant thereafter. The final pressure value was determined from steady state mass and energy balances. At steady state, the break flow equaled the sum of the HPI and LPI flows and removed core decay power. The steady state downcomer pressure was 0.97 MPa (140 psia). The steady state fluid temperature at the break was 320 K (120°F), and the break was covered with subcooled liquid.

Downcomer fluid temperature is shown in Figure 11-10. The temperature was calculated by the code before 1740 s and extrapolated by hand after 1740 s. The extrapolated temperature was constant between 1740 s, when the calculation terminated, and 2700 s, when the steam generator secondaries cooled to primary saturation temperature. The downcomer temperature was then assumed to cool to 310 K (100°F). The final downcomer temperature was 6 K (10°F) above the HPI/LPI temperature because of bypass and leakage flows within the reactor vessel.

The heat-transfer coefficient for the reactor vessel wall is shown in Figure 11-11. The heat-transfer coefficient was calculated by the code before 1740 s and extrapolated by hand after 1740 s. The extrapolation assumed a constant coefficient, equal to the average calculated value during the reflooding of the U-tubes, until the steam generator secondaries were cooled to primary saturation temperature at 2700 s. The heat-transfer coefficient then decreased to 320 W/m^2-K (58 Btu/hr-ft^2-°F) based on a forced convection heat-transfer correlation (Dittus-Boelter) and the combined HPI and LPI flow at 7200 s.

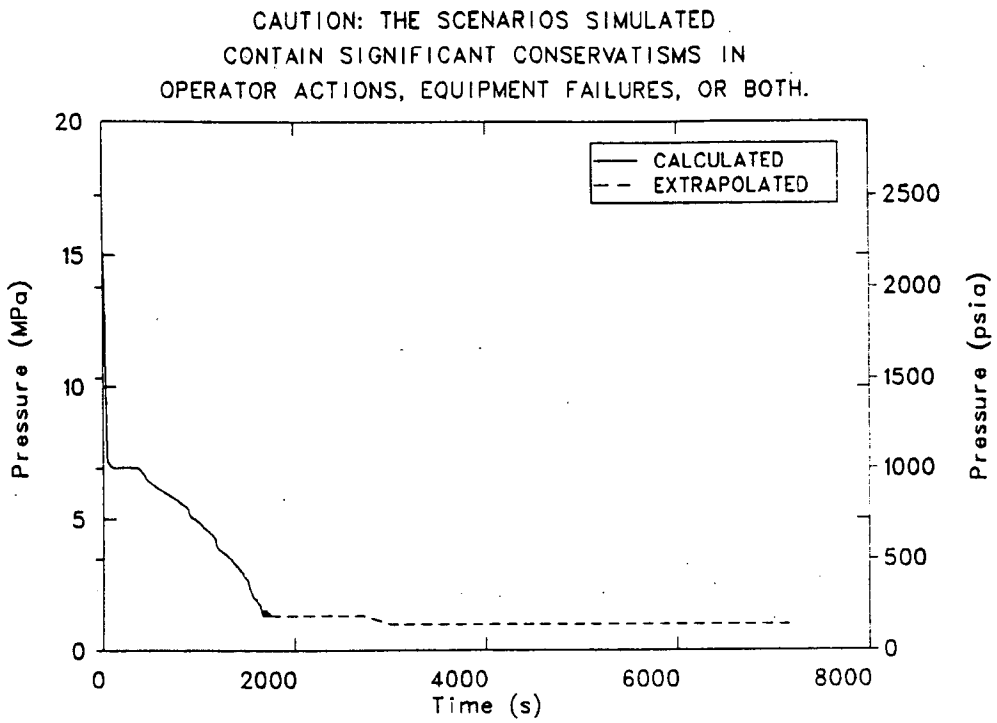

Figure 11–9. Scenario 8 extrapolated reactor vessel downcomer pressure.

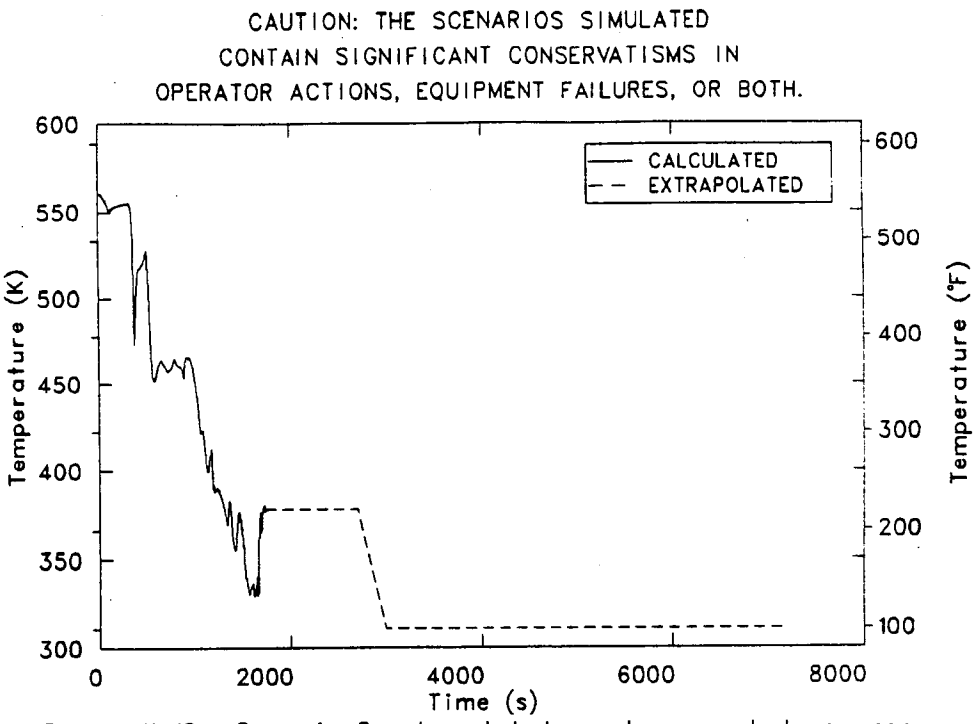

Figure 11–10. Scenario 8 extrapolated reactor vessel downcomer temperature.

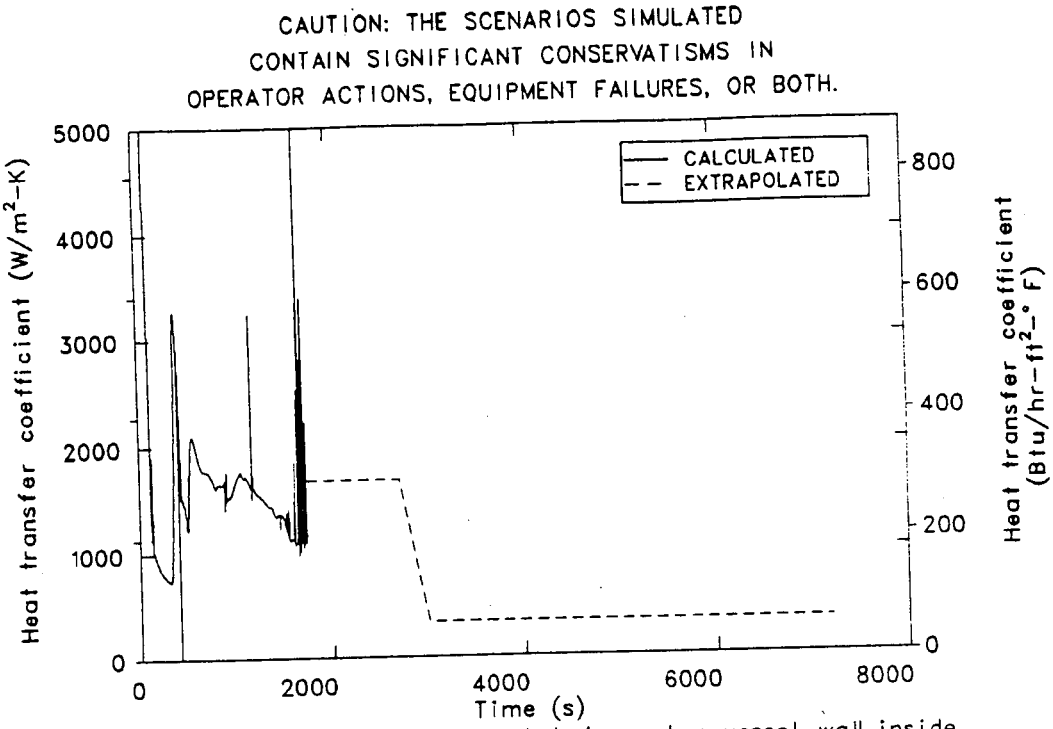

Figure 11–11. Scenario 8 extrapolated reactor vessel wall inside surface heat–transfer coefficient.

The mass flow rate in the A cold leg is shown in Figure 11-12. The mass flow rate was calculated by the code before 1740 s and extrapolated by hand after 1740 s. The B and C loop flow rates were not shown because the flow was similar in all three loops after 500 s. The extrapolation for the A loop flow was applicable for the other loops. The extrapolated flow equaled the sum of the HPI and LPI flows.

The fluid temperature in the A cold leg is shown in Figure 11-13. The temperature was calculated by the code before 1740 s and extrapolated by hand after 1740 s. The B and C loop temperatures were not shown because the temperatures in all three loops were similar after the loops finished draining at 900 s. The same extrapolation was applicable for all three loops. The extrapolated temperature was constant between 1740 s, when the calculation terminated, and 2700 s, when the steam generator secondaries cooled to primary temperature. The extrapolated temperature then decreased the 306 K (90°F), the temperature of the HPI and LPI.

11.4 Conclusions

The minimum calculated downcomer fluid temperature was 329 K (133°F) and occurred at 1616 s. The calculated downcomer pressure at 1616 s was 1.77 MPa (257 psia). The downcomer fluid temperature and pressure extrapolated to 7200 s were 310 K (100°F) and 0.97 MPa (140 psia), respectively. Three-dimensional effects within the downcomer were probably not important during this transient because all three loops responded similarly after 900 s, which was long before the minimum downcomer temperature occurred. The calculation was thought to be reasonable. No significant offsets or biases in the calculation were apparent.

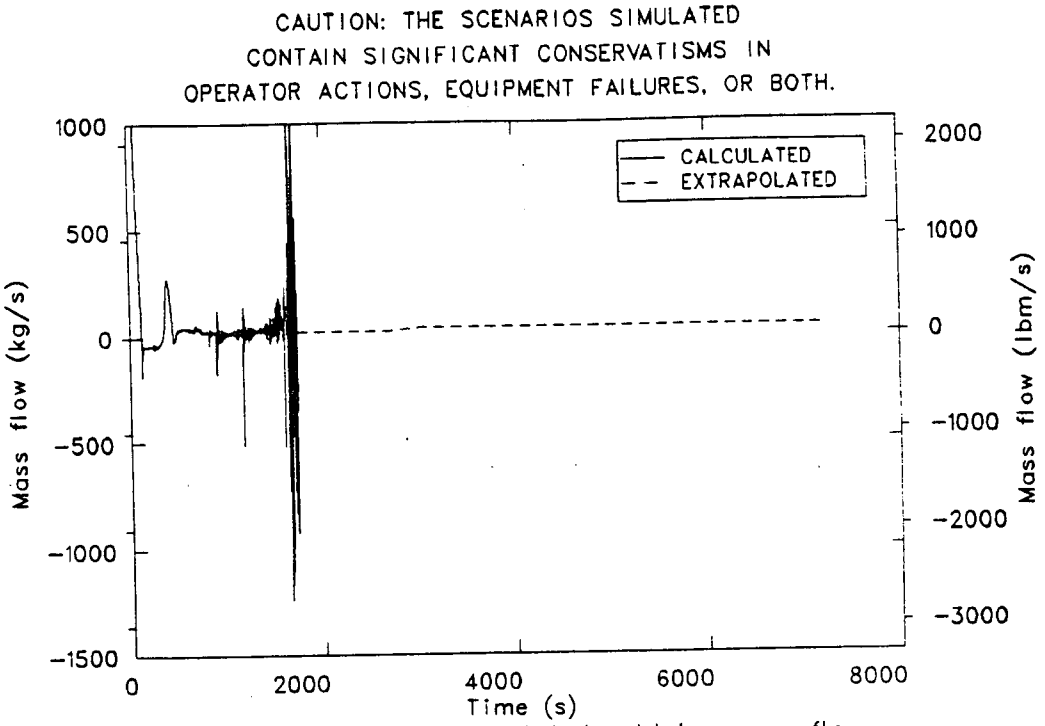

Figure 11-12. Scenario 8 extrapolated cold leg mass flow.

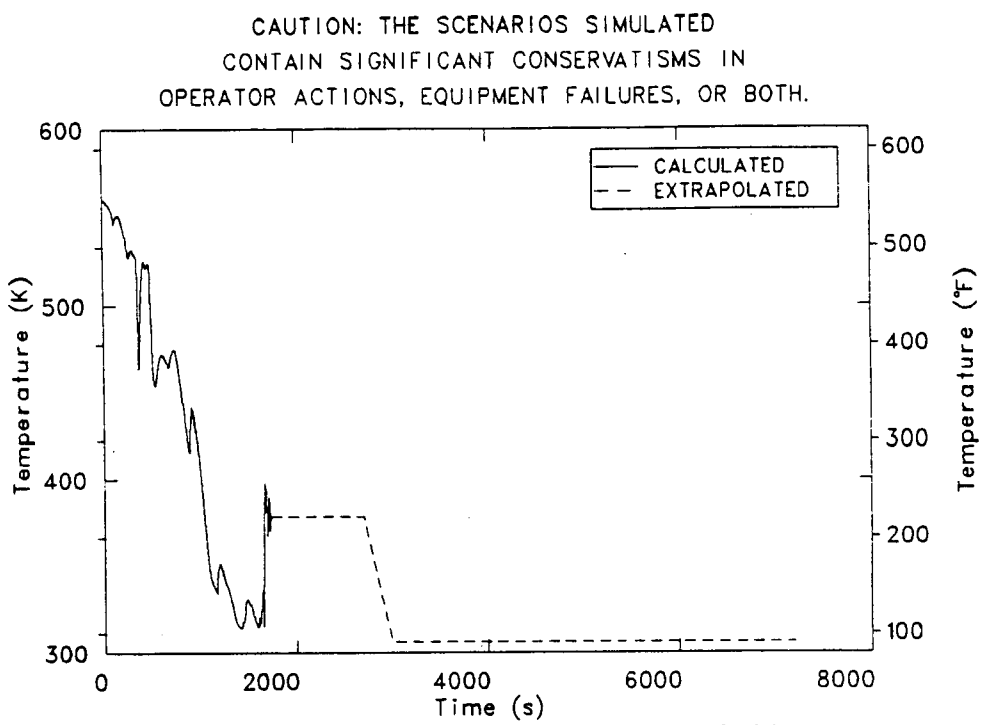

Figure 11-13. Scenario 8 extrapolated cold leg fluid temperature.

12. SCENARIO 9, STEAM GENERATOR TUBE RUPTURE AT HOT STANDBY

The following section describes the investigation of Scenario 9. This calculation was performed to evaluate the consequences of a postulated rupture of a single steam generator tube with the reactor at hot standby conditions.

A description of the scenario is provided in Section 12.1, followed by a discussion of the model changes required to perform the calculation in Section 12.2. The results of the calculation, the extrapolated results and the uncertainties associated with the calculation are described in Section 12.3. The conclusions regarding the calculation are presented in Section 12.4.

Scenarios investigated in this report generally include conservative assumptions concerning equipment failures, operator actions, or combinations of these. Conclusions relative to pressurized thermal shock severity are not to be drawn directly from the results presented in this report (see Section 15).

12.1 Scenario Description

A description of the scenario as developed at Oak Ridge National Laboratory, appears in Table 12-1.

The scenario is initiated with the double-ended rupture of a single tube in steam generator A with the reactor at hot standby conditions. The break is located at the tubesheet on the cold leg end of the tube. Operator actions are assumed to trip off reactor coolant pump (RCP) power when primary system pressure falls below 9.07 MPa (1315 psia) and restart RCPs if subcooling, pressure, and pressurizer level criteria are later satisfied. The operator is also assumed to throttle auxiliary feedwater to maintain 40% steam generator narrow-range levels.

TABLE 12-1. SCENARIO DESCRIPTION NO. 9

Plant Initial State - Just prior to transient initiator

General Description: Hot 0% Power, 0% Power after 100 hrs of shutdown
System Status

Turbine: Not latched, TSVs closed
Secondary PORV: Automatic control
Steam Dump Valves: Automatic control
Charging System: Automatic control
Pressurizer: Automatic control
Engineering Safety Features: Automatic control
PORVs: Automatic control
Reactor Control: Manual
Main Feedwater: In bypass mode, manual control to provide zero power level in S/G's; 1 condensate pump, 1 MFWP operating.
Aux Feedwater: Automatic control
MSIVs: Open, Automatic control
MFIVs: Closed, Automatic control

Transient Initiator - A steam generator tube rupture on the cold leg side of tube sheet of S/G A.

Equipment Failures which occur during the transient if the equipment is demanded.

None

Operator Reactions to Reported Information

1. If SIAS signal is generated, the operator will trip the reactor coolant pumps when RCS pressure reaches 1300 psig.

2. The operator will restart reactor coolant pumps 10 minutes after all the following criteria are met.

   A. > 40°F subcooled
   B. Pressurizer level ≥ 20% or increasing
   C. R.C. pressure > 325 psig

3. The operator will throttle AFW flow to maintain 40% S/G level.

The assumed operator actions represent those expected in response to a small break loss of coolant transient which the operator fails to recognize as a steam generator tube rupture event. That is, operating procedures to recover from a steam generator tube rupture event are not followed.

12.2 Model Changes

With the exception of nodalization changes necessary to simulate the broken steam generator tube, the model used to perform this calculation is described in Sections 2.1 and 2.2. The transient was initiated from the hot standby conditions presented in Section 2.3.3.

The broken steam generator tube was simulated by the nodalization shown in Figure 12-1. The tube primary side was represented by four cells. Heat transfer was represented between each cell and its adjacent steam generator secondary cell. In addition to wall friction, lumped flow losses were used at junctions 289, 291, and 292 representing contraction from plena to tube and expansions from tube to the secondary region.

12.3 Results

The following sections describe the analysis results for a calculation of Scenario 9 and extrapolation and uncertainty of those results.

12.3.1 Calculation Results

A sequence of events for this calculation is presented in Table 12-2.

At zero time a single tube in steam generator A was assumed to have ruptured at the tubesheet on the cold leg end. Figure 12-2 shows the break mass flow rates through both ends of the ruptured tube. The flow through the hot leg end was significantly less than that through the cold leg end due to the large wall friction pressure drop imposed on the fluid exiting through the full length of tube. Flow through both break paths was friction dominated, that is, the flow rates were determined by the flow losses of the paths and not by choking phenomena. Both paths passed single phase liquid throughout the calculation.

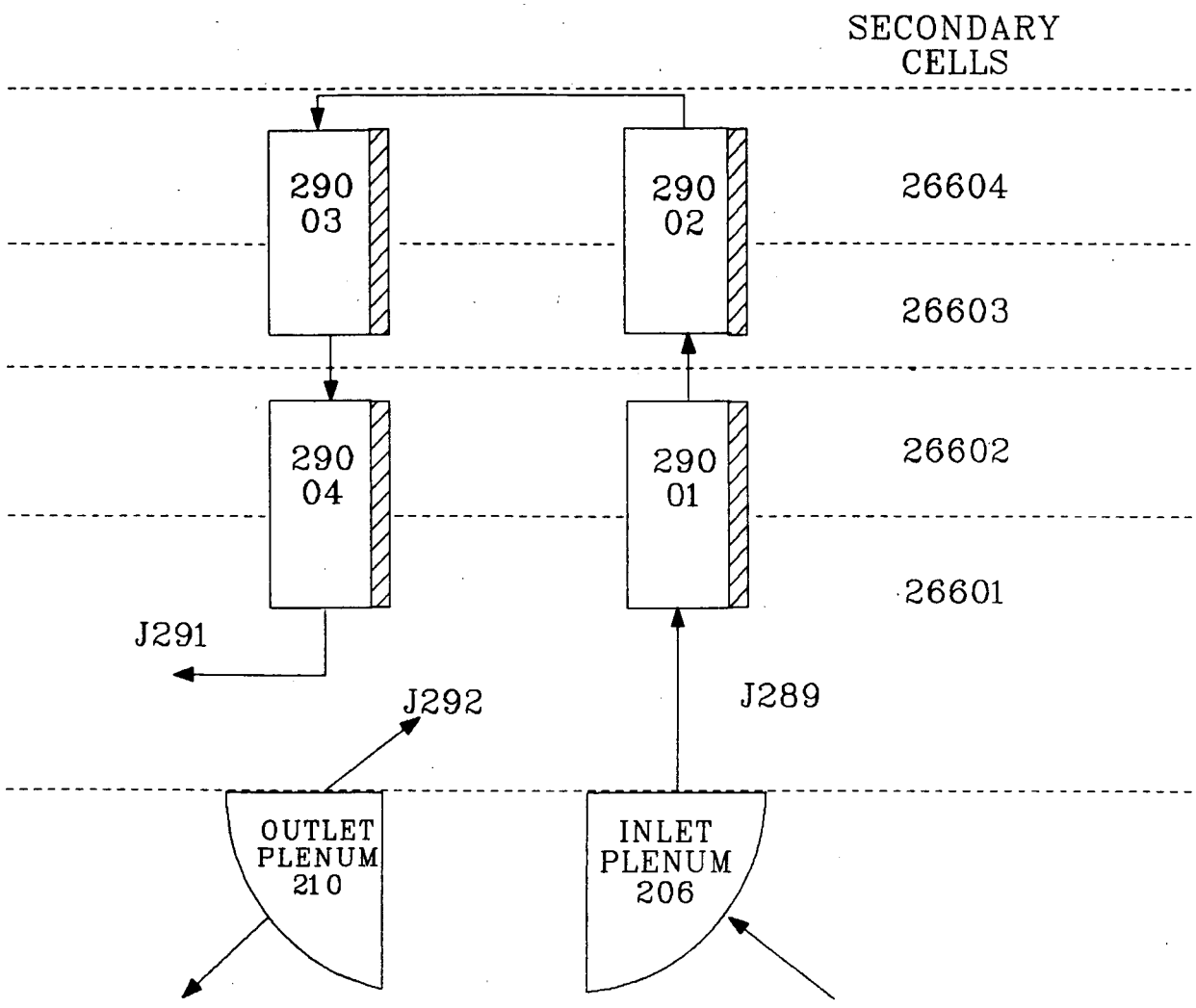

FIGURE 12–1. NODALIZATION FOR BROKEN TUBE IN STEAM GENERATOR A.

TABLE 12-2. SCENARIO 9 SEQUENCE OF EVENTS

Time (s)	Event
0	Tube rupture occurs
1	Proportional pressurizer heaters powered, makeup rate starts increasing
8	Backup pressurizer heaters powered
64	Pressurizer heaters depowered on low level
68	Makeup rate reaches maximum capacity
276	SIAS signal generated by low pressurizer pressure (1730 psia)
	Actions due to SIAS are: feedwater bypass valves closed, main feedwater pump tripped; main feedwater pump recirculaton flow terminated; motor-driven auxiliary feedwater initiated and steam generator levels controlled to 40% NR; HPI and LPI pumps started (shutoff head HPI: 1470 psia, LPI: 145 psia), letdown isolated.
366	HPI flow starts (1470 psia)
625	RC pump trip (1315 psia)
794	RC pump rotors stopped
1332	Affected steam generator separator flooded (void = 0.)
1530	Liquid flow to affected steam generator steam line begins
2500	Affected steam generator liquid solid
7200	Calculation terminated

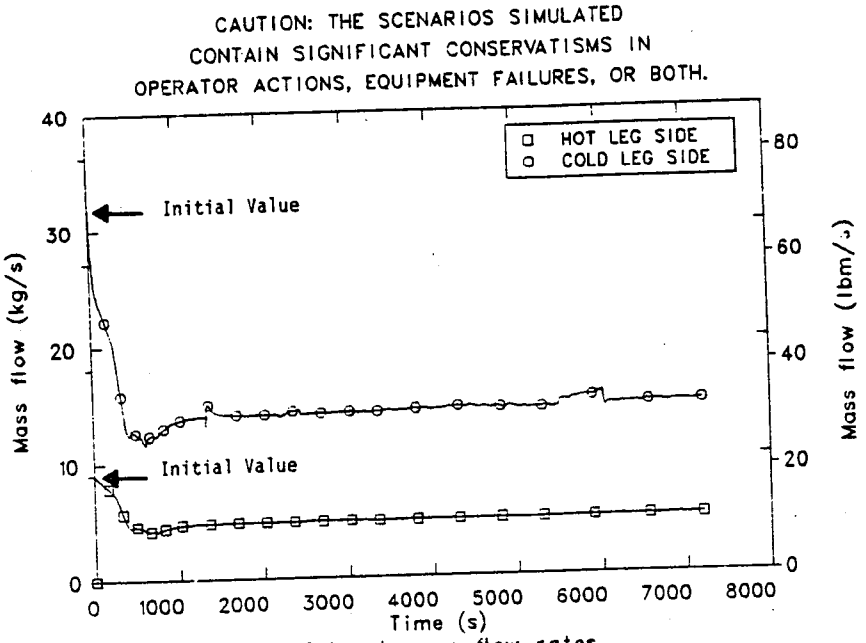

Figure 12-2. Scenario 9 break mass flow rates.

As a result of the break the primary system pressure fell, as shown in Figure 12-3, causing the pressurizer proportional heaters to be powered at 1 s and backup heaters to be powered at 8 s. The pressurizer level indication, shown in Figure 12-4 fell due to the fluid volume lost through the break and this first caused the makeup rate to increase and then tripped off pressurizer heater power. Because the pressurizer level indication did not recover, the reactor coolant pump restart criteria (see operator actions in Table 12-1) was never achieved.

The affected steam generator mass inventory increased dramatically as shown in Figure 12-5 and the associated increase in steam generator level caused a slight throttling back of main feedwater to the affected steam generator as shown in Figure 12-6. The transient was assumed to start with main feedwater under manual control with the reactor at hot standby conditions. Accordingly, there was an uncertainty as to what control, if any, should be placed on the affected steam generator's main feedwater bypass valve. Options included (1) freezing the valve at its pre-transient area, (2) allowing the valve to modulate at a rate consistent with that used prior to the transient, and (3) closing the valve. Option (1) assumes the operator does not observe the increasing level in steam generator; option (2) assumes he observes it and controls feedwater as he has been; option (3) assumes he observes it, recognizes a tube rupture has occurred and acts accordingly. The calculation was performed using option (2). The gradual initial decline in affected steam generator main feedwater bypass valve flow rate is an indication that the operator is slowly throttling back feedwater but does not recognize the transient as a tube rupture which would require isolation of feed and steam functions of the affected steam generator. This choice is consistent with the operator actions in the scenario description (Table 12-1) which indicates the operator is aware a small break transient is in progress but does not recognize it to be a steam generator tube rupture. The results of the calculation were insensitive, however, to the selection of options (1), (2), or (3) because the combined break mass flow rates (Figure 12-2) exceeded the affected steam generator main feedwater flow rate (Figure 12-6) by more than an order of magnitude. Thus results were relatively insensitive to the delivery of main feedwater.

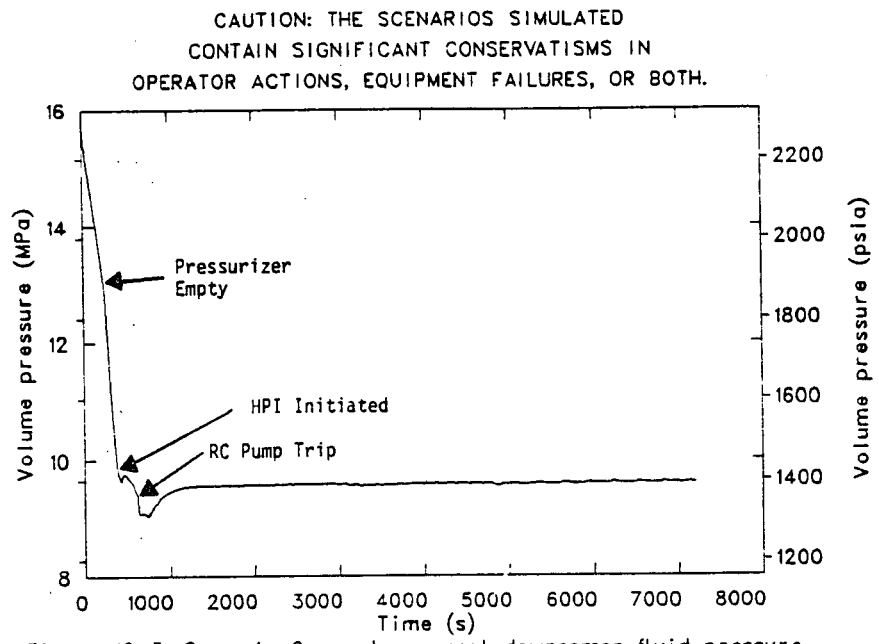

Figure 12-3. Scenario 9 reactor vessel downcomer fluid pressure.

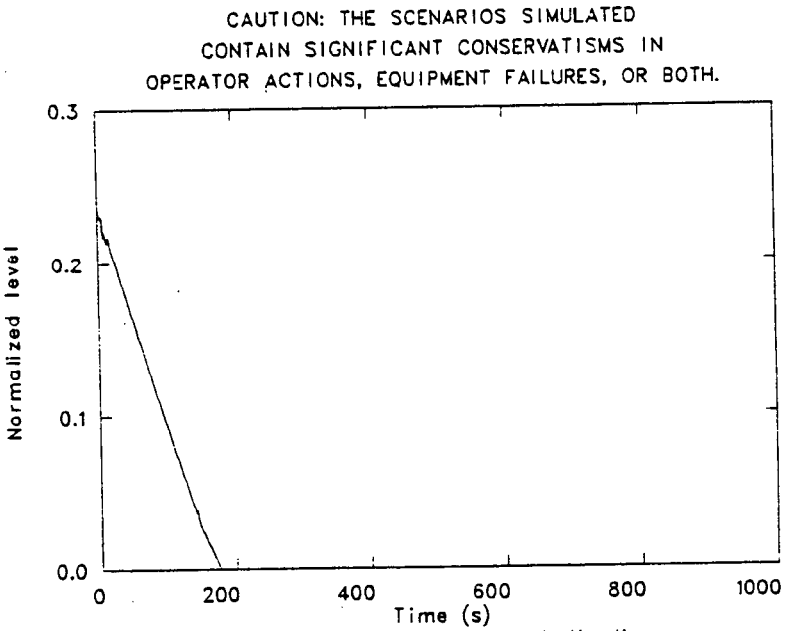

Figure 12-4. Scenario 9 pressurizer level indication.

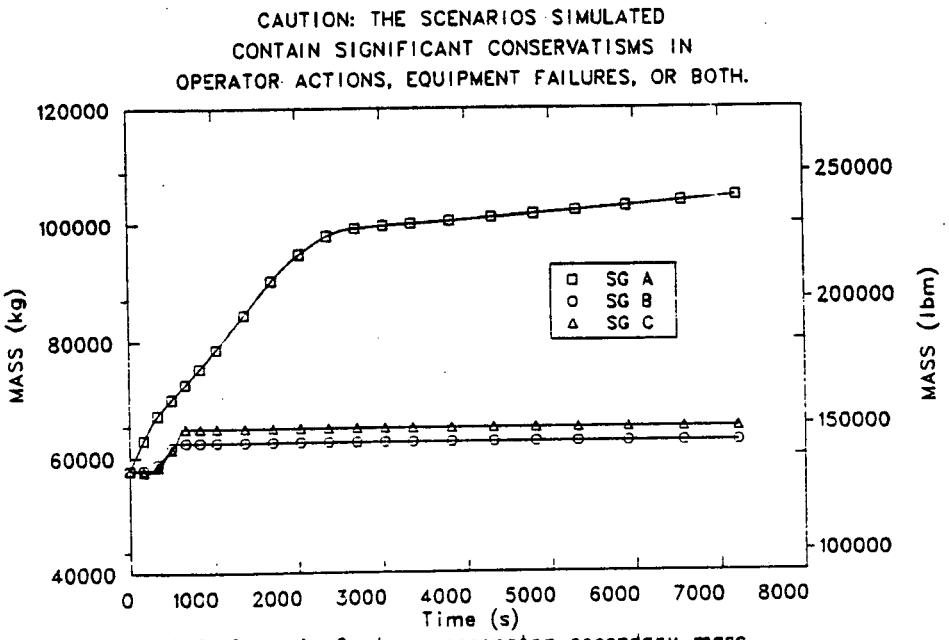

Figure 12-5. Scenario 9 steam generator secondary mass inventories.

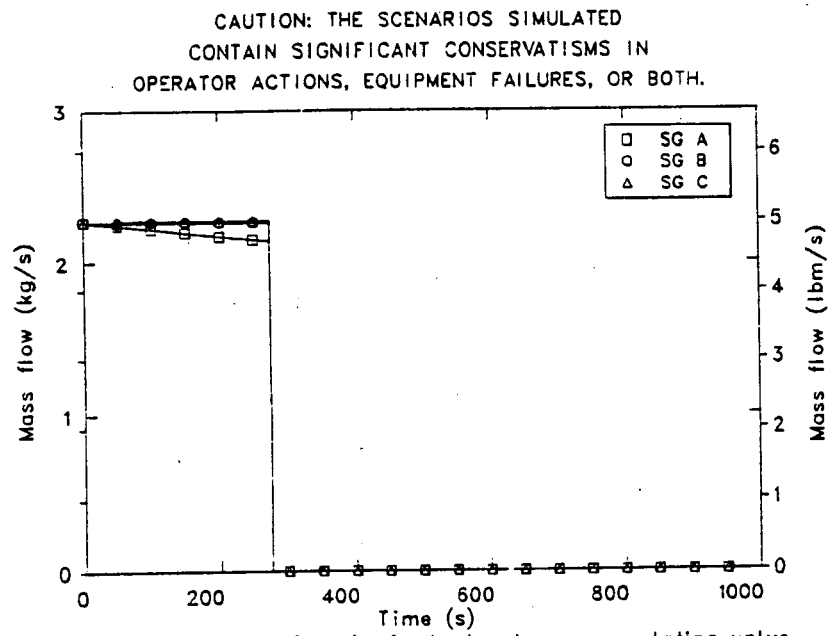

Figure 12-6. Scenario 9 main feedwater bypass regulating valve flow rates.

At 276 s the safety injection activation signal (SIAS) was generated due to low pressurizer pressure. As a result of the SIAS the following actions occurred: Main feedwater (MFW) bypass valves were closed, the MFW pump was tripped, MFW pump recirculation flow was terminated, motor-driven auxiliary feedwater (AFW) was initiated and controlled to each steam generator to maintain 40% narrow-range level indication, high and low pressure injection (HPI and LPI) pumps were started, and letdown was isolated.

Turbine-driven AFW initiation requires two-out-of-three low steam generator level indications and as a result was not started for this transient. Therefore, only motor-driven AFW was initiated during this transient.

Figure 12-7 shows a comparison of total injection and break mass flow rates. Injection flow combines the HPI rate for the three loops with the makeup rate. Break flow is a combination of the two break mass flow rates shown in Figure 12-2. Following initiation of HPI at 366 s the injection flow exceeded the break flow by a small amount throughout remainder of the transient. During this period the primary system pressure (Figure 12-3) was stabilized slightly below the HPI shutoff head with injection volumetric flow just balanced by break volumetric flow, the pressurizer virtually empty, and the pressurizer surge line flow virtually zero. The injection mass flow rate during this period was slightly higher than that of the break in Figure 12-7 because the injection flow density was higher than that at the break.

Figure 12-8 shows the steam generator secondary pressure responses and Figure 12-9 shows the steam generator heat removal rates. The heat removal rate shown for Steam Generator A does not include the break flow energy removal rate, only that energy removed through the tube walls. Steam Generator A (SGA) remained pressurized to the steam dump setpoint as a result of the broken tube break flows and became a primary system heat source at 511 s. Because the SGA level was elevated, no AFW was delivered to SGA. Steam Generators B and C (SGB and SGC) secondary pressures remained elevated until 593 and 703 s, respectively, when these generators

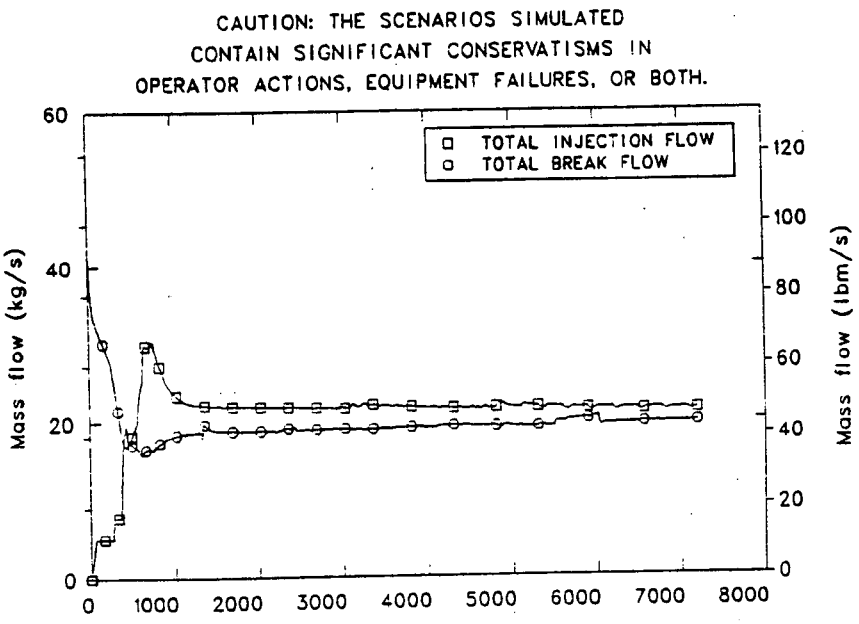

Figure 12-7. Scenario 9 comparison of injection and break mass flow rates.

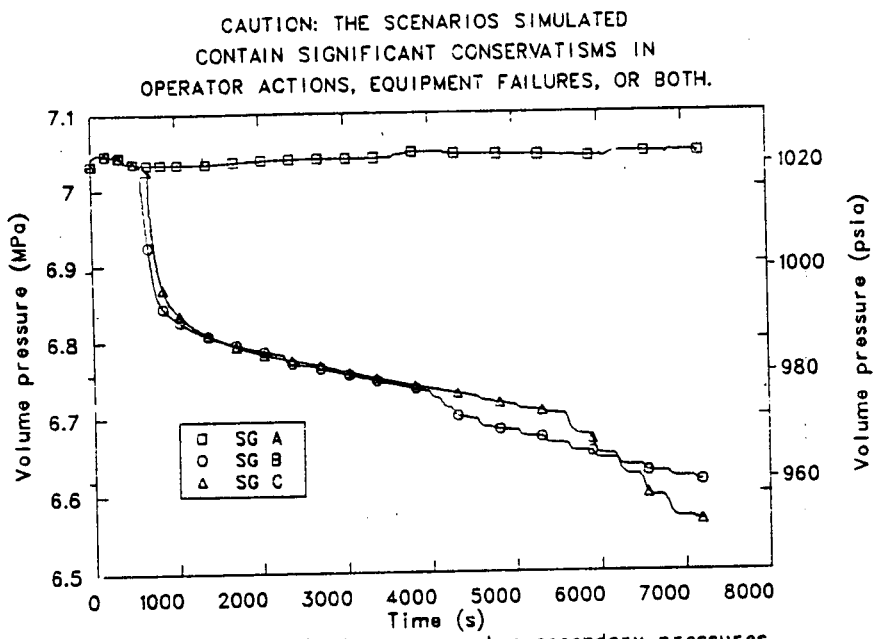

Figure 12-8. Scenario 9 steam generator secondary pressures.

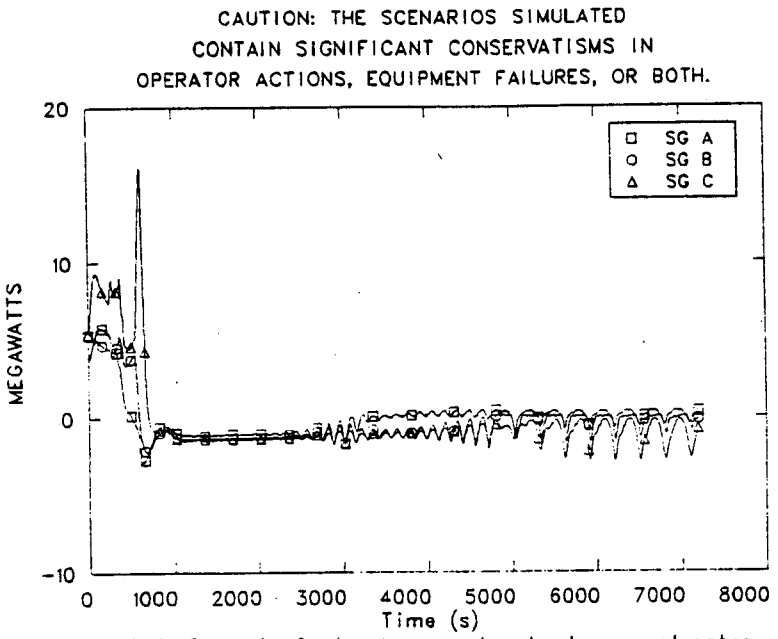

Figure 12-9. Scenario 9 steam generator heat removal rates.

became primary system heat sources. AFW was delivered to SGB from 276 s to 543 s and SGC from 276 to 617 s. AFW to these steam generators was terminated when their narrow range levels exceeded 40%. The initial high SGA heat removal rate was caused as hot pressurizer fluid entered the Loop C hot leg during the initial pressurizer outsurge. The peak in SGC heat removal rate occurred from 543 to 617 s when SGC was receiving all the AFW flow.

At 625 s the primary system pressure declined to 9.07 MPa (1315 psia) and power to all reactor coolant pumps was tripped off. The ensuing pump coastdown ended at 794 s when the pump rotors had stopped.

Mass flow rates between the HPI sites and reactor vessel in the three cold legs are shown in Figure 12-10. Following reactor coolant pump coastdown smooth natural circulation was established at around 1300 s. Due to the effects of the broken steam generator tube, the Loop A cold leg natural circulation flow rate was about one-third that in Loops B and C as shown in Figure 12-10 from about 1300 to 2200 s. After this time, flow oscillations in all three loops were observed. The oscillations were caused by phenomena occurring in the Loop A cold leg. Loop B and C flow oscillations were driven by the oscillations emanating from Loop A. The oscillation of Loop A flow was developed by a time-varying driving force for loop natural circulation flow caused by a time-varying loop A cold leg fluid temperature during periods of low flow or stagnant Loop A conditions. As loop flow approached stagnation, HPI fluid made up an increasing percentage of the fluid reaching the reactor vessel. The HPI fluid was colder than the fluid coming from the reactor coolant pump discharge so as stagnation was approached the reactor vessel downcomer fluid temperature decreased. As a result, the reactor vessel downcomer density increased and this caused the natural circulation flow rate to increase. One would suspect a steady equilibrium point might have been reached where the loop flow slowed until the natural circulation driving potential required to sustain that steady flow was achieved. This steady equilibrium is attainable, however, only if the natural circulation driving potential rapidly responds to changes in loop flow. In the calculation presented here this was not the case; loop velocities were less than about

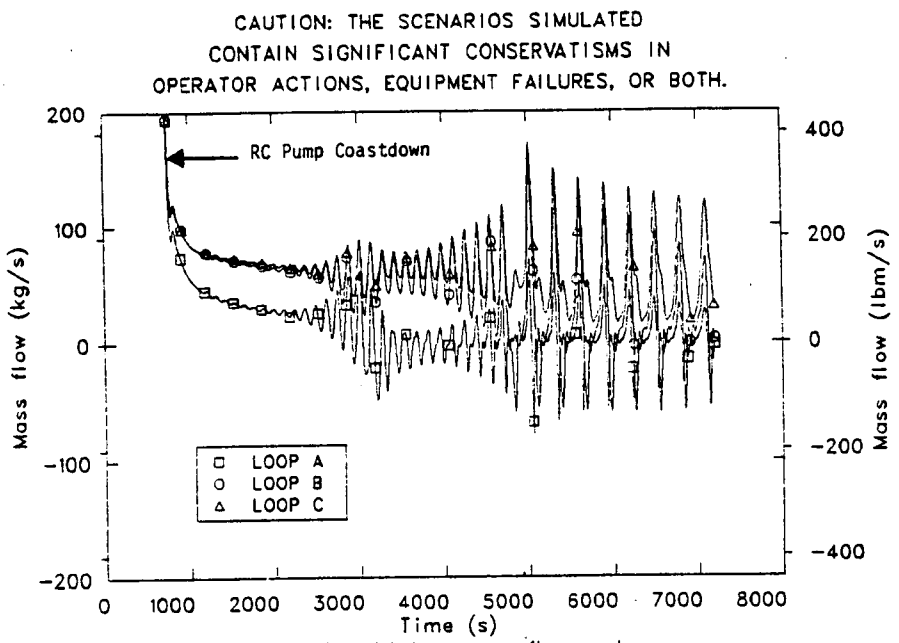

Figure 12-10. Scenario 9 cold leg mass flow rates.

0.05 m/s (0.2 ft/s). Thus a change in loop flow did not affect the natural circulation driving potential (by changing the liquid density in the downcomer) until significantly later in time. At a loop velocity of 0.05 m/s the transit time from the HPI site to the reactor vessel is 80 s. This delay is the cause of the loop oscillations observed in Figure 12-10. To further the investigation, a sensitivity RELAP5 calculation was performed in which the HPI injection sites were moved from the cold legs to the reactor vessel downcomer inlet at 5300 s. The oscillations damped out shortly after the injection sites were moved confirming the delay effect discussed above is responsible for the flow oscillations. The change in the nature of the oscillations at about 5000 s was caused by Loop B also reaching complete stagnation as shown in Figure 12-10. The discussion above is intended to explain the causes of the oscillations observed in the RELAP5 calculation. A discussion of whether or not these oscillations are physical is presented in Section 12.3.2.

Figure 12-11 shows the cold leg fluid temperatures between the HPI sites and the reactor vessel downcomer. All temperatures shown are generally decreasing as a result of continued primary system energy removal due to high pressure injection and break flow. The temperature oscillations are large but are explained fully by the loop flow oscillations just discussed. The minimum calculated downcomer fluid temperature was 451 K (352°F) as shown in Figure 12-12.

At 1332 s the affected steam generator separator was flooded and at 1530 s liquid flow to the affected steam generator steam line commenced. At 2500 s the affected steam generator secondary was liquid solid.

The calculation was terminated at 7200 s, the end of the pressurized thermal shock investigation period as defined at Oak Ridge National Laboratory.

12.3.2 Extrapolations and Uncertainties

Since the calculation was carried out to a full two hours after the initiating event, no extrapolation of data to this time was required.

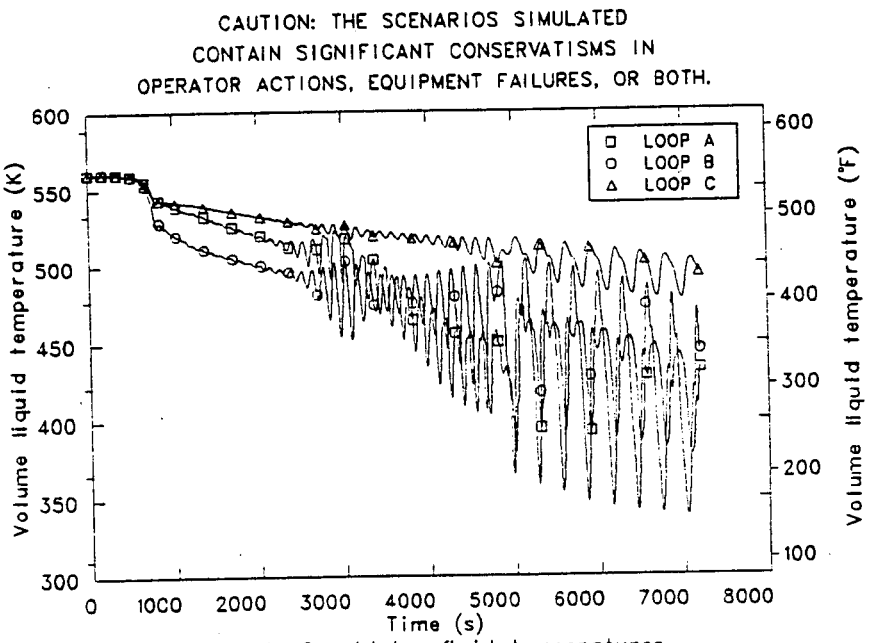

Figure 12-11. Scenario 9 cold leg fluid temperatures.

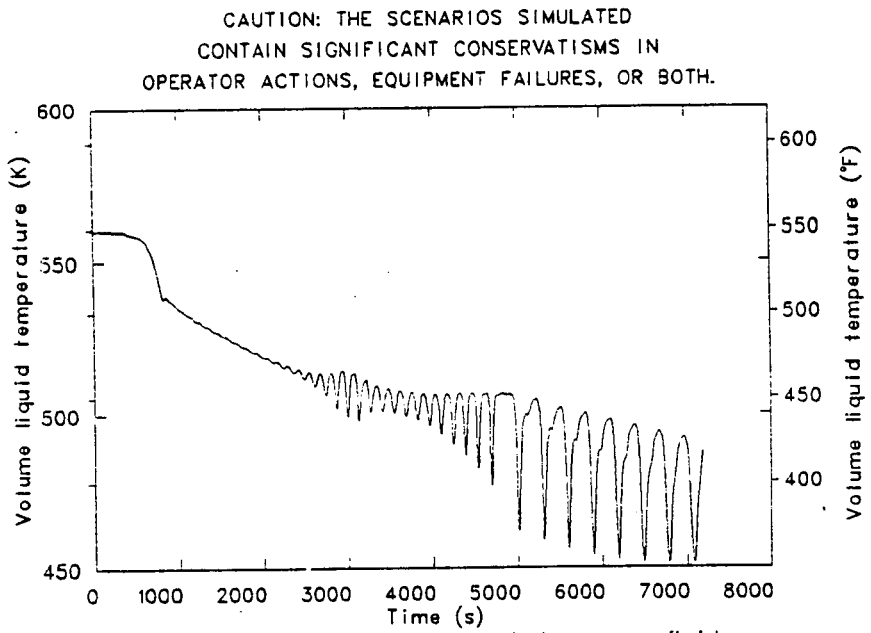

Figure 12-12. Scenario 9 reactor vessel downcomer fluid temperature.

The major uncertainty in the calculated results centers on the flow oscillations discussed in the previous section. The oscillations were determined to be caused by a delayed response of natural circulation driving potential to changes in loop flow. The delay is caused by long transit times of fluid from the HPI site to the reactor vessel. The uncertainty is whether or not the RELAP5-calculated delay phenomena in the affected loop cold leg represents reality.

RELAP5 is a water and steam, two-fluid computer code. If a cell is liquid-filled, such as is the cold leg during the oscillations, the liquid is considered to be homogeneous and represented by a single fluid temperature. The model contains three cells between the HPI site and reactor vessel. As long as loop flow is sufficiently large, a high degree of mixing between HPI and loop flow is to be expected and the model will faithfully represent reality. If the loop flow stagnates, as does Loop A after about 2400 s, a homogeneous model does not well represent the flow conditions expected within the cold leg. Specifically, under stagnant conditions a high degree of vertical thermal stratification of liquid within the cold legs is to be expected. Cold HPI liquid is expected to flow along the bottom of the cold leg cross section underneath warmer liquid flowing in the top. Under such circumstances, the average density of fluid reaching the reactor vessel cold leg nozzle would be smooth in time. Thus the flow oscillations observed during near-stagnant affected loop conditions are caused by a limitation of the computer model and are not physical. Because thermal stratification within the cold leg is to be expected, however, this sequence should be investigated further using a multi-dimensional computer model capable of simulating thermal stratification within the cold leg and reactor vessel downcomer regions.

Since the loop flow oscillations are not physical and have a significant effect on mixed cold leg and reactor vessel downcomer fluid temperatures (Figures 12-11 and 12-12) it was considered necessary to predict the responses to be expected with the oscillations removed. This prediction was accomplished by performing a RELAP5 sensitivity calculation in which the HPI and makeup were relocated from the cold leg to the reactor vessel inlet. As discussed in Section 12.3.1 this change succeeded in

damping out the flow oscillations. The sensitivity calculation was run for 1200 s, starting at 5300 s, and the results were used to generate the dashed lines which appear on the remaining figures in this section. The dashed lines represent the best estimate of plant responses for this sequence.

Figure 12-13 shows the reactor vessel downcomer fluid pressure. The dashed line indicates the best estimate pressure response. Very little change in pressure was observed as a result of damping out the loop flow oscillations. At 7200 s the best estimate pressure is 9.624 MPa (1396 psia).

Figure 12-14 shows the reactor vessel downcomer fluid temperature and Figure 12-15 the downcomer wall inside surface heat transfer coefficient. The dashed lines indicate the best estimate responses as determined through the use of the sensitivity calculation. At 7200 s the best estimate downcomer fluid temperature is 465 K (378°F).

Figures 12-16 through 12-18 show the mass flow rates between the HPI location and reactor vessel in each of the cold legs. The dashed line for each loop was based on the results of the sensitivity calculation with adjustments in loop flow expected if HPI and reactor coolant makeup injection are accounted for. The adjusted cold leg flow rates at the end of calculation are 3.6 kg/s (8 lb/s) in Loop A, 33.6 kg/s (74 lb/s) in Loop B and 60 kg/s (132 lb/s) in Loop C. Factors affecting these differences in loop flows are: (1) the effects of the break on Loop A flow, (2) all makeup injection occurring into Loop B, and (3) Loop C steam generator secondary fluid temperatures below those of Loop B. This latter factor caused less degradation of natural circulation driving head in Loop C than in Loop B, hence the higher Loop C flow.

Figures 12-19 through 12-21 show the cold leg fluid temperatures between the HPI injection locations and the reactor vessel. Adjustments, indicated by the dashed lines, have been made to account for the elimination of oscillatory behavior. The adjustments were accomplished by using the sensitivity calculation as an indication of loop flow rates and

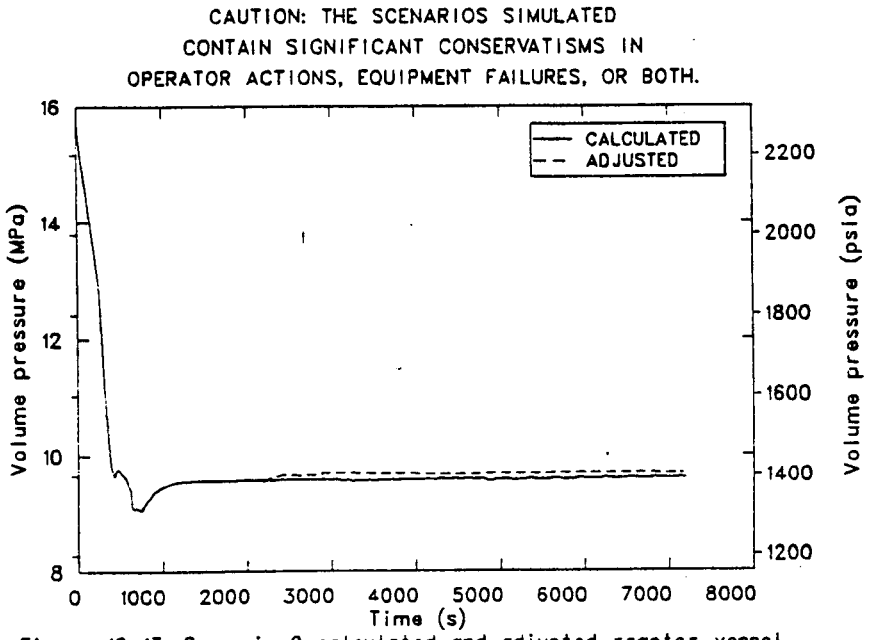

Figure 12-13. Scenario 9 calculated and adjusted reactor vessel downcomer fluid pressure.

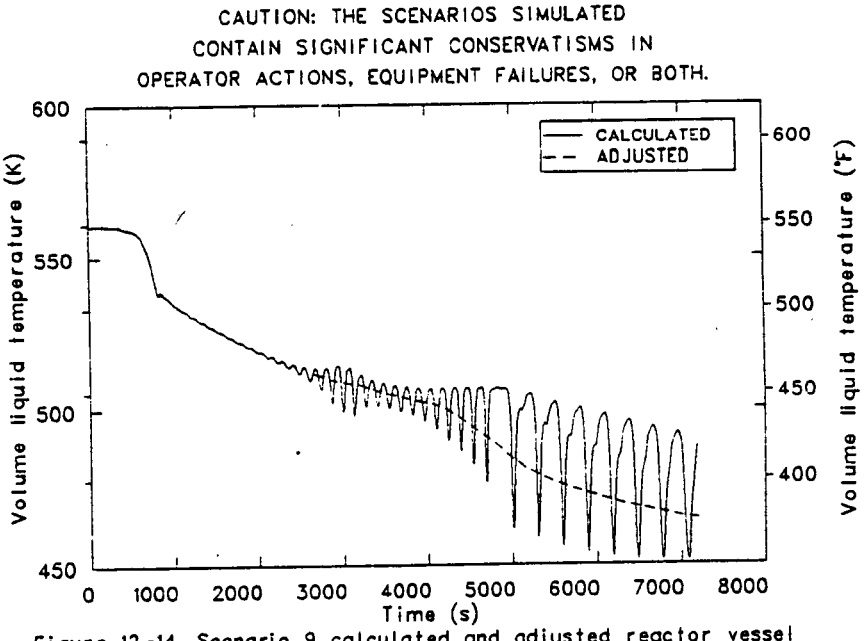

Figure 12-14. Scenario 9 calculated and adjusted reactor vessel downcomer fluid temperature.

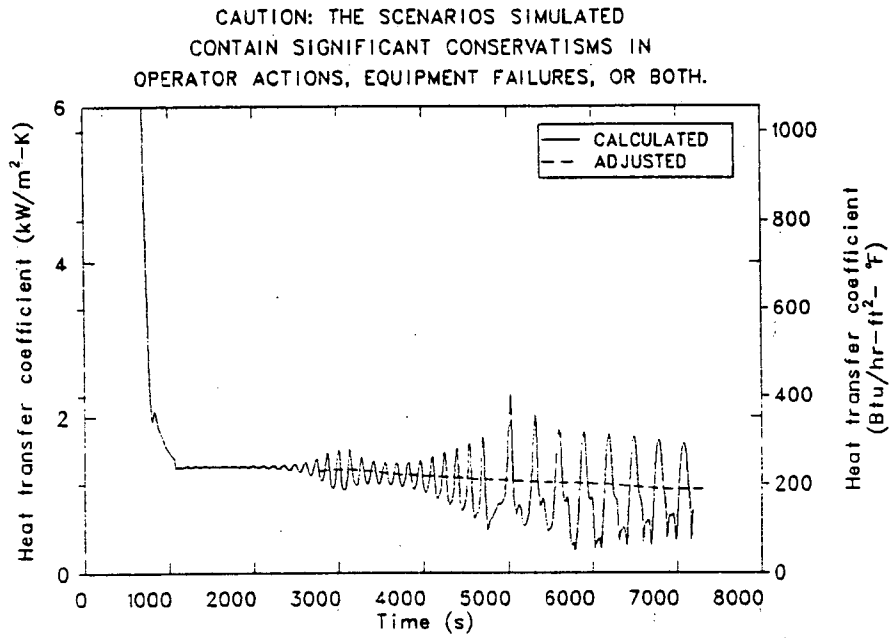

Figure 12-15. Scenario 9 calculated and adjusted reactor vessel downcomer inside surface heat transfer coefficient.

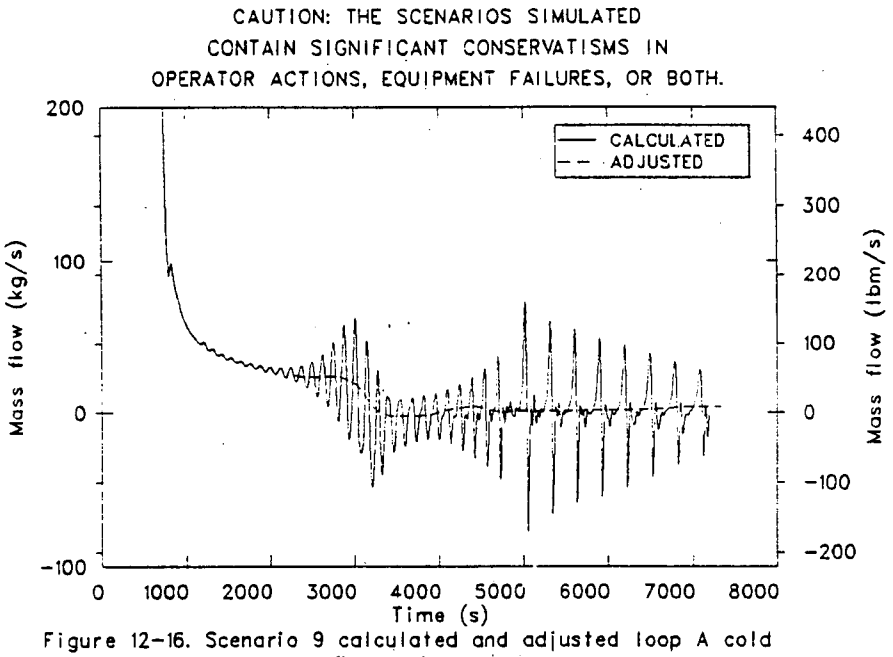

Figure 12-16. Scenario 9 calculated and adjusted loop A cold leg mass flow rate.

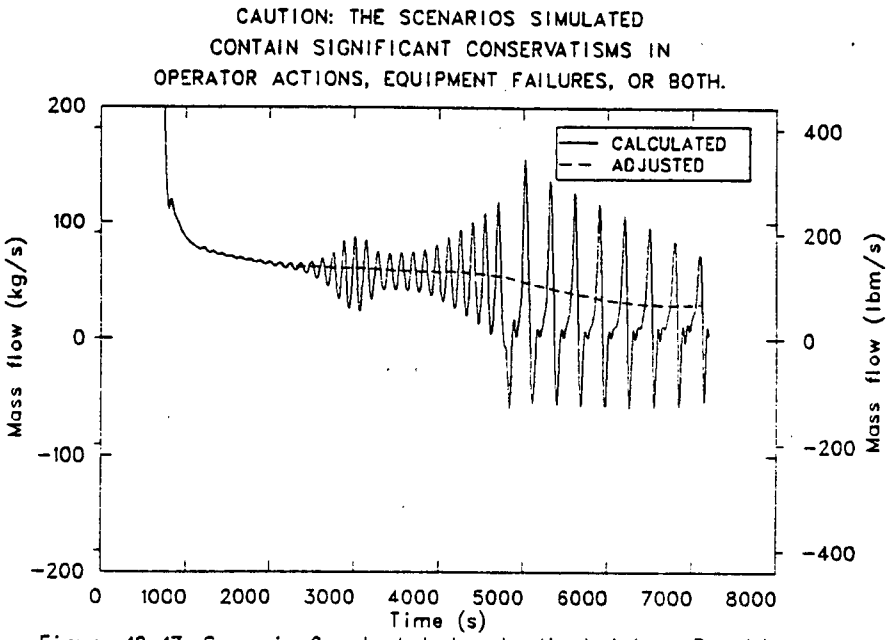

Figure 12-17. Scenario 9 calculated and adjusted loop B cold leg mass flow rate.

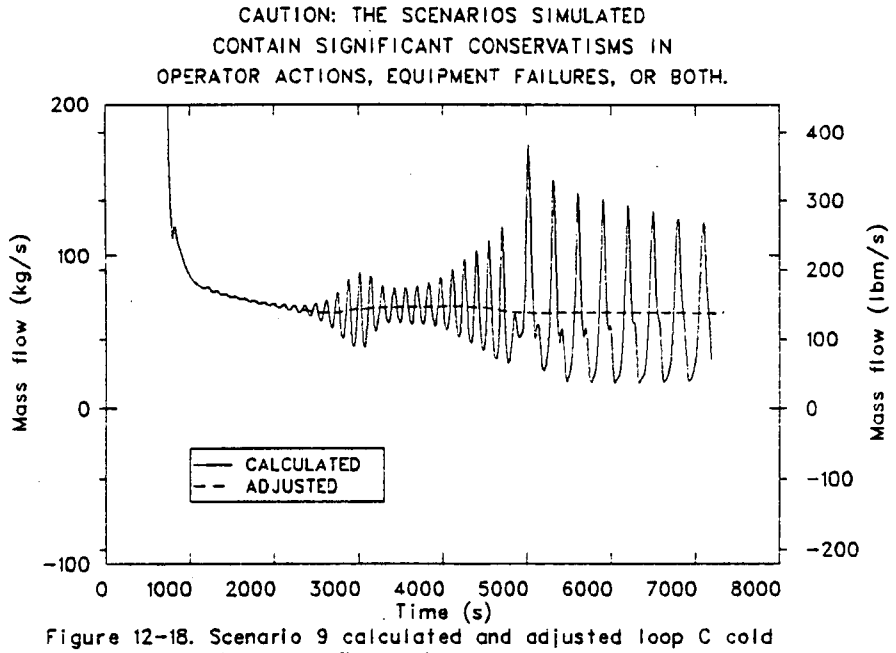

Figure 12-18. Scenario 9 calculated and adjusted loop C cold leg mass flow rate.

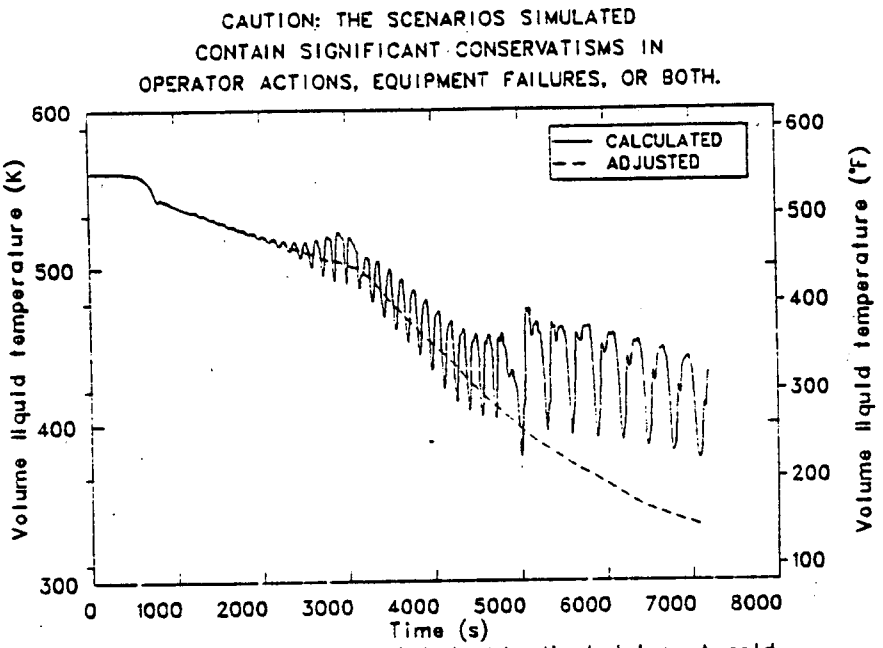

Figure 12-19. Scenario 9 calculated and adjusted loop A cold leg fluid temperature.

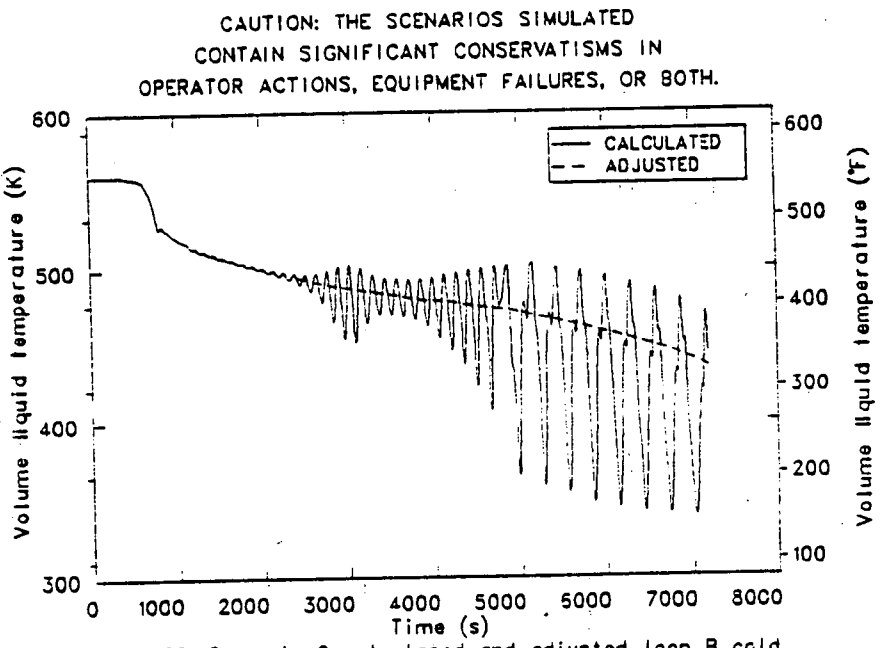

Figure 12-20. Scenario 9 calculated and adjusted loop B cold leg fluid temperature.

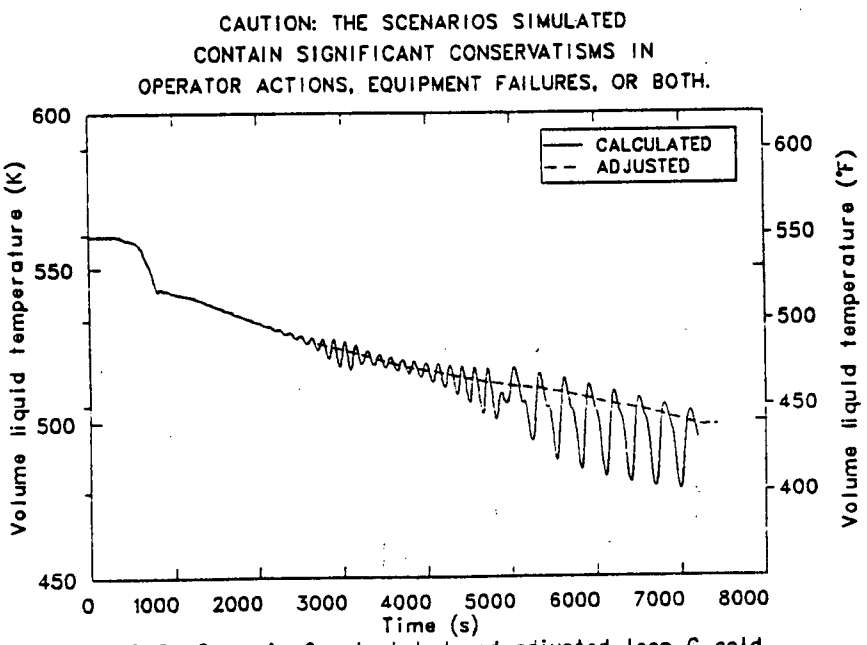

Figure 12–21. Scenario 9 calculated and adjusted loop C cold leg fluid temperature.

RCP discharge fluid temperatures. Mass-flow-weighted fluid temperature mixing calculations were then performed using the loop and HPI/makeup flow rates and temperatures. The Loop B and C adjusted temperatures were higher than those calculated due to higher-than-calculated adjusted loop flow rates as shown in Figures 12-17 and 12-18. Conversely, the adjusted Loop A temperature was lower-than-calculated as a result of the lower-than-calculated adjusted Loop A mass flow show in Figure 12-16. The adjusted cold leg fluid temperatures at 7200 s are 330 K (135°F) in Loop A, 433 K (320°F) in Loop B, and 502 K (444°F) in Loop C.

12.4 Conclusions

The calculated loop flow oscillations which are observed starting at about 3000 s are not physical and are caused by a limitation of the computer model during near-stagnant flow conditions. The computer model precludes calculation of thermal stratification effects within a liquid-filled cold leg which would remove the driving potential for the oscillations.

The minimum reactor vessel downcomer fluid temperature occurred at the end of the two-hour period. After adjustment for removal of the non-physical flow oscillations, the minimum downcomer temperature is 465 K (378°F). The associated downcomer fluid pressure is 9.624 MPa (1396 psia).

13. SCENARIO 10, STEAM GENERATOR TUBE RUPTURE AT FULL POWER

The following subsections contain the transient scenario description, modeling changes effected to perform this calculation, detailed analysis of the transient results, extrapolations and uncertainty analysis, and conclusions drawn from the analysis for Scenario 10; a single steam generator tube rupture at full power.

Scenarios investigated in this report generally include conservative assumptions concerning equipment failures, operator actions, or combinations of these. Conclusions relative to pressurized thermal shock severity are not to be drawn directly from the results presented in this report (see Section 15).

13.1 Transient Scenario Description

The transient is initiated from full power steady state (nominal temperature and pressure), and all system controls are in automatic control. The transient is begun by a double-ended break occurring in a single tube in the cold leg side of the Loop A steam generator. During the transient it is assumed that all systems operate automatically as designed. The only operator actions are: (1) trip the reactor coolant pumps when the primary pressure reaches 9.1 MPa (1315 psia) and a SIAS signal is generated, (2) throttle auxiliary feedwater flow to maintain a 40% narrow range level in each of the steam generators. It should be noted, as in Section 12, the above actions are not the normal procedures the operator would take in this type of transient. A transient scenario is provided in Table 13-1.

13.2 Model Changes

Changes made to the steady state model to incorporate the tube rupture include the addition of a pipe component describing a single tube, and are the same as for the steam generator tube rupture at hot standby, described in detail in Section 12.2.

TABLE 13-1. STEAM GENERATOR TUBE RUPTURE TRANSIENT SCENARIO AT FULL POWER

Plant Initial State - Just prior to transient initiator

General Description: 100% Power steady state

System Status

Turbine: Automatic control
Secondary PORV: Automatic control
Steam Dump Valves: Automatic control
Charging System: Automatic control
Pressurizer: Automatic control
Engineering Safety Features: Automatic control
PORVs: Automatic control
Reactor Control: Automatic
Main Feedwater: Automatic control
Aux Feedwater: Automatic control
MSIVs: Open, Automatic control
MFIVs: Open, Automatic control

Transient Initiator - A steam generator tube rupture on the cold leg side of the tube sheet on S/G "A".

Equipment Failures which occur during the transient if the equipment is demanded.

None

Operator Reactions to Reported Information

1. If SIAS signal is generated, the operator will trip the reactor coolant pumps when RCS pressure reaches 1300 psig.

2. The operator will throttle AFW flow to maintain 40% S/G level.

13.3 Transient Results

This section presents the results, and extrapolations and uncertainties of the steam generator tube rupture transient at full power.

13.3.1 Calculation Results

A calculated sequence of events for the transient is provided in Table 13-2.

The double-ended rupture of a single tube in the cold leg side of Steam Generator A was assumed to occur at time zero. Upon rupture of the tube, the primary system began to depressurize as shown in Figure 13-1. The pressurizer proportional and back-up heaters were automatically initiated as a result of the depressurization in an effort to recover primary system pressure. Also, as a result of the break, the pressurizer liquid level shown in Figure 13-2, began to decrease, resulting in an increase in the make-up flow rate to recover the level. At approximately 89 s a high turbine over-temperature ΔT signal in the reactor protection system was generated and the turbine governor valves began to run back. Between 95 and 114 s load rejection setpoints of 15, 35, and 55% were reached and steam dump valve banks 1, 2, and 3 were opened respectively as indicated by the total steam dump mass flow rate shown in Figure 13-3.

At 114 s into the transient, a reactor over-temperature ΔT signal tripped the reactor. Primary system pressure shown in Figure 13-1 rapidly decreased as a result of the decrease in core power at reactor trip and a delay in the reduction of primary to secondary heat removal rate as shown in Figure 13-4. The turbine stop valves closed as a result of reactor trip, and secondary pressure rapidly increased to approximately 6.9 MPa (1000 psia) as shown in Figure 13-5. The steam dump system switched from load rejection control to plant trip control mode due to reactor trip. The steam dump valves closed as a result of an overswing of a lead-lag controller in the plant trip control system logic, but opened thereafter, as shown in Figure 13-3, and modulated to bring the primary system average temperature down to 559 K (547°F). After reactor trip, the primary system

TABLE 13-2. SCENARIO 10 SEQUENCE OF EVENTS

Transient Time (s)	Event
0	Single tube rupture in Steam Generator A occurs Primary system begins to depressurize.
10	Pressurizer heaters turn on.
89	2/3 turbine high over-temperature ΔT signal, turbine valve began to run back.
95	15% load rejection setpoint reached and steam dump valve bank 1 opened.
101	35% load rejection actuation setpoint reached and steam dump valve bank 2 opened.
108	55% load rejection actuation setpoint reached and steam dump valve bank 3 opened.
114	Reactor tripped on 2/3 reactor over-temperature ΔT. Turbine stop valves close. Steam dump system switches to plant trip control mode and steam dump valves modulate to bring the plant Tave to 559 K (547°F).
130	Pressurizer level is less than 14.4% and heaters are tripped off. Main feedwater regulating valves close on reactor trip and low Tave.
137	Main feedwater pumps trip; motor-driven aux feed water system turned on.
199	SIAS signal received due to low pressurizer pressure.
275	Pressurizer and pressurizer surge line empty.
335	Pressure dropped below HPI pump head and HPI flow is established. Aux feed to Steam Generator A terminated.
370	Primary depressurization stopped.
560	Total aux feed flow goes to Steam Generator C for about 50 seconds.

TABLE 13-2. (continued)

600	Primary pressure increase began.
1130	Plant Tave dropped below 559 K (547°F) and steam dump system switched from plant trip control to steam pressure control. Aux feed flow to Steam Generator C increased .
1160	Level in Steam Generator C reached 40% narrow range level and aux feed flow to that generator is terminated.
1200	Level in Steam Generator B reached 40% narrow range level and aux feed flow was terminated.
2400	Transient terminated. Primary system pressure stable at 9.6 MPa (1400 psia) and vessel downcomer temperature stable at 560 K (549°F). Secondary heat removal was equal to core power, and total primary inlet flow equaled the break flow.

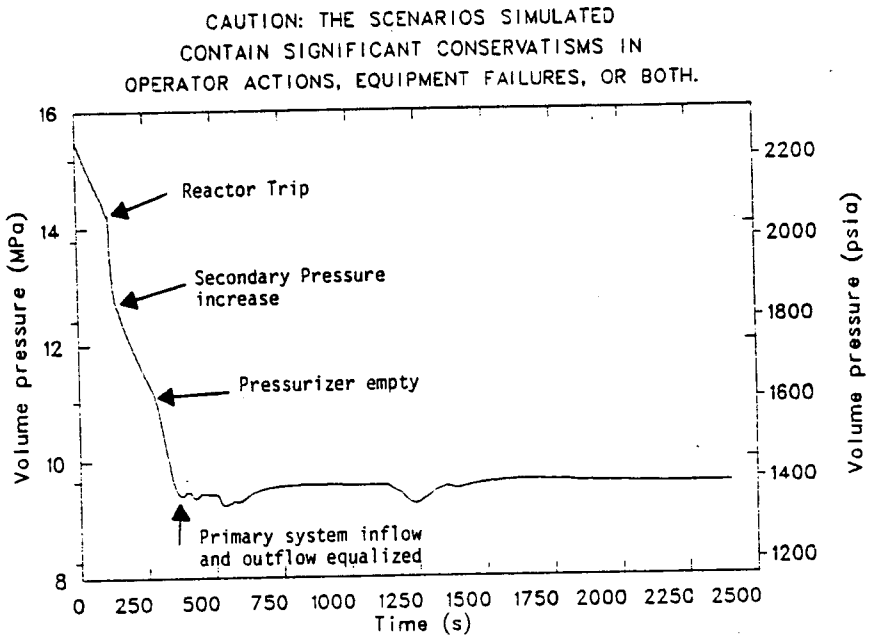

Figure 13-1. Scenario 10 primary system pressure.

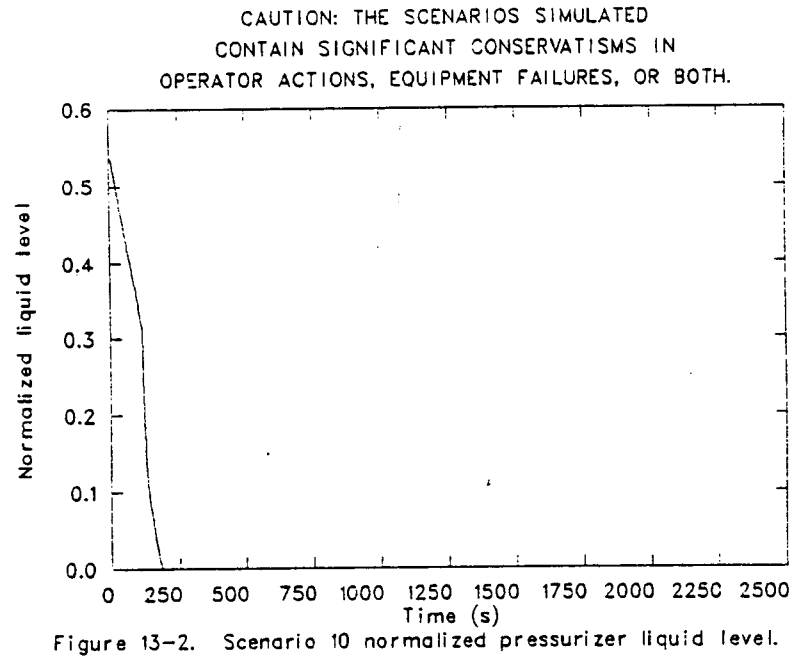

Figure 13-2. Scenario 10 normalized pressurizer liquid level.

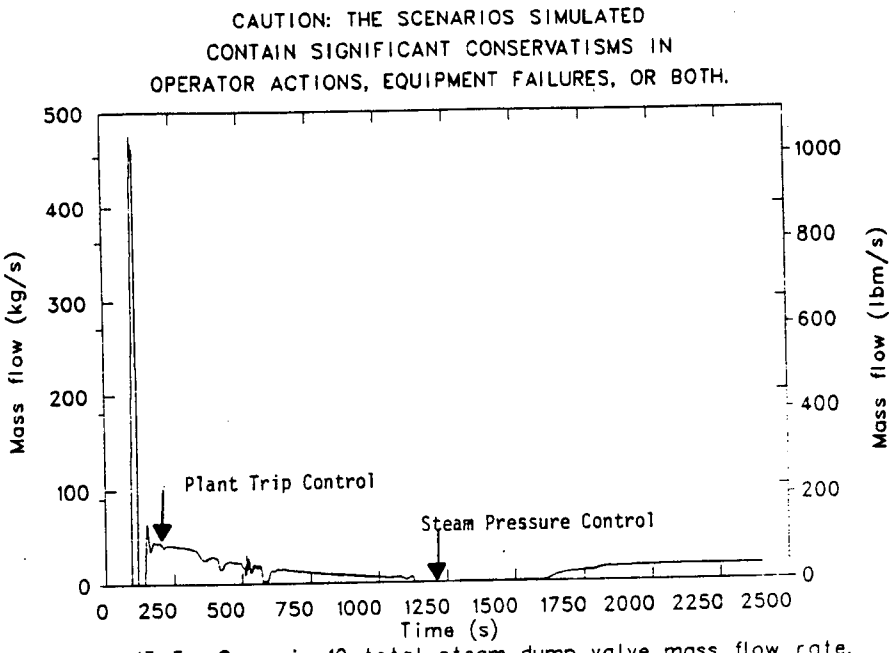

Figure 13-3. Scenario 10 total steam dump valve mass flow rate.

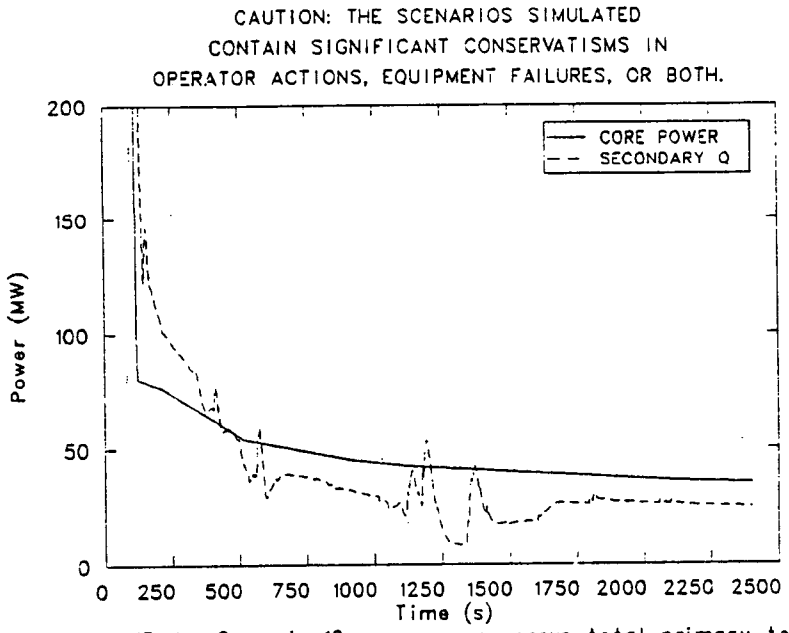

Figure 13-4. Scenario 10 core power versus total primary to secondary heat transfer rate.

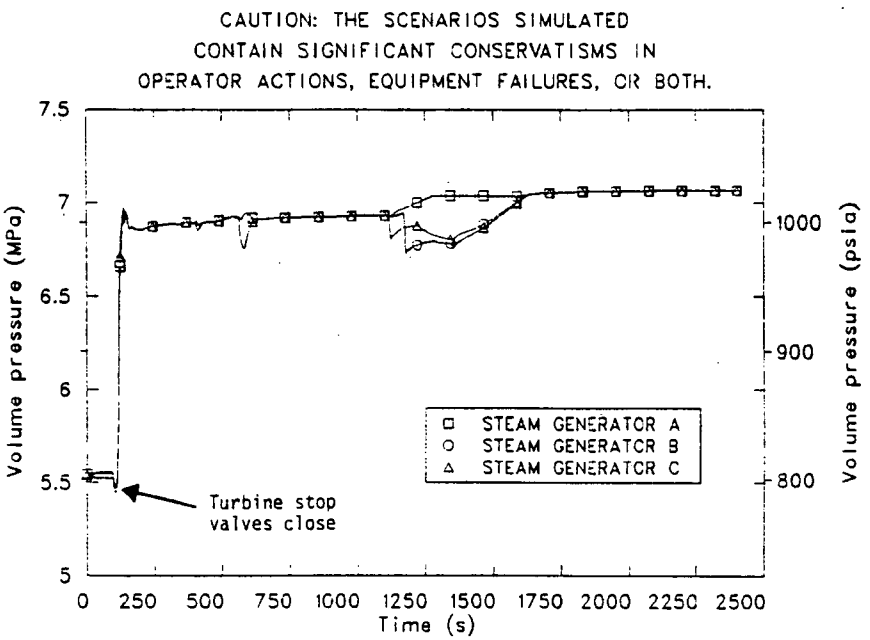

Figure 13-5. Scenario 10 steam generator secondary pressure.

pressure continued to decrease at a slower rate as shown in Figure 13-1, due to the reduction in primary system heat removal rate shown in Figure 13-4.

Break flow, shown in Figure 13-6, rapidly decreased upon reactor trip due to the reduction in primary system pressure and the increase in secondary system pressure. Choking, which dominated the break flow from the initiation of the transient, was terminated when the conditions at the break changed from saturated liquid to subcooled liquid due to the consequences of the reactor trip. The break mass flow rate increased as a result of subcooling at the break until the steam dump valves opened, as discussed above, at which time the break flow again decreased.

At 130 s the pressurizer liquid level decreased below 14.4% of the measured level range and the pressurizer proportional and back-up heater power was terminated. Also, at approximately this time the main feedwater regulating valves were closed due to the reactor trip and a low average temperature signal. No effort by the operator was assumed to open the bypass valves to maintain main feed flow to the generators. Approximately 7 s later the main feedwater pumps tripped and motor-driven auxiliary feedwater system was initiated. Turbine-driven auxiliary feedwater was not initiated as it requires 2-out-of-3 low steam generator level indications.

The secondary narrow range liquid level is shown in Figure 13-7 for all three generators. Initially, the level in the affected steam generator (Steam Generator A) increased due to the break flow into the secondary. Upon reactor trip, the turbine stop valves closed and the level in the generators collapsed due to an elimination of the flow effects on the differential pressure that is used in the level calculation. When the motor-driven auxiliary feedwater system was initiated at approximately 137 s the levels began to increase.

At approximately 200 s the pressure in the pressurizer dropped below 11.93 MPa (1730 psia), generating a SIAS signal of energizing the HPI pumps. By approximately 275 s the pressurizer and pressurizer surge line

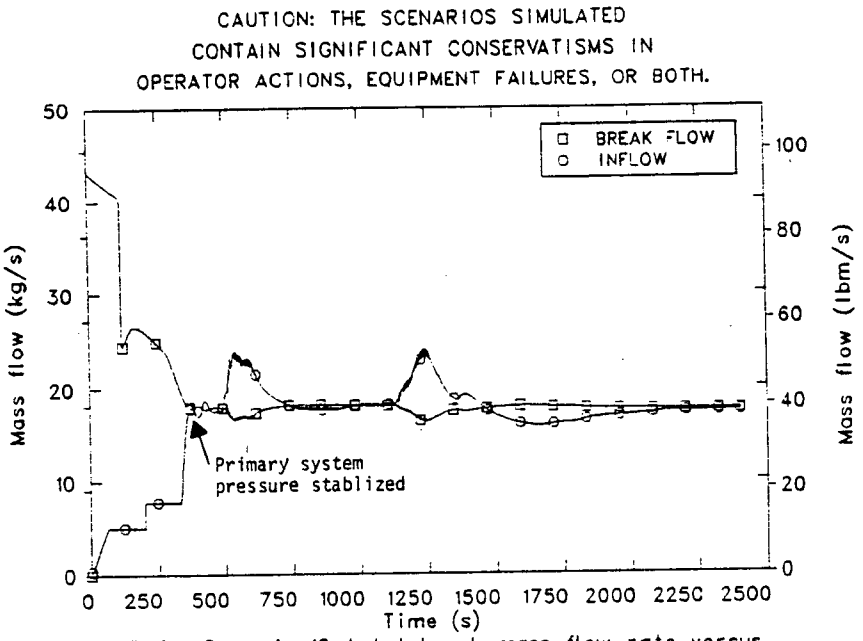

Figure 13-6. Scenario 10 total break mass flow rate versus total ECC CVCS mass flow rate.

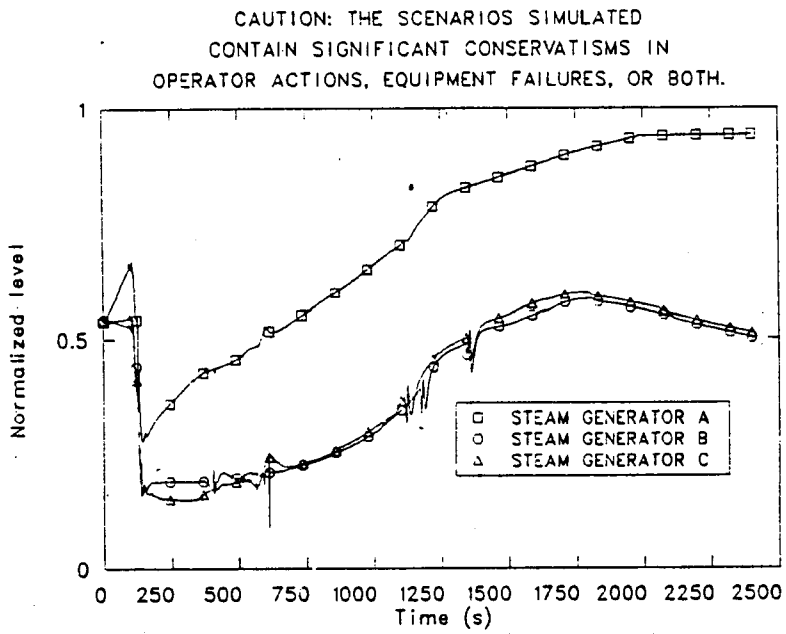

Figure 13-7. Scenario 10 normalized steam generator narrow range liquid level.

had emptied, the primary depressurization rate increased as shown in Figure 13-1, and the mass flow rate out the break decreased as shown in Figure 13-6.

By approximately 335 s primary pressure had dropped below the HPI pump head and HPI flow was initiated. Upon initiation of HPI, the total mass flow into the primary system equaled the break mass flow rate shown in Figure 13-6. The primary depressurization was terminated at approximately 9.4 MPa (1363 psia) as shown in Figure 13-1. The primary system pressure remained relatively stable until approximately 500 s, at which time, the pressurizer surge line began to fill with liquid. The incoming liquid interacted with the steam in the first volume of the surge line and resulted in condensation which depressurized the primary system. The volumetric condensation rate briefly exceeded the volumetric inflow to the primary side and the primary pressure decreased as shown in Figure 13-1. Also affected by the condensation was HPI flow, which increased, as shown in Figure 13-6, due to the decrease in primary pressure. At approximately 525 s the condensation in the surge line had stopped and primary pressure began to increase as shown in Figure 13-1. The increase was due to more heat being generated in the core than was removed by the secondary as shown in Figure 13-4.

Figure 13-8 shows the auxiliary feedwater flow into each of the steam generator secondaries. During the transient, the operator controlled the narrow range level to 40%. At approximately 335 s the 40% narrow range level in the affected steam generator was reached and auxiliary feedwater to that generator was terminated. Because of the common auxiliary feedwater header, the flow was split between the two unaffected steam generators. The amount of flow each generator received was determined by the pressure difference between the auxiliary feedwater header pressure and the steam generator pressure. As shown in Figure 13-8 at approximately 400 and 550 s auxiliary feed flow preferred the C steam generator for short periods of time. The effect of this behavior (notably at 550 s) enhanced the overall primary system heat removal (see Figure 13-4) such that primary repressurization at 550 s was arrested temporarily as shown in Figure 13-1. Condensation effects in the C steam generator were the major cause of the preferential auxiliary feedwater flow.

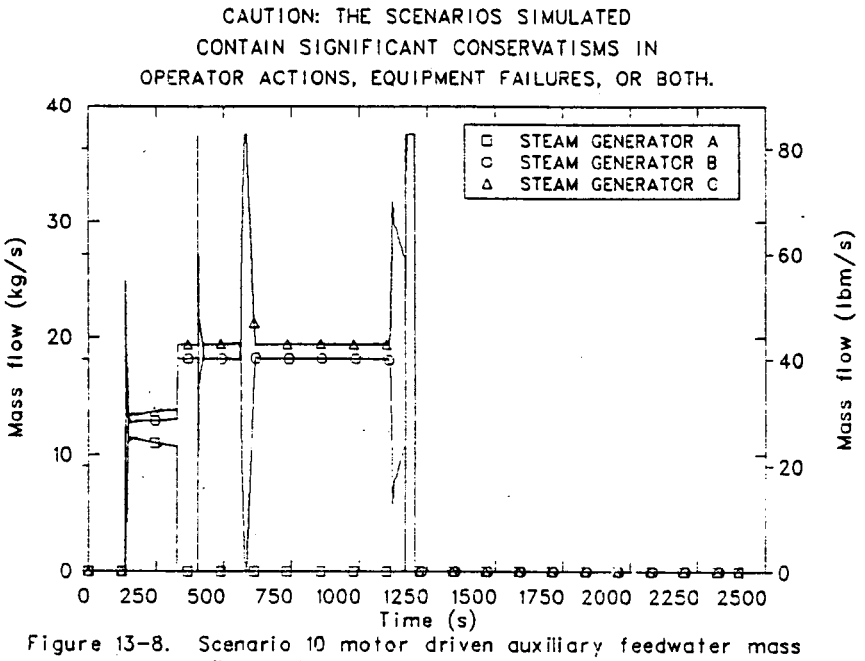

Figure 13-8. Scenario 10 motor driven auxiliary feedwater mass flow rate.

Between 620 and 1130 s primary system pressure had increased approximately to 9.6 MPa (1400 psia) and was stable due to the total primary inflow equaling the break flow, and the total energy being removed from the primary system (including energy removed at the break) equaling the core decay power. Also, the loop mass flow rates, shown in Figure 13-9, were very nearly equal during this time, whereas before, the Loop C mass flow rate was higher as a result of emptying the pressurizer.

At approximately 1130 s the auctioneered high average temperature dropped below 559 K (547°F) and the steam dump system switched from plant trip control to steam pressure control mode, and the steam dump valves closed. In steam pressure control, the steam dump valves modulate open if the secondary pressure increases to 7.0 MPa (1020 psia). As a result of the steam dump valve closure the secondary pressure in Steam Generators A and B increased, however the pressure in Steam Generator C decreased as shown in Figure 13-5 due to condensation effects from auxiliary feedwater entering the secondary. Auxiliary feedwater preferred the C steam generator because of the lower pressure, and therefore the level in that generator increased faster, reaching the 40% cutoff level at approximately 1160 s. Auxiliary feed flow was then terminated from the C steam generator and the B steam generator received all of the auxiliary feed flow. The effect of preferential auxiliary feed flow to one or the other steam generator was to increase the overall primary heat removal rate, as shown in Figure 13-4, which in turn resulted in a depressurization of the primary side (see Figure 13-1) and an increase in HPI flow (see Figure 13-6). The cold leg and reactor vessel downcomer temperatures, shown in Figure 13-10, during this time also decreased due to the increased cold HPI flow, and more energy being removed from the primary system than was being generated by decay heat.

At approximately 1200 s the level in the B steam generator reached 40% of the narrow range level and auxiliary feed flow to that steam generator was terminated, thus all feed flow to the steam generators was terminated. At that time the primary heat removal rate decreased and the primary pressure increased as shown in Figure 13-1. At approximately 1350 s condensation in the steam generator downcomer above the feed ring occurred

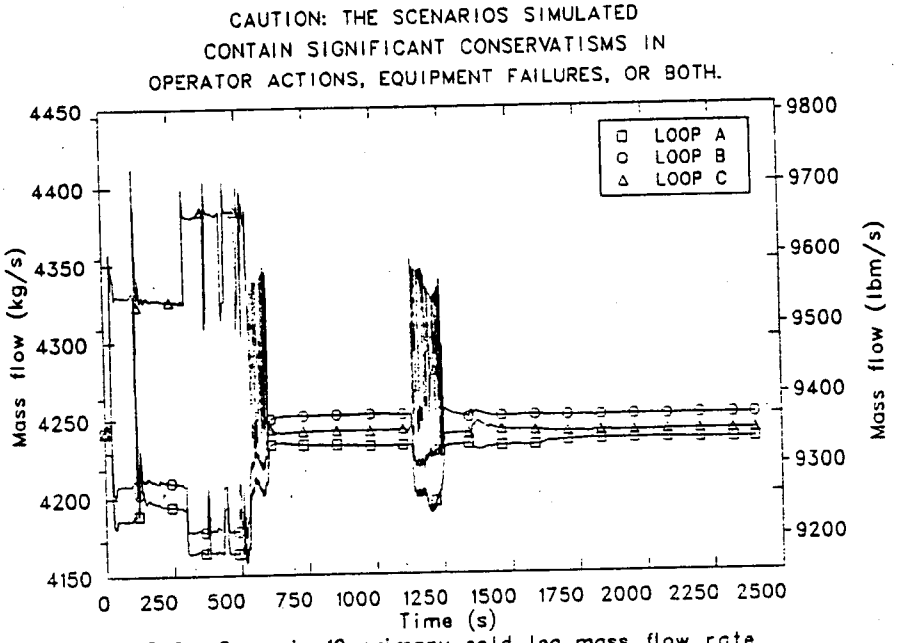

Figure 13–9. Scenario 10 primary cold leg mass flow rate.

in Steam Generators B and C. This condensation resulted in a temporary flow reversal in the secondary side which enhanced the primary to secondary heat transfer resulting in a small decrease in pressure and a small decrease in the cold leg loop fluid temperatures (see Figure 13-10).

Primary system pressure continued to increase until approximately 1700 s. At this time, a balance between the break flow rate and the total primary inflow (see Figure 13-6) existed. Also, a balance between the total primary system heat removal (heat transfer across the steam generator tubes and energy removal at the break) and core decay power existed. Because of a balance in these thermal-hydraulic mechanisms, the primary system pressure increase was terminated and the pressure remained stable to the end of the calculation at 2400 s. The primary system pressure at the end of the calculation was 9.6 MPa (1400 psia) and the reactor vessel downcomer temperature was stable at 560 K (549°F).

13.3.2 Extrapolations and Uncertainties

This section presents the extrapolations of the reactor vessel downcomer pressure, fluid temperature, wall inside surface heat transfer coefficient, and cold leg flow rates and fluid temperatures. Also, any known uncertainties in the calculation are addressed.

An extrapolation to two hours of the pressure, temperature and heat transfer coefficient curves in the reactor vessel downcomer and the mass flow rate and temperature curves in the cold legs are shown in Figures 13-11 through 13-15. The reactor vessel downcomer parameters are shown at an elevation equal to the top of the core. At the termination of the calculation the system was in a quasi-steady state, i.e., ECC flow equaled the break flow and the total energy removed from the primary system equaled the core decay heat, which resulted in a stable system behavior. This behavior was expected to remain stable throughout the two hour period, with minor perturbations as the system adjusts to the decreasing core decay power.

Figure 13-16 shows the vessel downcomer pressure response. As discussed in Section 13.3.1 the slight depressurization at approximately

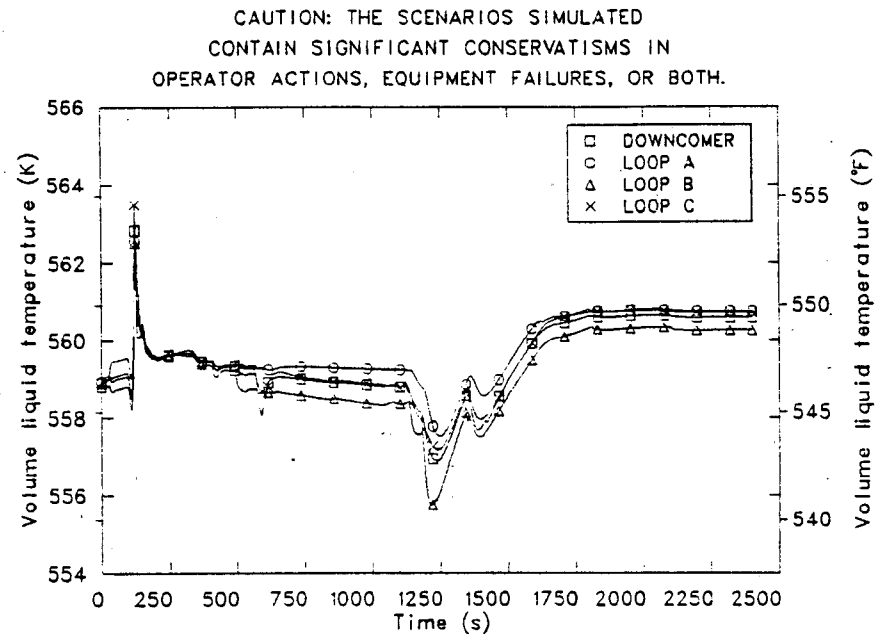

Figure 13–10. Scenario 10 primary cold leg fluid temperatures and vessel downcomer fluid temperature.

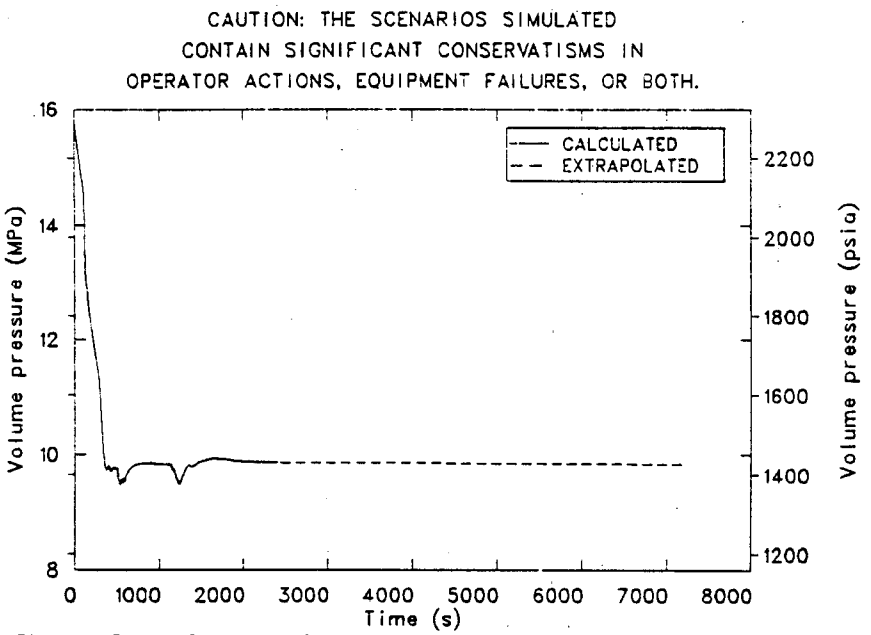

Figure 13–11. Scenario 10 extrapolated vessel downcomer pressure at elevation equal to the top of the core.

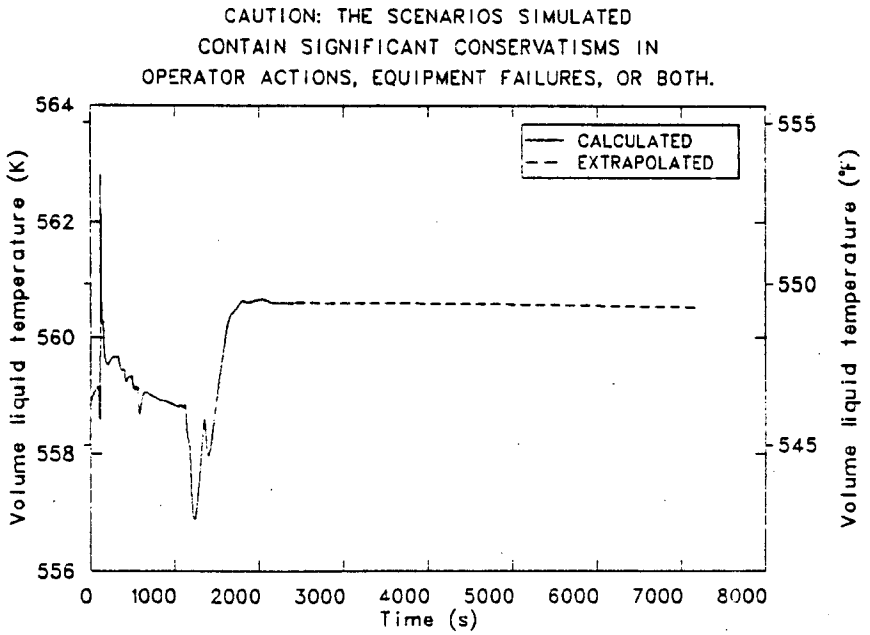

Figure 13-12. Scenario 1C extrapolated vessel downcomer fluid temperatures at elevation equal to the top of the core.

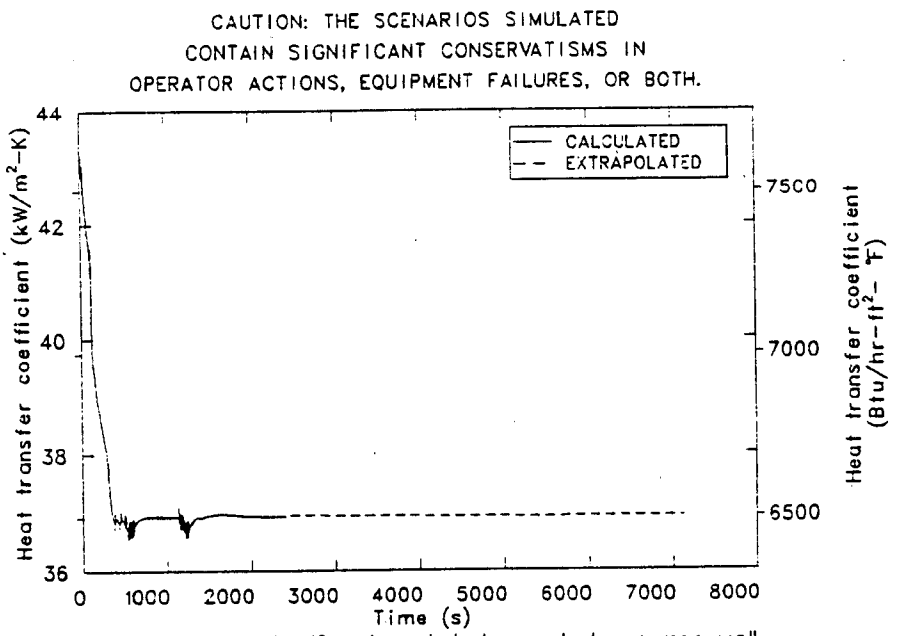

Figure 13-13. Scenario 1C extrapolated vessel downcomer wall inside surface heat transfer coefficient at elevation equal to the top of the core.

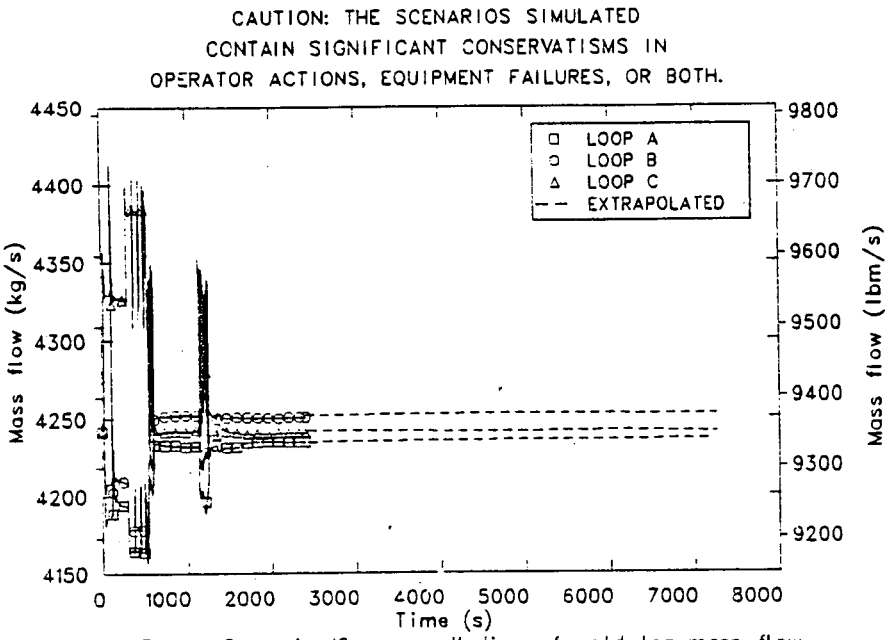

Figure 13-14. Scenario 10 extrapolation of cold leg mass flow rates.

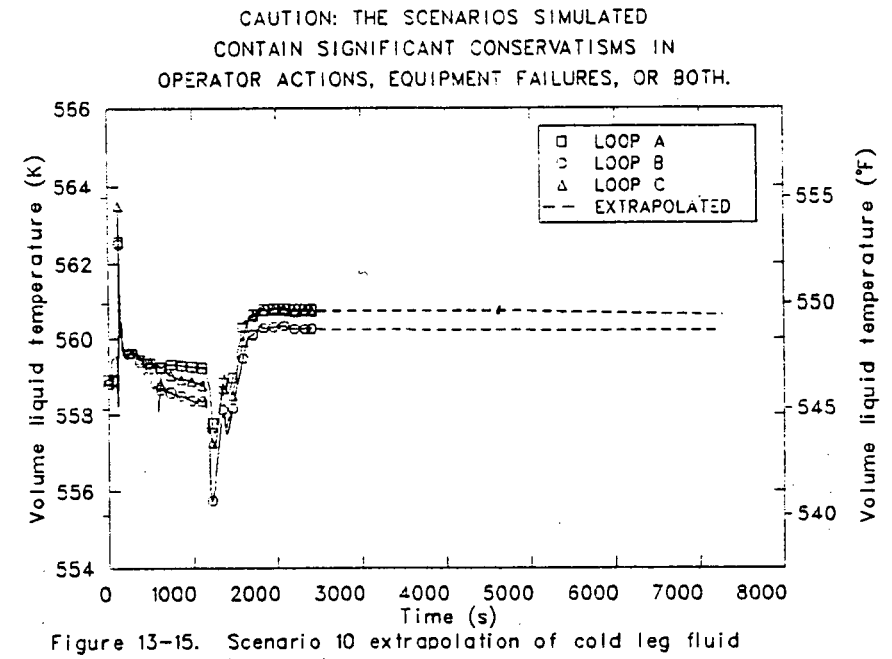

Figure 13-15. Scenario 10 extrapolation of cold leg fluid temperature.

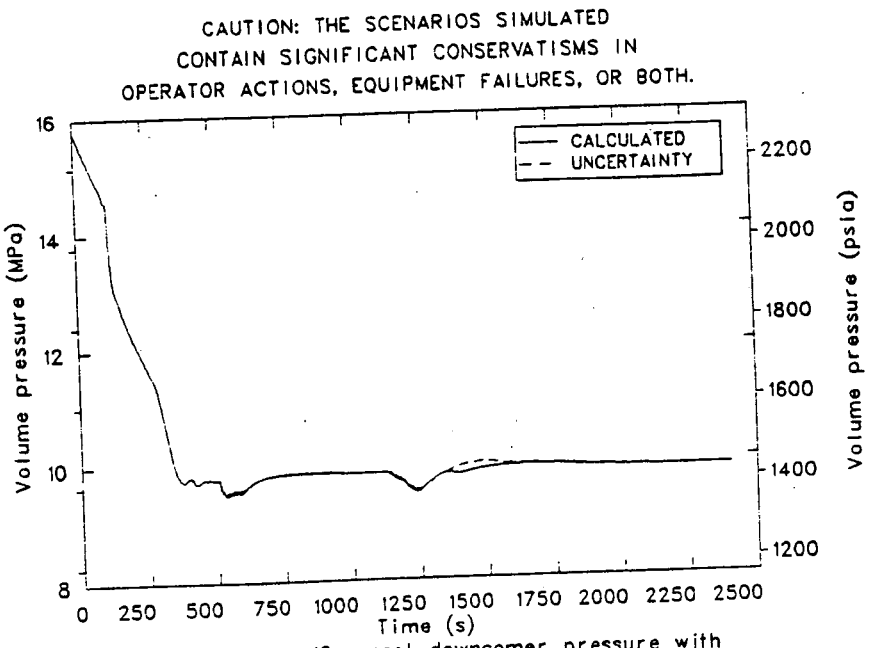

Figure 13-16. Scenario 10 vessel downcomer pressure with uncertainty.

1350 s was a result of a flow reversal in the steam generator secondary due to condensation in the upper portion of the generator downcomer. The flow reversal enhanced the primary system heat removal rate, resulting in a cooldown of the primary and thus a slight depressurization. The flow reversal may have been overstated and had it not occurred, the pressure would not have decreased, but increased as shown by the dashed line in Figure 13-16, until a balance in the system existed as described in Section 13.3.1. The major effect of this uncertainty was a decrease in reactor vessel downcomer temperature as shown in Figure 13-17. When the primary system pressure decreased, the HPI flow increased introducing more cold liquid into the primary system. Again, had this depressurization not occurred, the temperature would have responded in the manner of the dashed line shown in Figure 13-17.

13.4 Conclusions

As a consequence of the primary system pressure not decreasing below 9.1 MPa (1315 psia) during the transient, the reactor coolant pumps were never tripped. This resulted in good thermal mixing of the primary coolant fluid with the incoming ECC fluid and the vessel downcomer temperature did not vary more than 5.5 K (10°F) from the initial steady state value. Also, because the pumps did not trip, multi-dimensional effects in the loops and reactor vessel were negligible, therefore, multi-dimensional mixing calculations for this transient are not needed. The minimum reactor vessel downcomer temperature was 556.9 K (542.7°F), and the maximum subsequent pressure was 9.6 MPa (1400 psia).

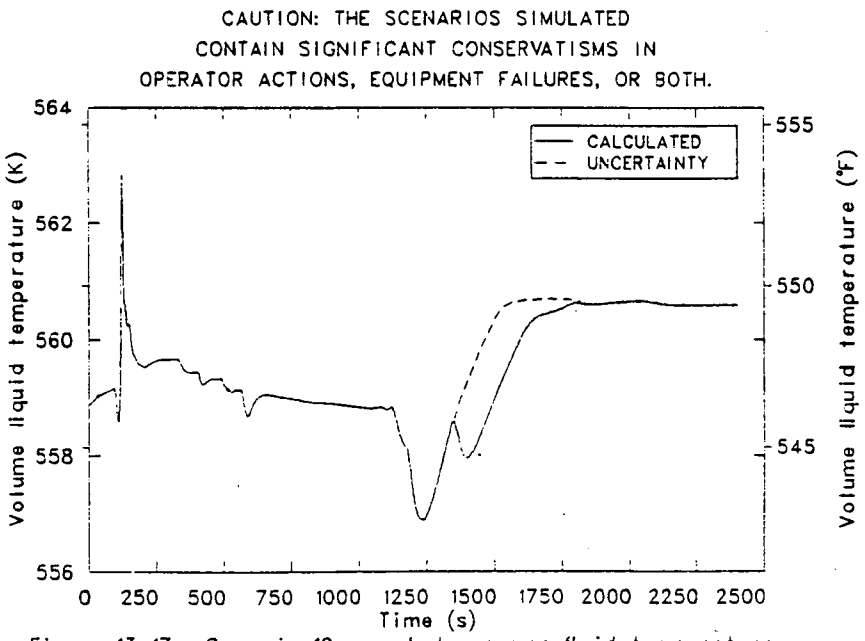

Figure 13-17. Scenario 10 vessel downcomer fluid temperature with uncertainty.

14. SCENARIO 11, LOSS OF SECONDARY HEAT SINK WITH PRIMARY SYSTEM FEED-AND-BLEED RECOVERY

The following section describes the results of the Scenario 11 calculation. This calculation was performed to evaluate the consequences of a postulated loss of secondary heat sink accompanied by an uncontrolled primary feed and bleed type of recovery. The feed and bleed was performed by opening both pressurizer power-operated relief valves (PORVs) and initiating high pressure injection (HPI).

A description of the scenario is provided in Section 14.1, followed by a discussion of the model changes required to conduct the calculation in Section 14.2. The calculated data, the extrapolated results, and the uncertainties in the calculation are described in Section 14.3. The conclusions regarding the calculation are presented in Section 14.4.

Scenarios investigated in this report generally include conservative assumptions concerning equipment failures, operator actions, or combinations of these. Conclusions relative to pressurized thermal shock severity are not to be drawn directly from the results presented in this report (see Section 15).

14.1 Scenario Description

A description of Scenario 11 is provided in Table 14-1. As with the other calculations, this scenario was developed by Oak Ridge National Laboratory (ORNL). The sequence of the calculation followed the scenario description through the required 7200 s. The calculation was extended for another 900 s to more adequately address the pressurized thermal shock (PTS) question.

14.2 Model Changes

The model described in Section 2 was changed as described below to satisfy the operator action requirements given in Table 14-1.

TABLE 14-1. SCENARIO DESCRIPTION NO. 11

Plant Initial State - Just prior to transient initiator

General Description: 100% power steady state
System Status
- Turbine: Not latched, TSVs closed
- Secondary PORV: Automatic control
- Steam Dump Valves: Automatic control
- Charging Systems: Automatic control
- Engineering Safety Features: Automatic control
- Pressurizer PORVs: Automatic control
- Reactor Control: Automatic control
- Main Feedwater: Automatic control
- Auxiliary Feedwater: Automatic control
- Main Steam Isolation Valves (MSIVs): Automatic control
- Main Feedwater Control Valves: Automatic control

Transient Initiator - Both Main Feedwater pumps trip simultaneously.

Equipment Failures that occur during the transient if the equipment is demanded--Auxiliary Feedwater pumps fail to start.

Operator Reactions to Reported Information

1. Operator trips reactor coolant pumps (RCPs) when 1/3 Steam Generator (S/G) wide range (WR) levels decrease below 5%.

2. Operator initiates safety injection (HPI) and opens the pressurizer PORVs after RCP trip and when the A Loop hot leg temperature has increased 5°F.

1. The RCP trip was changed from a low pressure trip (9.07 MPa, 1315 psia) to an evaluation of any SG WR level below 5%.

2. Additional control variables were added to the model to monitor the Loop A hot leg temperature, determine the minimum temperature at the Steam Generator A (SGA) inlet after RCP trip, and the difference between the minimum temperature and the current temperature. This temperature difference was used to start HPI and open the pressurizer PORVs.

The transient was initiated from the 2300 MW full power steady state conditions described in Section 2.3.1.

14.3 Results

The results of the Scenario 11 calculation are presented in this section. Included in the discussion of the results are the assumptions made in extrapolating the calculated results beyond the end of the RELAP5 calculation.

The first subsection describes the RELAP5 results. A discussion of the method used to extrapolate the calculated data and the uncertainties involved in the calculation are presented in the second subsection.

14.3.1 Calculation Results

The results of the RELAP5 calculation are described in this section. A synopsis of the events that occurred in the calculation are presented in Table 14-2.

The reactor vessel downcomer fluid temperature response is shown in Figure 14-1. The initial increase in downcomer temperature at the start of the transient was due to a combination of secondary pressure increase and decreasing feedwater flow. The increase in secondary pressure was due to the closing of the turbine stop valve (which was initiated by the tripping

TABLE 14-2. SCENARIO 11 SEQUENCE OF EVENTS

Time (s)	Event
0	Transient initiated by manually tripping MFW pumps Reactor and turbine tripped PTC initiated
5	MFW valves closed (feed train isolated from steam generators)
100	Primary pressure decreased to 14.27 MPa (2070 psia)
650	Primary pressure restored to 15.51 MPa (2250 psia)
1500	SGC FW header blowdown began
1700	SGB FW header blowdown began
1900	SGC feedwater header blowdown completed
2100	SGB feedwater header blowdown completed
3626	SGA WR level reached 5% - RCPs were manually tripped.
3718	Loop A T-hot increased by 2.78 K (5°F) Pressurizer PORVs opened and SIAS tripped on
3767	Primary system pressure reached HPI shutoff head
3817	PTC switched to SPC
3830	Vessel upper head began voiding.
3857	Natural circulation in loops degraded due to combination of voiding in hot leg and PORV flow.
3878	Pressurizer indicated level reached 100%.
3937	Natural circulation resumed
3960	Reactor vessel upper head completely voided.
4093	SGB secondary became primary system heat source

TABLE 14-2. (Continued)

Time (s)	Event
4096	SGA secondary became primary system heat source
4100	SGC secondary became primary system heat source
4444	Natural circulation ended in Loop C
5500	SGA feedwater header blew down.
6000	HPI and CVCS inflow exceeded PORV outflow
6026	Condensation depressurization in the Loop C pump suction.
7159	Condensation depressurization in reactor vessel upper downcomer
7160	Accumulator injection initiated
8100	Downcomer conditions : (at top nf downcomer) Pressure = 4.04 MPa Temperature = 468.6 K dT/dt (last 100 s) = - 90.9 K/hr (-163.6°F/hr) dP/dt (last 100 s) = -3.72 MPa/hr (-539.5 psi/hr)

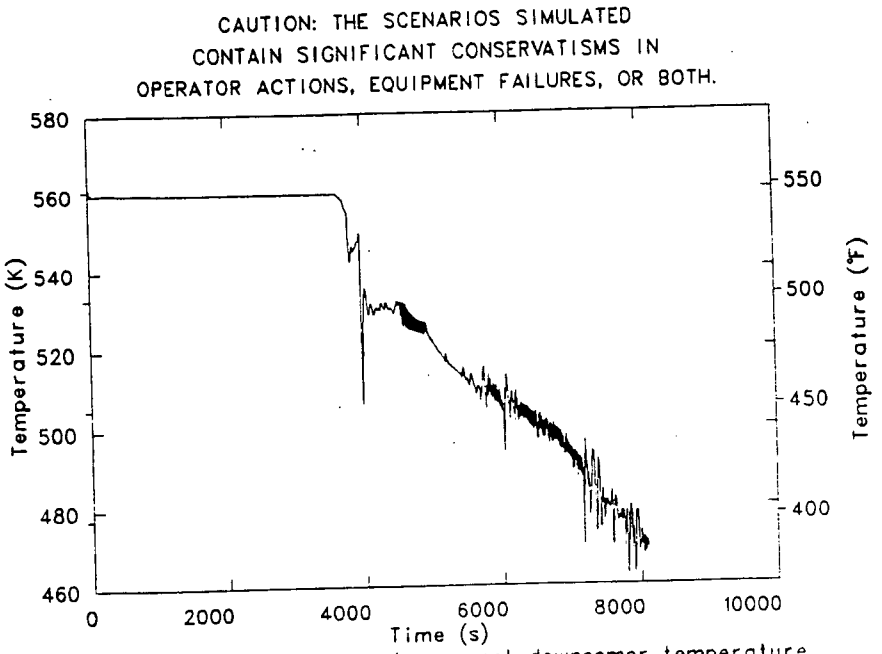

Figure 14-1. Scenario 11 reactor vessel downcomer temperature.

of the main feedwater (MFW) pumps). The constant downcomer temperature during the first 3600 s was the result of the plant trip control system (PTC) response, which was designed to control the steam dump valves to bring the primary average temperature down from the full power value (575 K, 575.4°F) to the no-load setpoint (559.3 K, 547°F).

The reactor vessel downcomer pressure response is shown in Figure 14-2. The initial decrease in pressure was due to a reactor trip caused by the turbine trip. The reduction in core power resulted in a coincident reduction in the hot leg temperatures, which caused a shrinkage of the pressurizer liquid volume. The reduction in pressure ended as the hot leg temperatures stabilized at 560 K (548°F) and the pressurizer heaters began recovering the pressure. The primary system pressure was restored to 15.51 MPa (2250 psia) by 650 s and remainded there until the RCPs were tripped.

The RCPs were tripped at 3626 s when the WR level in SGA had decreased to 5% of full range. The reduction in core flow resulted in an increase in the temperature rise across the core, which in turn caused the hot leg temperatures to increase. This temperature response continued until 3718 s when the pressurizer PORVs were opened and HPI initiated. These actions were taken, per the scenario description, when the Loop A hot leg temperature had increased by 2.78 K (5°F). Initiation of HPI was assumed to require a manual SIAS which in turn caused letdown to be isolated. The mass flow rates of the pressurizer PORVs, HPI, and the CVCS are shown in Figure 14-3.

The opening of the PORVs caused a rapid depressurization of the primary to 6.75 MPa (979 psia). The depressurization of the primary system resulted in reversed flow at 3818 s, which was halted at 3878 s due to voiding in the SG tube bundles and reactor vessel upper plena and head. The 0.70 MPa (102 psi) pressure increase between 3878 s and 3962 s was due to (a) the collapse of voids as the primary system refilled, and (b) the resumption of natural circulation through the SG tube bundles. The resumption of natural circulation resulted in increased heat transfer to the steam generator secondaries which caused the primary system to cool, and hence, depressurize.

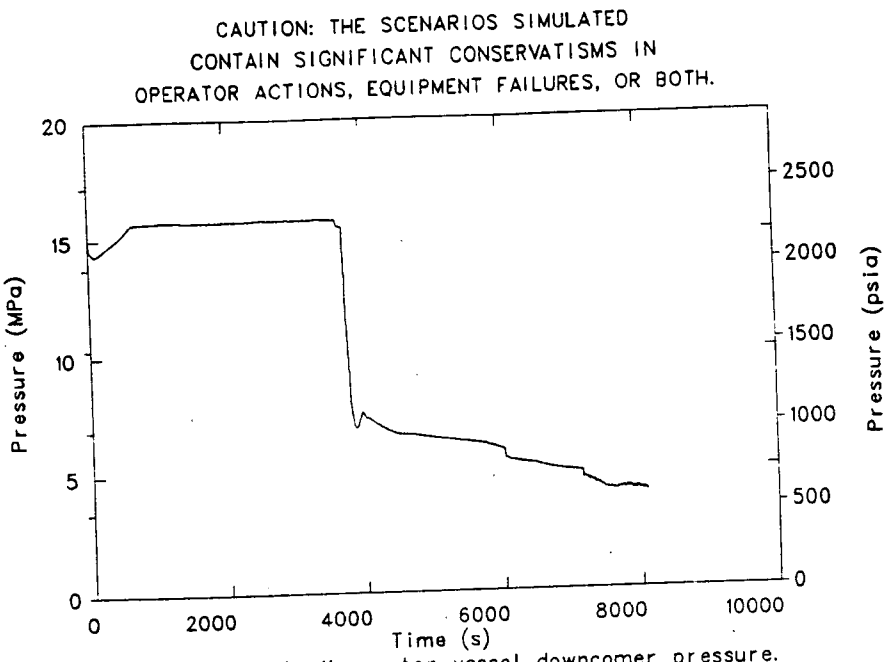

Figure 14-2. Scenario 11 reactor vessel downcomer pressure.

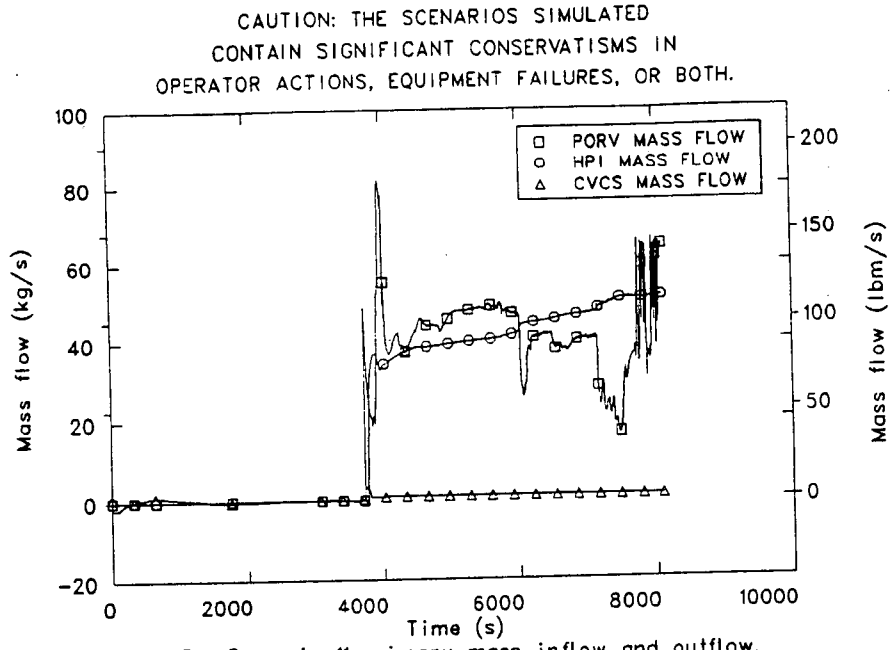

Figure 14-3. Scenario 11 primary mass inflow and outflow.

HPI was initiated at 3718 s, but no fluid was injected into the cold legs until the primary system pressure had decreased to the HPI shutoff head (10.135 MPa, 1470 psia) at 3767 s. The HPI and CVCS filled all but the upper volume of the pressurizer by 3878 s. The pressurizer upper head was never water solid due to the opened PORVs, which were capable of handling the total system inflow.

Isolation of the CVCS letdown valve resulted in an increase in the CVCS net injection flow rate of 3.41 l/s (54 GPM). The increase in injection flow rate was offset by the pressurizer level control system level error, and the net injection flow returned to 0.95 l/s (15 GPM). The increase in the calculated CVCS mass flow rate at 4000 s was due to a step change in the temperature of the injected fluid, which increased the CVCS fluid density.

Temperatures in the vessel downcomer (as shown in Figure 14-1) decreased between 3768 and 3817 s due to the HPI fluid from the three cold legs. The increase in temperature between 3817 s and 3937 s was the result of opening the PORVs, thereby causing reverse circulation in the three loops, which resulted in core fluid circulating back through the downcomer. The resumption of positive circulation at 3937 s resulted in a rapid temperature decrease due to the HPI fluid entering the downcomer. This decrease ended after the fluid in the cold legs was flushed through the downcomer, followed by the warmer fluid from the hot legs.

The constant downcomer temperature response between 4090 s and 4444 s was the result of nearly constant flow conditions, and heat additions to the primary coolant from the core and steam generator secondaries that were offset by heat removal due to the open PORV and the HPI fluid. The heat transfer from the secondary to the primary system was positive for the remainder of the calculation.

The minor temperature oscillations between 4500 and 4900 s were due to flow effects in the C Loop. During this period of time, SGC began voiding in the top of the tube bundle. This voiding induced a flow oscillation in the C Loop, which affected the amount of HPI fluid that flowed into the vessel downcomer. These oscillations were eventually damped out when the

tube bundle was sufficiently voided to prevent further natural circulation in that loop. Positive flow in the three loops for the next 900 s resulted in a steadily decreasing downcomer temperature which ended when SGC was completely drained.

The relatively large decrease in downcomer temperature at 6026 s was caused by condensation depressurization in the vessel in the Loop C pump suction. The decrease in pressure caused an increase in cold leg and HPI flow from the A and B loops into the vessel downcomer. This temperature oscillation lasted approximately 15 s and ended when the loop seal was refilled.

The flow rate responses of the three cold leg discharges are shown in Figure 14-4. The flow rates remainded essentially constant until the RCPs were tripped at 3626 s. The flow rates then decreased to 136 kg/s by the time the HPI shutoff head was reached (3767 s). The injection of HPI fluid resulted a brief period of flow rate increase before the initial voiding of the tube bundles resulted in flow stagnation. Natural circulation was reestablished at 3937 s in the three loops as the refill of the primary system collapsed the voids in the tube bundles. The mass flow rates through the three loops then increased until 3980 s as the reactor vessel upper plena and head drained into the hot legs. Flow rates then decreased to the natural circulation rate of 70 kg/s (154 lbm/s) until the Loop C tube bundle voided at 4400 s as a result of the PORV flows. The A and B loops maintained natural circulation for the remainder of the calculation. The flow rate in Loop C continued to decrease until 4444 s, and was essentially stagnant for the remainder of the transient.

The flow oscillations calculated for Loop C between 4500 s and 4900 s occurred when the SGC tube bundle refilled during the initial period of reverse flow (4444 to 4482 s) and then began voiding from the top down. The resultant bubble in the two upper volumes of the SGC tubes tended to compress during the refill periods, and decompress during the emptying periods. This process of compression-decompression continued until 4860 s, when the void fractions in the two upper volumes of the tube bundle were sufficiently large to damp out further oscillations. The tube bundle

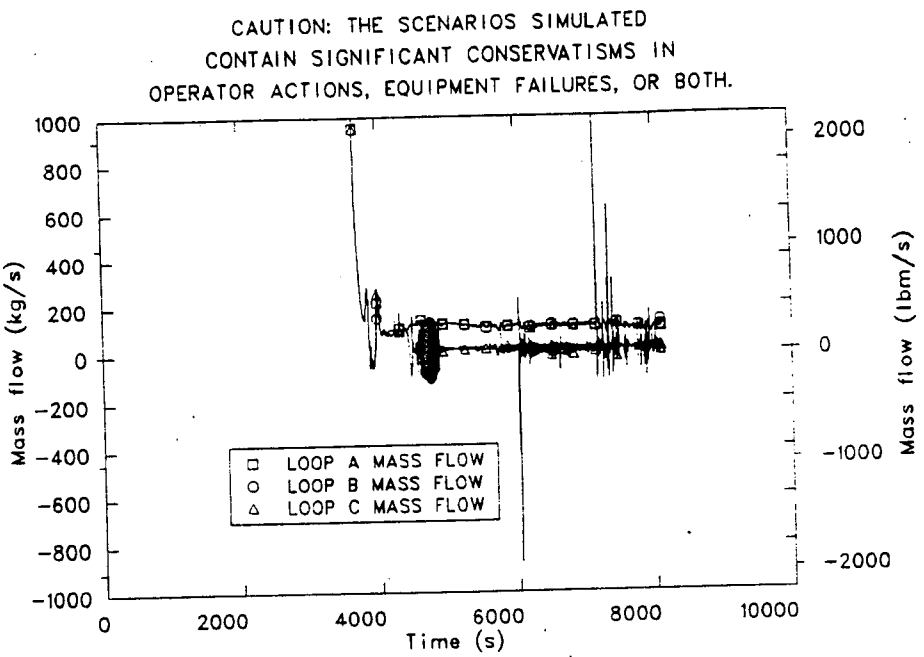

Figure 14-4. Scenario 11 cold leg flow rates.

continued to void until it was completely drained (4900 s). The draining of the SG resulted in a period of stable positive cold leg flow in the C Loop, with a correspondingly steady increase in the cold leg temperatures. This increase in cold leg temperature ended when the tube bundle completely drained. The temperature in the Loop C cold leg then became a function of the direction of flow, which varied from positive to negative for the remainder of the transient.

A condensation depressurization of the Loop C pump suction at 6026 s resulted in an increase in the A and B cold leg loop flow rates, and a reverse of the C loop cold leg flow rate. The pump suction depressurization stopped, but the reverse flow induced a condensation depressurization of the reactor vessel upper downcomer, which reestablished positive flow in Loop C cold leg. These loop flow oscillations continued (but with lower magnitudes) for the remainder of the transient.

Another condensation-induced depressurization occurred in the upper downcomer of the reactor vessel at 7159 s. The pressure in the cold legs was approximately 4.76 MPa (690 psia), and the depressurization of the primary system was sufficient to reduce the pressure to the accumulator injection pressure (4.62 MPa, 670 psia).

The downcomer temperature and pressure at the end of the calculation were 468.6 K (383.8°F) and 4.04 MPa (585 psia). The response during the last 100 s indicated a temperature decrease of 90.9 K/hr (163.6°F/hr), and a pressure decrease of 3.72 MPa/hr (540 psia/hr). It should be noted that the downcomer temperature is a combination of the three loop temperatures. The A and B loop cold leg temperatures downstream of HPI and accumulator injection point were 479.5 and 478.7 K (403.4 and 402.0°F), respectively; while the C loop cold leg temperature was 315.8 K (108.8°F).

The steam dump mass flow rate response is shown in Figure 14-5. The large flow spike at the beginning of the transient was due to the response of the plant trip controller (PTC). The function of the PTC is to reduce the primary average temperature to the no-load value, 559.3 K (547°F). The difference between the actual average temperature and the setpoint

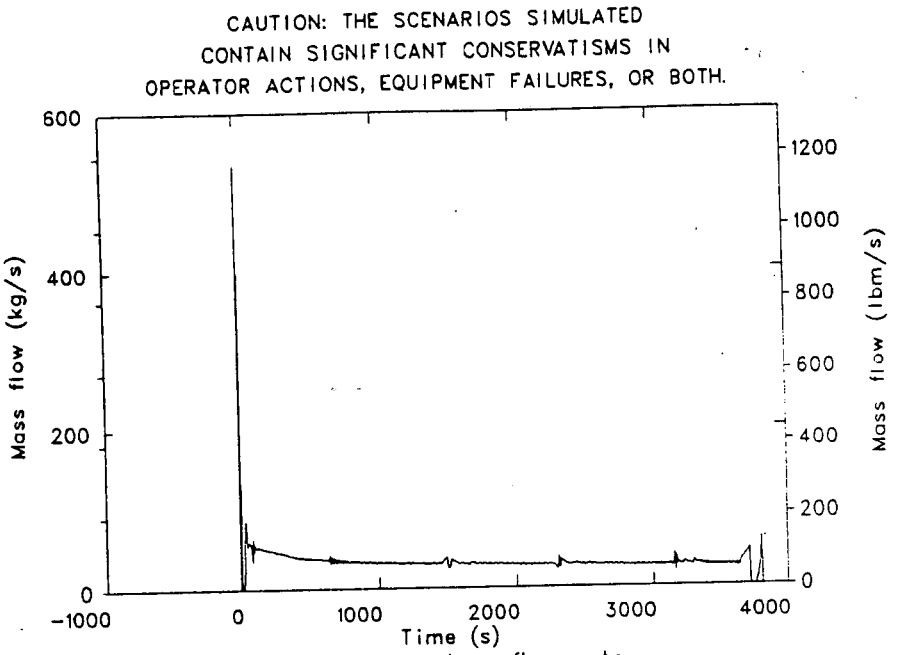

Figure 14-5. Scenario 11 steam dump flow rate.

temperature determines the steam dump valve area. At the beginning of the transient the primary average temperature was 575 K (575.4°F), which represents a PTC error of sufficient magnitude to cause the steam dump valve to trip almost completely open. This large error rapidly diminished due to the effect of the reactor trip. The rapid decrease in mass flowrate following the initial surge was due to the characteristic lead/lag response to the decreasing primary average temperature (lead/lag controllers tend to overrespond to sudden changes in the input variable). The initial temperature variations were gone within the first 50 s of the transient, to be followed by a more stable period of temperature behavior.

The minor oscillations in steam dump flowrate at 650, 1450, 2300 and 3150 s occurred as a result of changes in the heat transfer regimes in the SG boiler region as the secondary mass decreased. The changing heat transfer regimes caused minor fluctuations in the primary average temperature, which induced larger changes in the steam dump valve area demand. These oscillations were relatively short-lived and did not affect the results of the calculation.

The increase in secondary system mass flow rate at 3626 s was due to the effect of tripping the RCPs. The RCP trip reduced the flow rate in the primary coolant loops and consequently increased the primary system average temperature by increasing the temperature rise across the core. The increase in the primary average temperature resulted in an increased demand on the steam dump valve area from the PTC.

The decrease in secondary system mass flow rate at 3718 s occurred when the pressurizer PORVs were opened, causing a decrease in the primary system average temperature, and a corresponding overresponse in the PTC signal.

The flow reversal in the primary system due to the PORVs opening caused a temporary increase in the primary system average temperature with the expected steam dump valve response. The steam dump valves closed at 3817 s when the primary system average temperature finally decreased below the no-load setpoint of 559.3 K (547°F) and the PTC was switched over to the steam pressure control mode (SPC). The SPC regulates the steam dump

valve area based on secondary header pressure, which never became great enough to open the steam dump valves during the remainder of the transient.

The SG wide range (WR) level responses are shown in Figure 14-6. The initial oscillations in SG levels were due to changes in the secondary pressures in response to the closure of the turbine stop valve and the opening of the steam dump valve. The relatively smooth decrease in the SG levels from about 50 to 3817 s was due to the removal of the secondary mass through the open steam dump valve. The increases in SGB and SGC levels between 1500 and 2100 s were due to the respective feedwater headers blowing down as the SG pressures decreased. The SG A feedwater header did not blow down until 5500 s, and as a result, the SGA WR level was the level that tripped the RCPs at 3626 s.

The increase in SGA mass starting at 5500 s did not affect the results of the calculation because the temperature of the feedwater was approximately the same as the existing secondary temperature, and the heat transfer during this period of time was essentially zero, as shown in Figure 14-7, which presents the primary-to-secondary heat transfer response for the three SGs.

14.3.2 Extrapolations and Uncertainties

Uncertainties regarding the results of the Scenario 11 calculation, and predicted conditions at the end of the 2-hour period of interest are presented in this section. The parameters to be addressed are the vessel downcomer pressure, temperature and heat transfer coefficient; and the cold leg discharge volume mass flowrates and temperatures.

The reactor vessel downcomer pressure response for the last 4100 s is shown in Figure 14-8. The primary system pressure is expected to continue decreasing at an average rate of 3.72 MPa/hr (540 psi/hr) for the last 2900 s. The pressure at 11000 s is therefore expected to be approximately 1.034 MPa (150 psia).

The reactor vessel downcomer fluid temperature response for the last 4100 s is shown in Figure 14-9. As can be seen in this figure, the

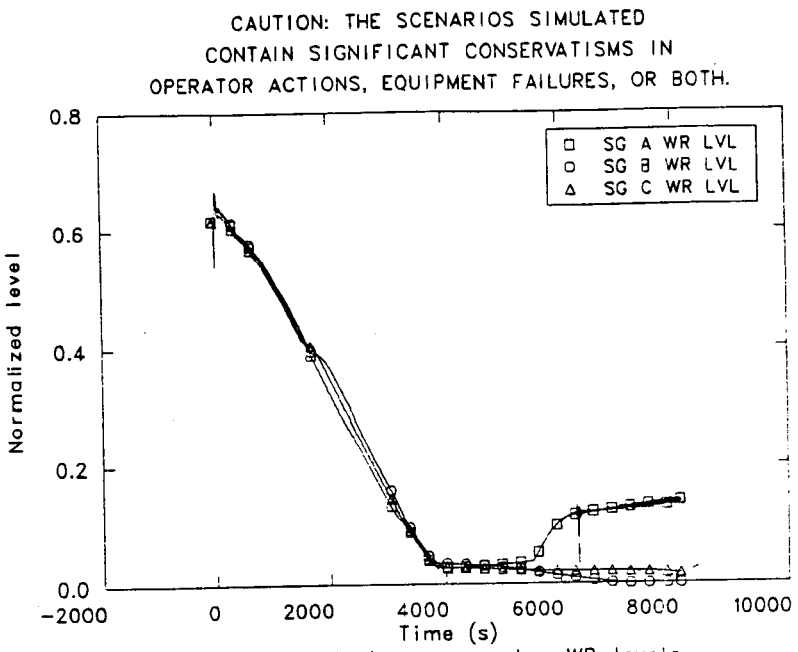

Figure 14-6. Scenario 11 steam generator WR levels.

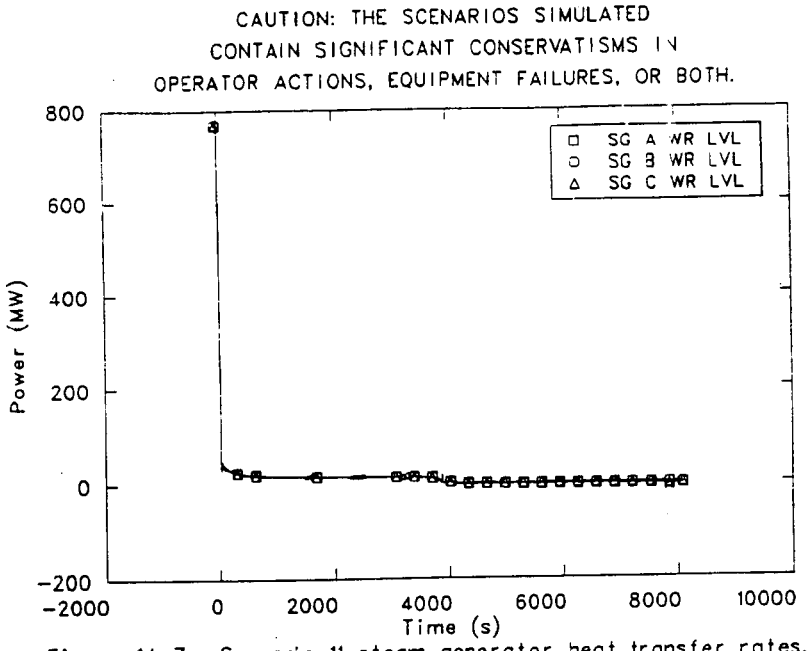

Figure 14-7. Scenario 11 steam generator heat transfer rates.

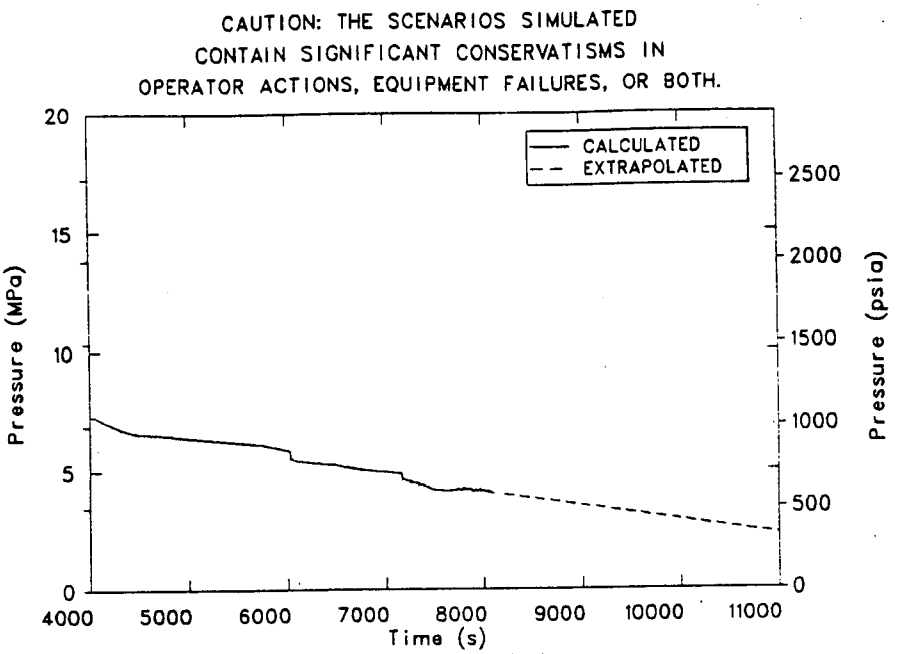

Figure 14-8. Scenario 11 reactor vessel downcomer pressure response, 4000-11000 s.

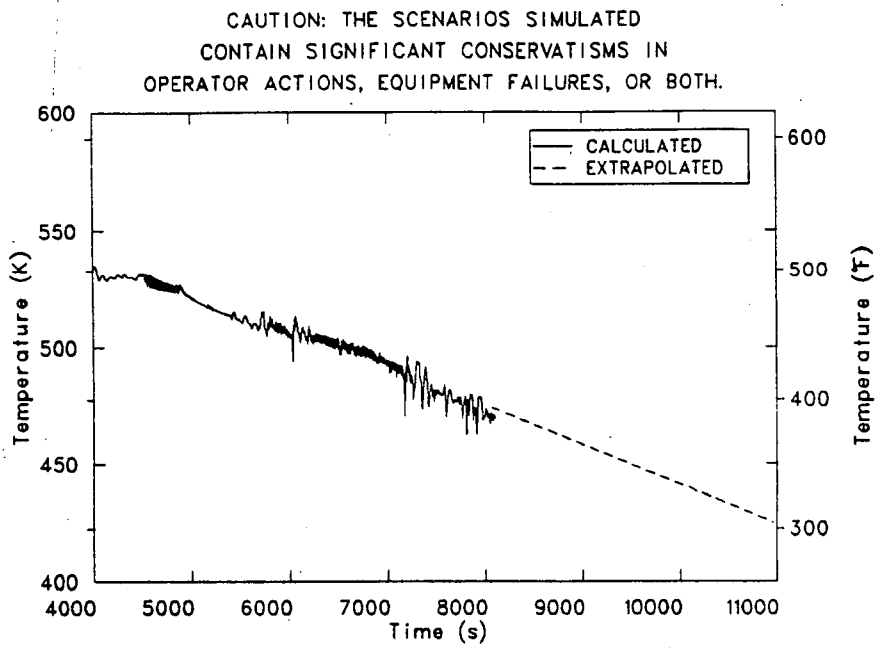

Figure 14-9. Scenario 11 reactor vessel downcomer temperature response, 4000-11000 s.

downcomer temperature was essentially independent of the condensation depressurization events at 6000 and 7200 s. The temperature response during this period of time was dominated by the A and B loops, which were only slightly affected by accumulator injection.

The reactor vessel downcomer fluid temperature is expected to continue decreasing at a constant rate of 57.8 K/hr (104°F/hr) through 11000 s. The final temperature based on the estimated rate of temperature decrease is approximately 422 K (300°F).

The reactor vessel downcomer wall heat transfer coefficient response during the last 4100 s of the calculation is shown in Figure 14-10. The relatively large spikes in the calculated data were the result of oscillations in the downcomer pressure, temperature and mass flow rate. These oscillations were due in part to the response of the primary system to the accumulator injection events. During periods of accumulator injection colder fluid was circulated into the reactor vessel downcomer from the cold legs. This colder fluid resulted in the higher heat transfer coefficients. These rapid changes in the heat transfer coefficient are qualitatively reasonable, but may be overstated. The heat transfer transfer coefficient is expected to remain nearly constant through 11000 s. The final value is estimated to be between 0.7 kW/m2-K (0.034 BTU/ft^2-°F) and 1.3 kW/m^2-K (0.064 BTU/ft2-°F).

The cold leg mass flow rate responses during the last 4100 s are shown in Figure 14-11. The Loop A and B discharge flowrate responses are essentially equal. Uncertainties regarding their responses are due to the effect of accumulator injection. As can be seen in Figure 14-11, the A and B loops behaved rather predictably and indicated no unusual response. The mass flow rates should remain nearly constant through the last 2900 s due to the effect of the driving head produced by the core decay heat coupled with the effect of the gradually increasing HPI flow. The flow rates of these two loops are expected to be approximately 100 kg/s (220 lbm/s) at 11000 s.

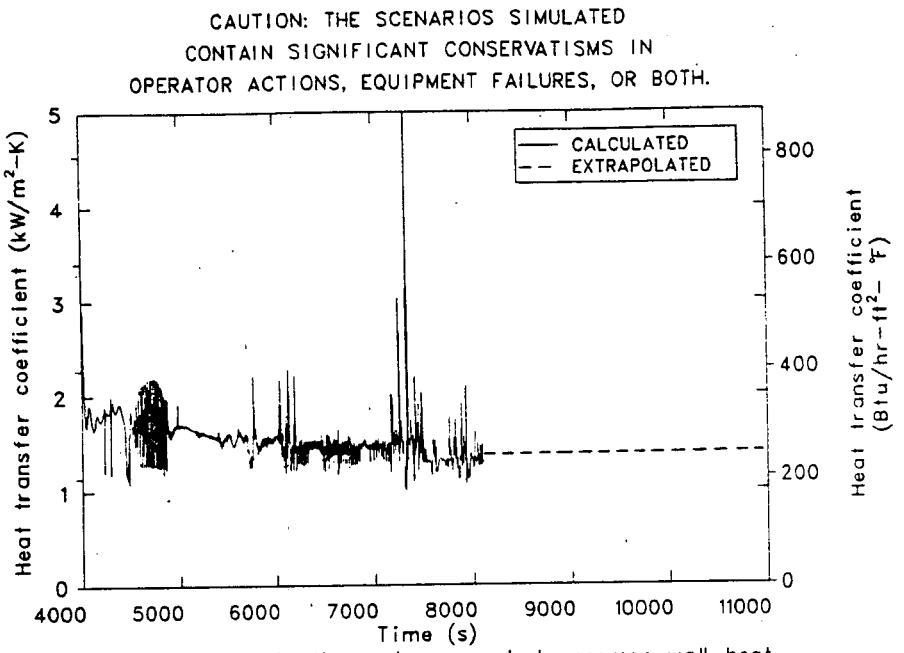

Figure 14-10. Scenario 11 reactor vessel downcomer wall heat transfer coefficient, 4000–11000 s.

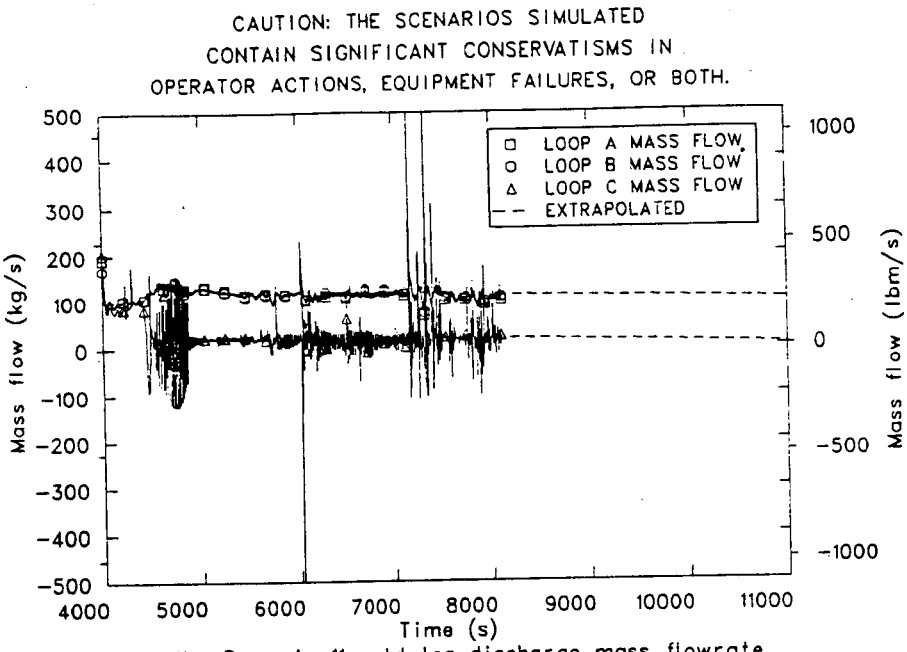

Figure 14-11. Scenario 11 cold leg discharge mass flowrate responses, 4000–11000 s.

The C loop cold leg discharge mass flow rate response was significantly affected by accumulator injection and condensation depressurization events. This was due to the nearly stagnant flow conditions existing in this loop. The large flow oscillations at 6000 s and between 7200 s and 7400 s were due to the effects of accumulator injection. These oscillations could be qualitatively correct, but in all likelihood, are significantly overpredicted. These oscillations are expected to continue for the duration of the desired period of the calculation, but at a reduced magnitude as the primary system continues to depressurize.

The Loop C cold leg discharge mass flow rate will continue to equal the HPI plus accumulator injection flow rate for the last 2900 s since this loop would be stagnant without these contributions. The flowrate at 11000 s is expected to be approximately 10 kg/s (22 lbm/s).

The cold leg temperature responses of the three cold leg discharge volumes for the last 4100 s are shown in Figure 14-12. The Loop A and B responses were predictably smooth since the flowrates through these two loops were nearly constant and nonoscillatory in behavior. The Loop C discharge volume temperature was significantly more erratic. The relatively large temperature oscillations at 6000 s, 7200 s, and 7700 s were the result of reverse flow during periods of accumulator injection. The reversed flow events were caused when the Loop C cold leg suction depressurized, thereby inducing the warmer downcomer fluid to flow into the cold leg discharge volume. The subsequent decreases in the Loop C discharge temperature were due to the resumption of positive flow back into the downcomer. These oscillations are the result of condensation depressurization events.

The Loop A and B cold leg discharge temperatures are expected to continue deceasing at a constant rate of approximately 60 K/s (108°F/s) for the last 2900 s. The final temperature of the fluid in these two loops will be approximately 420 K (489°F).

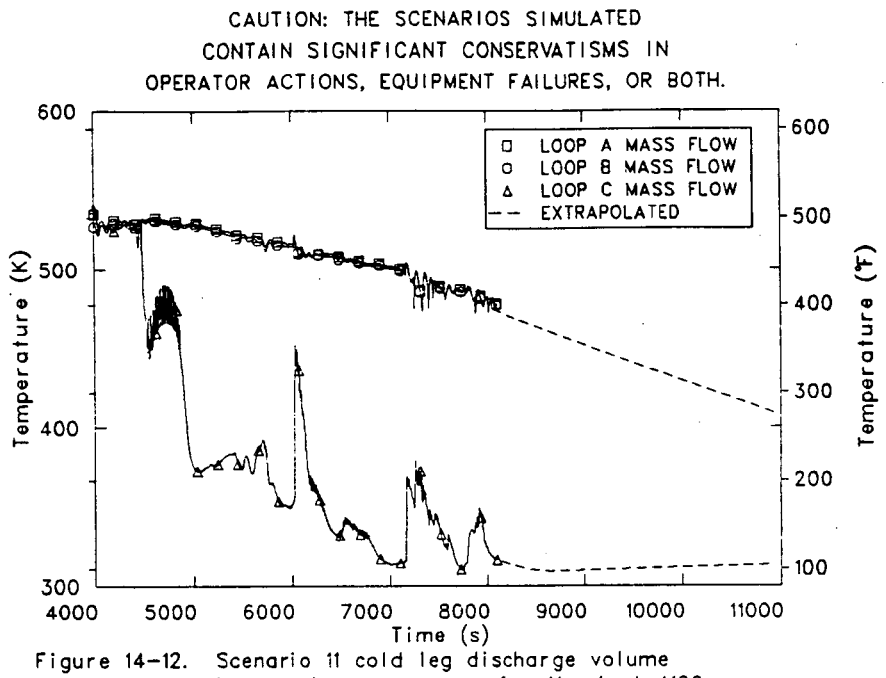

Figure 14-12. Scenario 11 cold leg discharge volume temperature responses for the last 4100 s.

The Loop C cold leg discharge temperature is expected to vary between 300 K (80°F) and 305 K (90°F) at 11000 s. The final temperature will be a function of the HPI and accumulator injection flow rates and the direction of flow in the Loop C cold leg discharge piping.

14.4 Conclusions

Conclusions regarding the results of the Scenario 11 calculation are presented in this section. A compilation of the values of the parameters described in Section 14.3 will be presented.

The extrapolated values from the Scenario 11 calculation corresponding to 11000 s are summarized in Table 14-3.

Extrapolation of the primary system pressure response through 11000 s indicates that the system pressure will continue to decrease until the low pressure injection (LPI) shutoff head is reached (0.97 MPA, 140 psia). Initiation of LPI will thereafter maintain the primary system pressure at the LPI shutoff head as long as the PORV is open.

The reactor vessel downcomer fluid temperature is expected to continue decreasing due to the influence of the HPI, accumulators and LPI. The minimum fluid temperatures will continue to be found in the Loop C cold leg discharge volumes.

The reactor vessel downcomer wall heat transfer coefficient should remain essentially constant except during periods of accumulator or LPI injection, which will cause brief periods of increased flow and decreased average fluid temperature. These changes in local fluid properties will tend to increase the heat transfer coefficient; however, these periods are expected to be transient in nature and should not significantly affect the overall heat transfer coefficient response.

The cold leg discharge mass flow rates are expected to remain essentially constant due to the driving head provided by the core decay

TABLE 14-3. SCENARIO 11 EXTRAPOLATED VALUES

Parameter	Value
Downcomer pressure	1.03 MPa (150 psia)
Downcomer temperature	395 K (251°F)
Downcomer wall heat transfer coefficient	0.7-1.3 kW/m2-K (0.034-0.064 BTU/ft2-°F)
Cold leg mass flow rates:	
Loops A and B	100 kg/s (45 lbm/s)
Loop C	10 kg/s (4.5 lbm/s)
Cold leg discharge temperatures:	
Loops A and B	420 K (296°F)
Loop C	303 K (85°F)

heat. The SGC bundle is not expected to refill due to the open PORV. If the PORV were to be closed, it is expected that the SGC tube bundle would refill and the primary system loop mass flow rates would eventually become about 70 kg/s (154 lbm/s) in all three loops.

The cold leg discharge fluid temperatures in the A and B loops are expected to continue decreasing due to the effect of the HPI, accumulator and LPI contributions. The Loop C cold leg fluid temperature was essentially at the HPI fluid temperature prior to 11000 s.

15. OVERVIEW AND CONCLUSIONS

This report presents analyses of twelve RELAP5 computer code calculations pertinent to the study of pressurized thermal shock (PTS) in the H. B. Robinson, Unit 2 (HBR-2) pressurized water reactor (PWR).

One of the calculations simulated a plant trip transient that occurred in the PWR. A comparison of code-calculated and measured data indicated generally good agreement thus providing an informal and limited, but useful, qualification of the computer model beyond the detailed quality assurance measures described in Section 2.

The remaining eleven calculations simulated hypothetical cooldown scenarios with varying potentials for primary system repressurization. These scenarios were defined at Oak Ridge National Laboratory (ORNL), integrator of the multi-laboratory PTS study. Detailed descriptions of the scenarios are presented in the "Scenario Description" subsections of Sections 4 through 14.

The computer calculations were performed using "best estimate" modeling assumptions for plant conditions and responses to the events specified in the scenario descriptions. The reader is cautioned, however, that for bounding purposes the scenario descriptions were based on extremely conservative assumptions concerning equipment malfunctions, operator actions and omissions, or combinations of these. Thus, while the computer calculations represent "best estimate" plant responses to the scenarios as defined, they do not represent the "most probable" plant responses to the scenario initiating events.

Table 15-1 shows a summary tabulation of minimum fluid temperatures and maximum subsequent fluid pressures in the reactor vessel downcomer for each of the eleven scenarios. The pressures and temperatures shown are located at an elevation adjacent to the top of the core. Note the pressures and temperatures shown are generally not coincident. The temperatures shown represent the lowest calculated or, in the event of

TABLE 15-1. SUMMARY TABULATION OF HBR-2 PTS ANALYTICAL RESULTS

Scenario	Description	Plant Condition	Minimum RV Downcomer Fluid Temperature (K)	Minimum RV Downcomer Fluid Temperature (°F)	Maximum Subsequent RV Downcomer Pressure (MPa)	Maximum Subsequent RV Downcomer Pressure (psia)
1	1 ft^2 steam line break	Hot standby	386	235	16.2	2350
2	Double-ended steam line break	Hot standby	370	206	16.2	2350
3	Stuck-open steam line PORV	Hot standby	397	256	11.1	1632
4	3 Steam dumps fail open	Full power	373	212	11.8	1711
5	SG overfill with AFW	Full power	535	503	16.0	2320
6	Small hot leg break	Full power	310	100	0.98	142
7	Stuck-open pressurizer PORV	Full power	538	509	17.5	2538
8	Small hot leg break	Hot standby	310	100	0.97	140
9	SG tube rupture	Hot standby	465	378	9.62	1396
10	SG tube rupture	Full power	557	543	9.65	1400
11	Loss of heat sink, primary feed and bleed recovery	Full power	422	300	1.03	150

calculations terminated before the end of the PTS 2-hour period of interest, the lowest extrapolated temperatures within the 2-hour period. The pressures and temperatures shown in the table have been adjusted, if required, for any uncertainty or bias identified in the calculations as discussed in the "Extrapolations and Uncertainties" subsections for each scenario. Table 15-1 is presented as a convenience to the reader and is not intended to be used as an indicator of pressurized thermal shock severity for each sequence. Determination of severity first requires an evaluation of the plotted information presented in the scenario results sections. Second, additional analyses of multidimensional effects and fracture mechanics, will be performed by other PTS study participants. Following these additional studies, judgements of severity will be made at ORNL.

APPENDIX A

Table A-1 presents a timing survey of the calculations presented in this report. Figures A-1 through A-12 show the continuous rate of CPU time usage during each of the calculations

The computer used to perform the calculations was the CDC 176 at the Idaho National Engineering Laboratory. The calculations were performed using the RELAP5/MOD1.6 computer code.

TABLE A-1. TIMING STATISTICS

	Scenario											
	Plant Trip	1	2	3	4	5	6	7	8	9	10	11
Total number volumes (#C)	213	193	198	224	223	223	224	223	224	222	222	223
Total number heat structures	218	200	203	218	218	218	218	218	218	226	226	218
Transient time seconds (RT)	900	1800	1581	3737	2491	3600	2800	2200	1737	7200	2400	8100
Total CPU seconds used	4944	5628	9392	18252	19795	21116	9697	5599	11915	20556	13704	31389
Total number of time steps (#DT)	18004	20172	34286	57663	58690	73465	30959	18844	34384	68972	48052	99127
CPU/real time	5.49	3.13	5.94	4.88	7.95	5.87	3.46	2.55	6.86	2.86	5.71	3.88
$\frac{CPU \times 10^2}{RT \times \#C}$	2.58	1.62	3.00	2.18	3.57	2.63	1.54	1.14	3.06	1.29	2.57	1.74
$\frac{CPU \times 10^6}{RT \times \#C \times \#DT}$	1.43	0.80	0.87	0.38	0.61	0.36	0.50	0.60	0.89	0.19	0.53	0.18
$\frac{CPU \times 10^3}{\#C \times \#DT}$	1.29	1.45	1.38	1.41	1.51	1.29	1.40	1.33	1.55	1.34	1.28	1.42

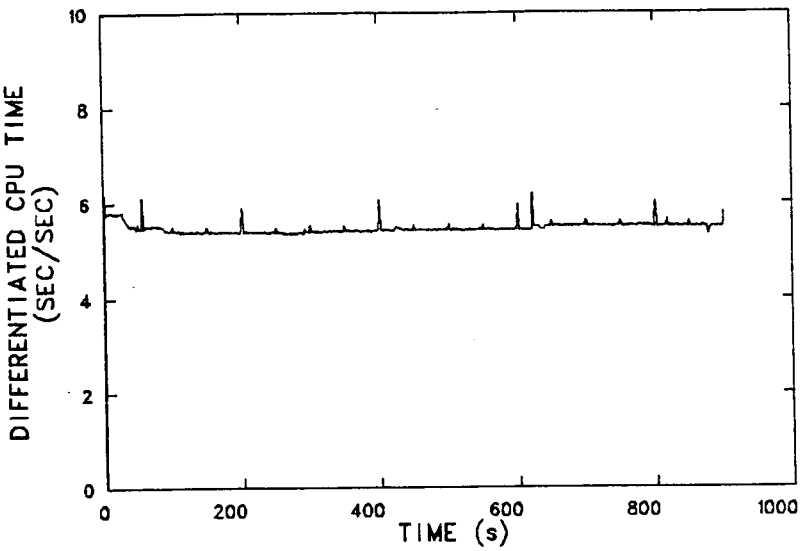

Figure A-1. Plant trip rate of CPU time usage.

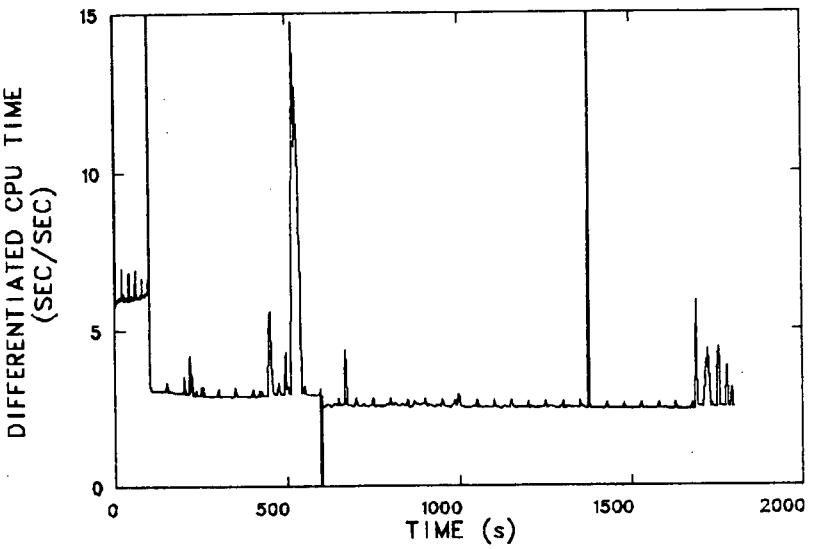

Figure A-2. Scenario 1 rate of CPU time usage.

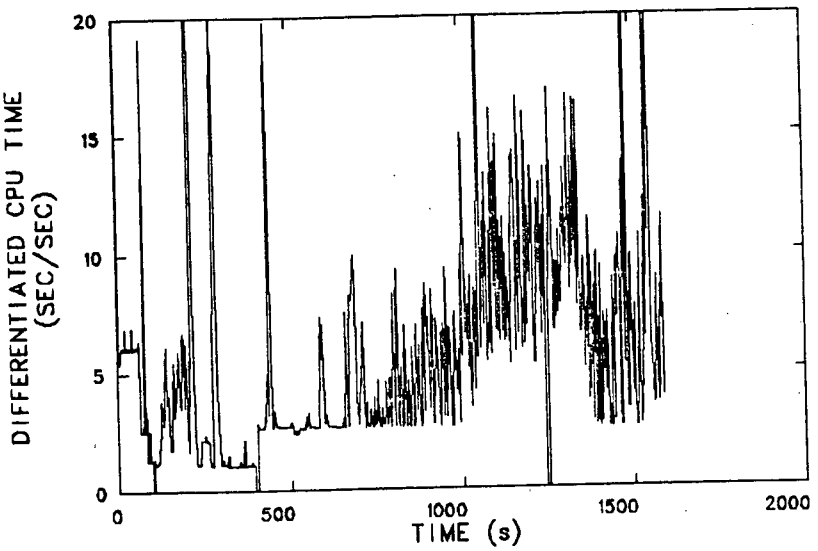

Figure A-3. Scenario 2 rate of CPU time usage.

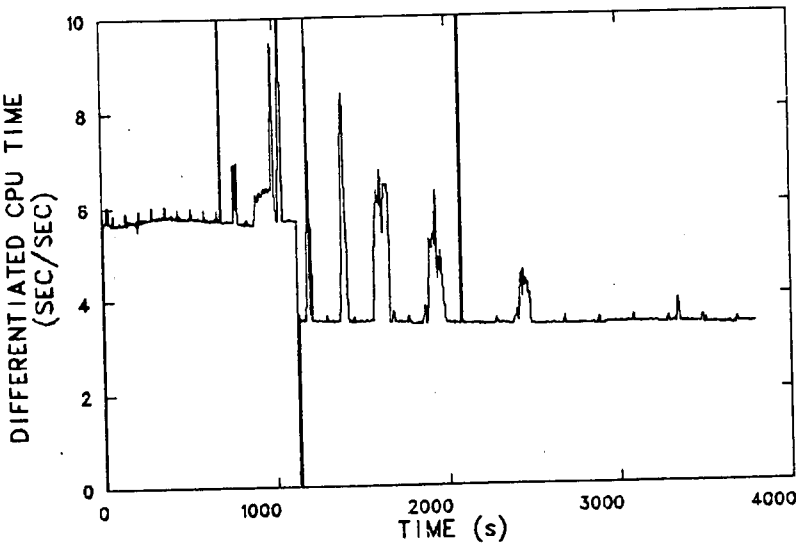

Figure A-4. Scenario 3 rate of CPU time usage.

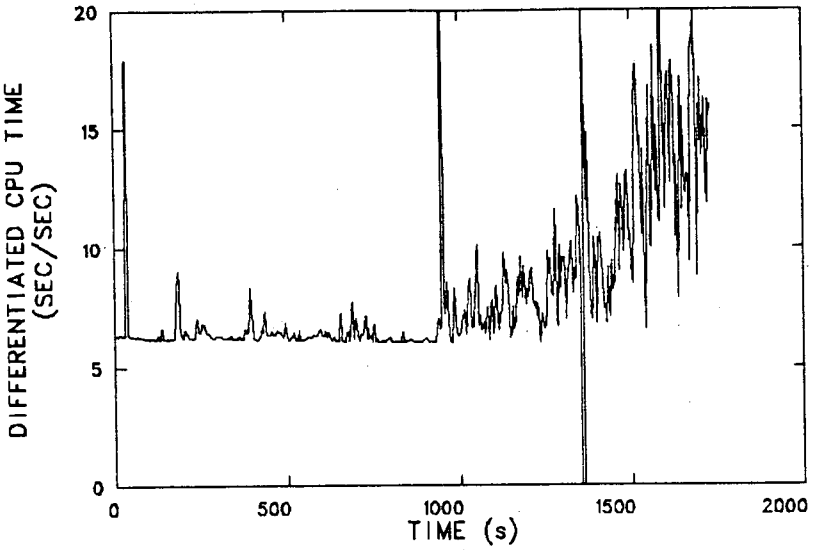

Figure A-5. Scenario 4 rate of CPU time usage.

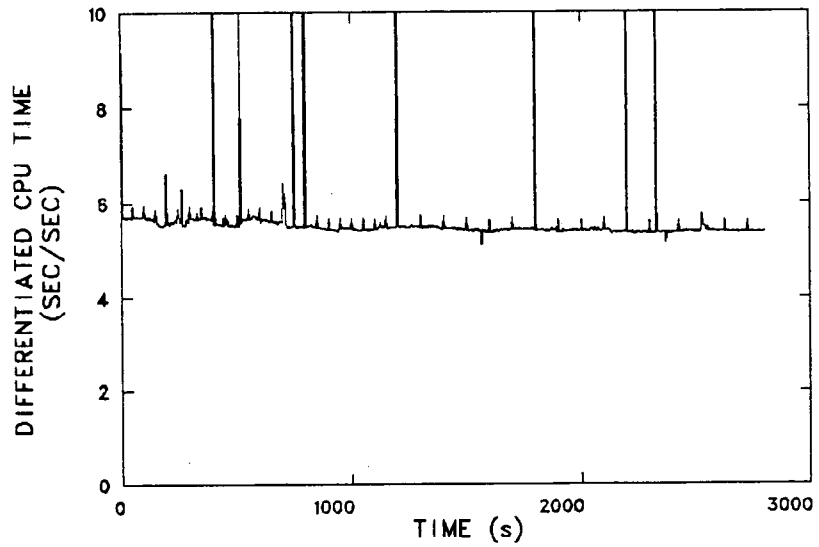

Figure A-6. Scenario 5 rate of CPU time usage.

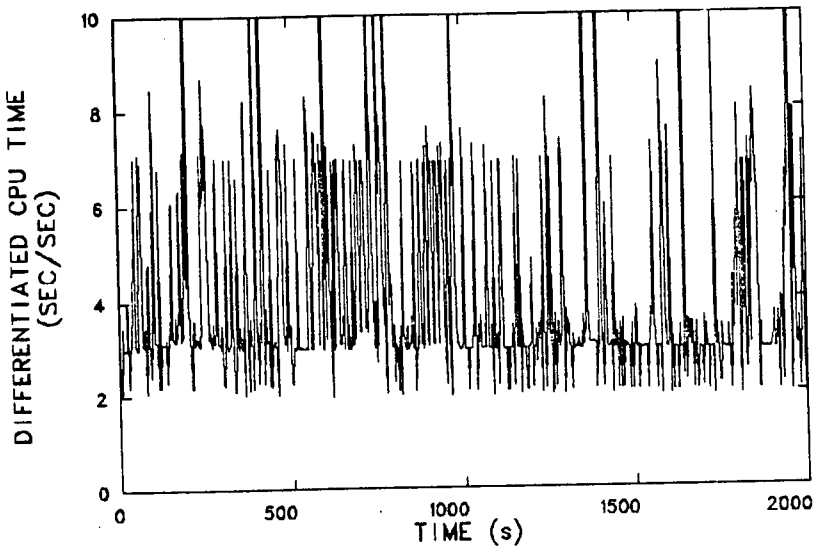

Figure A-7. Scenario 6 rate of CPU time usage.

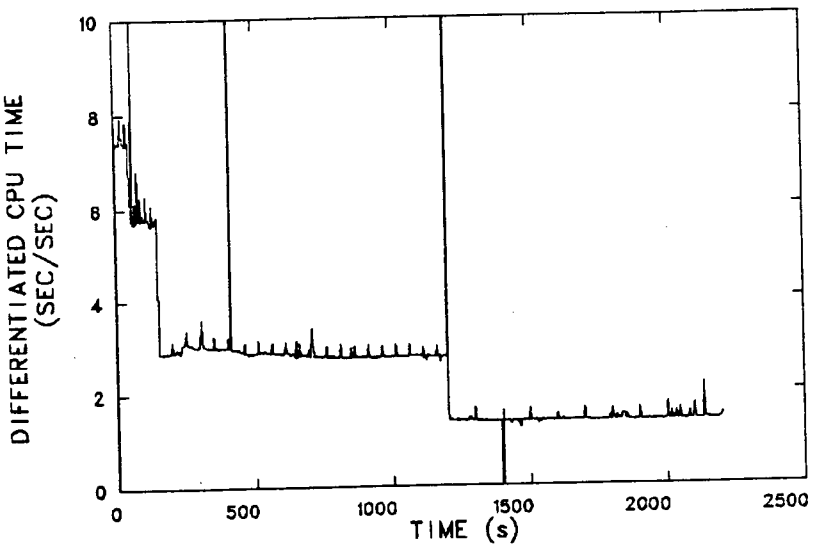

Figure A-8. Scenario 7 rate of CPU time usage.

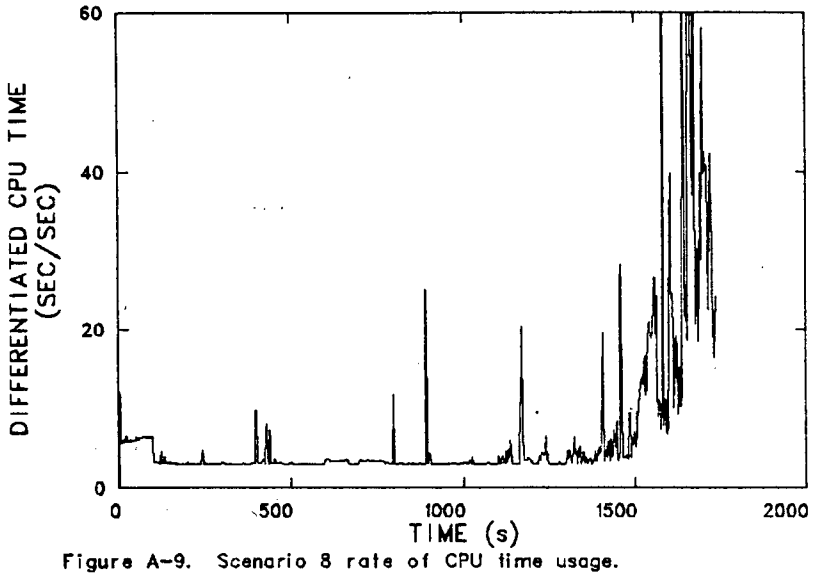

Figure A-9. Scenario 8 rate of CPU time usage.

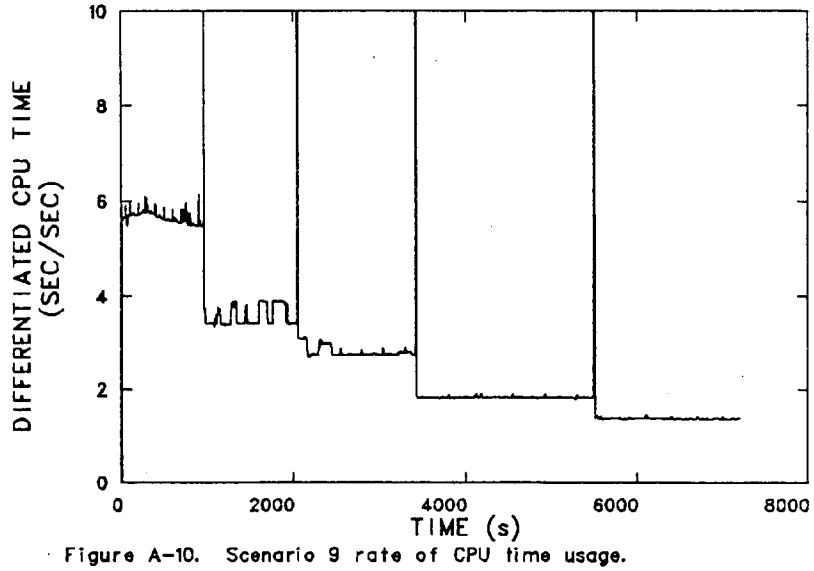

Figure A-10. Scenario 9 rate of CPU time usage.

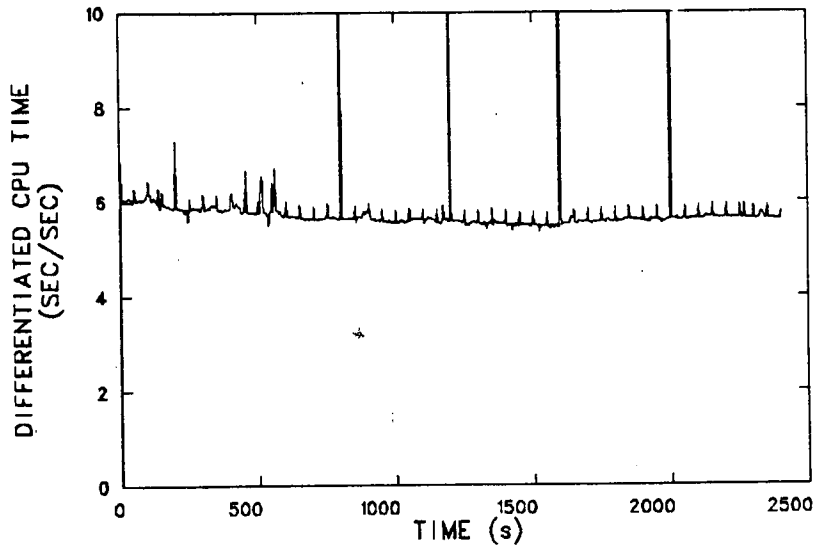

Figure A-11. Scenario 10 rate of CPU time usage.

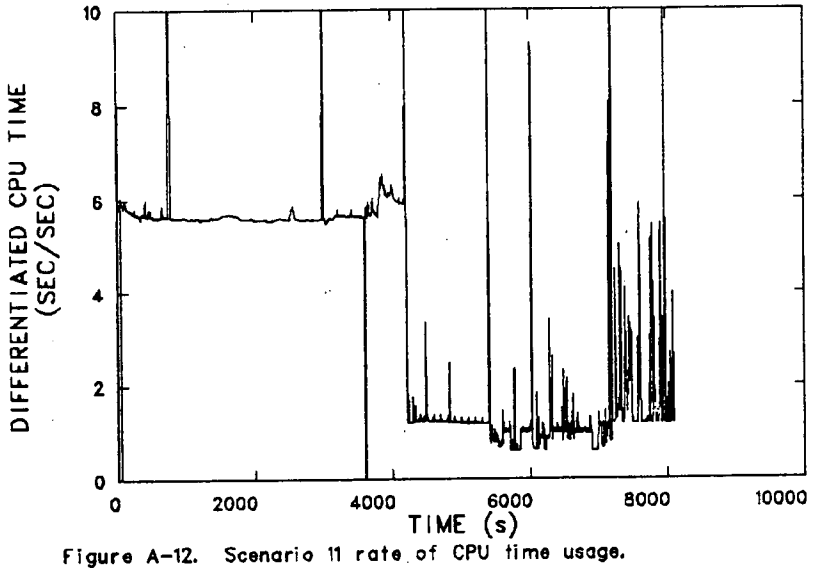

Figure A-12. Scenario 11 rate of CPU time usage.

NRC FORM 335 (11-81)

U.S. NUCLEAR REGULATORY COMMISSION

BIBLIOGRAPHIC DATA SHEET

1. REPORT NUMBER *(Assigned by DDC)*
EGG-SAAM-6476

4. TITLE AND SUBTITLE
RELAP5 Thermal-Hydraulic Analyses of Pressurized Thermal Shock Sequences for the H. B. Robinson Unit 2 Pressurized Water Reactor

2. *(Leave blank)*

3. RECIPIENT'S ACCESSION NO.

7. AUTHOR(S)
C. D. Fletcher, M. A. Bolander, M. E. Waterman, J. D. Burtt, B. D. Stitt, C. M. Kullberg, C. B. Davis, D. M. Ogden

5. DATE REPORT COMPLETED
MONTH: December YEAR: 1983

9. PERFORMING ORGANIZATION NAME AND MAILING ADDRESS *(Include Zip Code)*
EG&G Idaho, Inc.
Idaho Falls, ID 83415

DATE REPORT ISSUED
MONTH: December YEAR: 1983

6. *(Leave blank)*

8. *(Leave blank)*

12. SPONSORING ORGANIZATION NAME AND MAILING ADDRESS *(Include Zip Code)*
Division of Accident Evaluation
Office of Nuclear Regulatory Research
U.S. Nuclear Regulatory Commission
Washington, DC 20555

10. PROJECT/TASK/WORK UNIT NO.

11. FIN NO.
A6047

13. TYPE OF REPORT
Technical

PERIOD COVERED *(Inclusive dates)*

15. SUPPLEMENTARY NOTES

14. *(Leave blank)*

16. ABSTRACT *(200 words or less)*

Thermal-hydraulic analyses of eleven hypothetical pressurized thermal shock (PTS) scenarios for the H. B. Robinson, Unit 2 pressurized water reactor were performed at the Idaho National Engineering Laboratory (INEL) using the RELAP5 computer code. The scenarios, which were developed at Oak Ridge National Laboratory (ORNL), contain significant conservatisms concerning equipment failures, operator actions, or both.

The results of the thermal-hydraulic analyses presented here, along with additional analyses of multidimensional and fracture mechanics effects will be utilized by ORNL, integrator of the PTS study, to assist the U.S. Nuclear Regulatory Commission in resolving the pressurized thermal shock unresolved safety issue.

17. KEY WORDS AND DOCUMENT ANALYSIS

17a. DESCRIPTORS

17b. IDENTIFIERS/OPEN-ENDED TERMS

18. AVAILABILITY STATEMENT
Unlimited

19. SECURITY CLASS *(This report)*
Unclassified

21. NO. OF PAGES

20. SECURITY CLASS *(This page)*
Unclassified

22. PRICE
S